THE EFFECT OF CANNABINOIDS AND ANTI-AGING COMPOUNDS ON SKIN AGING AND REJUVENATION

MARTA GERASYMCHUK
Ph.D. (Pathological Physiology), Zaporizhzhia State Medical University, Ukraine, 2013
M.D. (General Medicine), Ivano-Frankivsk State Medical University, Ukraine, 2006

A thesis submitted
in partial fulfilment of the requirements for the degree of

DOCTOR OF PHILOSOPHY

in

BIOMOLECULAR SCIENCE

Department of Biological Sciences
University of Lethbridge
LETHBRIDGE, ALBERTA, CANADA

THE EFFECT OF CANNABINOIDS AND ANTI-AGING COMPOUNDS ON SKIN AGING AND REJUVENATION

MARTA GERASYMCHUK

Date of Defence: April 28, 2022

Dr. I. Kovalchuk	Professor	Ph.D.
Dr. O. Kovalchuk	Professor	Ph.D.
Thesis Co-supervisors		
Dr. T. Burg	Professor	Ph.D.
Thesis Examination Committee Member		
Dr. R. Gibb	Professor	Ph.D.
Thesis Examination Committee Member		
Dr. N. Thakor	Associate Professor	Ph.D.
Internal External Examiner		
Department of Chemistry and Biochemistry		
Faculty of Arts and Science		
Dr. K Riabowol	Professor	Ph.D.
External Examiner		
University of Calgary		
Calgary, Alberta		
Dr. T. Russell		
Chair, Thesis Examination Committee	Associate Professor	Ph.D.

This thesis is dedicated to my parents:

*my beloved mother - **Nadiya Holobyn** (1947 - 2022)*
for her nobleness,

*my father - Prof. **Roman Gerasymchuk** (1937 - 2019),*

and to all amazing people for being there every step of the way!

ABSTRACT

Cannabis sativa/indica has been used for medicinal and recreational purposes for over millennia. There are several approved medical indications for cannabis use in dermatological practice, including eczema, psoriasis, and severe pain. At the same time, there is a lack of scientific information about the anti-aging and rejuvenation properties of cannabinoids. We hypothesized that phytocannabinoids, cannabidiol (CBD) and tetrahydrocannabinol (THC), and nutrient signaling regulators (NSR), metformin, rapamycin, and triacetylresveratrol (TRSV), exert anti-aging and rejuvenating activity on skin fibroblasts. Results demonstrate that low doses of THC and CBD alone or combined with NSR lowered expression of senescence markers, stimulated ameliorative metabolic and functional activity, inhibited dermal aging processes, and positively affected the viability of skin fibroblasts. We found that TRSV alone or combined with THC/CBD might be a potential tool for enhancing regeneration and repair in injured tissues. The effectiveness of metformin or rapamycin alone or combined with phytocannabinoids was less effective.

ACKNOWLEDGEMENTS

First and foremost, I would like to express my deepest appreciation and sincere gratitude to Professor Igor Kovalchuk for the privilege of working in his research group, knowledge, guidance, and consistent support of my Ph.D. project and pursuits in research. His mentorship has greatly aided me during experiments and in writing this thesis. He has always encouraged me to think critically and evolve as an academic, to work hard and generate my ideas, criticism, and most importantly, to challenge my work and ensure my research is of the highest quality and experience mentoring students. Dr. Kovalchuk has provided me with sufficient independence and resources to fully complete this dissertation. Thank you for your prompt responses, wise advice, and always beneficial solutions. I could not have imagined having a better supervisor for my Ph.D. study.

I would also like to express my deepest gratitude to my co-supervisor, Dr. Olga Kovalchuk, for an excellent opportunity to work in her lab on this exciting project, for outstanding mentorship, continual support, and guidance along the way – and your confidence in me. Also, I am thankful for all of her friendly talks, advice, and encouragement. She has taught me to think outside the box and be critical of my work. Thank you so much for everything.

I would like to thank my Committee Members, Dr. Theresa Burg and Dr. Robbin Gibb. I want to express my gratefulness for your scientific and mental support during difficult periods in my life, helpful comments regarding my research, great advice and criticism, insightful comments, and especially for their challenging questions that reminded me to be aware and explore my research from various perspectives. In addition,

their enthusiasm and outstanding kind personalities have been instrumental to my thesis success.

I would also like to extend my appreciation to my External Examiners members, Dr. Karl Riabowol, Dr. Nehalkumar Thakor, and Dr. Tony Russell, Chair of my Thesis Examination Committee for their comments and suggestions concerning my research, their time, and effort. I could not have asked for a better committee.

The work performed in this dissertation would not have been possible without the support and guidance of many brilliant and caring individuals. I want to extend my deepest appreciation to Dr. Roy Golsteyn for permission to use his laboratory equipment, his patience, constant moral support, numerous pieces of advice, and expertise on this research project.

I would also like to thank Dr. Andy Hudson for his tremendous support of my research, sharing his experience, the guidance provided towards technical assistance and use of equipment, help with supplements and microscopy, and for being patient with my numerous questions.

I give special thanks to Dr. Steve Wiseman for the opportunity to work in his laboratory and share experience with incredibly smart graduate and undergraduate students, learn new toxicology techniques, test cannabinoids in oocyte maturation assay, your ongoing support, advice, and kind attention.

I'm very grateful to past and current Kovalchuk lab members. I want to give special thanks to Dr. Andrey Golubov, Dr. Bo Wang, Dr. Dongping Li, Dr. Santosh Suryavanshi, Rocio Rodriguez Juarez, Rommy Rodriguez Juarez, Olena Shymanovska, Dr. Slava

Ilnytsky, Araba Panyin Sagoe-Wagner, who taught me many of the biological techniques I used throughout my research project. They extended me a tremendous amount of time, support, and guidance during the early parts of my Ph.D. studies, always being there for me, answering questions, and being wonderful colleagues and friends.

I give special thanks and deepest appreciation to my colleague and amazing friend Gregory Ian Robinson for all of his immense enthusiasm and great help, without which I know I would not have reached the finish line in the time I did. He did tremendous work in QuPath analysis, provided countless suggestions, and assisted in lab work, including even opening the freezer and carrying heavy stuff. Greg input a lot of energy and effort for excellent proofreading of my thesis. During the last two years, he was not just an outstanding friend but also my guardian angel who always supported and helped no matter what encouraged me never to give up, and always created a cheerful atmosphere. I am really blessed to have a friend like Greg.

I would also like to thank our past lab members, Mariia Zayachuk and Nazar Pryimak, for helping during lab work and being good friends. I can not forget to mention great colleagues from other labs who helped me with techniques and proofreading my manuscripts, such as Sejer Meyhoff, Justin Dubiel, Lauren Zink, Katrina Taylor, Jaxson Reiter, Amanda Carpenter, and Suzanne Chmilar.

I am thankful for financial support received in the form of graduate assistantships and awards from the funding agency MITACS, the University of Lethbridge, and the School of Graduate Studies for the SGS Dean’s Scholarship, International Continuous SGS Tuition Award, Coca-Cola Scholarship, and InPlanta Biotechnology Inc., Pathway Rx, without the financial support of which, my work would not be completed.

My appreciation goes to my best friends, Dr. Natalia Vardinska, Dr. Taras Koval, Dr. Sylwia Szczepara, Viktor Karatov, Dr. Taras Koshyk, Dr. Toro Mario Damiano, Dr. Rafail Elevterov, Dr. Kristian Dachev, Dr. Musa Durlyov, Dr. Valentyna Volobueva, Dr. Iryna Belska, Dr. Solomiia Kerniakevych, Dr. Sergii Girnyi, Dr. Mykola Drosyk, Oleg Levytsky, Dr. Lydmyla Ivanyuk, Dr. Olena Bedenko, Rostyslav Lytvyn, and Dr. Vitaliy Shvets, who have been there for me through the good and the bad times and never failed to make me laugh when I needed it the most.

I want to share my gratitude to the very important and special people who invested in my success throughout my life and with regards to them, I became who I am. My deepest appreciation to Dr. Shevchuk Anatoliy and his family, Prof. Gryb Viktoriia, my god-father Dr. Ivan Ostapiyak, my god-mother Dr. Romanna Kuhtyak, rector of IFNMU Prof. Evgen Nejko, Prof. Kostyantyn Volkov, Prof. Nuncio Crimi, Prof. Carlo Vancheri, Prof. Anatoliy Kubyshkin, Dr. Anton Evseyev, Dr. Lydmila Anisimova, Dr. Nadiia Verbova, Dr. Alex Verbova, Dr. Marta Yuzkiv, and Dr. Francesco Foglino – I am forever thankful!

I offer a lot of thanks to the people who have made Canada my second home – my friends: Gregory Robinson, Justin Dubiel, Katrina Taylor, Chloe Devoy, Bailey Porter, Hunter Johnson, Kush Patel, Sejer Meyhoff, Teymur Gafarov, Justin Miller, Lauren Zink, and Svitlana Payant, – remember, you are the best!

I left to the end the most grateful, however bittersweet appreciation to my late parents, who are already not able to share my happiness and success in this world. You both, Nadiya and Roman, are the beginning of this journey, have shown me life, and have offered me opportunities that I would not have found without you. My beloved Mamusia, you loved me more than anything in this world, you taught me that the few most important

steps toward success are showing up, working hard, respecting others, and never giving up; you made me strong. Day after day, your support moved me toward my goals, and when I did mistakes, you constantly supported and taught me to come back the next day and try again, I have tried to emulate this and eventually always reached what I desired. My dear father, you showed me that there is a way to complete a job and there is a way to do a job right and directed me to use the second path whenever possible. You always encouraged me to believe in myself and to strive for excellence in everything I do. Thank you both for letting me be a child as long as possible. I know you are supporting me now even if I could not see it.

And in the end, I want to thank you to all the Ukrainian people who are heroically defending my home country, Ukraine! In this challenging time, Ukrainians are united in bravery, defense of their own land, culture, and traditions, as well as freedom for future generations not just in Ukraine but in the EU and globally against the biggest evil of the modern world provided by russian war in Ukraine. I wish my people to win and settle the peace. Glory to Ukraine!

TABLE OF CONTENTS

LIST OF TABLES

LIST OF FIGURES

LIST OF ABBREVIATIONS

2-AG – 2-arachidonoylglycerol
AADs – age-associated diseases
AC – adenylyl cyclase
AEA – anandamide
AGEs – advanced glycation end product
AMPK – AMP-activated protein kinase
AP-1 – activator protein – 1
ARD – age-related diseases
ATP – adenosine triphosphate
β-Gal – β-Galactosidase
BID – BH3 interacting-domain death agonist
BMPs – bone morphogenetic proteins
bp – base pair
BSA – bovine serum albumin
CB1 – cannabinoid receptor 1
CB2 – cannabinoid receptor 2
CBs - cannabinoids
CBC – cannabichromene
CBD – cannabidiol
CBDV – cannabidivarin
CBG – cannabigerol
CBGV – cannabigerovarin
CBN – cannabinol
CDK2 – cyclin-dependent kinase 2
CDKN1A – cyclin dependent kinase inhibitor 1A, gene coding protein p21
CDKN2A – cyclin dependent kinase inhibitor 2A, gene coding protein p16
CO_2 – carbon dioxide
COL1A1 – type I collagen
COL3A1 – type III collagen
COPD – chronic obstructive pulmonary disease
CR – calorie restriction
CV – crystal violet
CVD – cardiovascular diseases
DAGL – diacylglycerol lipase
DAPI – 4',6-diamidino-2-phenylindole
DMSO – dimethyl sulfoxide
DNA – deoxyribonucleic acid
eCBs – endocannabinoids
ECM – extracellular matrix
ECS – endocannabinoid system
EGF – epidermal growth factor

EGFR – epidermal growth factor receptor
ELN – elastin
ERK – extracellular signal-regulated kinases
ETC – electron transport chain
FAAH – fatty acid amide hydrolase
FDG – fluorogenic fluorescein digalactoside
FOXO – forkhead box O
GAPDH – glyceraldehyde-3-phosphate dehydrogenase
GDF11 – growth differentiation factor 11
GH – growth hormone
GPCRs – G-protein coupled receptors
GPR18 – G protein-coupled receptors 18
GPR55 – G protein-coupled receptors 55
GPR119 – G protein-coupled receptors 119
HAS1 – hyaluronan synthase 1
HDF – human dermal fibroblasts
HGPS – Hutchinson–Gilford progeria syndrome
HIF-1 – hypoxia-inducible factor 1
HPA – hypothalamic-pituitary axis
IGF-1 – insulin-like growth factor-1
JNK – c-Jun N-terminal kinase
kb – kilobase
MAGL – monoacylglycerol lipase
MAPK – mitogen-activated protein kinase
MF – mitotic fibroblast
MKI-67 – marker of proliferation Ki-67
MMP – matrix metalloproteinase
mtDNA – mitochondrial DNA
mTOR – mammalian target of rapamycin
mTORC1 – mammalian target of rapamycin complex 1
mTORC2 – mammalian target of rapamycin complex 2
NAD – Nicotinamide adenine dinucleotide
NADH – nicotinamide adenine dinucleotide+hydrogen (H)
NAEs – N-acylethanolamines
NAPE-PLD – NAPE-phospholipase D
nDNA – nuclear DNA
NF-κB – nuclear factor kappa-B
NR – neutral red
NSRs – nutrient signaling regulators
OD – optical density
OEA – N-oleoylethanolamide
OXPHOS – oxidative phosphorylation
p. – passage of cell culture

PBS – phosphate buffer sulfate
pCBs – phytocannabinoids
PD – population doubling
PDL – population doubling level
PEA – palmitoylethanolamine
PMF – postmitotic fibroblast
Rb – retinoblastoma protein
RNA – ribonucleic acid
ROS – reactive oxygen species
RS – replicative senescence
RT-PCR – Reverse transcription polymerase chain reaction
SAHF – senescence-associated heterochromatic foci
SASP – senescence-associated secretory phenotype
SD – standard deviation
SGK – Serum and glucocorticoid-induced kinase
SIPS – stress-induced premature senescence
TEWL – trans-epidermal water loss
TGF-β – transforming growth factor β
THC – Δ-9-tetrahydrocannabinol
THC-COOH – 11-nor-9-carboxy-D9-tetrahydrocannabinol
THC-OH – 11-Hydroxy-D9-THC
THCV – Δ9-tetrahydrocannabivarin
TIMP1 – tissue inhibitor of metalloproteinases 1
TKRs – tyrosine kinases receptors
TNF-α – tumor necrosis factor alpha
TRPV1 – transient receptor potential channels of the vanilloid subtype 1
TRPV2 – transient receptor potential channels of the vanilloid subtype 2
UVB – type B ultraviolet rays
WHO – World Health Organization
YLDs – years the global population lived with a disability

CHAPTER 1: GENERAL INTRODUCTION AND LITERATURE REVIEW

1.1. General principle of aging

The worldwide population is aging. The current world population is nearing 7.93 billion and despite COVID-19, it is anticipated that world will reach 10 billion people by 2057. According to the World Health Organization's (WHO) recent report the average age span is increasing gradulally every year (WHO, 2021). Moreover, the WHO reports that about 13% of the global population is 60 years old or over (WHO, 2018) and the rate of growth is about 3% per year (Sarcar et al., 2017; Spector, 2018). By 2030, 21 countries will be "super-aged," meaning more than 20% of their population will be 65 years or older. These countries include Japan, Canada, and New Zealand (Arensberg, 2018). According to the official Canadian Statistics in 2019, 25.9% of Canadian citizens are already 65 years or older, which equates to 2.7 million people. This is not far behind Japan that currently is the oldest country in the world where 26.6% of the population is over 65 years old (Wilson et al., 2019). Furthermore, prognoses demonstrate that people who are 60 years or older (except Africa) will constitute more than 25% of the global population by 2050 (Brunetta et al., 2020; Spector, 2018). Due to this increased longevity, scientists predict that most children born after the year 2000 will celebrate their 100th birthday (Vaupel, 2010).

Increased longevity throughout the world is positive, but it is a double-edged sword. On the one hand, older people have more opportunities to have an active lifestyle, stay with their families or continue to work and at the same time contribute to multiple areas of society, albeit, this is mainly dependent on their overall health. On the other hand, increased longevity is directly associated with developing age-related diseases (ARDs).

Correspondingly, this means that long-lived people will suffer from pain and disabilities for significantly longer periods of time due to degenerative processes and ARDs (cardiovascular, diabetes, cancer, Parkinson's, Alzheimer's diseases, and others). These morbidities drastically complicate a patient's life and hasten mortality. It is worth noting that clinical manifestations of the abovementioned ARDs are preceded by long (10-20 years) asymptomatic periods of illness development (Umansky, 2018). Moreover, according to the last WHO report, due to population growth and aging, the total number of years the global population lived with a disability (YLDs) as part of the entire disability-adjusted life year increased by 10% within the last decade (WHO, 2021). The predominant causative role is directly correlated with the most significant number of deaths – including diabetes, stroke, road injuries, Alzheimer's disease, ischaemic heart disease, COPD, also known as chronic obstructive pulmonary disease, and cancers (e.g., lung, colorectal) – have all increased by as much as twice as measured by YLDs. If no changes are implemented, prognosis will worsen and aging will become a significant social and economic burden (Matjusaitis et al., 2016). Increased life spans have created a pressing need for a better understanding of the pathogenesis of various ailments of old age. For this reason, the development of anti-aging or age-delaying medication is becoming a prevalent concept in preventative medicine. It will potentially bring more dividends than the treatment of associated diseases on its own.

The process of aging is associated with various physiological and pathological molecular mechanisms, including complex patterns of changes in gene expression leading to changes in the performance of various cell types, tissues, and organs. Insulated genetic aberrations in aging-relevant pathways trigger segmental, tissue-selective aging phenotypes (Horvath & Raj, 2018). Nevertheless, for the majority of tissues, it still

remains unknown which age-related modifications play a prominent etiological role in the aging mechanism, and which ones are just epiphenomena (Tigges et al., 2014).

The most obvious and visible symptoms of aging in humans are manifested by changing of the skin apperance. Skin is the first line of defense against abiotic and biotic environmental factors (Choi & Lee, 2015; Lämmermann et al., 2018). Thus, cutaneous aging has garnered significant attention from scientists, aesthetic medicine, and the cosmetic industry. Hence, the purpose of this review is to analyze the most evident physiological and pathological mechanisms influencing skin aging.

1.2. The general concept of aging and senescence

Aging is a somatic process of progressive deterioration in the ability to endure stress and injuries due to gradual loss of maximal functional activity, metabolic efficacy, and potential to adapt (Glass et al., 2013; Yang et al., 2019; Zhavoronkov et al., 2019). As aging is under control of individual (intrinsic or internal factors) and environmental (extrinsic or external) factors (Figure 1.1), it cannot be outlined by a single pathway or a single cause (Makrantonaki & Zouboulis, 2007). Concomitantly, the term ***senescence,*** in general, represents an irreversible and quite distinct form of quiescence as a result of trophic support deprivation (Kumar et al., 1992).

To date, the need to understand the fundamental changes in aging on the organismal level pushes scientists to dig deeper into the cellular level. ***Cellular aging*** is a result of the multifaceted process of gradual accumulation of damage over time albeit with the ability to maintain normal cell functions (Burton & Stolzing, 2018). ***Cellular senescence***, however, is an irreversible arrest of cell proliferation attributable to an incremental shortening of the tandem repeats protecting chromosome ends – telomeres (Hayflick,

1965; Kato et al., 1998; Nassour et al., 2016; Waldera Lupa et al., 2015). At the same time, this further leads to abnormal functional activity and establishes the development of a multi-component senescence-associated secretory phenotype (SASP) (Wiley & Campisi, 2016). The number of senescent cells increases with age in organisms, although at different rates in various organs (Kirkland & Tchkonia, 2017; Matjusaitis et al., 2016). Importantly, in mammalian development, cellular senescence has been increasingly accepted as a physiological process involved in tumor prevention, age-associated dysfunction in various tissues, and as a regulatory switch (Cavinato et al., 2017).

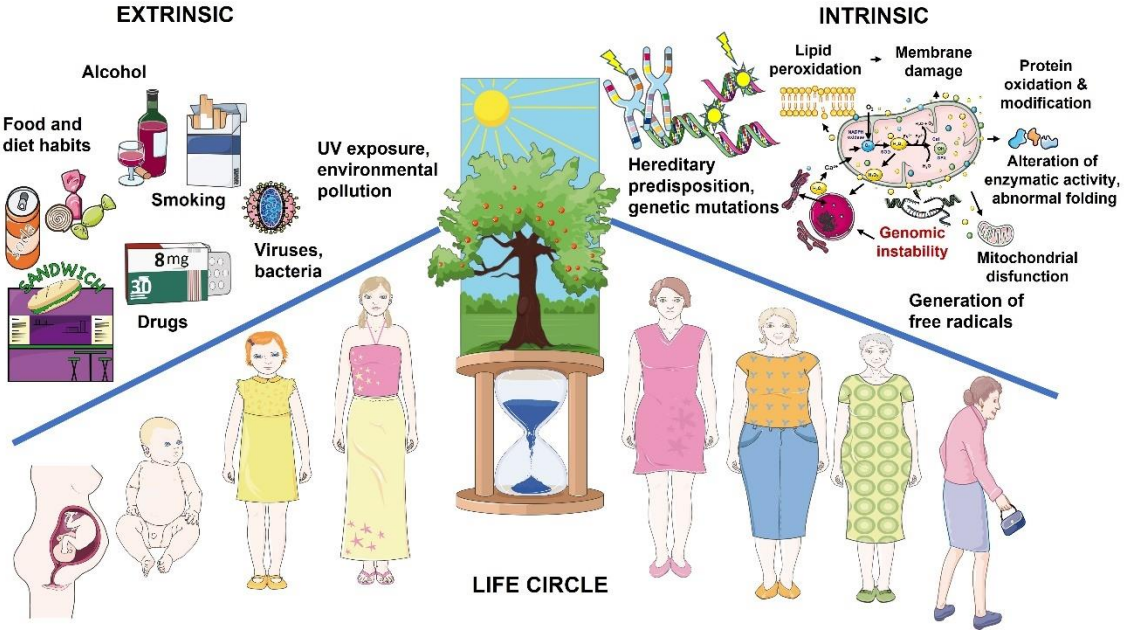

Figure 1.1. The main two groups of factors that trigger aging. This figure was created using images from Servier Medical Art Commons Attribution 3.0 Unported License (http://smart.servier.com).

Present-day studies consider that aging contains two principal determinants that occur in parallel: extrinsic and intrinsic processes. The extrinsic factors arise mostly because of environmental and socio-economic influences such as lifestyle and nutrition. These determine how the pre-set frame of opportunity is exploited during the individual

aging trajectory. Correspondingly, intrinsic factors, such as genetic background and hereditary predisposition, delineate molecular mechanisms in various aging pathways.

1.3. Theories of aging

For millennia, mankind has been looking for answers to aging and mortality. Currently, it is a fact that age is the leading risk factor for numerous degenerative diseases and many other non-degenerative illnesses. Nevertheless, the mechanisms of these processes remain a mystery (Harman, 1992). To date, different theories of aging and senescence have been proposed, but none seem to interpret it fully.

The progressive ideas of Darwin's theory of natural selection presented to society in 1859 in his book "On the Origin of Species" initiated the development of aging and senescence concepts. There are numerous theories describing the causative effects that deteriorate health, and almost all of them are based on the mechanisms that affect homeostasis at the genetic, molecular, cellular, tissue, and organismal levels (Gerasymchuk, 2021). Currently, more than 300 theories of aging have been proposed (Gkogkolou & Böhm, 2012). Most of them, in general, are possible to combine into two big groups: ***programmed-*** or ***error-based*** theories (Table 1.1) (Jin, 2010).

The group of ***programmed-based*** theories rely heavily on the development-dependent senescence of specific genes, with or without the involvement of the neuroendocrine and the immune system (Davidovic et al., 2010). Whereas ***error-based*** theories explain the aging process by the induction of cumulative damage at various levels of living organisms. It is assumed that most aging processes are related to general cellular depletion due to irreversible damage, loss of metabolic activities, accumulation of cross-linked proteins and potentiation of free radical generation that can cause mutations (Jin,

2010). This section discusses some of the significant theories which influence the process of accelerated organismal and skin aging.

Table 1.1. Theories of aging

Theory	Synopsis	Reference
	programmed-based	
August Weismann's programmed and altruistic theory (1882)	The accumulation of wearied cellular components exceeds the body's ability to self-repair and ultimately leads to cell degradation and death	Ahuja et al., 2017
Medawar's evolutionary theory (1952)	The accumulation of late-acting deleterious mutations	Kim et al., 2016; Wensink et al., 2014
Neuroendocrine-immune concept (1954)	The age-dependent rise of cortisol negatively decreases other hormone receptors' sensitivity and consequently negatively affects neuro-immune regulation and defense	Dilman et al., 1986; Fabris, 1990
Williams' antagonistic pleiotropy (1957)	The early-life mutations of specific alleles can be beneficial, albeit, in later stages of life, they can be detrimental	Gladyshev, 2016; Thoppil & Riabowol, 2020; Wensink et al., 2014; Williams, 1957
Kirkwood disposable soma theory (1977)	The energy-saving strategy of reduced error regulation in somatic cells is a trade-off between reproductive fitness and longevity that causes aging	Dilman et al., 1986; Fabris, 1990; Longo et al., 2005
	error-based	
Bjorksten's "crosslinkage theory" (1942)	The accumulation of cross-linked proteins in the cells initiates cellular damage and boosts their aging by slowing down their functions	Bjorksten, 1968
Harman's free radical theory (1956)	Excessive free radicals damage cellular membranes that subsequently render cells dysfunctional	Harman, 1956
Failla's somatic mutation theory	The increase in genetic mutation frequency inversely correlates with functionality in cellular, organ and whole organismal level and is the leading reason for aging	Failla, 1958

Replicative cellular senescence	The replicative cellular senescence or "Hayflick limit" occurs approximately after 50 subdivisions	Hayflick & Moorhead, 1961
Orgel's theory of error catastrophe	The accumulation of errors during protein translation followed by an accumulation of defective proteins	Orgel, 1963
Somatic DNA damage theory of aging	Rising and accumulation of DNA damage inhibits organismal defense and repair capabilities	Alexander, 1967; Freitas & De Magalhães, 2011
Telomere hypothesis	Each round of DNA replication is directly associated with a recurrent reduction of the DNA due to the inability of DNA polymerase to replicate telomeres, ultimately triggering cellular death.	Harley, 1991; Olovnikov, 1973
Mitochondrial DNA damage theory	Age-related phenotypes develop because of accumulation of mitochondrial oxidative damage with age	Wallace, 2001
Membrane hypothesis of aging	The combination of free radical and mitochondrial theories state that the decreased membrane permeability and subsequent deterioration of mitochondrial functions are provoked by ROS and by residual heat coming from nerve signals	Zs.-Nagy, 2014
Blagosklonny's hyperfunction theory	The over-activation of growth-promoting signaling pathways during development and hyperfunction of genes in the fertile age leads to hypertrophy resulting in aging	Blagosklonny, 2019; Gladyshev, 2016

1.3.1. Programmed-based evolutionary theories

Weismann's programmed theory of aging (also called a wear-and-tear theory) implies that the cell's structural components wear with time and lose functional activity. Damage in the cells, tissues, and organs gradually accumulate due to lack of ameliorating properties and eventually lead to cellular degradation and death (Ahuja et al., 2017). The theory discusses the role of programmed cell death and apoptosis in multicellular

organisms. It is a well-known fact that apoptosis is a fundamental process of organismal wellbeing. It is involved in ontogenesis, prevents cancerogenesis, and potentiates immune defense responses and other physiological processes (Longo et al., 2005).

The *evolutionary theory of aging* is extremely popular and has been studied from different perspectives. The most prominent key concepts were based on Haldane's (1941) perception that reduction of natural selection forces represents a function of aging. This insight was broadened considerably by Williams (1957) into the antagonistic pleiotropy idea. He emphasized that mutations in certain alleles might be beneficial or neutral early in life, accumulating in the process of active selection, but later in life such mutations may lead to pleiotropic deleterious effects on fitness (Gladyshev, 2016; Thoppil & Riabowol, 2020). It was explained by the inability of selection forces to eliminate mutations later in life. It is also worth noting the contributions made by Medawar who described the development of senescence as a result of an accumulation of late-acting deleterious mutations (Kim et al., 2016). Williams believed that two traits, beneficial and detrimental, could be under the influence of specific genes that might be evolutionarily selected. For instance, the first trait augments wellness in adolescence while the second one is harmful in later life. Hence, deleterious alleles presumably begin to act in the late stages of life and cause aging due to their accumulation throughout evolution.

Despite the perceptiveness of Williams and Medawar's evolutionary theory, it does not explain molecular mechanisms in aging. On the other hand, since aging is not an adaptive trait, there has been a good reason to doubt that the evolutionary conservation could apply to the aging process (Partridge, 2010).

Under the influence of August Weismann's ideas of repairable chemical and mechanical damage, and limitations of the effectiveness of molecular repair mechanisms

in the metabolic trade-off theories as well as Orgel's "error catastrophe" hypothesis (Orgel, 1963), T.B. Kirkwood proposed the *disposable soma theory* (Kirkwood, 1977). Kirkwood presumed that aging and subsequent mortality might be due to an energy-saving strategy of reduced error regulation in somatic cells. He emphasized limitations in the organismal maintenance of reproduction and repair processes (Longo et al., 2005). With the purpose of maintaining effectiveness and productivity, the organism tries to allocate essential resources to maintain metabolic, reproductive, and protective activities, which compete with each other for supplies (e.g., nutrients) and hence becomes less efficient, leading to damage accumulation (Gladyshev, 2016). Consistent with the abovementioned theory, it can be hypothesized that natural selection induces trade-offs between fecundity or growth and longevity (Kirkwood & Austad, 2000). It is worth noting that disposable theory before others has combined the mechanistic biology of aging and the evolutionary concept of aging. Despite that, it remains unclear why life duration of some organisms with sufficient resources is often shorter than those with limited resources (O'Brien et al., 2008). It has been observed that caloric restrictions, and not increased caloric intake, tend to prolong lifespan for a wide range of species (Mitteldorf, 2001). Taking into consideration that other processes appear to contribute to aging, further studies are necessary to determine whether the disposable soma theory might describe aging alone or in association with different concepts.

As a continuation of the "wear and tear" theory presented in the systemic *neuroendocrine-immune concept* of aging, Dr. Dilman created the "Neuroendocrine-Ontogenetic Theory," in 1954, also known as the "nervous-neuroendocrine" or "aging clock" (Diggs, 2008; Dilman et al., 1986). The central postulate of this theory is based on "The Law of the Deviation of Homeostasis." It addressed the hypothalamus and the

hypothalamic-pituitary axis (HPA), the crucial regulatory system controlling homeostasis of three main functions in humans, i.e., energy metabolism, reproduction, and adaptation (Dilman et al., 1986). It described the age-dependent gradual deterioration of the hormonal production-regulation function with simultaneous decrease in the sensitivity of receptors (Ahuja et al., 2017; Zjacic-Rotkvic et al., 2010). On the other hand, Dr. Walford developed a theory known as the "immune" hypothesis based on experimental studies by assessment of various biochemical and physiological criteria and found that the immune system loses its efficiency with age with further limited responses against pathogens. He has concluded that the pathogenesis of aging involves auto-immune reactions against self-proteins (Walford, 1964).

To date, the accumulation of scientific knowledge demonstrates a significant decline in the level of critical hormones and a reduction of their activity with age. Secretion of growth hormones, androgens and estrogens, and their precursors such as adrenal hormone dehydroepiandrosterone significantly decrease with age (Zjacic-Rotkvic et al., 2010). Consequently, this results in the reduction and further devastation of muscle mass, decreased insulin sensitivity, and diminished immune function that leads to a general decrease in the ability of organismal self-regulation and repair. The aforementioned events are directly dependent on HPA activity and cortisol as the primary stress hormone. Cortisol is one of the few hormones that increase with age and at the same time, decrease the level and efficacy of HPA resulting in enhanced catabolism. Moreover, its elevated levels lead to osteoporosis and fractures, breaking down of muscle tissue, as well as degradation of collagen, hyperglycemia, hypertension, and suppression of immune responses (Diggs, 2008; Farage, Miller, & I. Maibach, 2017). An interesting fact is that

cortisol is involved in the processes of destruction and atrophy in the hippocampus which further impairs the ability to encode and recall memories.

It is worth mentioning another vital signaling pathway involved in aging - the growth hormone (GH)/insulin-like growth factor-1 (IGF-1) axis. GH and IGF-1 regulate cellular development, proliferation, stress resistance and survival (Ashpole et al., 2015). It is known that the level of IGF-1 rises from birth to puberty, followed by a slow decline through adulthood and correlated with a reduction in the amplitude of GH secretion. Experimental studies have shown that IGF-1 expression is decreased in senescent dermal fibroblasts in vitro as well as in geriatric dermis *in vivo* (Khan et al., 2002). Furthermore, reduced IGF-1 expression in elderly skin positively correlates with inadequate protective response to type B ultraviolet (UVB) rays in exposure trials using geriatric volunteers. Diminished dermal expression of IGF-1 in the elderly might be one of the leading factors in the pathogenesis of the aging-related non-melanoma skin cancer (Lewis et al., 2010).

The endocrine component is an essential part of neuroendocrine-immune theory of aging. Albeit this concept is not unique, it can help in interpretation in combination with other concepts. The fidelity of the existing theories will be ascertained in the years ahead. Still, the role of hormones obviously will remain an essential component in the elucidation of the nature of the process of aging (Zjacic-Rotkvic et al., 2010).

1.3.2. Error or damage-based aging theories

In 1942, Dr. Johan Bjorksten proposed the *cross-linking theory* of aging (Bjorksten, 1968). He emphasized that crosslinking is based on covalent bonding that ties two or more large molecules (protein and other molecular structures) together (crosslink) by forming larger polymeric particles that have reduced elasticity and mobility (Ahuja et al., 2017;

Zs.-Nagy, 2014). For instance, in industry, this process is used commonly as natural rubber can be crosslinked or "vulcanized" using sulphur. Living biological species are exposed to various crosslinking agents such as sulphur, alkylating agents, aldehydes, quinones, antibodies, polybasic acids, lipid oxidation products, free radicals induced by ionizing radiation, and polyvalent metals (Bjorksten, 1968). However, in living organisms, the accumulation of crosslinked molecular aggregates provokes deterioration in tissue function (Jin, 2010). Thus, proteins become compromised and functionally insufficient leading to further damage to the tissues and entire organ systems.

It was presumed that cross-linkage affects the immunological function of proteins that might predispose auto-immune response. Cross-linking also destroys elasticity, thus causing microfractures in organs, including arterial endothelial lining as well as results in the transformation of proteins from hydrophilic to oleophilic, leading to the formation of atherosclerotic plaques (Bjorksten, 1968). Furthermore, cross-linking is implicated in decreased swelling capacity, increased resistance to hydrolases and other enzymes that eventually potentiate the aging process. Besides, human skin, like other organs, continuously experiences exposure to different extrinsic factors with a subsequent excessive generation of reactive oxygen species (ROS). In turn, ROS reacts with glucose, and DNA and boosts cross-linking of collagen. Therefore, skin becomes leathery, dry, and yellow, accompanied by the appearance of wrinkles and waning cutaneous elasticity (Ahuja et al., 2017). Current studies show strong, direct and indirect evidence that cross-linking reactions are involved in the age-related changes throughout life (Bjorksten & Tenhu, 1990; Gkogkolou & Böhm, 2012; Yamagishi et al., 2015).

Perhaps the largest impact on aging studies was made by Leonard Hayflick's and Paul Moorhead's (1961) breakthrough when they presented the concept of the *Hayflick*

limit and *replicative cellular senescence*. They found that cultivated human fibroblasts cell cultures had stopped dividing and were dying after about 50 sub cultivations (Hayflick, 1965; De Magalhães, 2004). As cell culture studies began in 1900 and were performed mostly on cancer cells, it was believed that cells are immortal. Also, it was a widespread consideration that aging by itself had nothing in common with intracellular events (Rattan, 2016). Hayflick opposed the dogma of those days that all cells are immortal and presented a statement that healthy human cells can only replicate and divide a limited number of times, about forty to sixty times. Apart from limited cellular division "memory" in healthy cells, it was observed that cryogenically preserved cells also could "remember" how many times they have divided when they were frozen. Such "memorization" was presented as a counting mechanism, and Hayflick proposed the term "replicometer" location of which was designated in the nucleus (Rattan, 2016). Later it was found that the replicative limit of healthy cells in a "biological clock" mechanism is independent of the passage of time but related to rounds of DNA replication and telomere shortening in particular (Rattan, 2016; Shay & E. Wright, 2000). Recent scientific trends regard cellular life as a "biological clock". Finite replicative life span of cells is accompanied by cell arrest at the G1 phase. Selective repression of growth regulatory genes might be one of the mechanisms guiding this process (Makrantonaki & Zouboulis, 2017).

The beginning of the 1970s was associated with the appearance of the *telomere hypothesis of aging* (Table 1.1). It was found that ends of linear DNA, later named telomeres, are not completely copied during the DNA replication process. DNA polymerase, which is responsible for the synthesis of the lagging-strand, is unable to completely replicate the 3′ end of linear duplex DNA, as the synthesis of Okazaki

fragments requires RNA primers attaching upstream of the synthesis point of the lagging strand. This leads to the shortening of the end of the chromosome after each duplication (Shay & Wright, 2000). In 1972, James Watson, one of the discoverers of the double helix, referred to this event as the end-replication problem (Watson, 1972).

Interconnected with Watson's idea of the end-replication problem is the *theory of marginotomy* presented by Alexandr Olovnikov (Olovnikov, 1973). Inspired by Hayflick's work, Olovnikov pondered the question of why normal cells have a limited capacity to replicate. The unexpected answer found him at the Moscow subway station (Olovnikov, 1996). He saw an analogy between the train moving along the tunnel that symbolized the DNA polymerase and the track representing the DNA. In his imagination, the inability of the polymerase to copy from the very beginning related to the presence of a dead zone between the front end of the polymerase molecule and its catalytic center (Olovnikov, 1973). This was similar to the dead zone between the front end of a train standing at the beginning of the subway platform and the next entrance door to the first car (Shay & Wright, 2000). Thus, if the train copied the DNA track beneath the car, the first DNA section would not be replicated due to the fact that it was beneath the engine at the start (Olovnikov, 1996). Olovnikov realized the fact that each round of DNA replication is directly associated with a recurrent reduction of the DNA molecule due to the inability of DNA polymerase to fully replicate chromosome ends (telomeres) ultimately triggering cellular death. Numerous studies discovered a robust connection between cutaneous aging and telomere attrition (Harley, 1991). Analysis of DNA samples from the sun-protected epidermis showed telomere lengths varies by age. It was found that at birth, the telomeric length is around 13.3 kb, with a subsequent rate of 36 bp reduction of TTAGGG repeats sequences per year (Nakamura et al., 2002). The data collected from

73–95-year-old patients showed a lowered length of epidermal telomeres, up to 7.8 kb (Jia & Nash, 2017; Lindsey et al., 1991; Sugimoto et al., 2006).

A couple of interesting concepts based on the evidence of accumulation of age-related DNA damage have found support and popularity as well. The *somatic mutation theory*, proposed by Failla (1958), claimed that the increase in genetic mutation frequency inversely correlates with functionality at the cellular, organ and whole organismal level. In 1963, Orgel presented a *theory of error catastrophe*. The aging process was explained as accumulation of errors during protein translation that was followed by a consequent accumulation of defective proteins (Brunk & Terman, 2002; Orgel, 1963). About a decade later, Alexander gave precedence to *DNA damage* rather than mutations as the leading reason for aging (Alexander, 1967) (Figure 1.2). This hypothesis was subsequently supported and proved by many scientists (Gensler & Bernstein, 1981; Holmes et al., 1992) and is currently known as the "*somatic DNA damage theory of aging*" (Freitas & De Magalhães, 2011).

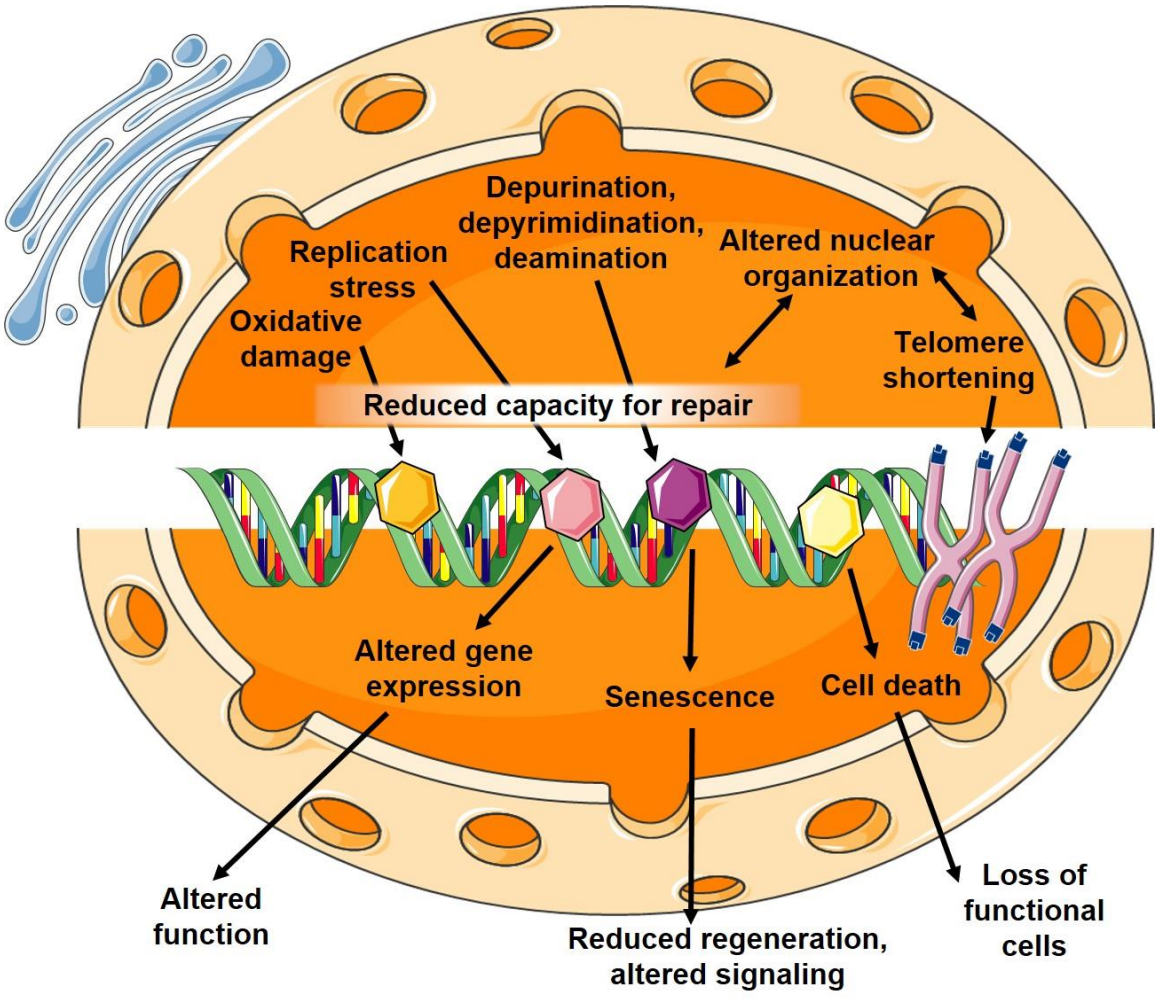

Figure 1.2. Mechanisms contributing to genomic instability and their role during aging. *Colored hexagons* represent DNA lesions, *arrows* indicate contributions of processes to the given outcomes, *two-directional* arrows indicate interplay between two processes. Retrieved and modified from C. Sidler, Genomic instability and aging – causes and consequences, Chapter 29, Figure 29.2; O. Kovalchuk and I. Kovalchuk, Genome stability: From virus to human application., 1st ed. Amsterdam: Elsevier Inc./Academic Press, 2016. This figure was created using images from Servier Medical Art Commons Attribution 3.0 Unported License (http://smart.servier.com).

Another significant aging concept that has branched into numerous studies is *the free radical theory*, proposed by Harman (1956). In this theory aging is considered as having a mechanistic cause whereby ROS that are produced as part of normal metabolism randomly damage cellular components (Khrapko & Turnbull, 2014; Rattan, 2006).

Consequently, the gradual accumulation of damaged cellular macromolecules and organelles are reflected as senescence (Gladyshev, 2016). As a result of multiple studies (Khrapko & Turnbull, 2014; Rattan, 2006), it was generally confirmed that ROS levels rise, and antioxidant activity reduces with advancing age. Skin by itself can regulate the production and degradation of ROS. This regulation is maintained in equilibrium by radical scavenging systems such as antioxidant enzymes and enzyme-like small molecules. Among them are peroxidases (heme-containing and selenium-containing glutathione peroxidase), superoxide dismutases, catalases, and low-molecular-weight antioxidants such as tocopherols, carnosine, ascorbic acid, and reduced nicotinamide adenine dinucleotide (NADH) which can donate an electron and then scavenge free radicals (Harman, 1992). Therefore, it is essential to focus on the association of free radicals with skin degeneration.

Skin is attacked daily by various external and internal factors such as radiation, pollution, temperature deviations, chemical (cosmetics, smoking, alcohol) and infection agents (bacteria, viruses, fungi) that triggers the activation of chain of internal defense mechanisms of immune responses. One of these mechanisms is *phagocytosis*, which is associated with an excess amount of ROS production. Immune defense is highly energy-dependent and leads to the intensification of oxidative phosphorylation that is related to mitochondrial ROS generation as it mainly takes place at the electron transport chain (ETC) located on the inner mitochondrial membrane. Thus, an increased ROS potentiates cellular damage, which encompasses oxidation of deoxyribonucleic acid (DNA), leading to mutations (Makrantonaki & Zouboulis, 2017). Furthermore, oxidation of membrane lipids results in reduced transport efficiency and altered transmembrane signaling, aggregation of waste products, and inter alia pigments such as lipofuscins which

accumulate to give an appearance of “age spots” (Ahuja et al., 2017; Zs.-Nagy, 2014). Lipofuscins is comprised of lipid-containing residues of lysosomal digestion and considered to be one of the aging or “wear-and-tear” pigments (Gray & Woulfe, 2005; Szweda et al., 2003). Thereby, they deteriorate cellular ability to repair and reproduce, violate DNA and RNA synthesis, inhibit protein synthesis, and additionally break down primary dermal fibers such as elastin and collagen and degrade cellular enzymes (Makrantonaki & Zouboulis, 2017).

By now it has been widely established that the corrupted stress response in somatic cells is linked with a defect in proteolytic systems such as ubiquitin-proteasome pathway, calpains, and lysosomal activity (Cuervo & Dice, 1998; Szweda et al., 2003). Hence, this leads to the cellular accumulation of misfolded and altered proteins, as they cannot be eliminated by the processes of macroautophagy and/or microautophagy (Cuervo & Dice, 1998; Leidal et al., 2018). Besides, there is ample evidence indicating that ROS accumulation plays a pivotal role by participating in diverse mitogen-activated protein kinase (MAPK) pathways (e.g., c-Jun terminal kinase, p38 kinases); activation of these pathways induces activator protein – 1 (AP-1) complex and inhibits transforming growth factor β (TGF-β) function. In turn, the signal cascade leads to deterioration of collagen metabolism and its further excessive degradation by increased activity of matrix metalloproteinase (MMP) (e.g., MMP-1, MMP-3 and MMP-9) (Makrantonaki & Zouboulis, 2017).

The process of continuous damage begins at birth, but it is not harmful in the juvenile years due to the body’s natural repair mechanisms. With time, cell functions are compromised and slowed down by the influence of cumulative effect of free radicals. Consequently, reduction of the body’s self-repair capabilities eventually leads to the

formation of the aging phenotype (coarse wrinkling, skin sagging and atrophy, irregularities in pigmentation, elastosis, telangiectasias).

On the other hand, it remains unclear why cells cannot handle oxidative stress as it is a part of the normal metabolic process as well as part of an immune response in phagocytosis. Therefore, an essential question to be addressed is whether free radicals and other detrimental factors are the primary cause of aging. Besides, another question is whether or not aging and death happen as a result of a hypothetical weakening of regulatory program of repair and replacement (Longo et al., 2005). Molecular aspects of these questions will be discussed in later sections.

Numerous publications demonstrate that with age, nuclear DNA is damaged less frequently than mitochondrial DNA (Ames, 1989; Khrapko & Turnbull, 2014). Indeed, throughout the last few decades a significant portion of studies examining aging have concentrated on genetic damage and instability of organellar genomes (Wallace, 2001). In particular, the *mitochondrial theory of aging* increased in popularity, which is mostly regarded as a refinement of Harman's *free radical hypothesis* (Jacobs, 2003; Tan, 2019). The basis for the oxyradical hypothesis is that aging and age-related phenotypes develop as a result of accumulation of mitochondrial oxidative damage with age (Harman, 1956; Ziegler et al., 2015). At the same time, some studies demonstrate that increased production of ROS does not obligatorily result in lifespan reduction, and actually can even increase lifespan (Yee et al., 2014) due to the activation of adaptive mechanisms (Scialo et al., 2020) and the necessity for maintaining physiological mechanisms (Figure 1.3). Experimental data demonstrate that in worms with impaired insulin/IGF-1 signaling the increase in lifespan could be mediated by retrograde ROS signaling, albeit inhibition of ROS activity using antioxidants can diminish such longevity by up to 60% (Zarse et al.,

2012). Also, increased longevity in *Caenorhabditis elegans* might be reached by diminishing respiration accompanied by a mild elevation in ROS levels and resulting in further activation of hypoxia-inducible factor 1 (HIF-1) transcription factor and following changes in the expression of nuclear genes (Lee et al., 2010; Son & Lee, 2019). These data demonstrate that apart from ROS elevation, additional factors might be involved in mechanisms of aging.

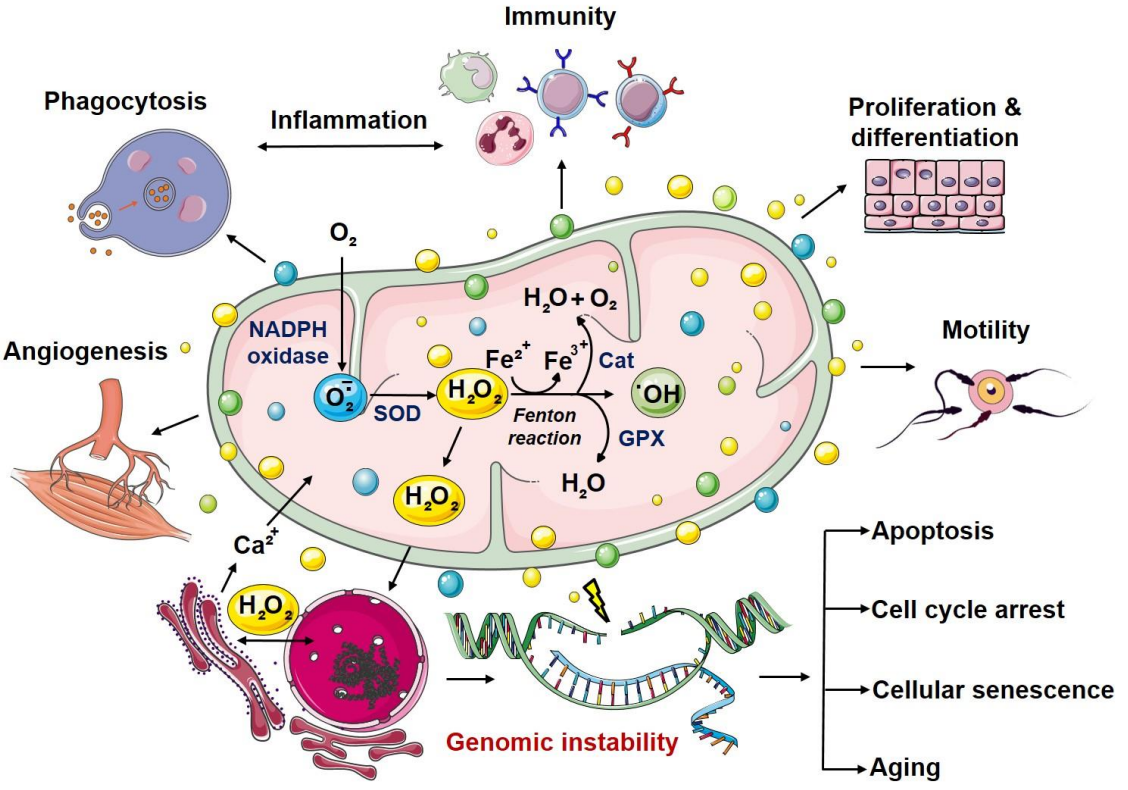

Figure 1.3. Generation of reactive oxygen species. Role of ROS in maintaining physiological processes. Cat, catalase; Fe^{3+} ferric ion; Fe^{2+}, ferrous ion; GPX, glutathione peroxidase; H_2O_2, hydrogen peroxide; OH•, hydroxyl; NADPH oxidase, nicotinamide adenine dinucleotide phosphate oxidase; ROS, reactive oxygen species, $O_2^{\bullet-}$, superoxide; SOD, superoxide dismutase. Retrieved from Gerasymchuk, M. (2021). Genomic instability and aging: Causes and consequences. *Genome Stability*, 533–553. https://doi.org/10.1016/B978-0-323-85679-9.00028-3. This figure was created using images from Servier Medical Art Commons Attribution 3.0 Unported License (http://smart.servier.com).

The *mitochondrial* theory of aging acknowledged that the deterioration of mitochondrial activity is one of the cornerstones of cellular dysfunction in the aging process (Lefkimmiatis et al., 2020; Nacarelli et al., 2016; Ziegler et al., 2015). Mitochondrial functions have traditionally been viewed as adenosine triphosphate (ATP) production by oxidative phosphorylation (OXPHOS) as well as transmission of adaptive regulatory signals to control immunity, apoptosis or survival, and homeostasis with strong effects in aging. Moreover, studies show that mitochondria are considered as one of the main hubs in the regulation of many age-related pathways such as senescence, unfolded protein response, autophagy, and inflammation (Son & Lee, 2019).

A lot of attention has been given to mitochondria for the purpose of aging research. Mitochondrial DNA (mtDNA) is a double-stranded, circular molecule that is 16,569 bp long in human (Druzhyna et al., 2008). Human mtDNAs are formed as protein-DNA complexes inside the mitochondrial matrix and known as mitochondrial nucleoids (Yasukawa & Kang, 2018). The mtDNA synthesis is in proximity to the ROS formation by the protein complexes I, II, and III of ETC at the inner mitochondrial membrane. In comparison to nuclear DNA (nDNA) mtDNA is not protected by histones and for this reason is more exposed to ROS attack (Tan, 2019). Moreover, since excision and recombination repair are less efficient in mitochondria as compared to the nucleus (Gebhard et al., 2014; Makrantonaki & Zouboulis, 2017), mutations accumulate progressively during life (Nacarelli et al., 2016). A vicious cycle develops with age (Druzhyna et al., 2008) in which mutations in mtDNA lead to disfunction of the respiratory chain, further reinforcing the production of DNA-damaging oxygen radicals (Jacobs, 2003). Thus, increased ROS production causes catastrophic and irreversible

gradual mtDNA injury and mutagenesis in mitochondria, substantially increasing oxidative damage and cellular dysfunction (Brunetta et al., 2020; Wisnovsky et al., 2016).

Nevertheless, the mitochondrial theory of aging cannot encompass all mechanisms of cellular and organismal deterioration changes with age. Additionally, it does not provide a reasonable explanation of some contradictory phenomena of aging. For instance, why prolonged antioxidant therapy did not attenuate age-related oxidative damage (Barja, 2019). Besides, a substantial body of circumstantial evidence indicates sufficient protection of mtDNA by a sturdy protein coating with mitochondrial transcription factor A and proteins, including antioxidant enzymes (Tan, 2019). An alternative concept proposed nearly a decade ago by M. Blagosklonny, was described as the hyperfunction theory of aging which represents a conjunction of ideas of mechanistic and evolutionary biology with amplified functions of genetics (Blagosklonny, 2008). The author suggested that aging is a consequence of over-activation of growth-promoting signalling pathways such as the TOR (well-known in mammals as mTOR and famous target of rapamycin) pathway. He proposed that sustained development and hyperfunction of genes in the fertile age leads to hypertrophy resulting in aging. At the same time, accumulation of molecular damage is considered a secondary factor (i.e., hyperfunction and hypertrophy cause damage, not the other way around) and has a limited influence on the aging process (Gladyshev, 2016). It is known that reactive oxygen species (ROS) induce molecular damage, but Blagosklonny gave the ROS theory of aging an alternative explanation: He has hypothesised that ROS-induced molecular damage is not life-limiting, simply because the effect of TOR on aging is much more profound.

Consequently, ROS plays a signalling role in the mTOR pathway, but not vice versa (Blagosklonny, 2008). Results of excessive mTOR and INS/IGF1 signalling activity could

be interpreted from the point of view of hyperfunction theory. Multiple studies showed that inhibition of these pathways is predicted to increase lifespan. Meanwhile, hypertrophy is usually associated with hyperfunction based on excessive activities that later lead to functional insufficiency and exhaustion. It could also be the secondary (i.e., following damage) evidence of aging or may demonstrate other potentially related deleterious processes as a result of insufficient protection or regulation (Gladyshev, 2016).

In 2014 Zs.-Nagy "upgraded" free radical and mitochondrial theories with a concept called the membrane hypothesis of aging. The central idea of this theory is the decreased membrane permeability and subsequent deterioration of mitochondrial functions provoked by ROS and by residual heat coming from nerve signals (Zs.-Nagy, 2014).

While supportive evidence exists for each of these theories, there appears to be extensive areas of overlap of concepts and processes between theories. For instance, the "mitochondrial theory of aging" is interrelated with the "free radical theory of aging." Mitochondrial dysfunction is characterized by reduced mitochondrial biogenesis, increased respiratory rates, or malfunction of the electron transport chain (Forrester et al., 2018), resulting in increased generation of free radicals such as reactive oxygen species (ROS) with age (Lee & Wei, 2012). At the same time, mitochondrial ROS production drives the range of physiological processes: cellular differentiation and proliferation, motility, angiogenesis, immune response, as well as an integral part of phagocytosis and apoptosis (Figure 1.3). Furthermore, the physiological aspects of mitochondrial activity deteriorate with age, whereas pathological progressively grows (Figure 1.4).

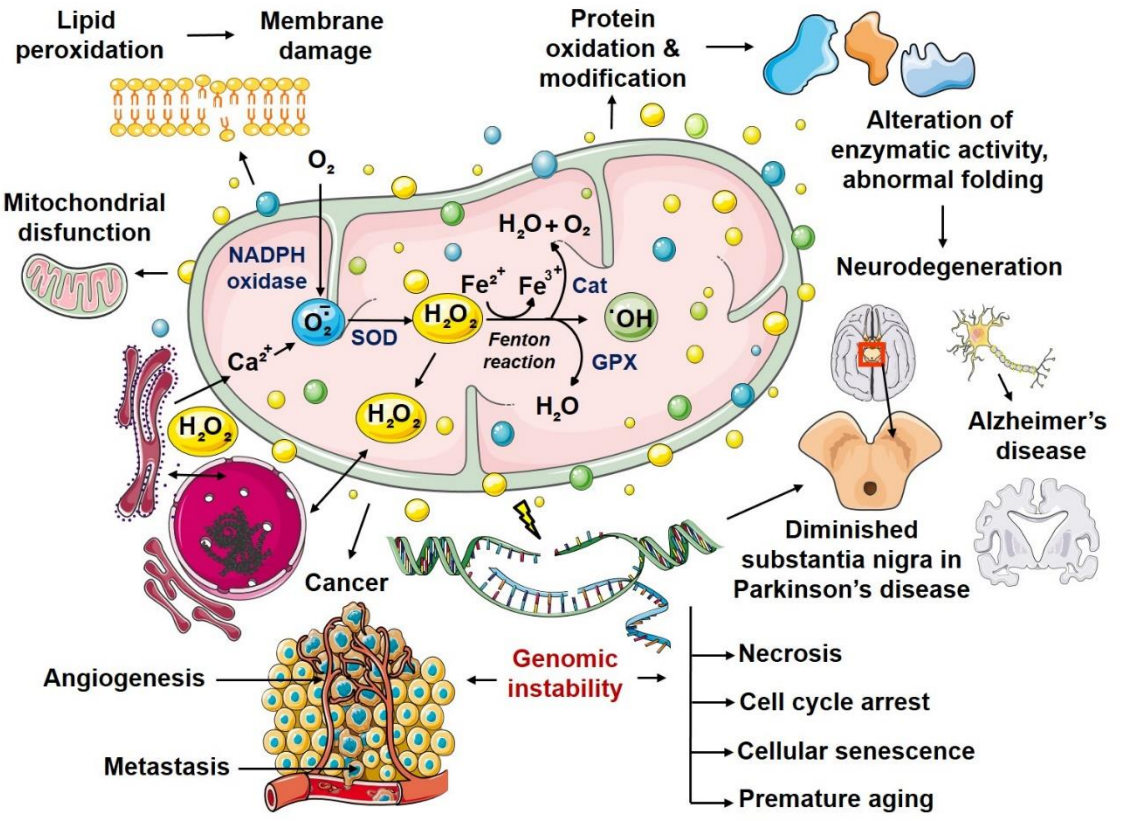

Figure 1.4. Generation of reactive oxygen species. Involvement of increased production of ROS on the pathological processes. Cat, catalase; Fe^{3+} ferric ion; Fe^{2+}, ferrous ion; GPX, glutathione peroxidase; H_2O_2, hydrogen peroxide; OH•, hydroxyl; NADPH oxidase, nicotinamide adenine dinucleotide phosphate oxidase; ROS, reactive oxygen species, $O_2^{\bullet-}$, superoxide; SOD, superoxide dismutase. Retrieved from Gerasymchuk, M. (2021). Genomic instability and aging: Causes and consequences. *Genome Stability*, 533–553. https://doi.org/10.1016/B978-0-323-85679-9.00028-3. This figure was created using images from Servier Medical Art Commons Attribution 3.0 Unported License (http://smart.servier.com).

The somatic mutation accumulation theory of aging postulates that accumulation of mutations with age results in functional decline and ultimately leads to an increasing chance of death at any given time (Failla, 1958; Szilard, 1959), and was later modified into the DNA damage accumulation theory of aging. As mentioned previously, organismal aging is caused by a complex interplay of different molecular changes affecting the

various tissues within the organism and resulting in their functional deterioration. While keeping this in mind, there is extensive evidence that indicates a central role of DNA damage accumulation and resulting genomic instability in aging.

It is evident that each presented theory has merit and discloses specific mechanisms of aging. All aforementioned theories and concepts have a place in the bigger picture of the aging pathogenesis; however, additional research is needed to understand the entire picture. Understanding the fundamental physiology of changes in the aging process as well as studying and testing its theories may disclose secrets of longevity, help in the treatment of age-associated diseases, and hence decrease general morbidity and mortality.

1.4. Skin as the aging-representative organ

The most evident and visible symptoms of aging in humans are manifested by changing skin appearance due to continuous exposure to exogenous irritants. Skin is the first line of defense against abiotic and biotic environmental factors (Choi & Lee, 2015; Lämmermann et al., 2018). Despite an ongoing renewal process, the cutaneous regenerative capacity reduces with age. A decrease in regenerative potential is often linked to a decline in the elimination of senescent cells, and their gradual accumulation results in the physiological aging of the tissue itself (Mancini et al., 2014). Many questions remain as to how to achieve longevity and healthy aging (Elsharawy et al., 2012). Skin seems to be an ideal health indicator because an alteration in its appearance directly signals the ongoing pathological changes in the organism. Thus, research on dermal health and aging is essential for an overall understanding of the processes of aging.

1.4.1. Skin structure and functions

Skin is the outermost organ and the largest one in the human body. It occupies about 8% of the total body mass of an adult human covering 1.8 m^2 of surface area (Krishnan et al., 2012). Apart from being a protective barrier, the skin is also responsible for maintaining homeostasis, including the prevention of percutaneous loss of electrolytes, fluid, and proteins; it also mediates immune activity and sensory perception as well as temperature regulation (Figure 1.5) (Cavinato et al., 2017; Farageet al., 2017; Horsburgh et al., 2017). The skin consists of three separate, but functionally interdependent, layers: the epidermis, dermis, and hypodermis (Figure 1.6). Their cellular components maintain the mechanical defense, photoprotection, immunosurveillance, nutrient metabolism, repair, and rejuvenation (Bíró et al., 2009; Elder et al., 2015).

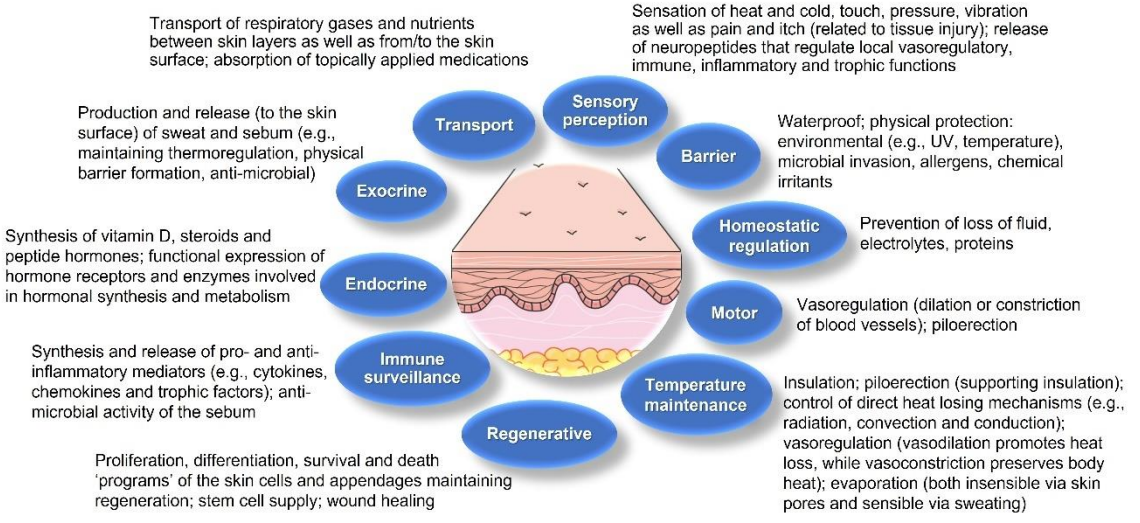

Figure 1.5. Skin functions. Schematic diagram showing the functions of the normal human skin. This figure was created using images from Servier Medical Art Commons Attribution 3.0 Unported License (http://smart.servier.com).

1.4.1.1. Epidermis

The epidermis is the outermost layer of the skin derived from the ectoderm and is tightly interlocked with dermal ridges. It mainly serves as a protective bulwark between the outside world and the internal environment of the body (Figure 1.5). Other epidermal functions are related to immunoprotection, thermoregulation, and the maintenance of energy metabolism, ultraviolet protection, and resistance to trauma. The epidermis consists of keratinocytes, Langerhans cells, melanocytes, neuroendocrine (Merkel) cells, and inflammatory cells (Figure 1.6) (Sewon Kang, 2019). Keratinocytes comprise over 90% of the cellular population of the epidermis and are connected by desmosomes and tight junctions. They produce and store an intracellular fibrous protein (keratin) that provides hardness and water-resistant properties to the skin and its appendages (hair and nails) (Kierszenbaum & Tres, 2019). Langerhans cells resemble macrophages by their functions and perform a phagocytic activity. Melanocytes produce the pigment melanin that gives hair and skin its color and are also involved in UVR damage protection. Merkel cells function as a touch-perception receptor (Kang, 2019).

Depending on the location in the body, the skin is classified into two types: thin skin and thick skin, respectively, made of four or five layers of epithelial cells in the epidermis. Thin skin consists of the following layers or strata (from the innermost layer to the outermost one): the *stratum basale* (the basal layer or stratum germinativum) which contains stem cells that attach the epidermis to the basal lamina; *stratum spinosum* (the spinous or prickle cell layer); *stratum granulosum* (the granular cell layer); *stratum corneum* (the cornified cell layer). The fifth layer, located between the stratum corneum and the stratum granulosum, is known as *stratum lucidum* (the clear cell layer) and is

found predominantly in thick skin which covers the palms of the hands and the soles of the feet (Elder et al., 2015; Kierszenbaum & Tres, 2019).

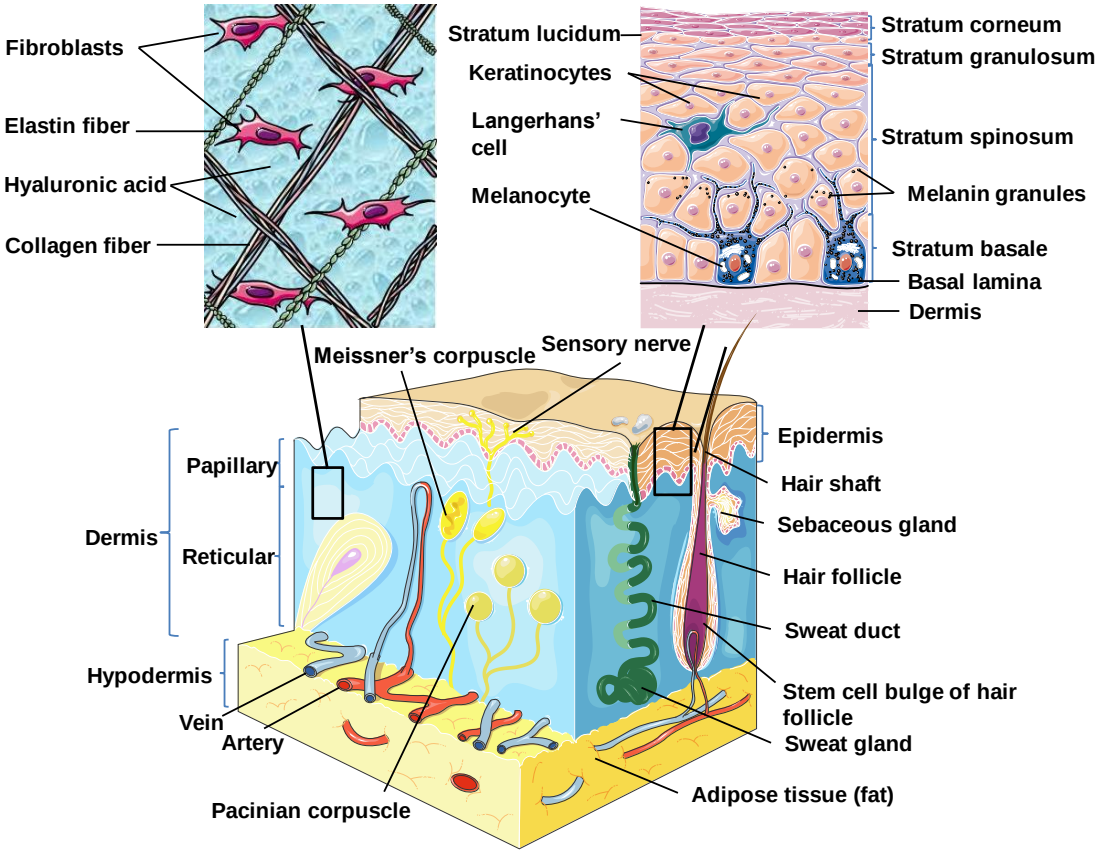

Figure 1.6. Skin structure. Schematic diagram showing the structural components of the normal human skin. Retrieved from M. Gerasymchuk, V. Cherkasova, O. Kovalchuk, and I. Kovalchuk, "The Role of microRNAs in organismal and skin aging," *Int. J. Mol. Sci.*, vol. 21, no. 15, p. 5281, 2020, doi: 10.3390/ijms21155281. This figure was created using images from Servier Medical Art Commons Attribution 3.0 Unported License (http://smart.servier.com).

1.4.1.2. Dermis

The dermal layer delivers nutrients and supports circulation (Singhvi et al., 2018). It is separated from the epidermis by a structurally and chemically complex basement membrane zone presented by intertwining collagen fibers. The dermal-epidermal interface is tightly interlocked and stabilized by hemidesmosomes (Kierszenbaum & Tres, 2019).

Structurally, the dermis is a connective tissue layer composed of an interconnected net of collagenous and elastin fibers embedded within the ground substance produced by fibroblasts (Figure 1.6); it is abundant with lymph and haemocirculation, nerves and additional structural components (hair follicles and sweat glands). The majority of dermis cells are presented by fibroblasts that possess a multifunctional capacity but are predominantly involved in the production of extracellular matrix (ECM) components (Elder et al., 2015). Apart from fibroblasts, the dermal layer is composed of a broad number of endothelial and neural cells, supporting elements as well as mast cells embedded within a matrix of collagen and glycosaminoglycans. In the dermis, there are also dendritic and nondendritic monocyte/macrophages, myofibroblasts along with dermal dendrocytes expressing factor XIIIa that are implicated in the hemostatic and inflammatory processes (Pagliari & Sotto, 2002; Włodarczyk et al., 2014).

The dermis consists of the papillary (upper) and reticular (lower) layers (Figure 5). The papillary layer starts at the epidermal basement membrane and is composed of loose areolar connective tissue with fibroblasts, collagen bundles, and thin elastic fibers that form a loose mesh and provide a mechanical anchor as well as nutrients to the overlying epidermis. Additionally, it contains phagocytes, lymphatic capillaries, nerve fibers, and touch receptors known as Meissner corpuscles (Kierszenbaum & Tres, 2019). The second layer is a reticular layer which is a thicker layer located between the papillary dermis and the subcutaneous adipose tissue. It is made up of irregular dense connective tissue with thick collagen bundles and coarse elastic fibers and is supported by wide vascularization and the sensory and sympathetic nerve supply. Elastin fibers in this layer render dermal elasticity and movement. While collagen fibers maintain the structural and tensile robustness, they are also responsible for the support of skin hydration by binding water.

They are widespread in the papillary compartment and hypodermal layer (Elder et al., 2015).

1.4.1.3. Hypodermis

The hypodermis (also called the subcutaneous layer of the skin or superficial fascia) is a layer directly below the dermis which transitions to the fascial layers (Figure 1.6). It consists of well-vascularized, loose, areolar connective tissue with a lesser collagen content and abundant adipose tissue that form a layer of variable thickness depending on its location in the body. The hypodermis facilitates cutaneous mobility. The adipose tissue serves as a storage of metabolic energy and provides thermal insulation, cushioning properties, and shock absorption for the integumentary system (Elder et al., 2015; Kierszenbaum & Tres, 2019).

About 30,000 of dermal cells die every minute in human body. At the same time, cutaneous development and normal physiology is a highly adapted process that depends on the cooperation between genetic networks and various regulatory factors (Fore, 2006). Despite daily exposure to environmental damage, the skin sustains continuous self-renewal to replace old or injured cells and repair damaged tissue (Pal & Sen, 2019). However, when pathogenic effects exceed the protective cutaneous capabilities or regenerative properties depleted with age, cellular senescence and different dermatological diseases results (Huang et al., 2013).

1.4.2. Molecular aspects of skin development

Cutaneous formation begins within the first two weeks of development. The ectoderm eventually forms the epidermis and melanocytes as well as the nervous system. The latter starts developing during the third week of fetal life when the ectoderm creates

the neural plate within it and initiates neural crest development. The mesoderm gives rise to blood vessels, muscles, bones, and fibroblasts, except for some subpopulations that are derived from the neural crest of ectoderm. The endoderm is not involved in cutaneous formation (Kang, 2019). It is believed that neural crest cells secrete the Wnt1 ligand, a signaling molecule that activates the transcription factor and cytoskeletal protein, β-catenin. The latter controls epithelial differentiation and the functioning of stem cells and appendages. Fibroblast growth factors induce the neural fate, while bone morphogenetic proteins (BMPs) and WNT signaling regulate the epidermal fate (Pal & Sen, 2019; Thulabandu et al., 2018).

1.4.2.1. The development of epidermis

The surface ectoderm stimulates the generation of a single layer of basal keratinocytes from germinativum – a layer of cuboidal undifferentiated and mitotically active cells. Keratinocytes are known for an abundant synthesis of intermediate filaments keratins. Germinativum expresses the gene p63 which is essential for the epidermal differentiation. Experiments demonstrate lethality in mice immediately following birth due to p63-deficiency (Mills et al., 1999). In humans, the TP63 mutation causes several autosomal dominant ectodermal dysplasias which are characterized by different combinations of limb, ectodermal, and orofacial abnormalities as well as alopecia, suggesting the role of p63 in maintaining stem cell proliferation (Duchatelet et al., 2020; Senoo et al., 2007).

Numerous signaling pathways control epidermis formation and stratification. For instance, the ligand Delta, or Jagged, binds the receptor Notch which initiates transcription and epidermal differentiation. The inhibition of the Notch pathway results in the deficiency of the development of the cutaneous barrier (Pan et al., 2004). The epidermis

fails to stratify in case of a low level of expression of the p63 transcription factor that consequently deteriorates appendage formation (Blanpain & Fuchs, 2009). The development of hair follicles and epidermal interfollicular lineages is regulated by the Notch 1 and 2 signaling pathways (Yamamoto et al., 2003). The MAPK signal transduction pathway (also known as the Ras-Raf-MEK-ERK pathway) likewise regulates epidermal proliferation and differentiation. The deletion of its key enzyme Mek1/2 (mitogen-activated protein dual kinases 1/2) results in cutaneous underdevelopment (Scholl et al., 2007). Conversely, the augmented activity of the epidermal growth factor (EGF) involved in the MAPK pathway potentiates proliferation and epidermal tumor growth (Janes & Watt, 2006).

Three distinct pools of stem cells are located in the interfollicular epidermis, the bulge, and the sebaceous gland supporting epidermal homeostasis. Skin stem cells undergo continuous self-renewal and differentiation into the required cell lineages to replenish cells such as keratinocytes which die due to programmed termination or injury (Horsburgh et al., 2017). The renewal of the cutaneous barrier occurs via the spinous transition of basal cells in mature skin in parallel with changes to gene expression (e.g., down-regulation of Keratin5/14 and up-regulation of Keratin1/10) controlled by p63 and the canonical Notch pathway (Blanpain & Fuchs, 2009).

1.4.2.2. The development of dermis

The dermis is formed from the mesodermal layer. The distinct boundary between the epidermis and the dermis appears at the eighth week of gestation. Fibroblasts represent the primary cell type that supports the dermis and demonstrate the ability to regulate epithelial cell function. They also abundantly secrete collagens and other extracellular matrix molecules. Fibroblasts also show a high level of heterogeneity depending on skin

location. Thus, early embryonic dermal fibroblast progenitors can potentially differentiate into several cell types. For instance, the upper dermal fibroblast progenitor cells (PDGFRa, Blimp1, Dlk−, Irig1 markers) become the dermal papillae (a ball of fibroblasts that control hair keratinocytes) and the arrector pili muscle (muscle attached to hair that causes goosebumps) (Driskell et al., 2013; Fujiwara et al., 2011). In the upper dermis there are papillary fibroblasts. The lower dermal fibroblast progenitor (PDGFRa, Blimp1−, Dlk1) generates the lower reticular fibroblasts and intradermal adipocytes/dermal white adipose tissues (Driskell et al., 2013; Thulabandu et al., 2018). Reticular fibroblasts have the lower density and are biased for collagen I over collagen III production. Moreover, during wounding, they differentiate to myofibroblasts, which promotes wound closure and presumably scarring (Driskell et al., 2013). The formation of the appendages is directly interrelated with the papillary dermis (Thulabandu et al., 2018). Skin development is not complete at birth because the final full barrier formation occurs afterwards.

1.5. Processes involved in skin aging

Biological aging is an integral process. It consists of multiple interrelated processes based on internal biochemical reactions, genetic programs, and the ongoing external influences. Aging affects all organs and systems, albeit at a different rate (Berman et al., 2012). The skin, like all other organs, undergoes distinguishable changes due to the progressive deterioration of morphological and physiological functions with increasing age. Thus, the barrier function and mechanical protection are compromised as a result of a gradual diminishing in the replacement of cellular components. Therefore, wound healing and immune responses are delayed, which is also accompanied by the disrupted thermoregulation along with the depleted sebum and sweat production. Furthermore, the

skin provides the first visible evidence of the aging process (Makrantonaki & Zouboulis, 2007).

Cutaneous aging is a complex phenomenon involving the two simultaneously occurring processes: an intrinsic aging known as chronological or natural aging which is genetically determined. Extrinsic aging, on the other hand, is caused by environmental factors such as chronic sun exposure (the total sunlight spectrum contains 45% of ultraviolet light) known as photoaging (Dudonné et al., 2011). The main symptoms of dermal aging are represented by the gradual process of wrinkle development combined with skin sagging and drooping. Naturally aged skin looks dry and has fine wrinkles, but is still smooth and light (Sunderland et al., 2017; Yi et al., 2006). In contrast, extrinsically photo-aged skin has thick layers (a leathery aspect) and coarse wrinkles, irregular pigmentation ("age-spots" which are actinic lentigines), capillary telangiectasia, elastosis, and precancerous lesions such as actinic keratosis and malignant tumors (Berneburg et al., 2004; Gkogkolou & Böhm, 2012; Kang et al., 2017; Toutfaire et al., 2017).

Both types of cutaneous aging reduce the proliferative capacity of fibroblasts, keratinocytes, and melanocytes (Dudonné et al., 2011). The morphological manifestations are the result of a decreased extracellular matrix (ECM) synthesis in the dermis due to the increased expression of matrix-degrading enzymes, and matrix metalloproteinases (MMPs) which are mainly secreted by epidermal keratinocytes and dermal fibroblasts (Kang et al., 2017). MMPs lead to the degradation and accumulation of a non-functional matrix due to cross-links in collagen fibers (intrinsic aging) or partially degraded elastin fibers (extrinsic aging) in combination with an increased oxidative stress and inflammatory process (Toutfaire et al., 2017).

Extrinsic and intrinsic types of dermal aging are based on the common pathogenic molecular pathways (Wlaschek et al., 2001). The interactive features of both types of cutaneous aging are the generation of reactive oxygen species (ROS), resulting in the degradation of the ECM by the overexpressed MMPs (Rittié & Fisher, 2015). The accumulation of ROS predominantly leads to the activation of tyrosine kinases receptors (TKRs) via the inactivation of protein tyrosine phosphatases. Then TKRs are phosphorylated and their subsequent signaling pathways are activated. These include the three families of mitogen-activated protein kinases (MAPKs): p38MAPK, c-Jun N-terminal kinase (JNK), and ERK (extracellular signal-regulated kinases). The activation of these MAPKs is followed by the increased expression of transcription factor activator protein-1 (AP-1). This stimulates the expression of different metalloproteinases (MMP-1, MMP-3, and MMP-9) and prevents the appearance of procollagen-1 (Batista et al., 2009; Rittié & Fisher, 2015; Toutfaire et al., 2017). The enhanced activities of MMPs eventually lead to ECM degradation that deteriorates the cutaneous structure and manifests as aged skin.

Although the fundamental mechanisms are still poorly understood, a growing body of evidence is in favor of multiple pathogenic pathways of skin aging. Chronological- and photo-aging skin types may occur in parallel or overlap, and their leading mechanism is intensified oxidative stress which presumably has one of the most detrimental effects on cutaneous aging.

1.6. Endocannabinoid system throughout the body

The endocannabinoid system (ECS) is an evolutionary conserved homeostatic network encompassing a group of cannabinoid receptors that endogenously synthesize

cannabinoids (endocannabinoids, eCBs) such as the anandamide (N-arachidonoylethanolamine; AEA) and 2-arachidonoylglycerol (2-AG), and wide-range of enzymes involved in their synthesis, transport, and degradation. The central ECS receptors are cannabinoid type 1 receptor (CB1) and cannabinoid type 2 receptor (CB2). These receptors are found on the cell surface and mitochondria and can be located on the same cell in relative proximity (Maroon & Bost, 2018). Structurally, they are a group of G-protein coupled receptors (GPCRs), known also as metabotropic, being predominantly coupled to the $G_{i/o}$ α proteins that inhibit adenylyl cyclase (AC) thereby reducing cellular cAMP levels (Río et al., 2018). However, coupling to other effector proteins has also been reported, including activation of Gq and Gs proteins, inhibition of voltage-gated calcium (Ca^{2+}) channels, stimulation of inwardly rectifying potassium (K^{+}) channels, and activation of mitogen-activated protein kinase (MAPK) signaling pathways and β-arrestin engagement. Thus, inhibition of Ca^{2+} channels and activation of K^{+} channels lead to the suppression of release of excitatory and inhibitory neurotransmitters (e.g., noradrenaline, dopamine, acetylcholine, and glutamate) from the vesicles of the pre-synaptic terminals (Sinclair, 2016).

Endocannabinoids (eCB) are endogenous ligands. Among the most studied are AEA and 2-AG which are produced on demand from membrane phospholipids in response to physiological or pathological stimuli (e.g., calcium influx after excessive glutamate release and neuronal excitability). They can also be accumulated and stored by intracellular transporters and storage organelles/pools in the membrane as phospholipid precursors (Chiurchiù, 2016). The synthesis of AEA is moderated by phospholipase D, whereas fatty acid amide hydrolase (FAAH) was shown to break it down. At the same time, diacylglycerol lipase (DAGL) is responsible for 2-AG production, while

monoacylglycerol lipase (MAGL) is a key enzyme in its hydrolysis (Cintosun et al., 2020; Jeong et al., 2019). The 2-AG is a primary endogenous ligand and physiological cannabinoid receptor agonist for the CB2 receptor (Ibsen et al., 2017).

Once synthesized, eCBs bind to, and functionally activate, their target receptors (mainly CB1 or CB2) triggering various signaling pathways and causing specific biological effects in designated organs or tissues (Chiurchiù, 2016).

Apart from the "classical" eCBs, recently, several other endogenous molecules have been discovered and classified as "cannabinoid-like" or "cannabinoid-related" including 2-AG-ether (noladin ether) and O-arachidonoylethanolamine (virodhamine), as well as two additional N-acylethanolamines (NAEs), namely N-oleoylethanolamide (OEA) and palmitoylethanolamine (PEA) (Chiurchiù, 2016). The OEA has been exhibited to bind cannabinoid-like G-coupled receptor GPE119 and considered as its endogenous ligand whereas PEA demonstrated an affinity to both newly discovered receptors GPR55 and GPR119 (Jeong et al., 2019).

1.6.1. Cannabinoid type 1 receptor (CB1)

The CB1 receptor in humans is encoded by the *CNR1* gene located in chromosome 6 (6q14-q15) (Kupczyk et al., 2009). The CB1 receptors are primarily expressed in the CNS mainly at the terminal ends of central and peripheral neurons and in nonneural cells throughout the body (Kupczyk et al., 2009). Additionally, psychotropic effects of THC and the adverse psychiatric side effects of CB1-targeting drugs are predominantly due to the activation of CB1 receptors (Xing et al., 2020). CB2 receptors are mainly expressed by cells (T and B lymphocytes) and peripheral tissues of the immune system (spleen and thymus) where it regulates immune suppression, apoptosis, and cell migration (Ibsen et al., 2017). The presence and activation of CB2 has also been widely documented in

neurons, astrocytes and activated microglial cells in response to various stimuli (e.g., biologically active substances released in the chronic inflammatory process of the nervous system) (Chiurchiù, 2016; Maccarrone et al., 2015). The density of CB1 in the brain stem, specifically the cardiopulmonary centers is very low and thus the lethality due to respiratory depression development in cannabis users is extremely low in comparison to overdose by opiates (Sinclair, 2016). CB1 receptors are also present in immune cells, epithelial cells, bone marrow, heart, vascular endothelium, lung, gastrointestinal tract, testis, several peripheral organs, and the eye where they are involved in cell proliferation, glucose metabolism, inflammation, and apoptosis (Ghosh et al., 2017). Consequently, at present evidence-based data demonstrates the presence of functional ECS in virtually all peripheral organ systems (Bíró et al., 2009).

1.6.2. Cannabinoid type 2 receptor (CB2)

Cannabinoid receptor type 2 is encoded by the *CNR2* gene and is localized on chromosome 1 (1p36,11) (26). Like CB1, it has been identified during pre- and postnatal developmental periods (Fride, 2008). CB2 is often called an immunocannabinoid system receptor as it is abundantly expressed by the cellular and tissue components of the immune system (Tóth et al., 2019). CB2 receptors have been found on B and T lymphocytes, CD4+ and CD8+, natural killer (NK) cells, monocytes, macrophages, and neutrophils, and at the marginal zone of the spleen, thymus and tonsillar tissue (Sinclair, 2016; Ständer et al., 2005; Xing et al., 2020). The presence of CB2 receptors on the surface of antigen-presenting cells stimulates their cytokine profile and subsequently that of T-helper cells. These interactions may explain to a certain extent mechanisms of anti-inflammatory and anti-hyperalgesic effects of cannabinoids acting through CB2 receptors (Howard et al., 2013; Sinclair, 2016). Moreover, the expression of CB2 has also been found in the skin,

suggesting that CB2 signaling might be involved in the maintaining of cutaneous homeostasis, a balancing act of skin functions (Akhmetshina et al., 2009). Overall, CB2 receptors are thought to play an integral role in the mechanisms of various pathological processes that encompass inflammation, metabolic dysregulation, pain, neurodegeneration, atherosclerosis, and bone loss (Gertsch et al., 2006).

1.6.3. Additional components of ECS

Other membrane and intracellular receptors are involved in response to cannabinoids. Among them are the ionotropic transient receptor potential (TRP) cation channels family, nuclear receptors/transcription factors called the peroxisome proliferator-activated receptor (PPAR) α and ɣ, along with the orphan GPCRs including GPR18 and GPR55, serotonin 1A receptor (5-HT1A), and the adenosine A2A receptor (Baron, 2018; Río et al., 2018; Tóth et al., 2019). Thus, TRP includes six subfamilies: TRPC (canonical), TRPV (vanilloid), TRPM (melastatin), TRPA (ankyrin), TRPP (polycystin) and TRPML (mucolipin). PPARα and PPARɣ are known partially to regulate endocannabinoid-induced immunomodulatory effects on different immune cells (Li et al., 2021; Majewski et al., 2021; Pontis et al., 2016). GPR55 was discovered to be expressed explicitly on NK cells and monocytes and is likely involved in the immune response initiation (Chiurchiù, 2016). TRPV-1 receptors have been found on the surface of several types of central neurons and perivascular sensory nerves, as well as on a couple of immune cells (e.g., macrophages, dendritic or Langerhans cells), endothelial, epithelial smooth muscle cells, epidermal, and hair follicle keratinocytes (Kupczyk et al., 2009). The main components of the ECS and the biosynthesis and degradation of endocannabinoids are schematically depicted in Figure 1.7.

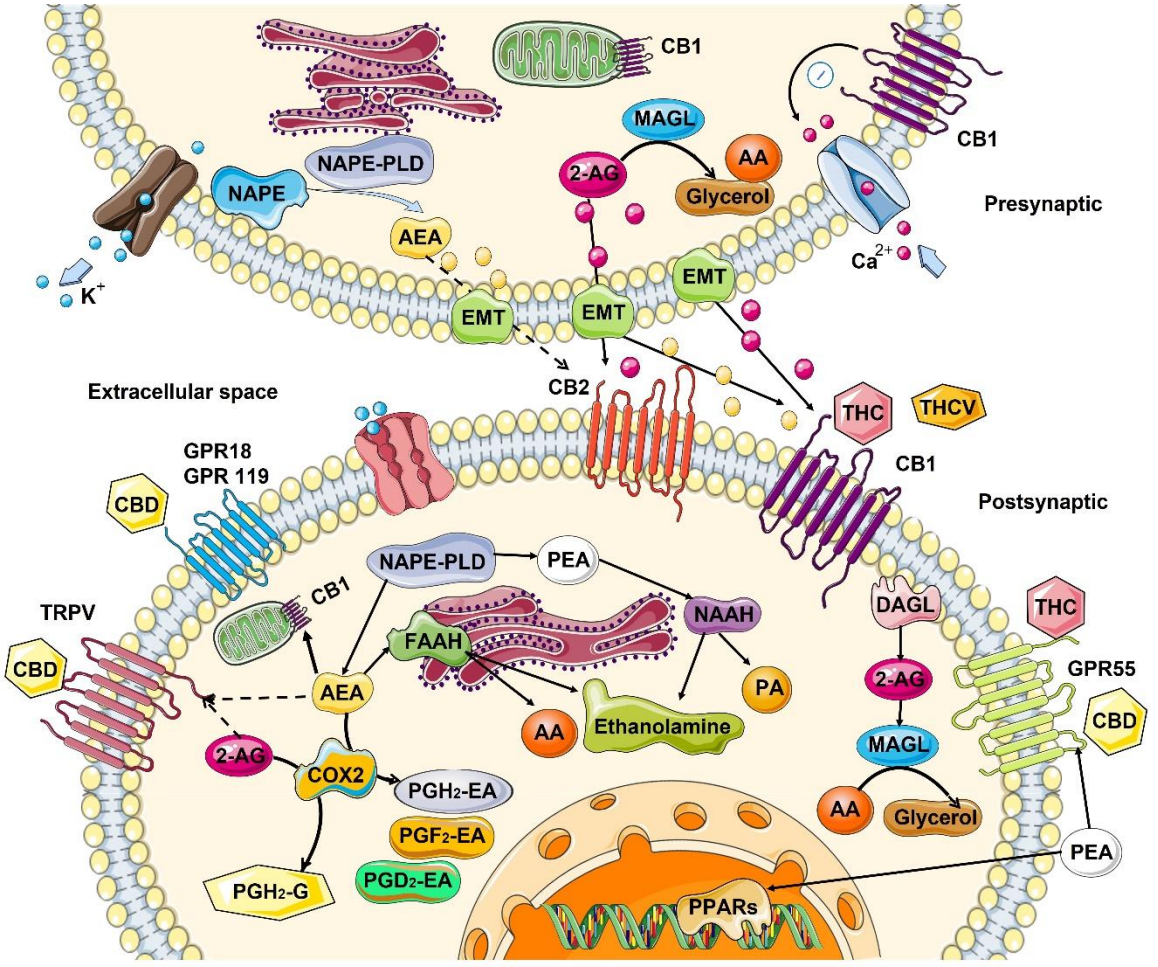

Figure 1.7. Biosynthesis, degradation, and action of endocannabinoids at cannabinoid receptors. Biosynthesis and the inactivation of the two endogenous lipid messengers, such as endocannabinoids N-Arachidonoylethanolamine or anandamide (AEA), 2-arachidonoylglycerol (2-AG), and N-palmitoylethanolamide (PEA) act on cannabinoid receptors. AEA and 2-AG are typically released on demand from membrane lipids. AEA synthesized from N-arachidonoyl-phosphatidylethanolamines (NAPE) via the activity of N-acyl-phosphatidylethanolamine-hydrolysing phospholipase D (NAPE-PLD) and hydrolyzed by fatty acid amide hydrolase (FAAH) to ethanolamine and arachidonic acid (AA). 2-AG is 2-AG can also be produced from sn-2-arachidonate-containing diacylglycerols by sn-1-acyl-2-arachidonoylglycerol lipase (DAGL), and degraded by lipase (MAGL), releasing glycerol and AA. PEA is hydrolyzed by N-acylethanolamine-hydrolysing acid amidase (NAAA) into ethanolamine and palmitic acid (PA). Cyclooxygenase-2 (COX-2) can also oxidize anandamide and 2-AG, followed by prostaglandin synthases to produce prostamides (from anandamide) and prostaglandin-ethanolamide, PG-EA (from 2-AG). Both AEA and 2-AG move across the plasma membrane via a purported endocannabinoid membrane transporter (EMT) and target CB1 and CB2, which show an extracellular binding site. 2-AG, AEA, and PEA directly activate orphan G-protein-coupled receptors (GPR55, GPR18, GPR119), the transient receptor potential of vanilloid (TRPV) channel, and peroxisome proliferator-activated nuclear receptors (PPARs). Dashed lines denote low-affinity bindings. Phytocannabinoids Δ9-

tetrahydrocannabinol (THC), cannabidiol (CBD), and Δ9-tetrahydrocannabivarin (THCV) showed to activate cannabinoid receptors. CB1, cannabinoid receptor 1; CB2, cannabinoid receptor 2; ER, endoplasmic reticulum. This figure was created using images from Servier Medical Art Commons Attribution 3.0 Unported License (http://smart.servier.com).

1.6.4. Phyto- and endocannabinoids act through cannabinoid receptors

Phytocannabinoids (pCBs) found in cannabis plants are well-known to interact with CB1 and CB2 receptors. Among them, the most common are γ-trans-Δ9-tetrahydrocannabinol (THC), Δ9cannabichromene (THCV), cannabidiol (CBD), cannabidivarin (CBDV), cannabigerol (CBG), cannabigerovarin (CBGV), cannabinol (CBN) and cannabichromene (CBC) (Bonini et al., 2018). It has been established that both eCBs and pCBs operate through the activation of presynaptic CB1 receptors as retrograde messengers that provide feedback inhibition of both excitatory and inhibitory transmission in the brain (Maroon & Bost, 2018). Altering CB1 and CB2 receptors, and their endogenous ligands along with endocannabinoid degradative enzymes, have already given promising results in the treatment of cancer, neurodegenerative diseases, and some dermal pathology.

A significant number of studies have found robust evidence that eCBs and pCBs, depending on their concentration, are capable of activating, antagonizing, or inhibiting various cellular targets including several metabotropic (e.g., CB1 or CB2), ionotropic (e.g., TRP) and nuclear (e.g., PPARs) receptors (Tóth et al., 2019). Furthermore, in some situations, they might enforce antagonistic biological actions on the same target molecule. Despite a large number of identified mechanisms of action of endocannabinoids and function of ECS in the regulation of certain diseases or organs, to date, there are still a lot of unknowns surrounding the biological activity and effects of cannabinoids.

For the past decade a great deal of research has been dedicated to identifying ECS mechanisms of action and response towards physiological regulation and functioning of tissues, organs, and the entire organism. Two primary cannabinoid receptors CB1 and CB2 were found to play crucial roles in a variety of physiological processes, including appetite regulation, immunomodulation (Guzmán, 2003), peripheral energy metabolism, pain sensation, and memory (Fride et al., 2005; Hua et al., 2020; Xing et al., 2020). At the same time, multiple questions were addressed about ECS's role in pathological conditions, morbidity, and mortality. Nevertheless, there is a gap in understanding the role of ECS in aging, the functioning of the integumentary system during physiological and pathological processes, and its regenerative capabilities in aged organisms.

1.6.5. Endocannabinoid system of skin

As an active neuroendocrine-immune organ, the skin is also a complex defensive system representing physicochemical, immunological, and microbiological barriers that provide cutaneous protection (Bíró et al., 2009).

The results of numerous dermatological studies have demonstrated that components of the ECS are present in the skin and were found to modulate numerous functions (Bíró et al., 2009). For instance, ECS is involved in cell growth regulation, differentiation, and survival (Tóth et al., 2011), immune and inflammatory responses, as well as sensory perception (Lau & Vaughan, 2014). Cutaneous cannabinoid receptors are typically located in suprabasal layers of the epidermis, hair follicles, and sporadic regions of the basal layer (Río et al., 2018). Thus, CB1 expression was found in keratinocytes localized in the spinous and granular epidermal layers, as well as in epithelial cells of the infundibulum and inner root sheet of hair follicles and differentiated sebaceous cells. In contrast, CB2

receptors are expressed in basal keratinocytes along with undifferentiated sebaceous cells and undifferentiated infundibular hair follicle cells. Presence of CB1/2 receptors has also been verified in the other cutaneous cells such as dermal fibroblasts (Garcia-Gonzalez et al., 2009), melanocytes (Pucci et al., 2012), and myoepithelial cells of eccrine sweat glands (Ständer et al., 2005).

The wide distribution of cannabinoid receptors was found in the nervous and vascular tissues throughout the skin. Like in the CNS and peripheral nervous tissues, both CB1 and CB2 were also identified in cutaneous nerve fibers. Also, the presence of these two cannabinoid receptors was determined in vascular endothelium (Gasperi et al., 2014; Liu et al., 2000), and the subcutaneous layer in pre-adipocytes and mature adipocytes (Río et al., 2018; Roche et al., 2006).

The most abundant cutaneous cells such as keratinocytes (Maccarrone et al., 2003), fibroblasts (McPartland, 2008), and melanocytes (Pucci et al., 2012) (Fig. 1.6) demonstrate a fully functional ECS. Notably, they were shown to synthesize AEA and 2-AG in large quantities. The expression of FAAH, an enzyme that metabolizes anandamide, was found to be low in the suprabasal epidermal layers, the outer root sheath of hair follicles, and in skin sebaceous glands (Wohlman et al., 2016).

Apart from traditional components, PPARγ and TRPV1 are additional receptors and similar to CB1/CB2 receptors in that they are involved in ECS signaling mechanisms throughout the skin. PPARγ expression was found in fibroblasts (Shi-Wen et al., 2010), keratinocytes (Ellis et al., 2000), melanocytes (Kang et al., 2004) and sebocytes (Dozsa et al., 2014) within different cutaneous layers. Similarly, vanilloid receptors are also found in different cutaneous cells (Río et al., 2018).

Cutaneous interactions between TRPV1 and AEA in cellular signaling directly affect cell growth, differentiation, proliferation, and survival. Curiously, depending on the cell type, this interaction may manifest itself by way of synergism, antagonism, or independently from the stimulation of CB1/2 receptors (Bíró et al., 2009; Dobrosi et al., 2008; Telek et al., 2007). Furthermore, it has been determined that the interactions between CB1 and TRPV1 are dose dependent. Based on the activation of CB1 by the phospholipase C (PLC)-PKC or inhibition by the adenylate cyclase (AC)-PKA pathways, CB1 can either stimulate or inhibit the TRPV1 channel activity, respectively (Christie et al., 2018). Hence, distinct mechanisms of various signaling systems provide collaborative work of all parts of the cutaneous barrier complex, with the skin cannabinoid system, named by Toth as a "c[ut]annabinoid" one, playing one of the essential roles (Tóth et al., 2019).

1.7. THESIS RATIONALE, HYPOTHESIS, AND AIMS

The aging process starts directly after birth and lasts through the entire lifespan. For most of the population, it becomes a pressing problem around age 40–60 when the middle-age period of life free of diseases is followed by the period associated with the beginning of age-related diseases (ARDs) that eventually leads to a shortening of life (Gerasymchuk et al., 2020).

Skin is the largest organ in the human body (Río et al., 2018). It is the first defense line against continuous external detrimental factors (e.g., UV exposure, environmental pollution, dietary habits, and numerous chemical compounds). Due to these circumstances, skin primarily demonstrates the main aging symptoms: wrinkles, aging

spots, dullness, and sagging texture. The critical areas to understanding dermal aging are studying the biological mechanisms, such as decreasing extracellular matrix protein synthesis or increasing its degradation, molecular aspects of the cell cycle, and metabolic regulations on the cellular level (Lago & Puzzi, 2019). In addition to mechanisms of skin aging, there are plenty of questions about anti-aging and rejuvenation mechanisms and strategies.

UV radiation and oxidative stress are the primary factors that cause skin aging and potentiating stress response that elicits a permanent cell cycle arrest known as cellular senescence (Lee et al., 2022). The last one provides beneficial activity, for instance, induction of acute senescence protects against cancer and limits fibrosis, however, lingering senescent cells drive ARDs (Birch & Gil, 2020).

Humankind is constantly looking for anti-aging, rejuvenation, and life-extension remedies over millennia, but unfortunately, there is little success in anti-aging therapeutics. Within the last few decades, scientists have developed numerous strategies. One of the most interesting is targeting senescent cells to delay aging and limit dysfunction, known as “senotherapy,” which is gaining momentum. Accordingly, drugs that selectively kill senescent cells termed “senolytics” constitute a significant focus and emerge as alternatives to target ARDs (Birch & Gil, 2020; Thoppil & Riabowol, 2020). Another up-and-coming anti-aging remedy group is natural signaling regulators (NRS) maintaining nutrient-sensitive signaling pathways and are vital for biological processes (Zhu et al., 2020). They are involved in the regulation of pathways responsible for organismal survival, growth, metabolism, signaling systems, including Sirtuin, mTOR, AMPK, and may allow the design of novel therapeutic approaches to ARDs (Cummings

& Lamming, 2017; Ramis et al., 2015). Among the most studied in this group are Sirtuin regulators (e.g., resveratrol and its metabolite piceatannol, Selisistat, a selective SIRT1 inhibitor) (Curry et al., 2021; Mayack et al., 2020; Yessenkyzy et al., 2020), mTOR inhibitors (e.g., rapamycin) (Bai et al., 2021; Fletcher et al., 2013; Qin et al., 2018; Yoshizaki et al., 2010), AMPK activators (e.g., metformin) (Barzilai et al., 2016; Shetty et al., 2018; Soydas et al., 2018, 2021). These NSRs have been shown *in vitro* and *in vivo* studies to extend the lifespan, alleviate ARDs and delay senescence. At the same time, there is almost no available data about their anti-aging and rejuvenation activity in the dermatological field.

In parallel, natural compounds, compared to synthetic ones, remained more attractive in research and industry fields. One class of fascinating natural compounds are phytocannabinoids produced by the cannabis plant. *Cannabis sativa* produces over 100 active medical ingredients called phytocannabinoids (pCBs), and the most abundant are Δ-9-tetrahydrocannabinol (Δ9-THC or THC) and cannabidiol (CBD) (Lim & Kirchhof, 2018). THC works primarily as a weak partial agonist on cannabinoid 1 (CB1) and cannabinoid 2 (CB2) receptors with well-known psychoactive effects, antiemetic, neuroprotective, anticancer, and anti-inflammatory properties (Dhadwal & Kirchhof, 2018). In contrast to THC, CBD has a little direct affinity to CB1 and CB2 receptors, and demonstrates neuroprotective, and anti-inflammatory properties, as well as improves common skin disorders such as psoriasis, eczema, dermatitis, lupus, acne, and nail-patella syndrome (Ardigò et al., 2020; Grant et al., 2011; Maghfour et al., 2021; Oláh et al., 2014, 2016, 2017; Sivesind et al., 2022). Currently, cannabis compounds are popular ingredients

in modern beauty products available on the general market, however, reliable information about the possible anti-aging and rejuvenation properties of pCBs is absent.

This study was performed to determine if applications of phytocannabinoids at relevant doses could delay senescence and stimulate the rejuvenation of aged fibroblasts.

It was hypothesized that cannabinoids THC and CBD alone and in combination with anti-aging compounds exert anti-aging effects in human skin fibroblasts by inhibiting inflammatory processes, activating collagen production, delaying cell senescence, and stimulating rejuvenation.

Aims of the study:

1. Determine if phytocannabinoids have anti-aging properties and delay the natural senescence of cells.

2. Determine if phytocannabinoids in different concentrations exert a rejuvenation effect in skin fibroblasts.

3. Compare the anti-aging effect of phytocannabinoids with other anti-aging compounds such as metformin, rapamycin, and triacetylresveratrol.

1.8. REFERENCES

Ahuja, A., Singh, N., Gupta, P., Mishra, S., & Rani, V. (2017). Influence of exogenous factors on skin aging. In M. A. Farage, K. W. Miller, & H. I. Maibach (Eds.), *Textbook of Aging Skin* (2nd ed., pp. 563–577). Springer, Berlin, Heidelberg. https://doi.org/10.1007/978-3-662-47398-6

Akhmetshina, A., Dees, C., Busch, N., Beer, J., Sarter, K., Zwerina, J., Zimmer, A., Distler, O., Schett, G., & Distler, J. H. W. (2009). The cannabinoid receptor CB2 exerts antifibrotic effects in experimental dermal fibrosis. *Arthritis and Rheumatism*, *60*(4), 1129–1136. https://doi.org/10.1002/art.24395

Alexander, P. (1967). The role of DNA lesions in the processes leading to aging in mice. *Symposia of the Society for Experimental Biology*, *21*, 29–50.

Ames, B. N. (1989). Endogenous oxidative DNA damage, aging, and cancer. *Free Radical Research Communications*, *7*(3–6), 121–128. https://doi.org/10.3109/10715768909087933

Ardigò, M., Franceschini, C., Campione, E., Cosio, T., Lanna, C., Bianchi, L., & Milani, M. (2020). Efficacy of a topical product containing purified omental lipids and three anti-itching compounds in the treatment of chronic pruritus/ *prurigo nodularis* in elderly subjects: A prospective, assessor-blinded, 4-week trial with transepidermal water loss and optical coherence tomography assessments. *Clinical, Cosmetic and Investigational Dermatology*, *13*, 1051–1058. https://doi.org/10.2147/CCID.S292636

Arensberg, M. B. (2018). Population aging: Opportunity for business expansion, an invitational paper presented at the Asia-Pacific Economic Cooperation (APEC) International Workshop on Adaptation to Population Aging Issues, July 17, 2017, Ha Noi, Viet Nam. *Journal of Health, Population and Nutrition*, *37*(1), 7. https://doi.org/10.1186/s41043-018-0138-0

Ashpole, N. M., Sanders, J. E., Hodges, E. L., Yan, H., & Sonntag, W. E. (2015). Growth hormone, insulin-like growth factor-1 and the aging brain. *Experimental Gerontology*, *68*, 76–81. https://doi.org/10.1016/j.exger.2014.10.002

Bai, G. L., Wang, P., Huang, X., Wang, Z. Y., Cao, D., Liu, C., Liu, Y. Y., Li, R. L., & Chen, A. J. (2021). Rapamycin protects skin fibroblasts from UVA-induced photoaging by inhibition of p53 and phosphorylated HSP27. *Frontiers in Cell and Developmental Biology*, *9*(February), 633331. https://doi.org/10.3389/fcell.2021.633331

Barja, G. (2019). Towards a unified mechanistic theory of aging. *Experimental Gerontology*, *124*(June), 1–14. https://doi.org/10.1016/j.exger.2019.05.016

Baron, E. P. (2018). Medicinal properties of cannabinoids, terpenes, and flavonoids in cannabis, and benefits in migraine, headache, and pain: An update on current evidence and cannabis science. *Headache*, *58*(7), 1139–1186. https://doi.org/10.1111/head.13345

Barzilai, N., Crandall, J. P., Kritchevsky, S. B., & Espeland, M. A. (2016). Metformin as a tool to target aging. *Cell Metabolism*, *23*(6), 1060–1065. https://doi.org/10.1016/j.cmet.2016.05.011

Batista, L. F. Z., Kaina, B., Meneghini, R., & Menck, C. F. M. (2009). How DNA lesions are turned into powerful killing structures: Insights from UV-induced apoptosis. *Mutation Research - Reviews in Mutation Research*, *681*(2–3), 197–208. https://doi.org/10.1016/j.mrrev.2008.09.001

Berman, A. E., Leontieva, O. V, Natarajan, V., Mccubrey, J. A., Demidenko, Z. N., & Nikiforov, M. A. (2012). Recent progress in genetics of aging, senescence and longevity focusing on cancer-related genes. *Oncotarget*, *3*(12), 1522–1532. https://doi.org/10.18632/oncotarget.889

Berneburg, M., Plettenberg, H., Medve-König, K., Pfahlberg, A., Gers-Barlag, H., Gefeller, O., & Krutmann, J. (2004). Induction of the photoaging-associated mitochondrial common deletion in vivo in normal human skin. *Journal of Investigative Dermatology*, *122*(5), 1277–1283. https://doi.org/10.1111/j.0022-202X.2004.22502.x

Birch, J., & Gil, J. (2020). Senescence and the SASP: Many therapeutic avenues. *Genes & Development*, *34*, 1565–1576. https://doi.org/10.1101/gad.343129

Bíró, T., Tóth, B. I., Haskó, G., Paus, R., & Pacher, P. (2009). The endocannabinoid system of the skin in health and disease: Novel perspectives and therapeutic opportunities. *Trends in Pharmacological Sciences*, *30*(8), 411–420. https://doi.org/10.1016/j.tips.2009.05.004

Bjorksten, J. (1968). The crosslinkage theory of aging. *Journal of the American Geriatrics Society*, *16*(4), 408–427. https://doi.org/10.1111/j.1532-5415.1968.tb02821.x

Bjorksten, J., & Tenhu, H. (1990). The crosslinking theory of aging - added evidence. *Experimental Gerontology*, *25*(2), 91–95. https://doi.org/10.1016/0531-5565(90)90039-5

Blagosklonny, M. V. (2008). Aging: ROS or TOR. *Cell Cycle*, *7*(21), 3344–3354. https://doi.org/10.4161/cc.7.21.6965

Blagosklonny, M. v. (2019). Rapamycin for the aging skin. *Aging*, 11(24), 12822–12826). https://doi.org/10.4161/cc.5.18.3288

Blanpain, C., & Fuchs, E. (2009). Epidermal homeostasis: A balancing act of stem cells in the skin. *Nature Reviews. Molecular Cell Biology*, *10*(3), 207–218. https://doi.org/10.1038/nrm2636

Bonini, S. A., Premoli, M., Tambaro, S., Kumar, A., Maccarinelli, G., Memo, M., & Mastinu, A. (2018). Cannabis sativa: A comprehensive ethnopharmacological review of a medicinal plant with a long history. *Journal of Ethnopharmacology*, *227*(May), 300–315. https://doi.org/10.1016/j.jep.2018.09.004

Brunetta, H. S., Holwerda, A. M., van Loon, L. J. C., & Holloway, G. P. (2020). Mitochondrial ROS and aging: Understanding exercise as a preventive tool. *Journal of Science in Sport and Exercise*, *2*(1), 15–24. https://doi.org/10.1007/s42978-019-00037-1

Brunk, U. T., & Terman, A. (2002). The mitochondrial-lysosomal axis theory of aging. Accumulation of damaged mitochondria as a result of imperfect autophagocytosis. *European Journal of Biochemistry*, *269*(8), 1996–2002. https://doi.org/10.1046/j.1432-1033.2002.02869.x

Burton, D. G. A., & Stolzing, A. (2018). Cellular senescence: Immunosurveillance and future immunotherapy. *Ageing Research Reviews*, *43*(January), 17–25. https://doi.org/10.1016/j.arr.2018.02.001

Cavinato, M., Koziel, R., Romani, N., Weinmüllner, R., Jenewein, B., Hermann, M., Dubrac, S., Ratzinger, G., Grillari, J., Schmuth, M., & Jansen-Dürr, P. (2017). UVB-induced senescence of human dermal fibroblasts involves impairment of proteasome and enhanced autophagic activity. *Journals of Gerontology - Series A Biological Sciences and Medical Sciences*, *72*(5), 632–639. https://doi.org/10.1093/gerona/glw150

Chiurchiù, V. (2016). Endocannabinoids and immunity. *Cannabis and Cannabinoid Research*, *1*(1), 59–66. https://doi.org/10.1089/can.2016.0002

Choi, M., & Lee, C. (2015). Immortalization of primary keratinocytes and its application to skin research. *Biomolecules and Therapeutics*, *23*(5), 391–399. https://doi.org/10.4062/biomolther.2015.038

Christie, S., Wittert, G. A., Li, H., & Page, A. J. (2018). Involvement of TRPV1 channels in energy homeostasis. *Frontiers in Endocrinology*, *9*(July), 1–14. https://doi.org/10.3389/fendo.2018.00420

Cintosun, A., Lara-Corrales, I., & Pope, E. (2020). Mechanisms of cannabinoids and potential applicability to skin diseases. *Clinical Drug Investigation*, *40*, 293–304. https://doi.org/10.1007/s40261-020-00894-7

Cuervo, A. M., & Dice, J. F. (1998). How do intracellular proteolytic systems change with age? *Frontiers in Bioscience*, *3*(8), d25-43. https://doi.org/10.2741/a264

Cummings, N. E., & Lamming, D. W. (2017). Regulation of metabolic health and aging by nutrient-sensitive signaling pathways. *Molecular and Cellular Endocrinology*, *455*, 13–22. https://doi.org/10.1016/j.mce.2016.11.014

Curry, A. M., White, D. S., Donu, D., & Cen, Y. (2021). Human Sirtuin regulators: The "Success" stories. *Frontiers in Physiology*, *12*, 752117. Frontiers Media S.A. https://doi.org/10.3389/fphys.2021.752117

Davidovic, M., Sevo, G., Svorcan, P., Milosevic, D. P., Despotovic, N., & Erceg, P. (2010). Old age as a privilege of the "selfish ones." *Aging and Disease*, *1*(2), 139–146.

Dhadwal, G., & Kirchhof, M. G. (2018). The risks and benefits of cannabis in the dermatology clinic. *Journal of Cutaneous Medicine and Surgery*, *22*(2), 194–199. https://doi.org/10.1177/1203475417738971

Diggs, J. (2008). Neuroendocrine (Aging Clock) theory of aging. In S. J. Loue & M. Sajatovic (Eds.), *Encyclopedia of Aging and Public Health*. Springer. https://doi.org/10.1007/978-0-387-33754-8_311

Dilman, V. M., Revskoy, S. Y., & Golubev, A. G. (1986). Neuroendocrine-ontogenetic mechanism of aging: Toward an integrated theory of aging. *International Review of Neurobiology*, *28*(C), 89–156. https://doi.org/10.1016/S0074-7742(08)60107-5

Dobrosi, N., Tóth, B. I., Nagy, G., Dózsa, A., Géczy, T., Nagy, L., Zouboulis, C. C., Paus, R., Kovács, L., & Bíró, T. (2008). Endocannabinoids enhance lipid synthesis and apoptosis of human sebocytes via cannabinoid receptor-2-mediated signaling. *The FASEB Journal*, *22*(10), 3685–3695. https://doi.org/10.1096/fj.07-104877

Dozsa, A., Dezso, B., Toth, B. I., Bacsi, A., Poliska, S., Camera, E., Picardo, M., Zouboulis, C. C., Bíró, T., Schmitz, G., Liebisch, G., Rühl, R., Remenyik, E., & Nagy, L. (2014). PPARγ-mediated and arachidonic acid-dependent signaling is involved in differentiation and lipid production of human sebocytes. *Journal of Investigative Dermatology*, *134*(4), 910–920. https://doi.org/10.1038/jid.2013.413

Driskell, R. R., Lichtenberger, B. M., Hoste, E., Kretzschmar, K., Simons, B. D., Charalambous, M., Ferron, S. R., Herault, Y., Pavlovic, G., Ferguson-Smith, A. C., & Watt, F. M. (2013). Distinct fibroblast lineages determine dermal architecture in skin development and repair. *Nature*, *504*(7479), 277–281. https://doi.org/10.1038/nature12783

Druzhyna, N. M., Wilson, G. L., & Ledoux, S. P. (2008). Mitochondrial DNA repair in aging and disease. *Mechanisms of Ageing and Development*, *129*(7–8), 383–390. https://doi.org/10.1016/j.mad.2008.03.002

Duchatelet, S., Russo, C., Osterburg, C., Mallet, S., Bole-Feysot, C., Nitschké, P., Richard, M. A., Dötsch, V., Missero, C., Nassif, A., & Hovnanian, A. (2020). A TP63 mutation causes prominent alopecia with mild ectodermal dysplasia. *Journal of Investigative Dermatology*, *140*(5), 1103-1106.e4. https://doi.org/10.1016/j.jid.2019.06.154

Dudonné, S., Coutière, P., Woillez, M., Mérillon, J.-M., & Vitrac, X. (2011). DNA macroarray study of skin aging-related genes expression modulation by antioxidant plant extracts on a replicative senescence model of human dermal fibroblasts. In *Phytotherapy research: PTR*, *25*(5), 686–693. https://doi.org/10.1002/ptr.3308

Elder, D. E., Elenitsas, R., Rosenbach, M., Murphy, G. F., Rubin, A. I., & Xu, X. (2015). *Lever's Histopathology of the Skin* (R. E. editor in chief, David E. Elder; associate editors & X. X. Misha Rosenbach, George F. Murphy, Adam I. Rubin, Eds.; 11th ed.). Wolters Kluwer.

Ellis, C. N., Varani, J., Fisher, G. J., Zeigler, M. E., Pershadsingh, H. A., Benson, S. C., Chi, Y., & Kurtz, T. W. (2000). Troglitazone improves psoriasis and normalizes models of proliferative skin disease: Ligands for peroxisome proliferator-activated receptor-Inhibit keratinocyte proliferation (Clinical Trial). *Archives of Dermatology*, *136*(5), 609–616. https://doi.org/10.1001/archderm.136.5.609

Elsharawy, A., Keller, A., Flachsbart, F., Wendschlag, A., Jacobs, G., Kefer, N., Brefort, T., Leidinger, P., Backes, C., Meese, E., Schreiber, S., Rosenstiel, P., Franke, A., & Nebel, A. (2012). Genome-wide miRNA signatures of human longevity. *Aging Cell*, *11*(4), 607–616. https://doi.org/10.1111/j.1474-9726.2012.00824.x

Fabris, N. (1990). A neuroendocrine-immune theory of aging. *International Journal of Neuroscience*, *51*(3–4), 373–375. https://doi.org/10.3109/00207459008999749

Failla, G. (1958). The aging process and cancerogenesis. *Annals of the New York Academy of Sciences*, *71*(6), 1124–1140. https://doi.org/10.1111/j.1749-6632.1958.tb54674.x

Farage, M. A., Miller, K. W., & I.Maibach, H. (2017). Textbook of Aging Skin. In *Textbook of Aging Skin* (2nd ed.). Springer-Verlag Berlin Heidelberg. https://doi.org/10.1007/978-3-662-47398-6

Farage, M. A., Miller, K. W., & Maibach, H. I. (2017). Degenerative changes in aging skin. In M. A. Farage, K. W. Miller, & H. I. Maibach (Eds.), *Textbook of aging skin* (2nd ed., pp. 15–30). Springer, Berlin, Heidelberg. https://doi.org/10.1007/978-3-662-47398-6

Fletcher, L., Evans, T. M., Watts, L. T., Jimenez, D. F., & Digicaylioglu, M. (2013). Rapamycin treatment improves neuron viability in an in vitro model of stroke. *PLoS ONE*, *8*(7), e68281. https://doi.org/10.1371/journal.pone.0068281

Fore, J. (2006). A review of skin and the effects of aging on skin structure and function. *Ostomy/Wound Management*, *52*(9), 24–35.

Forrester, S. J., Kikuchi, D. S., Hernandes, M. S., Xu, Q., & Griendling, K. K. (2018). Reactive oxygen species in metabolic and inflammatory signaling. *Circulation Research*, *122*(6), 877–902. https://doi.org/10.1161/CIRCRESAHA.117.311401

Freitas, A. A., & De Magalhães, J. P. (2011). A review and appraisal of the DNA damage theory of ageing. *Mutation Research - Reviews in Mutation Research*, *728*(1–2), 12–22. https://doi.org/10.1016/j.mrrev.2011.05.001

Fride, E. (2008). Multiple roles for the endocannabinoid system during the earliest stages of life: Pre- and postnatal development neuroendocrinology. *Journal of Neuroendocrinology*, *20*(1), 75–81. https://doi.org/10.1111/j.1365-2826.2008.01670.x

Fride, E., Bregman, T., & Kirkhamt, T. C. (2005). Endocannabinoids and food intake: Newborn suckling and appetite regulation in adulthood. *Experimental Biology and Medicine*, *230*(4), 255–234.

Fujiwara, H., Ferreira, M., Donati, G., Marciano, D. K., Linton, J. M., Sato, Y., Hartner, A., Sekiguchi, K., Reichardt, L. F., & Watt, F. M. (2011). The basement membrane of hair follicle stem cells is a muscle cell niche. *Cell*, *144*(4), 577–589. https://doi.org/10.1016/j.cell.2011.01.014

Garcia-Gonzalez, E., Selvi, E., Balistreri, E., Lorenzini, S., Maggio, R., Natale, M. R., Capecchi, P. L., Lazzerini, P. E., Bardelli, M., Laghi-Pasini, F., & Galeazzi, M. (2009). Cannabinoids inhibit fibrogenesis in diffuse systemic sclerosis fibroblasts. *Rheumatology*, *48*(9), 1050–1056. https://doi.org/10.1093/rheumatology/kep189

Gasperi, V., Evangelista, D., Chiurchiù, V., Florenzano, F., Savini, I., Oddi, S., Avigliano, L., Catani, M. V., & Maccarrone, M. (2014). 2-Arachidonoylglycerol modulates human endothelial cell/leukocyte interactions by controlling selectin expression through CB1 and CB2 receptors. *International Journal of Biochemistry and Cell Biology*, *51*(1), 79–88. https://doi.org/10.1016/j.biocel.2014.03.028

Gebhard, D., Mahler, B., Matt, K., Burger, K., & Bergemann, J. (2014). Mitochondrial DNA copy number – but not a mitochondrial tandem CC to TT transition – is increased in sun-exposed skin. *Experimental Dermatology*, *23*(3), 209–211. https://doi.org/10.1111/exd.12327

Gensler, H. L., & Bernstein, H. (1981). DNA damage as the primary cause of aging. *The Quarterly Review of Biology*, *56*(3), 279–303. https://doi.org/10.1086/412317

Gerasymchuk, M. (2021). Genomic instability and aging: Causes and consequences. *Genome Stability*, 533–553. https://doi.org/10.1016/B978-0-323-85679-9.00028-3

Gerasymchuk, M., Cherkasova, V., Kovalchuk, O., & Kovalchuk, I. (2020). The role of microRNAs in organismal and skin aging. *International Journal of Molecular Sciences*, *21*(15), 5281. https://doi.org/10.3390/ijms21155281

Gertsch, J., Raduner, S., & Altmann, K. H. (2006). New natural noncannabinoid ligands for cannabinoid Type-2 (CB2) receptors. *Journal of Receptors and Signal Transduction*, *26*(5–6), 709–730. https://doi.org/10.1080/10799890600942674

Ghosh, S., González-Mariscal, I., Egan, J. M., & Moaddel, R. (2017). Targeted proteomics of cannabinoid receptor CB1 and the CB1b isoform. *Journal of Pharmaceutical and Biomedical Analysis*, *144*, 154–158. https://doi.org/10.1016/j.jpba.2016.11.003

Gkogkolou, P., & Böhm, M. (2012). Advanced glycation end products: Key players in skin aging? *Dermato-Endocrinology*, *4*(3), 259–270. https://doi.org/10.4161/derm.22028

Gladyshev, V. N. (2016). Aging: Progressive decline in fitness due to the rising deleteriome adjusted by genetic, environmental, and stochastic processes. *Aging Cell*, *15*, 594–602. https://doi.org/10.1111/acel.12480

Glass, D., Viñuela, A., Davies, M. N., Ramasamy, A., Parts, L., Knowles, D., Brown, A. A., Hedman, Å. K., Small, K. S., Buil, A., Grundberg, E., Nica, A. C., Meglio, P. Di, Nestle,

F. O., Ryten, M., Durbin, R., McCarthy, M. I., Deloukas, P., Dermitzakis, E. T., … Spector, T. D. (2013). Gene expression changes with age in skin, adipose tissue, blood and brain. *Genome Biology*, *14*(7), R75. https://doi.org/10.1186/gb-2013-14-7-r75

Grant, J. E., Odlaug, B. L., Chamberlain, S. R., & Kim, S. W. (2011). Dronabinol, a cannabinoid agonist, reduces hair pulling in trichotillomania: A pilot study. *Psychopharmacology*, *218*(3), 493–502. https://doi.org/10.1007/s00213-011-2347-8

Gray, D. A., & Woulfe, J. (2005). Lipofuscin and aging: A matter of toxic waste. *Science of Aging Knowledge Environment: SAGE KE*, *5*, 1–5. https://doi.org/10.1126/sageke.2005.5.re1

Guzmán, M. (2003). Cannabinoids: Potential anticancer agents. In *Nature Reviews Cancer*, *3*(10), 745–755. European Association for Cardio-Thoracic Surgery. https://doi.org/10.1038/nrc1188

Harley, C. B. (1991). Telomere loss: Mitotic clock or genetic time bomb? *Mutation Research DNAging*, *256*(2–6), 271–282. https://doi.org/10.1016/0921-8734(91)90018-7

Harman, D. (1956). Aging: A theory based on free radical and radiation chemistry. *Journal of Gerontology*, *11*(3), 298–300. https://doi.org/10.1093/geronj/11.3.298

Harman, D. (1992). Free radical theory of aging. *Mutation Research/DNAging*, *275*, 257–266.

Hayflick, L. (1965). The limited in vitro lifetime of human diploid cell strains. *Experimental Cell Research*, *37*(3), 614–636. https://doi.org/10.1016/0014-4827(65)90211-9

Hayflick, L., & Moorhead, P. S. (1961). The serial cultivation of human cell strains. *Experimental Cell Research*, *25*(3), 585–621. https://doi.org/10.1016/0014-4827(61)90192-6

Holmes, G. E., Bernstein, C., & Bernstein, H. (1992). Oxidative and other DNA damages as the basis of aging: A review. *Mutation Research DNAging*, *275*(3–6), 305–315. https://doi.org/10.1016/0921-8734(92)90034-M

Horsburgh, S., Fullard, N., Roger, M., Degnan, A., Todryk, S., Przyborski, S., & O'Reilly, S. (2017). MicroRNAs in the skin: Role in development, homoeostasis and regeneration. *Clinical Science*, *131*(15), 1923–1940. https://doi.org/10.1042/CS20170039

Horvath, S., & Raj, K. (2018). DNA methylation-based biomarkers and the epigenetic clock theory of ageing. *Nature Reviews Genetics*, *19*(6), 371–384. https://doi.org/10.1038/s41576-018-0004-3

Howard, P., Twycross, R., Shuster, J., Mihalyo, M., & Wilcock, A. (2013). Cannabinoids. *Journal of Pain and Symptom Management*, *46*(1), 142–149. https://doi.org/10.1016/j.jpainsymman.2013.05.002

Hua, T., Li, X., Wu, L., Iliopoulos-Tsoutsouvas, C., Wang, Y., Wu, M., Shen, L., Johnston, C. A., Nikas, S. P., Song, F., Song, X., Yuan, S., Sun, Q., Wu, Y., Jiang, S., Grim, T.

W., Benchama, O., Stahl, E. L., Zvonok, N., … Liu, Z. J. (2020). Activation and signaling mechanism revealed by cannabinoid receptor-Gi complex structures. *Cell*, *180*(4), 655-665.e18. https://doi.org/10.1016/j.cell.2020.01.008

Huang, H. C., Chang, T. M., Chang, Y. J., & Wen, H. Y. (2013). UVB irradiation regulates ERK1/2- and p53-dependent thrombomodulin expression in human keratinocytes. *PLoS ONE*, *8*(7), 1–10. https://doi.org/10.1371/journal.pone.0067632

Ibsen, M. S., Connor, M., & Glass, M. (2017). Cannabinoid CB1 and CB2 receptor signaling and bias. *Cannabis and Cannabinoid Research*, *2*(1), 48–60. https://doi.org/10.1089/can.2016.0037

Jacobs, H. T. (2003). The mitochondrial theory of aging: Dead or alive? *Aging Cell*, *2*(1), 11–17. https://doi.org/10.1046/j.1474-9728.2003.00032.x

Janes, S. M., & Watt, F. M. (2006). New roles for integrins in squamous-cell carcinoma. *Nature Reviews Cancer*, *6*(3), 175–183. https://doi.org/10.1038/nrc1817

Jeong, S., Kim, M. S., Lee, S. H., & Park, B. D. (2019). Epidermal endocannabinoid system (EES) and its cosmetic application. *Cosmetics*, *6*(2), 1–10. https://doi.org/10.3390/COSMETICS6020033

Jia, Q., & Nash, J. F. (2017). Pathology of aging skin. In M. A. Farage, K. W. Miller, & H. I. Maibach (Eds.), *Textbook of Aging Skin.* (2nd ed., pp. 363–385). Springer, Berlin, Heidelberg. https://doi.org/10.1007/978-3-662-47398-6

Jin, K. (2010). Modern biological theories of aging. *Aging and Disease*, *1*(2), 72–74.

Kang H. Y., Chung E., Lee M., Cho Y., & Kang W. H. (2004). Expression and function of peroxisome proliferator-activated receptors in human melanocytes. *British Journal of Dermatology*, *150*(3), 462–468. https://doi.org/10.1111/j.1365-2133.2004.05844.x

Kang, S. M., Han, S., Oh, J. H., Lee, Y. M., Park, C. H., Shin, C. Y., Lee, D. H., & Chung, J. H. (2017). A synthetic peptide blocking TRPV1 activation inhibits UV-induced skin responses. *Journal of Dermatological Science*, *88*(1), 126–133. https://doi.org/10.1016/j.jdermsci.2017.05.009

Kato, D., Miyazawa, K., Ruas, M., Starborg, M., Wada, I., Oka, T., Sakai, T., Peters, G., & Hara, E. (1998). Features of replicative senescence induced by direct addition of antennapedia-p16 sxuRe fusion protein to human diploid fibroblasts. *Federation of European Biochemical Societies. Letters*, *427*, 203–208.

Khan, A. S., Sane, D. C., Wannenburg, T., & Sonntag, W. E. (2002). Growth hormone, insulin-like growth factor-1 and the aging cardiovascular system. *Cardiovascular Research*, *54*, 25–35. https://doi.org/10.1016/S0008-6363(01)00533-8

Khrapko, K., & Turnbull, D. (2014). Mitochondrial DNA mutations in aging. In *Progress in Molecular Biology and Translational Science* (1st ed). Elsevier Inc. https://doi.org/10.1016/B978-0-12-394625-6.00002-7

Kierszenbaum, L. A., & Tres, L. (2019). *Histology and cell biology: An introduction to pathology E-Book*.

Kim, S. Y., Metcalfe, N. B., & Velando, A. (2016). A benign juvenile environment reduces the strength of antagonistic pleiotropy and genetic variation in the rate of senescence. *Journal of Animal Ecology*, *85*(3), 705–714. https://doi.org/10.1111/1365-2656.12468

Kirkland, J. L., & Tchkonia, T. (2017). Cellular senescence: A translational perspective. *EBioMedicine*, *21*, 21–28. https://doi.org/10.1016/j.ebiom.2017.04.013

Kirkwood, T. B. L. (1977). Evolution of ageing. *Nature*, *270*(November), 301–304.

Kirkwood, T. B. L., & Austad, S. N. (2000). Why do we age? *Nature*, *408*(6809), 233–238. https://doi.org/10.1038/35041682

Krishnan, R., Rajeswari, R., Venugopal, J., Sundarrajan, S., Sridhar, R., Shayanti, M., & Ramakrishna, S. (2012). Polysaccharide nanofibrous scaffolds as a model for in vitro skin tissue regeneration. *Journal of Materials Science: Materials in Medicine*, *23*(6), 1511–1519. https://doi.org/10.1007/s10856-012-4630-6

Kumar, S., Millis, A. J., & Baglioni, C. (1992). Expression of interleukin 1-inducible genes and production of interleukin 1 by aging human fibroblasts. *Proceedings of the National Academy of Sciences*, *89*(10), 4683–4687. https://doi.org/10.1073/pnas.89.10.4683

Kupczyk, P., Reich, A., & Szepietowski, J. C. (2009). Cannabinoid system in the skin - a possible target for future therapies in dermatology. *Experimental Dermatology*, *18*(8), 669–679. https://doi.org/10.1111/j.1600-0625.2009.00923.x

Lago, J. C., & Puzzi, M. B. (2019). The effect of aging in primary human dermal fibroblasts. *PLoS ONE*, *14*(7), e0219165. https://doi.org/10.1371/journal.pone.0219165

Lämmermann, I., Terlecki-Zaniewicz, L., Weinmüllner, R., Schosserer, M., Dellago, H., de Matos Branco, A. D., Autheried, D., Sevcnikar, B., Kleissl, L., Berlin, I., Morizot, F., Lejeune, F., Fuzzati, N., Forestier, S., Toribio, A., Tromeur, A., Weinberg, L., Higareda Almaraz, J. C., Scheideler, M., … Grillari, J. (2018). Blocking negative effects of senescence in human skin fibroblasts with a plant extract. *Npj Aging and Mechanisms of Disease*, *4*(1), 4. https://doi.org/10.1038/s41514-018-0023-5

Lau, B. K., & Vaughan, C. W. (2014). Targeting the endogenous cannabinoid system to treat neuropathic pain. *Frontiers in Pharmacology*, *5*(28), 1-4. https://doi.org/10.3389/fphar.2014.00028

Lee, H.-C., & Wei, Y.-H. (2012). Mitochondria and aging. In R. Scatena, P. Bottoni, & B.Giardina (Eds.), *Advances in Mitochondrial Medicine. Advances in Experimental Medicine and Biology* (Vol. 942, pp. 311–327). Springer, Dordrecht. https://doi.org/10.1007/978-94-007-2869-1

Lee, J. J., Ng, S. C., Hsu, J. Y., Liu, H., Chen, C. J., Huang, C. Y., & Kuo, W. W. (2022). Galangin reverses H_2O_2-induced dermal fibroblast senescence via SIRT1-PGC-1α/Nrf2

signaling. *International Journal of Molecular Sciences*, *23*(3), 1387. https://doi.org/10.3390/ijms23031387

Lee, S. J., Hwang, A. B., & Kenyon, C. (2010). Inhibition of respiration extends *C. elegans* life span via reactive oxygen species that increase HIF-1 activity. *Current Biology*, *20*(23), 2131–2136. https://doi.org/10.1016/j.cub.2010.10.057

Lefkimmiatis, K., Grisan, F., Iannucci, L. F., Surdo, N. C., Pozzan, T., & Di Benedetto, G. (2020). Mitochondrial communication in the context of aging. *Aging Clinical and Experimental Research*, *33*(5), 1367-1370. https://doi.org/10.1007/s40520-019-01451-9

Leidal, A. M., Levine, B., & Debnath, J. (2018). Autophagy and the cell biology of age-related disease. *Nature Cell Biology*, *20*(12), 1338–1348. https://doi.org/10.1038/s41556-018-0235-8

Lewis, D. A., Travers, J. B., Somani, A., & Spandau, D. F. (2010). The IGF-1/IGF-1R signaling axis in the skin: A new role for the dermis in aging-associated skin cancer. *Oncogene*, *29*, 1475–1485. https://doi.org/10.1038/onc.2009.440

Li, C., Muñoz-Rojas, A. R., Wang, G., Mann, A. O., Benoist, C., & Mathis, D. (2021). PPARγ marks splenic precursors of multiple nonlymphoid-tissue Treg compartments. *PNAS*, *18*(13), e2025197118. https://doi.org/10.1073/pnas.2025197118/-/DCSupplemental

Lim, M., & Kirchhof, M. (2018). Dermatology-related uses of medical cannabis promoted by dispensaries in Canada, Europe, and the United States. *J Cutan Med Surg*, *23*(2), 178–184. https://doi.org/10.1177/1203475418808761

Lindsey, J., McGill, N. I., Lindsey, L. A., Green, D. K., & Cooke, H. J. (1991). In vivo loss of telomeric repeats with age in humans. *Mutation Research/DNAging*, *256*(1), 45–48. https://doi.org/10.1016/0921-8734(91)90032-7

Liu, J., Gao, B., Mirshahi, F., Sanyal, A. J., Khanolkar, A. D., Makriyannis, A., & Kunos, G. (2000). Functional CB1 cannabinoid receptors in human vascular endothelial cells. *Biochem. J.*, *346*, 835–840.

Longo, V. D., Mitteldorf, J., & Skulachev, V. P. (2005). Programmed and altruistic ageing. *Nature Reviews Genetics*, *6*(November), 866–873.

Maccarrone, M., Bab, I., Bíró, T., Cabral, G. A., Dey, S. K., Di Marzo, V., Konje, J. C., Kunos, G., Mechoulam, R., Pacher, P., Sharkey, K. A., & Zimmer, A. (2015). Endocannabinoid signaling at the periphery: 50 years after THC. *Trends in Pharmacological Sciences*, *36*(5), 277–296. https://doi.org/10.1016/j.tips.2015.02.008

Maccarrone, M., di Rienzo, M., Battista, N., Gasperi, V., Guerrieri, P., Rossi, A., & Finazzi-Agrò, A. (2003). The endocannabinoid system in human keratinocytes: Evidence that anandamide inhibits epidermal differentiation through CB1 receptor-dependent

inhibition of protein kinase C, activating protein-1, and transglutaminase. *Journal of Biological Chemistry*, *278*(36), 33896–33903. https://doi.org/10.1074/jbc.M303994200

Maghfour, J., Rundle, C. W., Rietcheck, H. R., Dercon, S., Lio, P., Mamo, A., Runion, T. M., Fernandez, J., Kahn, J., Dellavalle, R. P., & Yardley, H. (2021). Assessing the effects of topical cannabidiol in patients with atopic dermatitis. *Dermatology Online Journal, 27* (2), 15. Dermatology Online Journal. https://doi.org/10.5070/d3272052393

Majewski, G., Craw, J., & Falla, T. (2021). Accelerated barrier repair in human skin explants induced with a plant-derived ppar-α activating complex via cooperative interactions. *Clinical, Cosmetic and Investigational Dermatology*, *14*, 1271–1293. https://doi.org/10.2147/CCID.S325967

Makrantonaki, E., & Zouboulis, C. C. (2007). Characteristics and pathomechanisms of endogenously aged skin. *William J. Cunliffe Scientific Awards Prize 2006. Dermatology*, *214*, 352–360. https://doi.org/10.1159/000100890

Makrantonaki, E., & Zouboulis, C. C. (2017). Pathomechanisms of endogenously aged skin. In M. A. Farage, K. W. Miller, & H. I. Maibach (Eds.), *Textbook of Aging Skin* (2nd ed., pp. 111–120). Springer, Berlin, Heidelberg. https://doi.org/10.1007/978-3-662-47398-6

Mancini, M., Lena, A. M., Saintigny, G., Mahé, C., di Daniele, N., Melino, G., & Candi, E. (2014). MicroRNAs in human skin ageing. *Ageing Research Reviews*, *17*, 9–15. https://doi.org/10.1016/j.arr.2014.04.003

Maroon, J., & Bost, J. (2018). Review of the neurological benefits of phytocannabinoids. *Surgical Neurology International*, *9*(April 26), 91. https://doi.org/10.4103/sni.sni_45_18

Matjusaitis, M., Chin, G., Sarnoski, E. A., & Stolzing, A. (2016). Biomarkers to identify and isolate senescent cells. *Ageing Research Reviews*, *29*, 1–12. https://doi.org/10.1016/j.arr.2016.05.003

Mayack, B. K., Sippl, W., & Ntie-Kang, F. (2020). Natural products as modulators of sirtuins. *Molecules 25*(14), 3287. MDPI AG. https://doi.org/10.3390/molecules25143287

McPartland, J. M. (2008). Expression of the endocannabinoid system in fibroblasts and myofascial tissues. *Journal of Bodywork and Movement Therapies*, *12*(2), 169–182. https://doi.org/10.1016/j.jbmt.2008.01.004

Mills, A. A., Zheng, B., Wang, X. J., Vogel, H., Roop, D. R., & Bradley, A. (1999). p63 is a p53 homologue required for limb and epidermal morphogenesis. *Nature*, *398*(6729), 708–713. https://doi.org/10.1038/19531

Mitteldorf, J. (2001). Can experiments on caloric restriction be reconciled with the disposable soma theory for the evolution of senescence? *Evolution*, *55*(9), 1902–1905.

Nacarelli, T., Torres, C., & Sell, C. (2016). Mitochondrial reactive oxygen species in cellular senescence. In Rattan S. & Hayflick L. (Eds.), *Cellular Ageing and Replicative*

Senescence. Healthy Ageing and Longevity (pp. 169–185). Springer, Cham. https://doi.org/10.1007/978-3-319-26239-0

Nakamura, K.-I., Izumiyama-Shimomura, N., Sawabe, M., Arai, T., Aoyagi, Y., Fujiwara, M., Sasajima, K., Nakachi, K., & Takubo, K. (2002). Comparative analysis of telomere lengths and erosion with age in human epidermis and lingual epithelium. *Journal of Investigative Dermatology*, *119*(5), 1014–1019. https://doi.org/10.1046/j.1523-1747.2002.19523.x

Nassour, J., Martien, S., Martin, N., Deruy, E., Tomellini, E., Malaquin, N., Bouali, F., Sabatier, L., Wernert, N., Pinte, S., Gilson, E., Pourtier, A., Pluquet, O., & Abbadie, C. (2016). Defective DNA single-strand break repair is responsible for senescence and neoplastic escape of epithelial cells. *Nature Communications*, *7*, 1–16. https://doi.org/10.1038/ncomms10399

O'Brien, D. M., Min, K., Larsen, T., & Tatar, M. (2008). Use of stable isotopes to examine how dietary restriction extends Drosophila lifespan. *Current Biology*, *18*, 155–156.

Oláh, A., Markovics, A., Szabó-Papp, J., Szabó, P. T., Stott, C., Zouboulis, C. C., & Bíró, T. (2016). Differential effectiveness of selected non-psychotropic phytocannabinoids on human sebocyte functions implicates their introduction in dry/seborrhoeic skin and acne treatment. *Experimental Dermatology*, *25*(9), 701–707. https://doi.org/10.1111/exd.13042

Oláh, A., Szabó-Papp, J., Soeberdt, M., Knie, U., Dähnhardt-Pfeiffer, S., Abels, C., & Bíró, T. (2017). Echinacea purpurea-derived alkylamides exhibit potent anti-inflammatory effects and alleviate clinical symptoms of atopic eczema. *Journal of Dermatological Science*, *88*(1), 67–77. https://doi.org/10.1016/j.jdermsci.2017.05.015

Oláh, A., Tóth, B. I., Borbíró, I., Sugawara, K., Szöllõsi, A. G., Czifra, G., Pál, B., Ambrus, L., Kloepper, J., Camera, E., Ludovici, M., Picardo, M., Voets, T., Zouboulis, C. C., Paus, R., & Bíró, T. (2014). Cannabidiol exerts sebostatic and antiinflammatory effects on human sebocytes. *Journal of Clinical Investigation*, *124*(9), 3713–3724. https://doi.org/10.1172/JCI64628

Olovnikov, A. M. (1973). A theory of marginotomy. The incomplete copying of template margin in enzymic synthesis of polynucleotides and biological significance of the phenomenon. *Journal of Theoretical Biology*, *41*(1), 181–190. https://doi.org/10.1016/0022-5193(73)90198-7

Olovnikov, A. M. (1996). Telomeres, telomerase, and aging: Origin of the theory. *Experimental Gerontology*, *31*(4), 443–448. https://doi.org/10.1016/0531-5565(96)00005-8

Orgel, L. E. (1963). The maintenance of the accuracy of protein synthesis and its relevance to ageing. *Proceedings of the National Academy of Sciences of the United States of America*, *49*(4), 517–521. https://doi.org/10.1073/pnas.49.4.517

Pagliari, C., & Sotto, M. N. (2002). Correlation of factor XIIIa+ dermal dendrocytes with paracoccidioidomycosis skin lesions. *Medical Mycology*, *40*(4), 407–410. https://doi.org/10.1080/mmy.40.4.407.410

Pal, D., & Sen, C. K. (2019). MicroRNAs in skin development, function and disorders. In P. V. Peplow, B. Martinez, G. A. Calin, & A. Esquela-Kerscher (Eds.), *MicroRNAs in diseases and disorders: emerging therapeutic targets* (1st ed., Vol. 6, pp. 275–292). Royal Society of Chemistry. https://doi.org/10.1039/9781788016421-00275

Pan, Y., Lin, M. H., Tian, X., Cheng, H. T., Gridley, T., Shen, J., & Kopan, R. (2004). γ-Secretase functions through Notch signaling to maintain skin appendages but is not required for their patterning or initial morphogenesis. *Developmental Cell*, *7*(5), 731–743. https://doi.org/10.1016/j.devcel.2004.09.014

Partridge, L. (2010). The new biology of ageing. *Philosophical Transactions of the Royal Society B: Biological Sciences*, *365*(1537), 147–154. https://doi.org/10.1098/rstb.2009.0222

Pedro De Magalhães, J. (2004). From cells to ageing: A review of models and mechanisms of cellular senescence and their impact on human ageing. *Experimental Cell Research*, *300*(1), 1–10. https://doi.org/10.1016/j.yexcr.2004.07.006

Pontis, S., Ribeiro, A., Sasso, O., & Piomelli, D. (2016). Macrophage-derived lipid agonists of PPAR-α as intrinsic controllers of inflammation. *Critical Reviews in Biochemistry and Molecular Biology 51*(1), 7–14. https://doi.org/10.3109/10409238.2015.1092944

Pucci, M., Pasquariello, N., Battista, N., di Tommaso, M., Rapino, C., Fezza, F., Zuccolo, M., Jourdain, R., Agrò, A. F., Breton, L., & Maccarrone, M. (2012). Endocannabinoids stimulate human melanogenesis via type-1 cannabinoid receptor. *Journal of Biological Chemistry*, *287*(19), 15466–15478. https://doi.org/10.1074/jbc.M111.314880

Qin, D., Ren, R., Jia, C., Lu, Y., Yang, Q., Chen, L., Wu, X., Zhu, J., Guo, Y., Yang, P., Zhou, Y., Zhu, N., Bi, B., & Liu, T. (2018). Rapamycin protects skin fibroblasts from ultraviolet B-induced photoaging by suppressing the production of reactive oxygen species. *Cellular Physiology and Biochemistry*, *46*(5), 1849–1860. https://doi.org/10.1159/000489369

Ramis, M. R., Esteban, S., Miralles, A., Tan, D. X., & Reiter, R. J. (2015). Caloric restriction, resveratrol and melatonin: Role of SIRT1 and implications for aging and related diseases. *Mechanisms of Ageing and Development 146–148*, 28–41. Elsevier Ireland Ltd. https://doi.org/10.1016/j.mad.2015.03.008

Rattan, S. I. S. (2006). Theories of biological aging: Genes, proteins, and free radicals. *Free Radical Research*, *40*(12), 1230–1238. https://doi.org/10.1080/10715760600911303

Rattan, S. I. S. (2016). Origins of the Hayflick system, the phenomenon and the limit. In Suresh I.S. Rattan & L. Hayflick (Eds.), *Cellular Ageing and Replicative Senescence.*

Healthy Ageing and Longevity (pp. 3–14). Springer, Cham. https://doi.org/10.1007/978-3-319-26239-0_1

Río, C. del, Millán, E., García, V., Appendino, G., DeMesa, J., & Muñoz, E. (2018). The endocannabinoid system of the skin. A potential approach for the treatment of skin disorders. *Biochemical Pharmacology*, *157*(August), 122–133. https://doi.org/10.1016/j.bcp.2018.08.022

Rittié, L., & Fisher, G. J. (2015). Natural and sun-induced aging of human skin. *Cold Spring Harbor Perspectives in Medicine*, *5*(1), a015370. https://doi.org/10.1101/cshperspect.a015370

Roche, R., Hoareau, L., Bes-Houtmann, S., Gonthier, M. P., Laborde, C., Baron, J. F., Haffaf, Y., Cesari, M., & Festy, F. (2006). Presence of the cannabinoid receptors, CB1 and CB2, in human omental and subcutaneous adipocytes. *Histochemistry and Cell Biology*, *126*(2), 177–187. https://doi.org/10.1007/s00418-005-0127-4

Sarcar, S., Munteanu, C., Jokinen, J. P. P., Oulasvirta, A., Silpasuwanchai, C., Charness, N., Dunlop, M., & Ren, X. (2017). Designing mobile interactions for the ageing populations. *Proceedings of the 2017 CHI Conference Extended Abstracts on Human Factors in Computing Systems - CHI EA '17*, 506–509. https://doi.org/10.1145/3027063.3027074

Scholl, F. A., Dumesic, P. A., Barragan, D. I., Harada, K., Bissonauth, V., Charron, J., & Khavari, P. A. (2007). Mek1/2 MAPK kinases are essential for mammalian development, homeostasis, and Raf-induced hyperplasia. *Developmental Cell*, *12*(4), 615–629. https://doi.org/10.1016/j.devcel.2007.03.009

Scialo, F., Sriram, A., Stefanatos, R., Spriggs, R. V, Samantha, H. Y., Martins, L. M., & Sanz, A. (2020). Mitochondrial complex I derived ROS regulate stress adaptation in *Drosophila melanogaster*. *Redox Biology*, *32*, 101450. https://doi.org/10.1016/j.redox.2020.101450

Senoo, M., Pinto, F., Crum, C. P., & McKeon, F. (2007). p63 is essential for the proliferative potential of stem cells in stratified epithelia. *Cell*, *129*(3), 523–536. https://doi.org/10.1016/j.cell.2007.02.045

Kang, S. (2019). *Fitzpatrick's Dermatology* (Kang S., Amagai M., A. H. E. Bruckner A. L., Margolis D. J., McMichael A. J., & Orringer J. S., Eds.; 9th ed.). McGraw-Hill Education.

Shay, J. W., & E. Wright, W. (2000). Hayflick, his limit, and cellular ageing. *Nature Reviews Molecular Cell Biology*, *1*(1), 72–76. https://doi.org/10.1038/35036093

Shetty, A. K., Kodali, M., Upadhya, R., & Madhu, L. N. (2018). Emerging anti-aging strategies – Scientific basis and efficacy. *Aging and Disease*, *9*(6), 1165–1184. International Society on Aging and Disease. https://doi.org/10.14336/AD.2018.1026

Shi-Wen, X., Eastwood, M., Stratton, R. J., Denton, C. P., Leask, A., & Abraham, D. J. (2010). Rosiglitazone alleviates the persistent fibrotic phenotype of lesional skin scleroderma fibroblasts. *Rheumatology*, *49*(2), 259–263. https://doi.org/10.1093/rheumatology/kep371

Sinclair, J. (2016). An introduction to cannabis and the endocannabinoid system. *Australian Journal of Herbal Medicine*, *28*(4), 107–117.

Singhvi, G., Manchanda, P., Rapalli, V. K., Dubey, S. K., Gupta, G., & Dua, K. (2018). MicroRNAs as biological regulators in skin disorders. *Biomedicine & Pharmacotherapy*, *108*(September), 996–1004. https://doi.org/10.1016/j.biopha.2018.09.090

Sivesind, T. E., Maghfour, J., Rietcheck, H., Kamel, K., Malik, A. S., & Dellavalle, R. P. (2022). Cannabinoids for the treatment of dermatologic conditions. *JID Innovations*, *2*(2), 100095. https://doi.org/10.1016/j.xjidi.2022.100095

Son, J. M., & Lee, C. (2019). Mitochondria: Multifaceted regulators of aging. *BMB Reports*, *52*(1), 13–23. https://doi.org/10.5483/BMBRep.2019.52.1.300

Soydas, T., Sayitoglu, M., Sarac, E. Y., Cınar, S., Solakoglu, S., Tiryaki, T., & Sultuybek, G. K. (2021). Metformin reverses the effects of high glucose on human dermal fibroblasts of aged skin via downregulating RELA/p65 expression. *Journal of Physiology and Biochemistry*, *77*(3), 443–450. https://doi.org/10.1007/s13105-021-00823-y

Soydas, T., Yaprak Sarac, E., Cinar, S., Dogan, S., Solakoglu, S., Tuncdemir, M., & Kanigur Sultuybek, G. (2018). The protective effects of metformin in an in vitro model of aging 3T3 fibroblast under the high glucose conditions. *Journal of Physiology and Biochemistry*, *74*(2), 273–281. https://doi.org/10.1007/s13105-018-0613-5

Spector, M. (2018). Biomedical materials to meet the challenges of the aging epidemic. *Biomedical Materials (Bristol)*, *13*(3), 1–3. https://doi.org/10.1088/1748-605X/aab171

Ständer, S., Schmelz, M., Metze, D., Luger, T., & Rukwied, R. (2005). Distribution of cannabinoid receptor 1 (CB1) and 2 (CB2) on sensory nerve fibers and adnexal structures in human skin. *Journal of Dermatological Science*, *38*(3), 177–188. https://doi.org/10.1016/j.jdermsci.2005.01.007

Sugimoto, M., Yamashita, R., & Ueda, M. (2006). Telomere length of the skin in association with chronological aging and photoaging. *Journal of Dermatological Science*, *43*(1), 43–47. https://doi.org/10.1016/j.jdermsci.2006.02.004

Sunderland, N., Skroblin, P., Barwari, T., Huntley, R. P., Lu, R., Joshi, A., Lovering, R. C., & Mayr, M. (2017). MicroRNA biomarkers and platelet reactivity: the clot thickens. *Circulation Research*, *120*(2), 418–435. https://doi.org/10.1161/CIRCRESAHA.116.309303

Szilard, L. (1959). On the nature of the aging process. *Proceedings of the National Academy of Sciences of the United States of America*, *45*(1), 30–45. https://doi.org/10.1073/pnas.45.1.30

Szweda, P. A., Camouse, M., Lundberg, K. C., Oberley, T. D., & Szweda, L. I. (2003). Aging, lipofuscin formation, and free radical-mediated inhibition of cellular proteolytic systems. *Ageing Research Reviews*, *2*(4), 383–405. https://doi.org/10.1016/S1568-1637(03)00028-X

Tan, D.-X. (2019). Aging: an evolutionary competition between host cells and mitochondria. *Medical Hypotheses*, *127*(April), 120–128. https://doi.org/10.1016/j.mehy.2019.04.007

Telek, A., Bíró, T., Bodó, E., Tóth, B. I., Borbíró, I., Kunos, G., & Paus, R. (2007). Inhibition of human hair follicle growth by endo-and exocannabinoids. *The FASEB Journal*, *21*(13), 3534–3541. https://doi.org/10.1096/fj.06-7689com

Thoppil, H., & Riabowol, K. (2020). Senolytics: A translational bridge between cellular senescence and organismal aging. *Frontiers in Cell and Developmental Biology*, *7*, 367. Frontiers Media S.A. https://doi.org/10.3389/fcell.2019.00367

Thulabandu, V., Chen, D., & Atit, R. P. (2018). Dermal fibroblast in cutaneous development and healing. *Wiley Interdisciplinary Reviews: Developmental Biology*, *7*(2), 1–13. https://doi.org/10.1002/wdev.307

Tigges, J., Krutmann, J., Fritsche, E., Haendeler, J., Schaal, H., Fischer, J. W., Kalfalah, F., Reinke, H., Reifenberger, G., Stühler, K., Ventura, N., Gundermann, S., Boukamp, P., & Boege, F. (2014). The hallmarks of fibroblast ageing. *Mechanisms of Ageing and Development*, *138*, 26–44. https://doi.org/10.1016/j.mad.2014.03.004

Tóth, B. I., Dobrosi, N., Dajnoki, A., Czifra, G., Oláh, A., Szöllsi, A. G., Juhász, I., Sugawara, K., Paus, R., & Bíró, T. (2011). Endocannabinoids modulate human epidermal keratinocyte proliferation and survival via the sequential engagement of cannabinoid receptor-1 and transient receptor potential vanilloid-1. *Journal of Investigative Dermatology*, *131*(5), 1095–1104. https://doi.org/10.1038/jid.2010.421

Tóth, K. F., Ádám, D., Bíró, T., & Oláh, A. (2019). Cannabinoid signaling in the skin: Therapeutic potential of the "c(ut)annabinoid" system. *Molecules*, *24*(5), 1–56. https://doi.org/10.3390/molecules24050918

Toutfaire, M., Bauwens, E., & Debacq-Chainiaux, F. (2017). The impact of cellular senescence in skin ageing: A notion of mosaic and therapeutic strategies. *Biochemical Pharmacology*, *142*, 1–12. https://doi.org/10.1016/j.bcp.2017.04.011

Umansky, S. (2018). Aging and aging-associated diseases: A microRNA-based endocrine regulation hypothesis. *Aging*, *10*(10), 2557–2569. https://doi.org/10.18632/aging.101612

Vaupel, J. W. (2010). Biodemography of human ageing. *Nature*, *464*(7288), 536–542. https://doi.org/http://dx.doi.org/10.1038/nature08984

Waldera Lupa, D. M., Kalfalah, F., Safferling, K., Boukamp, P., Poschmann, G., Volpi, E., Götz-Rösch, C., Bernerd, F., Haag, L., Huebenthal, U., Fritsche, E., Boege, F., Grabe, N., Tigges, J., Stühler, K., & Krutmann, J. (2015). Characterization of skin aging-associated secreted proteins (SAASP) produced by dermal fibroblasts isolated from intrinsically aged human skin. *Journal of Investigative Dermatology*, *135*(8), 1954–1968. https://doi.org/10.1038/jid.2015.120

Walford, R. L. (1964). The immunologic theory of aging. *The Gerontologist*, *4*(4), 195–197. https://doi.org/10.1093/geront/4.4.195

Wallace, D. C. (2001). Mitochondrial defects in neurodegenerative disease. *Mental Retardation and Developmental Disabilities Research Reviews*, *7*(3), 158–166. https://doi.org/10.1002/mrdd.1023

Watson, J. D. (1972). Origin of concatemeric T7DNA. *Nature New Biology*, *239*(94), 197–201. https://doi.org/10.1038/newbio239197a0

Wensink, M. J., Wrycza, T. F., & Baudisch, A. (2014). No senescence despite declining selection pressure: Hamilton's result in broader perspective. *Journal of Theoretical Biology*, *347*(1), 176–181. https://doi.org/10.1016/j.jtbi.2013.11.016

WHO. (2018). *Ageing and health*. World Health Organization. https://www.who.int/news-room/fact-sheets/detail/ageing-and-health

WHO. (2021). *World health statistics 2021: monitoring health for the SDGs, sustainable development goals*.

Wiley, C. D., & Campisi, J. (2016). From ancient pathways to aging cells - connecting metabolism and cellular senescence. *Cell Metabolism*, *23*(6), 1013–1021. https://doi.org/10.1016/j.cmet.2016.05.010

Williams, G. C. (1957). Pleiotropy, natural selection, and the evolution of senescence. *Evolution*, *11*(4), 398–411. https://doi.org/10.2307/2406060

Wilson, D. M., Errasti-Ibarrondo, B., & Low, G. (2019). Where are we now in relation to determining the prevalence of ageism in this era of escalating population ageing ? *Ageing Research Reviews*, *51*(February), 78–84. https://doi.org/10.1016/j.arr.2019.03.001

Wisnovsky, S., Jean, S. R., Liyanage, S., Schimmer, A., & Kelley, S. O. (2016). Mitochondrial DNA repair and replication proteins revealed by targeted chemical probes. *Nature Chemical Biology*, *12*(7), 567–573. https://doi.org/10.1038/nchembio.2102

Wlaschek, M., Tantcheva-Poór, I., Naderi, L., Ma, W., Schneider, L. A., Razi-Wolf, Z., Schüller, J., & Scharffetter-Kochanek, K. (2001). Solar UV irradiation and dermal photoaging. *Journal of Photochemistry and Photobiology B: Biology*, *63*(1–3), 41–51. https://doi.org/10.1016/S1011-1344(01)00201-9

Włodarczyk, M., Sobolewska, A., Lesiak, A., & Narbutt, J. (2014). The role of factor XIII-A in the development of inflammatory skin lesions. *Central European Journal of Biology*, *9*(9), 869–873. https://doi.org/10.2478/s11535-014-0319-9

Wohlman, I. M., Composto, G. M., Heck, D. E., Heindel, N. D., Lacey, C. J., Guillon, C. D., Casillas, R. P., Croutch, C. R., Gerecke, D. R., Laskin, D. L., Joseph, L. B., & Laskin, J. D. (2016). Mustard vesicants alter expression of the endocannabinoid system in mouse skin. *Toxicology and Applied Pharmacology*, *303*, 30–44. https://doi.org/10.1016/j.taap.2016.04.014

Xing, C., Zhuang, Y., Xu, T. H., Feng, Z., Zhou, X. E., Chen, M., Wang, L., Meng, X., Xue, Y., Wang, J., Liu, H., McGuire, T. F., Zhao, G., Melcher, K., Zhang, C., Xu, H. E., & Xie, X. Q. (2020). Cryo-EM structure of the human cannabinoid receptor CB2-Gi signaling complex. *Cell*, *180*(4), 645-654.e13. https://doi.org/10.1016/j.cell.2020.01.007

Yamagishi, S., Fukami, K., & Matsui, T. (2015). Evaluation of tissue accumulation levels of advanced glycation end products by skin autofluorescence: A novel marker of vascular complications in high-risk patients for cardiovascular disease. *International Journal of Cardiology*, *185*, 263–268. https://doi.org/10.1016/j.ijcard.2015.03.167

Yamamoto, N., Tanigaki, K., Han, H., Hiai, H., & Honjo, T. (2003). Notch/RBP-J signaling regulates epidermis/hair fate determination of hair follicular stem cells. *Current Biology*, *13*(4), 333–338. https://doi.org/10.1016/s0960-9822(03)00081-2

Yang, Z., Jiang, S., Shang, J., Jiang, Y., Dai, Y., Xu, B., & Yu, Y. (2019). LncRNA: Shedding light on mechanisms and opportunities in fibrosis and aging. *Ageing Research Reviews*, *52*(April), 17–31. https://doi.org/10.1016/j.arr.2019.04.001

Yasukawa, T., & Kang, D. (2018). An overview of mammalian mitochondrial DNA replication mechanisms. *Journal of Biochemistry*, *164*(3), 183–193. https://doi.org/10.1093/jb/mvy058

Yee, C., Yang, W., & Hekimi, S. (2014). The intrinsic apoptosis pathway mediates the pro-longevity response to mitochondrial ROS in C. elegans. *Cell*, *157*(4), 897–909. https://doi.org/10.1016/j.cell.2014.02.055

Yessenkyzy, A., Saliev, T., Zhanaliyeva, M., Masoud, A. R., Umbayev, B., Sergazy, S., Krivykh, E., Gulyayev, A., & Nurgozhin, T. (2020). Polyphenols as caloric-restriction mimetics and autophagy inducers in aging research. *Nutrients*, *12*(5), 1344. MDPI AG. https://doi.org/10.3390/nu12051344

Yi, R., O'Carroll, D., Pasolli, H. A., Zhang, Z., Dietrich, F. S., Tarakhovsky, A., & Fuchs, E. (2006). Morphogenesis in skin is governed by discrete sets of differentially expressed microRNAs. *Nature Genetics*, *38*(3), 356–362. https://doi.org/10.1038/ng1744

Yoshizaki, A., Yanaba, K., Yoshizaki, A., Iwata, Y., Komura, K., Ogawa, F., Takenaka, M., Shimizu, K., Asano, Y., Hasegawa, M., Fujimoto, M., & Sato, S. (2010). Treatment with rapamycin prevents fibrosis in tight-skin and bleomycin-induced mouse models of

systemic sclerosis. *Arthritis and Rheumatism*, *62*(8), 2476–2487. https://doi.org/10.1002/art.27498

Zarse, K., Schmeisser, S., Groth, M., Priebe, S., Beuster, G., Kuhlow, D., Guthke, R., Platzer, M., Kahn, C. R., & Ristow, M. (2012). Impaired insulin/IGF1 signaling extends life span by promoting mitochondrial L-proline catabolism to induce a transient ROS signal. *Cell Metabolism*, *15*(4), 451–465. https://doi.org/10.1016/j.cmet.2012.02.013

Zhavoronkov, A., Mamoshina, P., Vanhaelen, Q., Scheibye-knudsen, M., Moskalev, A., & Aliper, A. (2019). Artificial intelligence for aging and longevity research: Recent advances and perspectives. *Ageing Research Reviews*, *49*(September 2018), 49–66. https://doi.org/10.1016/j.arr.2018.11.003

Zhu, M., Meng, P., Ling, X., & Zhou, L. (2020). Advancements in therapeutic drugs targeting of senescence. *Therapeutic Advances in Chronic Disease*, *11*, 1–26. https://doi.org/10.1177/2040622320964125

Ziegler, D. V, Wiley, C. D., & Velarde, C. (2015). Mitochondrial effectors of cellular senescence: Beyond the free radical theory of aging. *Aging Cell*, *14*(1), 1–7. https://doi.org/10.1111/acel.12287

Zjacic-Rotkvic, V., Kavur, L., & Cigrovski-Berkovic, M. (2010). Hormones and aging. *Acta Clinica Croatica*, *49*(4), 549–554. https://doi.org/10.1016/s0531-5565(96)00055-1

Zs.-Nagy, I. (2014). Aging of cell membranes: facts and theories. *Interdisciplinary Topics in Gerontology*, *39*, 62–85. https://doi.org/10.1159/000358900

CHAPTER 2: MODELING OF THE SKIN FIBROBLASTS' SENESCENCE-ASSOCIATED PHENOTYPE

2.1. ABSTRACT

Modern understanding of aging is based on the accumulation of cellular damage during the life span due to the gradual deterioration of regenerative mechanisms in response to the continuous effect of stress, lifestyle, and environmental factors, followed by increased morbidity and mortality. Simultaneously, aging organisms exponentially accumulate the number of senescent cells. Cell culture models are valuable tools to investigate the mechanisms of aging by inducing cellular senescence in stress-induced premature senescence (SIPS) models. Here, we explain the three-step and one-step H_2O_2-induced senescence models of SIPS designed and reproduced on different dermal fibroblasts cell-line (CCD-1064Sk, CCD-1135Sk, and BJ-5ta). In both SIPS models, it was evident that the fibroblasts developed similar aging characteristics as cells with replicative senescence. Among the most noticeable senescent biomarkers were the increased β-gal expression, high level of p21 protein, altered levels of cell-cycle regulators (i.e., CDK2 and c-Jun), compromised extracellular matrix (ECM) composition, reduced cellular viability, and delayed wound healing properties. Based on the significant increase in senescence biomarkers in fibroblast cultures, along with the reduced functional and metabolic activity, the one-step senescence model was chosen as a feasible and reliable method for future testing of antiaging compounds.

2.2. INTRODUCTION

2.2.1. Main hallmarks of cutaneous aging

Aging can be viewed as the accumulation of consecutive changes over time in response to stress, lifestyle, and environmental factors, ultimately causing irreparable damage and maladaptation in the function of cells, ECM, cell communication, intercellular signalling, etc., leading to age-related diseases and death (Boraldi et al., 2010; Kalfalah et al., 2014). Cutaneous aging is a complex phenomenon involving two simultaneously occurring processes: an intrinsic one, known as *chronological aging*, which is genetically determined, and *extrinsic aging* which is due to environmental factors such as chronic sun exposure, known as *photoaging* (Dudonné et al., 2011). It is manifested by the gradual process of wrinkles development, skin sagging and drooping. The naturally (intrinsically) aged skin looks dry and has fine wrinkles, but it is still smooth and light (Tobin, 2017). In contrast, the extrinsically photo-aged skin has thick layers ("leathery aspect") and rough wrinkles with pigmentation ("age-spots", which are actinic lentigines) and capillary telangiectasia (Berneburg et al., 2004; Kang et al., 2017; Toutfaire et al., 2017).

The are several biomarkers of senescence that could be detected in all somatic cells. The most well-known among them are: (i) senescence-associated beta-galactosidase (β-Gal) activity, (ii) the overexpression of cell cycle arrest proteins such as p16, p21, p53, (iii) the depletion of mitochondrial DNA (mtDNA), (iv) changes in the expression of senescence-associated microRNAs, (v) telomere attrition, (vi) and decreased expression of Ki-67 protein, which is associated with cell proliferation (Bertschmann et al., 2019; Kemp et al., 2017; Lin'kova et al., 2016; Toutfaire et al., 2017).

2.2.2. Fibroblasts as a cornerstone of dermal functional stability

Among all cutaneous layers, the dermis is the target source for current anti-aging and rejuvenation therapies. This dermal layer is rich in fibroblasts which produce ECM or skin scaffold, which mainly consists of collagen, elastin, and hyaluronic acid (Rittié & Fisher, 2015). Older skin demonstrates exhaustion of all these ECM components. Age-related increases in matrix metalloproteinases (MMPs) production are directly responsible for collagen degradation leading to a decline in collagen content at about 2% per year (Ashcroft et al., 1997; Farage et al., 2017). Dermal fibroblasts experience an alteration in the keeping of equilibrium between the synthesis of collagen and the synthesis of collagen-degrading enzymes under the influence of various stressors throughout life with further enhancement of dermal structural impairment (Varani et al., 2006). Moreover, increased accumulation of degraded collagen fibers works as entrapment that manifests itself in the reduction of fibroblast functional quality and quantity; likewise, a decline in collagen and other ECM proteins renewal capacity is observed with age (Farage et al., 2017). This is why a detailed analysis of fibroblast function is important to understand the pathogenesis of aging.

Fibroblasts represent the most abundant and permanent cell component of the connective tissue. They continuously produce and release glycoproteins, proteoglycans, and multiple precursor molecules of different fiber structures of ECM. The production of these macromolecules by fibroblasts are utilized to generate elastic fibers and various collagen types which are then embedded in an amorphous gelatinous material composed chiefly of proteoglycans, water, and minerals. Thus, the structural components of the basal membrane contain various types of collagen proteins. For instance, type III collagen is a

part of reticular fibers and is present in the reticular lamina, while the basal lamina has type IV collagen. The basement membrane contains other fibroblast products like fibronectin and heparan sulfate proteoglycans. In contrast to collagen and reticular fibers, elastic fibers lack collagen protein (Kierszenbaum & Tres, 2019).

Fibroblasts express vimentin, which is used as a marker to distinguish cells of mesodermal origin. Periadnexal skin fibroblasts typically demonstrate CD10 immunoreactivity. It is essential to mention that active fibroblasts exhibit myofibroblasts' ultrastructural and immunohistochemical features during wound healing (Eyden, 2001). Furthermore, apart from vimentin, myofibroblasts may express desmin and smooth muscle actin, which is vital for regeneration purposes (Elder et al., 2015).

In summary, fibroblasts produce and regenerate components of ECM, participate in wound healing and like other cells, deteriorate in functional capabilities with age. Consequently, cultured human diploid fibroblasts (HDF) have become popular *in vitro* cell systems in types of research designed to study conditions associated with alterations in replicative potentials, such as cancer or senescence. The limited replicative ability of HDF makes them a suitable model for cellular aging and potentially for rejuvenation studies. Moreover, senescent fibroblasts exert distinct morphology and diminished metabolic and functional qualities.

2.2.3. Models of cellular senescence

Present-day studies in the field of biogerontology interchangeably use the terms *cell senescence*, *cellular aging*, and *replicative senescence* for utilizing normal diploid cells in culture, which undergo a multitude of changes during serial sub-cultivation resulting in the permanent termination of cell division known as the *Hayflick limit* (Rattan, 2016). The

in vitro studies of age-related changes in the physiology, biochemistry, mechanobiology, and molecular biology of cultured cells have considerably boosted the understanding of the fundamental principles of cellular senescence. Numerous *in vitro* models have been proposed to explain the aging process via cellular senescence, but none of them appear to be fully comprehensive.

In 1961, Hayflick and Moorhead described the first model based on serial passaging of fibroblasts in culture that was considered as the process of cellular aging; it resulted in the end-stage irreversible growth arrest in G1/G0, known as replicative senescence (RS). In this state, cells are alive, exhibit low level of metabolic activity, and generally resist undergoing apoptosis (Campisi & D'Adda Di Fagagna, 2007; Rattan, 2016). Thus, these cells are *in vitro* senescent aged cells and are one of the widely used cellular aging models. Interestingly, the intrinsic limit of divisions resulting in RS directly correlated with the duration of the replicative lifespan of cultured cells. It was observed that cells from older organisms reach RS faster due to diminished *in vitro* replicative capacity than those from younger organisms, which needed a multitude of subcultures to do so (Ott et al., 2018). Thus, induction of RS is a continuous long-term process of cell passaging that might take anywhere from a few months up to a year, or even longer, and require expensive maintenance. Considering this, most research groups are looking into models of cellular senescence that does not require waiting for the replicative limit to be reached.

At the end of the last century, Toussaint and Remarcle (1995) presented research data showing that cellular aging can be accelerated by using a wide range of non-lethal stressors and proposed the term stress-induced premature senescence (SIPS) typically based on the principles of oxidative stress (Brack et al., 2000; Toussaint et al., 1995, 2000). In accordance with multiple experimental data and theoretical studies fibroblasts,

keratinocytes, melanocytes, or umbilical vascular endothelial cells were exposed to chronic and acute oxidative stress protocols including sublethal stresses such as UV, hyperoxia, hypoxia, hydrogen peroxide, ethanol, bleomycin, mitomycin C (Chen et al., 1995; Ott et al., 2018; Toussaint et al., 2000). To date, HDFs are routinely used as a "gold standard" for *in vitro* senescence research. Of note, there are seven morphological types of HDFs: three mitotic fibroblast (MF) types called MF I, MF II, and MF III, and four postmitotic fibroblast (PMF) types called PMF IV, V, VI, and VII. Shifts in the frequencies of the mitotic and postmitotic fibroblasts in mass populations are accompanied by alterations in the [35S]-methionine polypeptide pattern of the developing mass populations (Bayreuther et al., 1988). These types are used in SIPS models during *in vivo* and *in vitro* aging studies.

Most of the experimental setups for SIPS models depend on the cell type and are modulated via single or multiple applications of designated stressors for diverse periods of time in subcytotoxic doses. Advantages of those models were highlighted by high feasibility, low cellular recovery, fast exhaustion of the replicative potential, and eventually irreversible growth arrest that allowed reduced time and cost maintenance. Albeit the stressors mentioned above have many advantages, neither of them are optimal to reflect all mechanisms involved in cellular senescence.

Among commonly used SIPS models are:

a) Ultraviolet light exposure.

It is generally accepted that effects of chronic solar insolation have been mostly attributed to the deleterious impact of ultra-violet (UV) radiation involving a combination of UVB (280–320 nm) and UVA (320–400 nm) (Marionnet et al., 2010). UV radiation has long been known to generate photoproducts in genomic DNA, which promote genetic

mutations that drive premature aging based on enhancing fibroblasts' senescence process, apoptotic sunburn keratinocytes, and cutaneous carcinogenesis (Kemp et al., 2017; Toutfaire et al., 2017).

According to Batista (2009), the sunlight spectrum contains 45% of UV light. Daily, humans are typically exposed to the UV wavelengths of sunlight that are primarily composed of UVA (90%–95%) and UVB (5%–10%). These wavelengths of light are absorbed by multiple cellular molecules, including genomic DNA (Berneburg et al., 2004; Marionnet et al., 2010). The most dangerous for cells are short-wave radiation (UVB under 300 nm and UVC). Short-wave radiation can damage DNA because their wavelengths coincide with the absorption spectra of DNA, RNA, and proteins (Gebhard et al., 2014). UV exposure results in bulky lesions such as cyclobutane pyrimidine dimers (CPDs) and 6-4 photoproducts (6-4 PPs) (Kemp et al., 2017).

CPD formation occurs preferentially at thymine-containing dipyrimidine sites and likely also at methyl CpG-associated dipyrimidine sites, which include the TCG sequence (Ikehata, 2018), and can lead directly or indirectly to DNA strand breaks that induce mutations and neoplastic transformation (Debacq-Chainiaux et al., 2012). It is known that both CPDs and 6-4PPs are generated by UVB wavelengths of light, however, DNA absorbs UVC light more effectively than UVB. CPD formation could be also stimulated by UVA through direct photon absorption and via a chemiexcitation in the skin. The latter is based on reactive oxygen and nitrogen compounds created by the combination of electron excitation by UVA in melanin fragments that ultimately stimulate genomic DNA to induce CPD production (Douki et al., 2003).

UVB exposure in subcytotoxic doses of 250 mJ/cm^2 (doses of 375 mJ/cm^2 are cytotoxic) is a popular method to induce SIPS. It triggers enhanced β-gal activity, HDFs

growth arrest, mediated by overexpression of p53, p21, and p16 as well as mitochondrial DNA deletions (Debacq-Chainiaux et al., 2012; Gebhard et al., 2014; Greussing et al., 2013; Huang et al., 2013). DNA photodamage and the subsequent formation of mainly CPDs and other photoproducts were indicated as predominant pathogenic factors in DNA alterations, causing both transient and permanent genotoxicity followed by declined proliferative potential and growth arrest (Kang et al., 2017; Marionnet et al., 2010).

b) *X-ray and γ-irradiation.*

It is important to note that X-rays and gamma rays have the same characteristics and health effects but originate from different subatomic processes. Gamma rays are generated inside the nucleus, while X-rays are emitted from processes outside the nucleus. In γ-irradiation models, cells or animals are exposed to the γ-radiation that induces DNA damage and double-strand breaks followed by SIPS development. It was previously reported that umbilical vein endothelial cells exposed to 2 - 4 Gy (applied via a Cs^{137} γ-ray source at a dose rate of 2.82 Gy per minute) exhibit a variety of senescence features such as changes in cell architecture, β-gal activity elevation, and suppression of angiogenic activity in human (Kim et al., 2014). Data generated in our laboratory showed the appearance of senescence-associated alterations in different internal organs of mice (i.e., skin, spleen, liver, brain, gonads) after a single exposure (acute or fractionated) to 0.5 Gy of X-rays (Dickey et al., 2011; Ilnytskyy et al., 2009; Kovalchuk et al., 2004; Sidler, Li, et al., 2014). Induced changes corresponded to previously mentioned typical morphological, biomolecular, and genetic alterations found in SIPS.

c) *Mitomycin C, Bleomycin, or Actinomycin D induced SIPS.*

Antibiotics such as mitomycin C, bleomycin, and actinomycin D can induce DNA-crosslinking and inhibit RNA and protein synthesis by alkylation. When mitomycin C was

used on proliferative cells such as lung and skin fibroblasts, endothelial cells, melanocytes, and retinal pigment epithelial cells, DNA damage occurred after a 48 h exposure at a concentrations of 0.2 μM (De Magalhães, 2004; Rodemann, 1989). Furthermore, 12 h applications of actinomycin (0.04 mg/ml) or bleomycin sulfate (0.06 units/ml) were reported to induce senescence hallmarks (i.e., increasing the expression of both p21 and p16) (Robles & Adami, 1998).

d) *Hydrogen peroxide (H_2O_2).*

Oxidative stress induced by H_2O_2 is one of the most popular and reproducible models of cellular senescence. H_2O_2 causes DNA strand breaks and activates poly (APD-ribose) polymerase, leading to depletion of the cellular pool of NAD+ and ATP (Kirkland, 1991). The excessive amount of reactive oxygen species (ROS) produced from H_2O_2 damages the cellular membrane, decreases antioxidant activity, and more vigorously potentiates endogenous free radical generation (see Chapter 1).

The effectiveness of the H_2O_2-induced premature senescence model depends on the cell-line type, maintaining procedures, dose, time of exposure, and kind H_2O_2 solvent (i.e., cultured medium, phosphate buffered saline (PBS)).

Sanders and colleagues treated HDF with 100 or 200 mM H_2O_2 for 2 hours in a fresh cell culture medium (Sanders et al., 2013). Another group exposed neonatal foreskin fibroblasts to different concentrations of H_2O_2 (0-100 μM) diluted in PBS. Following incubation with H_2O_2, cells were washed with PBS and grown for an additional 48 hours (Shlush et al., 2011). They indicated 25 μM H_2O_2 as an optimal concentration for SIPS induction based on the typical senescence biomolecular and morphological markers. At the same time, cell death occurred when cells were treated with H_2O_2 concentrations higher than 50 μM. In contrast, Caldini et al. (1998) exposed subconfluent cultures to

various concentrations (0–0.5 mM) of H_2O_2 in a PBS for 30 min. They induced adaptation to stress, previously exposing young cells to low oxidant levels. After that, fibroblast treatments were repeated with 50 mM H_2O_2 for 30 min, every two days within eight days (Caldini et al., 1998). They found that young MRC5 fibroblasts pretreated with low doses of H_2O_2 were less prone to exhibit further oxidative damage to DNA, thus reproducing a senescent-like profile of sensitivity, whereas old cultures incubated in a NAD precursor-free medium exerted reduced resistance to H_2O_2-induced DNA strand breaks mimicking DNA sensitivity of young cells.

One modification of the H_2O_2 senescence model is treatment of H_2O_2 in combination with calorie restriction. Chen and Ames (1994) treated F65 cells with 200 µM H_2O_2 for 2 h. Cells were harvested and split into dishes containing 10 ml of medium followed by ten days of cultivation; cells were serum-starved for 24 h in DMEM containing 0.2% bovine serum albumin (BSA) (Chen & Ames, 1994). Following a 2 h application with 200 µM H_2O_2, the cells failed to respond to a stimulus of serum, platelet-derived growth factor, basic fibroblast growth factor, or epidermal growth factor by synthesizing DNA. In addition, the loss of response could not be recovered by 4 days, and the number of the population doublings in the rest of the life span decreased by 35.3 +/- 10.3%.

Sasaki Kajiya's group exposed NHEKs cells to 800 µM of H_2O_2 dissolved in D-MEM with 10% fetal bovine serum for 0–72 h. Moreover, in some experiments, keratinocytes were incubated in a culture medium supplemented with 5-AzazC (10 µM) or menadione (10 µM) (Sasaki et al., 2014). It was detected that H_2O_2 significantly increased the number of NHEKs positive in β-Gal activity, the expression of $p21^{cip1}$ and $p16^{INK4a}$, which was observed 3 h after the treatment with a concentration of H_2O_2 greater than 300 µM, indicating ROS induced cellular senescence. However, CDK inhibitor p53

in NHEKs, which is also associated with the cellular senescence markers, was not affected, while the expression of CDKs in cell cycling, especially CDK4 and CDK6, were reduced. Moreover, the other ROS inducer menadione (10 µM) also increased the expression of mRNA and protein of p16INK4a in a time-dependent manner. At the same time, the pre-treatment with the antioxidant drug N-acetylcysteine (NAC; 10 µM) suppressed the H_2O_2-induced upregulation of $p16^{INK4a}$ proteins in keratinocytes.

To date, there is no unique protocol that can cover all the aspects and needs related to cell culture and supplements which is why research groups use different variations of H_2O_2 exposure to establish an efficient senescence model.

2.3. METHODS AND MATERIALS

2.3.1. Main reagents

1. Hydrogen Peroxide 30% (Merck®, Cat# 1072091000)

2. Dulbecco's phosphate-buffered saline (D-PBS) (*MULTICELL*, Cat# 311-425-CL)

2.3.2. Cell culture and maintenance

Healthy human neonatal foreskin fibroblasts CCD-1064Sk (ATCC® CRL-2076™), human adult skin fibroblasts CCD-1135Sk (ATCC® CRL-2691™), and human foreskin BJ-5ta hTERT-immortalized cell lines (CRL-4001™) were obtained from the American Type Culture Collection (Rockville, MD, USA). Cells were cultivated in ISCOVE's Modified Dulbecco's Medium (IMDM) 1X (MULTICELL, Cat# 319-106-CL) containing 10% heat-inactivated Premium Grade Fetal Bovine Serum (Cat# 97068-085, VWR

International LLC, Radnor, USA), and 1% Penicillin-Streptomycin (10,000 IU Penicillin and 10 mg/ml Streptomycin, Cat# 450-201-EL, WISENT INC., Quebec, Canada). All cells were grown and harvested in our BSL 2 laboratory at the University of Lethbridge. Experimental cell lines were incubated in a humidified Forma Steri-Cycle CO_2 Incubator (Thermo Scientific) at 37℃ with 5% CO_2. Cell culture media were replaced with fresh media every three days until cell confluency reached 90%-100% for further experiments. The cells were subcultured every six or seven days. The replication speed or population doubling (PD) numbers of the cell lines were determined for each subculture as $\Delta PD = \log_2(n_f/n_i)$, where n_i is the number of cells initially seeded and n_f is the final number of cells in a culture. Cells for the senescence model were not older than 24-30 population doublings when employed in the experiments.

2.3.3. Senescence associated phenotype modelling

2.3.3.1. Three steps model of skin fibroblast senescence

Newborn skin fibroblasts CCD-1064Sk were subcultured to passage 11 (24 PDL) and exposed to H_2O_2 utilizing the three-step model (Figure 2.1). H_2O_2 was dissolved in the IMDM cell culture medium with 10% FBS in the following concentrations: 25 µM, 50 µM, 100 µM, 150 µM, 200 µM, 250 µM, 300 µM, and 350 µM. Each step started when cell confluency was approximately 60% with daily one-hour H_2O_2 exposure followed by complete fresh medium replacement. After 5 days of H_2O_2 treatment, cells were harvested and subcultured for the next step.

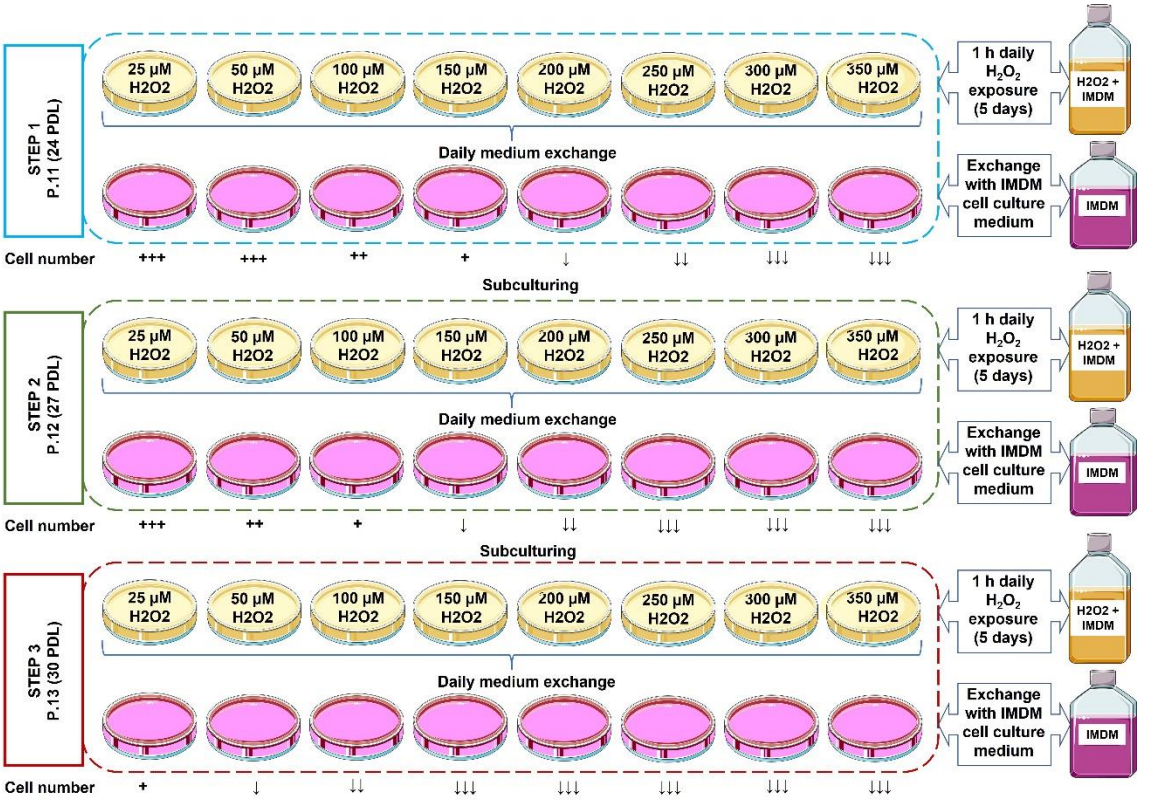

Figure 2.1. Three-step model of hydrogen peroxide stimulated premature cellular senescence. Cultivated cells were treated daily with H_2O_2 for one hour over a five-day period in each step. Each step started when cell confluency was approximately 60%. Speed of cellular growth and cell number was characterized as: +++, high and equal to healthy cells; ++, normal and equal to healthy cells; +, present but slower than healthy cells; ↓, lower number of cells with slower growth than healthy cells; ↓↓, small number of cells with almost absent cellular growth; ↓↓↓, rare presence of cells or cellular debris and absence of cellular growth. This figure was created using images from Servier Medical Art Commons Attribution 3.0 Unported License (http://smart.servier.com).

2.3.3.2. One-step hydrogen peroxide skin fibroblast senescence model

Skin fibroblasts (CCD-1064Sk) at 70% confluency were treated for 1 hour with 25 µM concentration of hydrogen peroxide solution (H_2O_2 dissolved in D-PBS) in 100 x 15 mm petri plates in aseptic conditions (Figure 2.2). Petri plates with skin fibroblasts were maintained in a humidified incubator at 37°C with 5% CO_2.

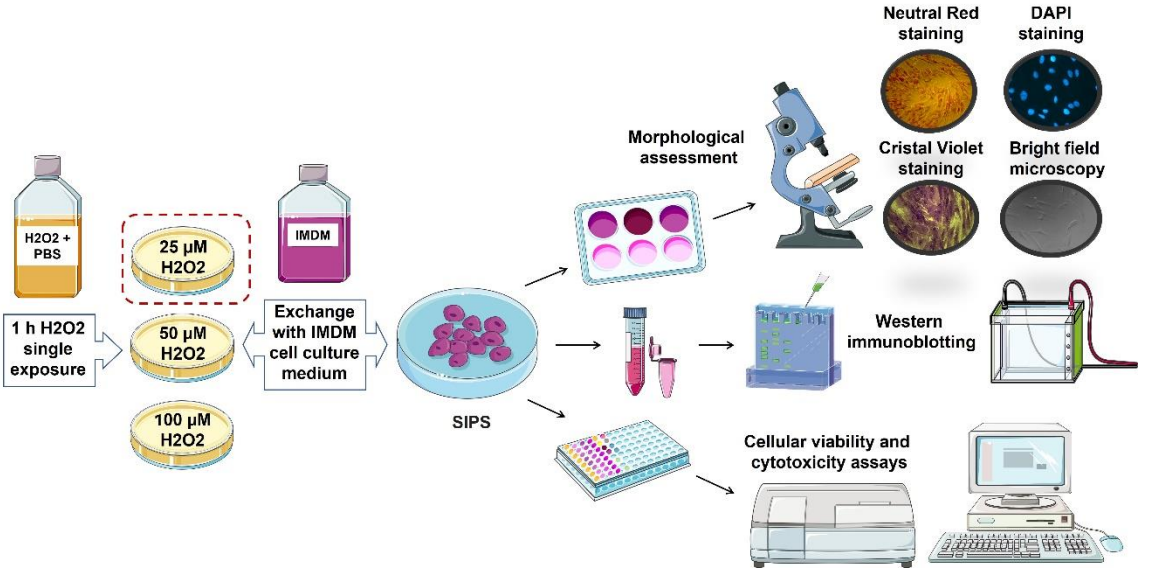

Figure 2.2. One-step model of hydrogen peroxide stimulated premature cellular senescence. SIPS, stress-induced premature senescence. This figure was created using images from Servier Medical Art Commons Attribution 3.0 Unported License (http://smart.servier.com).

After a single 1-hour treatment, H_2O_2 solution was poured out and substituted with cell culture medium. Subsequently, SIPS features, and biomarkers were determined via microscopy, β-galactosidase senescence assay, MTT and Neutral red colorimetric cell viability assays, Crystal violet cytotoxicity assay, western immunoblotting, reverse transcription-polymerase chain reaction, wound-healing assay (WHA), and nuclear DAPI staining.

2.3.4. β-galactosidase analysis

The activity of β-Galactosidase (β-Gal) in fibroblasts was detected by the beta-Galactosidase Detection Kit (Fluorometric) (ab176721, Abcam) following the manufacturer instructions. Briefly, the cell lysate was prepared from normal and premature aged cells with H_2O_2 with protein lysis buffer (included in the kit). Sample protein concentration was quantified using a Bradford protein assay and samples were diluted to 1 µg/mL protein concentration. Then, 50 µl of the standard and samples (diluted in 1× lysis buffer) were added to 96-well black plates followed by 50 µl of fluorogenic fluorescein digalactoside (FDG) working solution to each well and incubated at 37 °C for 4 hours. After adding 50 µl of the stop buffer, fluorescence in each sample was quantified with a FLUOstar Omega (BMG LABTECH) filter-based multi-mode microplate reader at 490 nm for excitation and 525 nm for emission. Cell senescence was established by β-Gal levels in each sample utilizing a β-galactosidase standard curve prepared for each experiment. All experiments were repeated three times; each test was done in triplicate.

2.3.5. Cell viability/cytotoxicity assays

2.3.5.1. The micro-culture tetrazolium assay (MTT)

Cell viability on CCD-1064Sk, CCD-1135Sk, and BJ-5ta human skin fibroblast was measured by the micro-culture tetrazolium assay MTT (3-[4,5-dimethylthiazol-2-yl]-2,5-diphenyltetrazolium bromide; thiazolyl blue) colorimetric metabolic activity assay with the cell proliferation kit I (#11465007001, Roche, Ontario, Canada) according to the manufacturer's instructions.

Cells were plated at 3.0 x 10^3 cells/well in 150 µL of cell culture medium in a 96-well assay plate and cultivated for 24-48 h before treatment depending on cell confluency. A broad range of H_2O_2 concentrations or other treatments such as cannabinoids (see Chapter 3) or anti-aging drugs (see Chapter 4) were examined to determine the appropriate effective/cytotoxic concentration for each designated treatment. Unless otherwise indicated, all measurements were performed in triplicate at specific time points (0, 1, 2, 3, 4, and 5 days). After the desired treatment time, 10 µL of MTT labeling reagent was added to each well without removing media and incubated for 4 h. Afterward, 100 µL of MTT solubilization solution (10% SDS in 0.01 M HCl) was added to each well, followed by overnight incubation. Cell viability was calculated by comparing it to the control treatment. All experiments were repeated three times; each test was done in triplicate.

2.3.5.2. Neutral red assay and microscopy

The Neutral red assay is based on the ability of viable cells to incorporate and bind neutral red dye in the lysosomes (Repetto et al., 2008). It was used to provide a qualitative estimation of the presence of viable cells in the fibroblast cell cultures.

Cells were cultivated in a 96-well cell culture plates and treated appropriately. The medium was removed from the fibroblast cell cultures and the cultures were washed with PBS. After that, 100 µL of Neutral red (N7005, Sigma-Aldrich) dissolved in a cell culture medium (40 µg ml^{-1}) was added for each well, followed by 4 h incubation at the appropriate culture conditions. After incubation, cells were gently washed twice with 150 µL of PBS. Images were taken using a Zeiss Observer Z1 epifluorescence microscope with AxioVision Rel 4.8 software. PBS was replaced with 150 µL of neutral red destain solution per well and incubated at room temperature on a microtiter plate shaker for 20

min. Neutral red's optical density (OD) was measured at 540 nm in a microtiter plate spectrophotometer, using blanks containing no cells as a reference.

2.3.5.3. Crystal violet assay

The viability of cultured fibroblasts was evaluated by detecting maintained adherence of cells by staining attached cells with crystal violet dye, which binds to proteins and DNA (Feoktistova et al., 2016). It is worth noting that a reduced amount of crystal violet staining in cell culture represents cells that undergo cell death and simultaneously lose their adherence and die.

Cells were cultivated in 96-well cell culture plates and treated appropriately. The medium was aspirated from the fibroblast cell cultures, and cells were washed twice with PBS. Then, 50 μL of 0.5% crystal violet staining solution was added to each well and incubated for 20 min at room temperature on a bench rocker with a frequency of 20 oscillations per minute.

After incubation, plates were gently washed four times in a stream of tap water, and they were inverted on filter paper and tapped the plates gently to remove any remaining liquid. Then, plates without their lids were left air-dry for at least 2 h at room temperature.

Images were taken using a Zeiss Observer Z1 epifluorescence microscope with AxioVision Rel 4.8 software.

With the purpose to evaluate fibroblasts viability, 200 μL of methanol was added to each well, and plates with lids were incubated for 20 min at room temperature on a bench rocker with a frequency of 20 oscillations per minute. The OD of each well was measured at 570 nm (OD570) with a microtiter plate reader spectrophotometer, using blanks containing no cells as a reference.

2.3.6. Protein extraction and quantification

The three cell lines of dermal fibroblasts were harvested by using TRYPSIN/EDTA (0.25% Trypsin and 2.21 mM EDTA-4Na, Cat#325-043-EL, WISENT INC., Quebec, Canada). The mixture was centrifuged at 1,600 rpm for five min. The supernatant was discarded, and the pellets were washed twice with ice-cold 1× PBS. The pellet was solubilized in100-150 µl RIPA lysis buffer with 10 mM Tris-HCl (pH 7.5), 100 mM NaCl, 1 mM EDTA, 1% Triton X-100, 10% glycerol, 0.1% SDS, 0.5% deoxycholate, 1 mM sodium orthovanadate, and 1 mM PMSF. Whole cellular protein lysate was sonicated using a Braunsonic model 1510 sonicator (B. Braun Germany) operating at 80% sonication capacity. Lysates were centrifuged at 12,000 ×g for 10 min and the supernatant was decanted for use. Using the Bradford protein assay with bovine serum albumin as the standard, protein concentrations were determined via NanoDrop 2000/2000c Spectrophotometer (ThermoFisher Scientific Company, Wilmington, DE).

2.3.7. Western immunoblotting

Western immunoblotting was conducted as described previously (Silasi et al., 2004). In brief, an equal amount of protein sample (30-100 µg) was prepared with 4 × loading buffer (0.0625 M Tris, 2% SDS, 10% glycerol, 0.01% bromophenol blue, and 1% 2-mercaptoethanol) and RIPA lysis buffer and heated at 95℃ for 10 min. The protein sample and PageRuler Plus Prestained Protein Ladder (Cat#26620, Thermo Scientific, Massachusetts, USA) were loaded and electrophoretically separated by SDS-PAGE into slab gels of 10-15% polyacrylamide at 100V. Polyvinylidene difluoride membranes (Amersham Biosciences, Baie d'Urfé, Québec) were used to transfer resolved proteins for 2 h on ice. Then, membranes were incubated for two hours in a blocking solution (5% dry

skimmed milk in PBS, 0.5% Tween 20) at room temperature and incubated with specific primary antibodies specified in Table 2.1 at 4°C overnight.

After overnight incubation, the membranes were washed three times with 0.1% Tween-20 in PBS (PBS-T). Then membranes were incubated with 1:10,000 dilution of either Bovine anti-mouse secondary antibody or Donkey anti-Rabbit secondary antibodies (Table 2.1) for two hours at room temperature. The rationale for including or not including proteins was based on the senescence and longevity pathways (Suppl. Figures 21-23).

Membranes were washed three times with PBS-T and then exposed to ECL Prime Western Blotting System (Cat#GERPN2232, GE Healthcare, Chicago, USA). Chemiluminescence was detected using the FluorChem HD2 Imaging System (Cell Biosciences, California, United States). Unaltered PVDF membranes were stained with Coomassie blue (BioRad, Hercules, CA) to confirm equal protein loading. Signals were quantified using the NIH Image J64 software and normalized relative to GAPDH or Coomassie staining as indicated.

Table 2.1. Antibodies used for Western blots

Antibody	Supplier, Cat No	Dilution
Mouse anti-NFκB p65	Santa Cruz, sc-8008	1:500 in 5% milk (PBST)
Rabbit anti-p-NFκB p65	Santa Cruz, sc-33039	1:500 in 5% milk (PBST)
Mouse anti-CB1/Cannabinoid Receptor 1/CNR1 (2F9)	Santa Cruz, sc-293419	1:100 in 5% milk (PBST)
Mouse anti-CB2/Cannabinoid Receptor 2/CNR2 (3C7)	Santa Cruz, sc-293188	1:200 in 5% milk (PBST)
Mouse anti-COL1A (COL-1)	Santa Cruz, sc-59772	1:100 in 5% milk (PBST)
Mouse anti-COL3A1 (B-10)	Santa Cruz, sc-271249	1:100 in 5% milk (PBST)
Mouse anti-elastin (BA-4)	Santa Cruz, sc-58756	1:200 in 5% milk (PBST)
Mouse anti-SIRT1 (B-7)	Santa Cruz, sc-74465	1:100 in 5% milk (PBST)
Rabbit anti-SIRT2	Santa Cruz, sc20966	1:500 in 5% milk (PBST)
Mouse anti-SIRT6 (2G1H1)	Santa Cruz, sc-517196	1:200 in 5% milk (PBST)
Mouse anti-MT-MMP-1 (C-7)	Santa Cruz, sc-377097	1:100 in 5% milk (PBST)
Mouse anti-MMP-2 (8B4)	Santa Cruz, sc-13595	1:100 in 5% milk (PBST)

Mouse anti-CDKN2A/p16INK4a (F-12)	Santa Cruz, sc-1661	1:500 in 5% milk (PBST)
Mouse anti-p21 Waf1/Cip1/CDKN1A (F-5)	Santa Cruz, sc-6246	1:500 in 5% milk (PBST)
Mouse anti-PCNA	Santa Cruz, sc-56	1:1000 in 5% milk (PBST)
Mouse anti-pro BDNF (5H8)	Santa Cruz, sc-65514	1:500 in 5% milk (PBST)
Mouse anti-cyclin D1 (DCS-6)	Santa Cruz, sc-20044	1:500 in 5% milk (PBST)
Mouse anti-CDK2	Santa Cruz, sc6248	1:500 in 5% milk (PBST)
Rabbit anti-p-AKT1/2/3 Thr308	Santa Cruz, sc-16646	1:200 in 5% milk (PBST)
Mouse anti-c-Jun (G-4)	Santa Cruz, sc-74543	1:200 in 5% milk (PBST)
Mouse anti-BID (E-7)	Santa Cruz, sc-514622	1:200 in 5% milk (PBST)
Mouse anti-TGFβ1 (3C11)	Santa Cruz, sc-130348	1:200 in 5% milk (PBST)
Mouse anti-EGFR (A-10)	Santa Cruz, sc-373746	1:200 in 5% milk (PBST)
Mouse anti-vinculin (7F9)	Santa Cruz, sc-73614	1:500 in 5% milk (PBST)
Mouse anti-p53 (DO-1)	Santa Cruz, sc-126	1:500 in 5% milk (PBST)
Mouse anti-p-p53 (D-9)	Santa Cruz, sc-377567	1:500 in 5% milk (PBST)
Mouse anti-MMP-9 (2C3)	Santa Cruz, sc-21733	1:500 in 5% milk (PBST)
Mouse anti-p-Akt1/2/3 (B-5)	Santa Cruz, sc-271966	1:500 in 5% milk (PBST)
Rabbit anti-AKT1	Abcam, ab-32505	1:1000 in 5% BSA (PBST)
Rabbit anti-Actin	Abcam, ab-179467	1:500 in 5% BSA (PBST)
Mouse anti-GAPDH (0411)	Santa Cruz, sc-47724	1:1000 in 5% milk (PBST)
	Secondary antibody	
Bovine anti-Mouse	Santa Cruz, sc-2371	1:10000 in 5% milk (PBST)
Donkey anti-Rabbit	Santa Cruz, sc-2313	1:10000 in 5% milk (PBST)

Abcam, Abcam Inc, Cambridge, United Kingdom; BSA, Bovine Serum Albumin; PBST, 1x Phosphate-Buffered Saline, 0.1 % Tween® 20; Santa Cruz, Santa Cruz Biotechnology, Inc., Texas, United States; Cell Signaling, Cell Signaling Technologies, Massachusetts, United States

2.3.8. RNA isolation

RNA was isolated from monolayer fibroblast cultures, using TRIzol® Reagent (Invitrogen, Carlsbad, CA); purified using an RNAesy kit (Qiagen), according to the manufacturer's instructions; and quantified using NanoDrop 2000c (ThermoScientific).

2.3.9. Reverse transcription polymerase chain reaction (RT-PCR)

Reverse transcription polymerase chain reaction (RT-PCR) was performed on skin fibroblast samples from all experimental groups. According to the manufacturer's

instructions, cDNA was generated with 500 ng RNA using the iScriptTM Select cDNA synthesis kit (Cat# 1708897, BioRad, Hercules, CA). PCR reactions were based on the SsoFastTM EvaGreen® Supermix (Cat# 1725202, BioRad) and 500 nM of forward and reverse primers specific for target sequences of interest. Primers were designed using the https://www.idtdna.com/Primerquest platform (Table 2.2). Primers were checked before on dilution series of normal fibroblasts cDNA. Reference genes (GAPDH, RPL13A, and UBC) were analyzed with the GeNorm method (Vandesompele et al., 2002). The reactions were analyzed on a C1000TM Thermo Cycler equipped with a CFX96 Touch™ Real-Time PCR Detection System (BioRad). The PCR programs were run according to the SSoFastTM guidelines with annealing temperatures as specified for the specific primer pairs. Expression analysis was performed with the BioRad Software (CFX Manager) and was based on the ΔΔCt method with the reference genes that were stably expressed in the GeNorm analysis.

Each experiment included three biological replicates for each group and two technical replicates per sample.

Table 2.2. Primer sequences and accession number for RT-PCR analysis

Target Gene	Sequence Forward (5' → 3')	Sequence Reverse (5' → 3')
CNR1 (CB1R)	CAAGCCTCTCTGGCACTTT	CTGGTGGTTGGGCCTATTT
CNR2 (CB2R)	CCTCCCAAAGTGCTAGGATTAC	CTTGTTCTCCTCCCTCATAAGC
COL1A1	CCACGACAAAGCAGAAACATC	GCAACACAGTTACACAAGGAAC
COL3A1	CTGGCATTCCTTCGACTTCT	AGCTTCAGGGCCTTCTTTAC
COL7A1	GCCTGGAAAGCCTGGTATT	TGTTCTCCACGTTCTCCTTTC
GDF11	TCTCAGAGCTAGTGTGGTAGAA	CCTCCCGGATCACTTTCAATAG
ELN	CTCAAAGCTGGATTCGCTCTA	AAGGGCAAGGTGGCTATTC

MMP1	CAGAAAGAGACAGGAGACATGAG	GAAGAGTTATCCCTTGCCTATCC
MMP2	AGAGAACCTCAGGGAGAGTAAG	CCTCGAACAGATGCCACAATA
HAS1	GTCTCCAGGGAGGGTATTTATTG	TCCTGATCACACAGTAGAAATGG
CDKN2A (P16)	AGCTGTCGACTTCATGACAAG	GAGCTTTGGTTCTGCCATTTG
EGFR	CAAGGAAGCCAAGCCAAATG	CCGTGGTCATGCTCCAATAA
MKI67	GGAGCCAGGTGACATCATAAA	CATGGATGACGCTGTGAGAA
CDKN1A (P21)	CCTTCCAGCTCCTGTAACATAC	TCGAGAGGTTTACAGTCTAGGT
SIRT1	AGAACCCATGGAGGATGAAAG	TCATCTCCATCAGTCCCAAATC
SIRT3	CCTCCTTCCTAGCATCACATTAC	CCTGGGAGTCACTGTCATTAAA
SIRT4	GAACCTGGAACAGGGACTTT	CTTTGTCAGTGCACCCTACT
SIRT6	CCTCTGACTTGCTGTGTTGT	GAGGGAGTTCACTCCTGTTTAAG
TP53	AGGGATGTTTGGGAGATGTAAG	CCTGGTTAGTACGGTGAAGTG
NFKB1	GAGACATCCTTCCGCAAACT	GGTCCTTCCTGCCCATAATC
TIMP1	TCCCAGATAGCCTGAATCCT	TGCTGGGTGGTAACTCTTTATT
GAPDH	CAGGAGGCATTGCTGATGAT	GAAGGCTGGGGCTCATTT
RLP13A	GGGAGCCAGAAGACTGATTG	CCAAGTGCTTGCACATTCTAAC
UBC	TGAAGACCCTGACTGGTAAGA	GAGGGATGCCTTCCTTATCTTG
PPIA	AGGGTTCTTAACCCAGCAATC	GCAGAAGGAACCAGACAGTAAA
SDHA	GATCTTCCTGACTCAGCCTTC	GAGACCCTGTCCCTACAATTAC

2.3.10. Wound-healing assay

Cells were cultivated to >90% confluence in 24-well plates. 10 µL pipette tips were used to scrape a scratch/wound line through the middle of each well simulating a wound. Cells were washed twice in PBS before adding cell culture growth medium or designated treatments. Images of the healing process were taken on the following time points: 1 h, 6 h, 24 h, 48 h, and 72 h throughout the assay.

The Infinity3 camera was used to collect images within the linear dynamic range representing the range in which the relationship between signal intensity and the amount of material is likely to be linear. Images were analyzed with ImageJ (IJ 1.46r) software.

At least seven measurements were counted per sample, and samples were designed in triplicates

2.3.11. Immunocytochemistry

Cells were plated on glass coverslips for 48 h, treated in 6-well plates, and then fixed in 3% formaldehyde for 20 min at room temperature. Cells were quenched with 50 mM NH_4Cl in PBS, permeabilized for 5 min in 0.2% Triton X-100, and blocked with 3% BSA for 30 min. After washing, nuclei were stained with 300 nM 4',6-diamidino-2-phenylindole (DAPI) (Thermo Fisher Scientific, Cat #D1306) in PBS for 15 min before mounting according to the manufacturer's instructions. Images were taken using a Zeiss Observer Z1 epifluorescence microscope with AxioVision Rel 4.8 software. DAPI produces a blue fluorescence when bound to DNA with excitation at 360 nm and emission at 460 nm. Specimens were stored at 4˚C. Experiments were prepared in triplicates.

2.3.12. QuPath Analysis

QuPath 0.2 was used for quantitative analysis of cell number and stained area for the nuclei of the fibroblasts. Images were taken using a Zeiss Observer Z1 epifluorescence microscope with AxioVision Rel 4.8 software and imported into QuPath. Nuclei were quantified using the cell detection function on the region of interest with parameters optimized to identify nuclei accurately and were confirmed by visual inspection. Any nuclear overlapping or partial nuclei captured erroneously identified as nuclei were deleted. Once nuclei were correctly identified, QuPath provided the following parameters:

a) Nuclei number is the number of distinct nuclei that were identified

b) Area of the nucleus (μm^2) is the number of pixels that enclosed within the nuclear perimeter.

c) Perimeter of the nucleus (μm) or length is the number of adjacent pixels in the boundary of the nucleus.

d) Nucleus circularity is an area-to-perimeter ratio which demonstrates the roundness of the nuclear perimeter. This is calculated by multiplying the area by four pi and divided by the square of the convex perimeter. For circular nuclei, the ratio equals 1, whereas nuclei that depart from circularity have ratios less than one.

e) Nuclear max caliper (μm) is the distance between farthest parallel endpoints touching opposite sides of the nucleus.

f) Nuclear min caliper (μm) is the distance between closest parallel endpoints touching opposite sides of the nucleus.

g) Nuclear eccentricity, also known as ellipticity, is a ratio of the min caliper/max caliper. It shows how oval-shaped the nuclei are.

All data were automatically converted from pixels to the appropriate units and were extracted from QuPath 0.2 software to Microsoft® Office Excel 365 files. Data were imported into the GraphPad Prism software 9.3.1 for statistical analysis (GraphPad Software, LLC, USA).

2.3.13. Statistical analysis

The number of cells PDL and biological repeats (n) for each experiment are indicated in the figure captions. Results are presented as mean of at least three samples per group with standard deviation (SD) of the mean or 95% confidence interval as indicated. Mean values ± SD and statistical analyses were calculated and plotted using

GraphPad Prism 9 (GraphPad Software, San Diego, CA) unless stated otherwise. Statistical analysis of data quantification was performed using an ANOVA test (Tukey post-hoc multiple comparison test) and an unpaired Student's t-test was used for analysis with two groups.

2.4. RESULTS

2.4.1. Setup of the senescence model system

To understand age-dependent changes that occur in the skin, we designed and tested two different models of senescence using dermal fibroblasts. First, normal human fibroblasts cell lines CCD-1064Sk, CCD-1135Sk, and BJ-5ta were treated with H_2O_2 at various concentrations to find a line that would recapitulate the development of SIPS without direct lethal effect. Thus, in the three-step senescence model, dermal fibroblasts were consistently exposed to the 25 µM, 50 µM, 100 µM, 150 µM, 200 µM, 250 µM, 300 µM, and 350 µM of H_2O_2 for 15 days divided into three five-day-steps (Figure 2.1). H_2O_2 treatment solution was prepared in the IMDM cell culture medium with 10% FBS that gave additional nutrients source to the cells and decreased harmful effect of higher doses of H_2O_2. Additionally, SIPS in experimental fibroblasts culture developed very slow increasing the cost of studies and complicated results consistency after repetition of experiments. At the same the time three-step senescence model showed robust SIPS changes in different dermal fibroblast cell lines (see below).

The second senescence model focused on the fast induction of SIPS in skin fibroblasts. In this model, we also exposed cells to various concentrations of H_2O_2 from 25 µM to 350 µM, however, fibroblasts were treated with H_2O_2 for one hour just once (Figure 2.2). Since fibroblasts are only treated with H_2O_2 once, this method is called a one-

step model. In addition, H_2O_2 was dissolved in the PBS to eliminate the protective effect of the cell culture medium and induce stress-like brief calory restriction conditions. PBS did not show adverse effects on cell culture within one hour and was used in the subsequent experiments as a solvent for H_2O_2. Our tests found that 25 μM concentration of H_2O_2 was the most reliable for the relatively stable induction of SIPS in different cell lines of dermal fibroblasts. We will compare these two senescence models and the effects of various concentrations of H_2O_2 in the SIPS development in this chapter.

2.4.2. Senescence induced morphological transition

Normal human fibroblasts have a limited *in vitro* lifespan when cells enter a non-dividing, senescent state, known as the Hayflick limit, which is one of the markers of senescence (Hayflick, 1965; Hayflick & Moorhead, 1961). Neonatal foreskin CCD-1064Sk fibroblasts have approximately ≥ 50 population doubling level (PDL) that usually corresponds to cultured passage 25-28 for this specific cell line, while PDL of normal human adult skin fibroblasts CCD-1135Sk is around ≥ 46 (15-20 passages). In contrast, human foreskin normal BJ-5ta hTERT-immortalized cell line (CRL-4001™) was TERT-immortalized at PDL of 58. Cell stocks obtained from ATCC were subcultured to reach three different passages depending on the type of cell line. To determine the senescence status of those cells, firstly we monitored their PDL, evaluated morphological changes, and senescence ratios as by β-Gal assay (Dimri et al., 1995). We then tested molecular senescence biomarkers and functional capabilities of the aged cells.

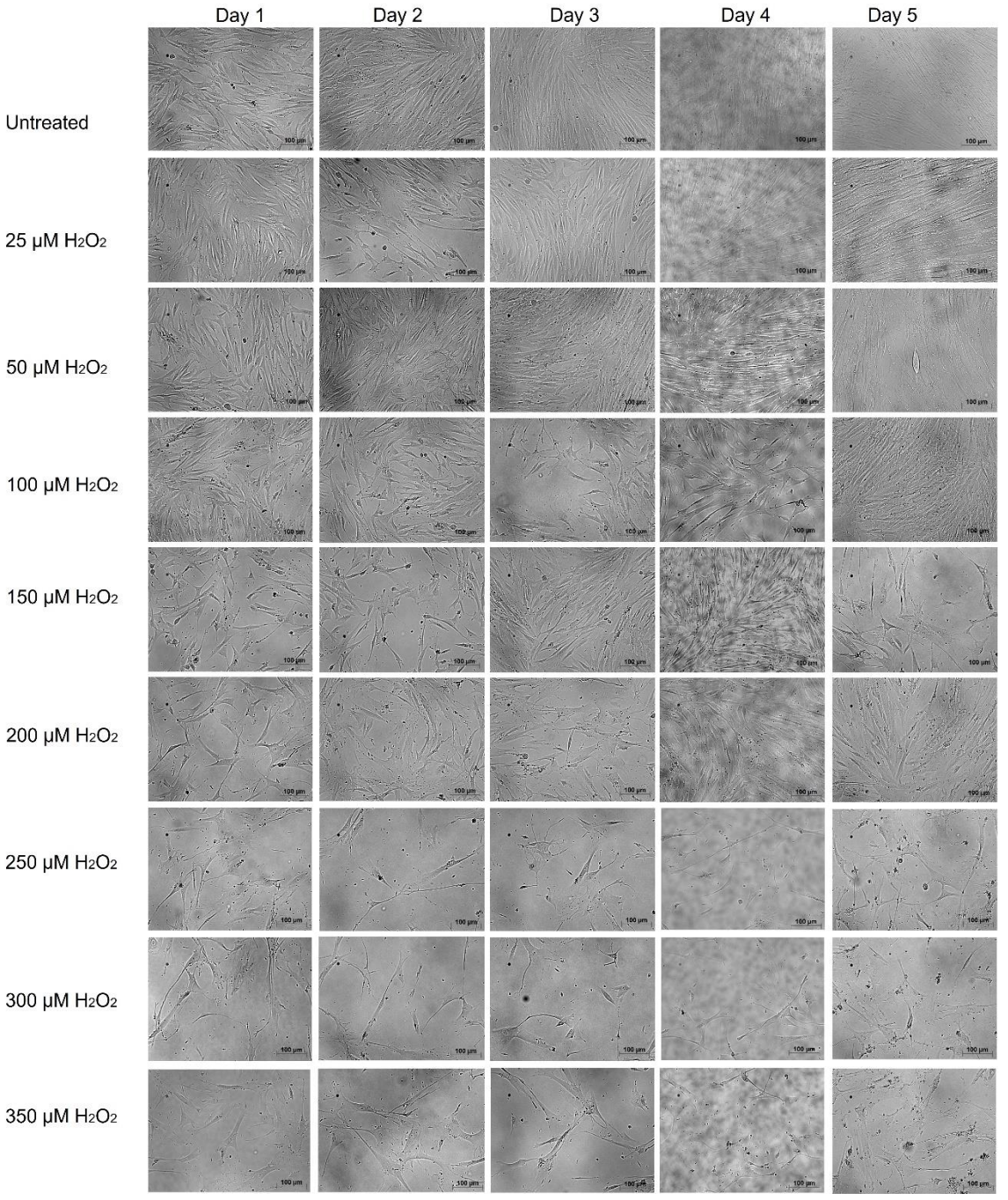

Figure 2.3. Human skin fibroblasts (CCD-1064Sk), 24 PDL exposed to H_2O_2 (Step 1 of the three-step senescence model). The figure represents gradual changes in cell quantity and quality within five days of H_2O_2 (doses of 25 μM, 50 μM, 100 μM, 150 μM, 200 μM, 250 μM, 300 μM, and 350 μM H_2O_2).

Phase-contrast imaging was used to characterize senescent dermal fibroblasts (Figure 2.3). While early fibroblast passages formed dense cultures and had small, elongated cell bodies, late passages displayed shape changes with large, flat cellular morphology, whereby cell and nuclear features looked nearly transparent. In addition, another critical aspect of passaging was determined – the loss of replicative capacity. We observed RS in prolonged culture fibroblasts (Figure 2.4). Like late passage fibroblasts, prematurely aged fibroblasts treated with H_2O_2 showed a substantially reduced growth speed and developed characteristics similar to other senescence models designed in our laboratory, albeit, they still demonstrated some replicative ability.

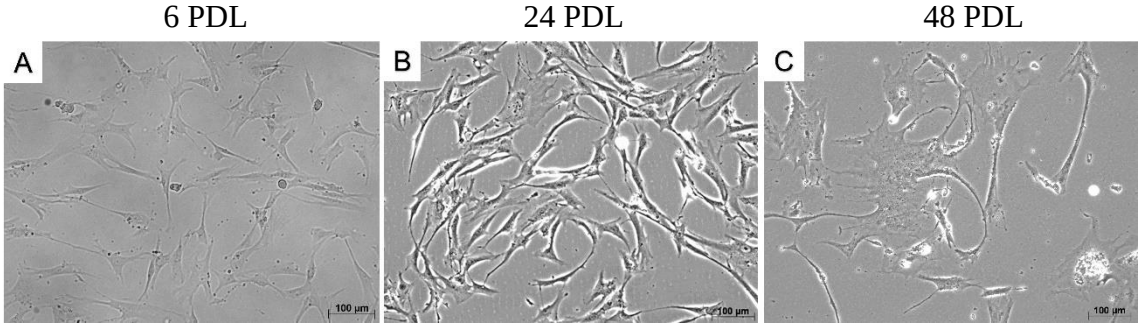

Figure 2.4. Human skin fibroblasts (CCD-1064Sk) at different population doubling levels**.** A. "Early" passage of fibroblast cell culture (6 PDL); B. "Middle" passage of fibroblast cell culture (24 PDL); C. Replicative senescence (48 PDL).

To find the optimal concentration of H_2O_2 for SIPS induction and to reduce the number of H_2O_2 treatments, we took images of potentially aged fibroblasts for both models with and without staining procedures (Figure 2.5). The morphological results of both senescence models showed 150 µM H_2O_2 concentrations or higher affected cells perniciously. H_2O_2 concentrations of 50 µM and 100 µM showed a progressive detrimental impact on cell viability and number. At the same time, 25 µM H_2O_2 showed a significant reduction in fibroblasts viability and replicative ability.

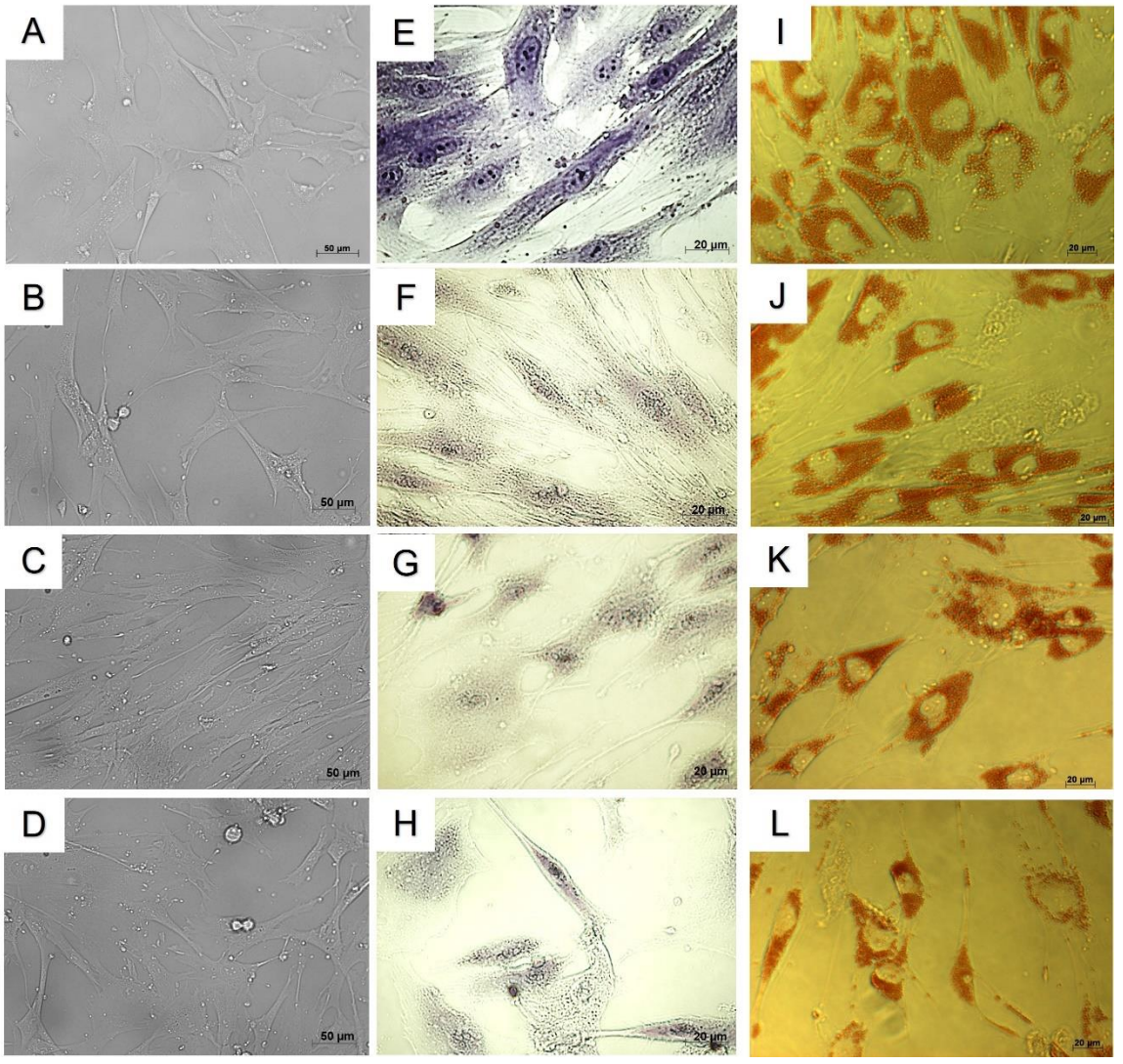

Figure 2.5. Human skin fibroblasts (CCD-1064Sk) 24 PDL, 24 hours after 1-hour H_2O_2 exposure (One-step senescence model). Phase-contrast microscopy: A, Untreated; B, 25 µM H_2O_2; C, 50 µM H_2O_2; D, 100 µM H_2O_2; Crystal violet staining: E, Untreated; E, 25 µM H_2O_2; G, 50 µM H_2O_2; H, 100 µM H_2O_2; Neutral red staining: I, Untreated; J, 25 µM H_2O_2; K, 50 µM H_2O_2; L, 100 µM H_2O_2.

2.4.3. β-galactosidase as a biomarker for senescence-associated phenotype

To determine the extent of senescence in the culture of dermal fibroblasts during serial passaging or the proposed senescence-induced models, we measured the senescence-associated beta-galactosidase (β-Gal) levels (Figure 2.6), which is commonly

used as biomarker for senescence (Debacq-Chainiaux et al., 2009; Dimri et al., 1995; Lee et al., 2006).

The three-step senescence model demonstrated a progressive decline in fibroblast number (Figure 2.6, A-H) and conversely, a significant increase in β-Gal levels (Figure 2.6, I). Importantly, we noticed a relative decline in β-Gal levels in fibroblasts treated with 100 µM H_2O_2 and 150 µM H_2O_2. This was likely due to a significant shortage in the number of fibroblasts at the end of step 3 of the three-step senescence model. Due to the limited number of cells treated with 200 µM H_2O_2, 250 µM H_2O_2, 300 µM H_2O_2, and 350 µM H_2O_2, β-Gal measurements were unreliable or undetectable (data not shown). In future experiments, we plan to use the senescence β-Galactosidase Staining Kit designed to detect β-gal activity at pH 6, with subsequent calculation of the positively stained cells.

Compared to the late PDL cultures, the β-Gal levels in early passages were lower (Figure 2.6, J). β-Gal levels were also significantly increased in the prematurely aged fibroblasts during the one-step model of senescence (Figure 2.6, K).

2.4.4. Senescence-associated changes in nuclear morphology

Morphologically, young fibroblasts were identified as elongated cells exhibiting a spindle-like shape that adhered to plates (Figure 2.4, A). Senescent fibroblasts and those exposed to the H_2O_2, demonstrated cellular size enlargement and irregular shape, while appearing to be reduced in cell number (Figure 2.4, C and Figure 2.5).

Findings obtained during microscopy examinations of cell cultures with and without staining motivate us to investigate whether H_2O_2 exposure influenced nuclear architecture. Therefore, fibroblasts were stained with DAPI, a fluorescent stain that binds strongly to adenine–thymine-rich regions in DNA.

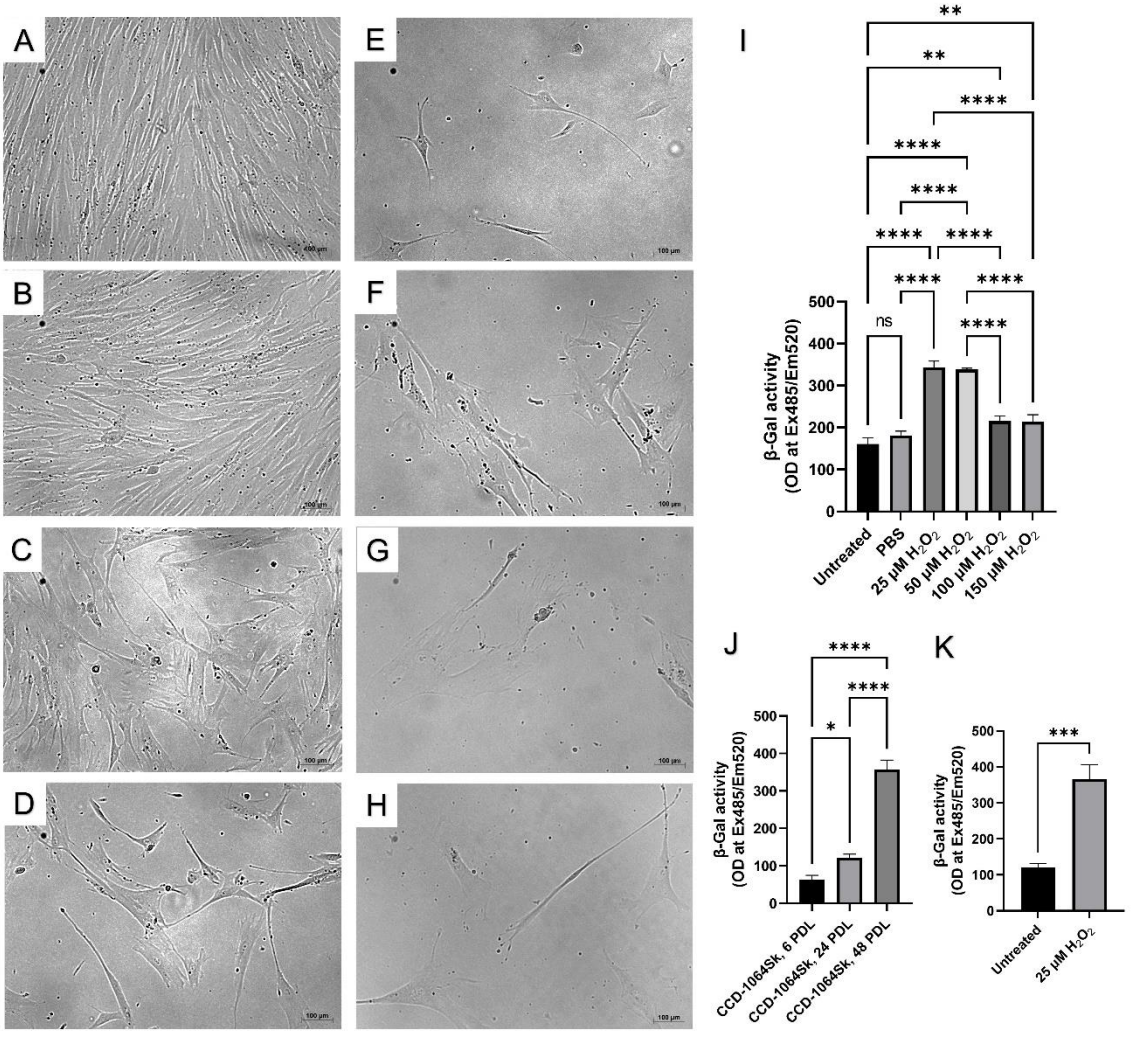

Figure 2.6. Human skin fibroblasts (CCD-1064Sk) 30 PDL exposed to H_2O_2 (Step 3 of the three-step senescence model). The images represent gradual changes in cell quantity and quality after five days of exposure to different concentrations of H_2O_2: A, 25 μM; B, 50 μM; C, 100 μM; D, 150 μM; E, 200 μM; F, 250 μM; G, 300 μM; H, 350 μM. I, Levels of β-Gal activity after H_2O_2 exposure on day five, step 3 (three-step model), were compared with untreated cells (CCD-1064, 30 PDL) and PBS, phosphate buffer sulfate. J, Levels of β-Gal activity in different passages of dermal fibroblasts; K, Levels of β-Gal activity after H_2O_2 exposure on day five (one-step model of senescence). Data were analyzed with an ANOVA test (Tukey post-hoc multiple comparison test) (I, J), and an unpaired Student's t-test was used for analysis with two groups (K). Significance isindicated within the figures using the following scale: *, $p<0.05$; **, $p<0.01$; ***, $p<0.001$; ****, $p<0.0001$. Bars represent mean ± SD.

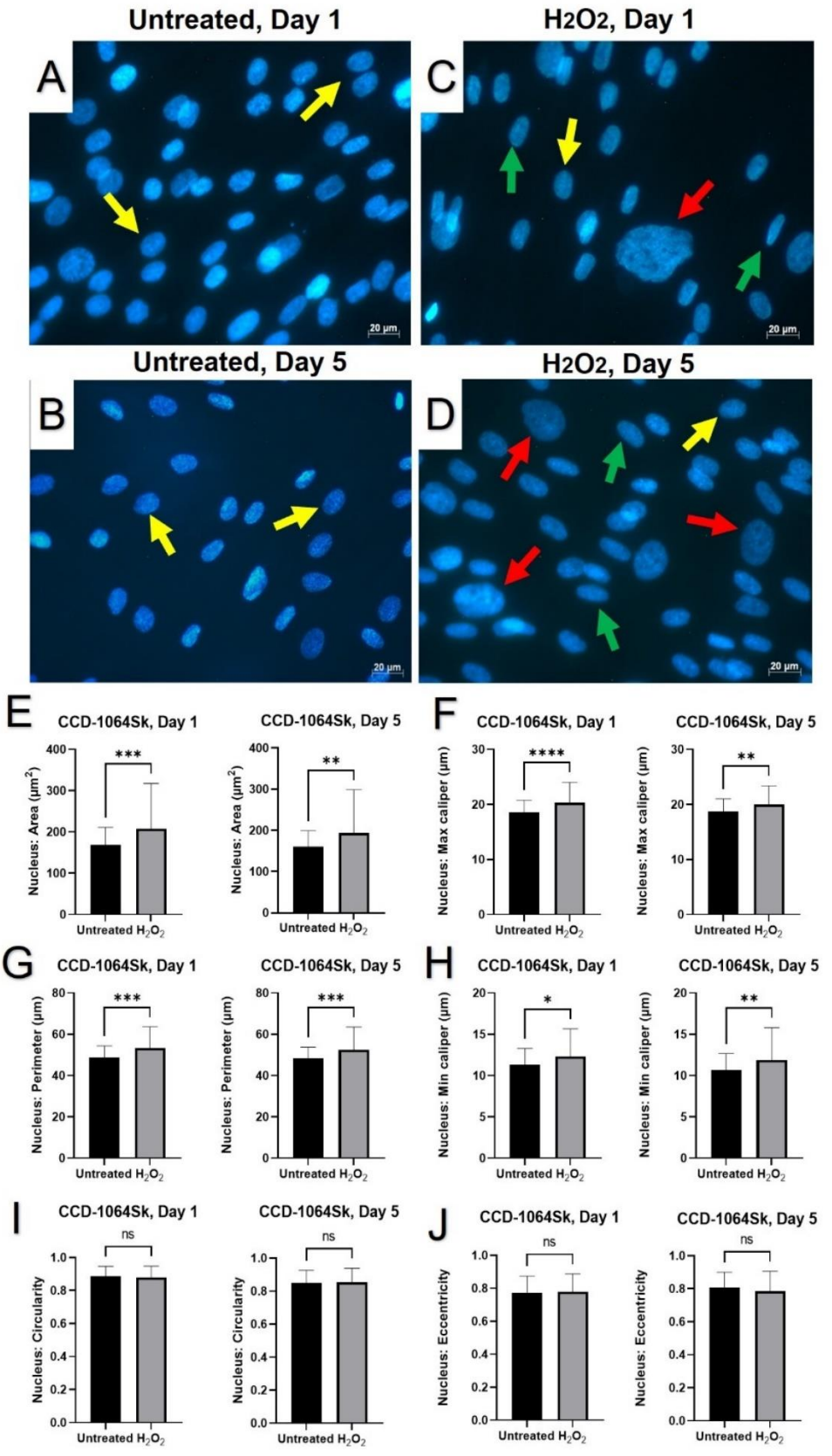
Untreated, Day 1
H2O2, Day 1
A
C
20 µm
Untreated, Day 5
H2O2, Day 5
B
D
E
CCD-1064Sk, Day 1
CCD-1064Sk, Day 5
Nucleus: Area (µm²)
***
**
Untreated H2O2
F
Nucleus: Max caliper (µm)
****
G
Nucleus: Perimeter (µm)
H
Nucleus: Min caliper (µm)
*
I
Nucleus: Circularity
ns
J
Nucleus: Eccentricity

Figure 2.7. DAPI stained nuclei of dermal fibroblasts (CCD-1064Sk), 24 PDL (one-step senescence model). Pictures A-D represent nuclear changes observed by immunofluorescence microscopy on days 1 and 5 after single 25 μM H_2O_2 exposure. Arrows point to nuclei with specific nuclear shapes: yellow – round, green – elongated, and red – gigantic/irregular. A, Untreated cells on day 1; B, prematurely aged fibroblasts after H_2O_2 exposure on day 1; C, Untreated cells on day 5; D, senescent fibroblasts on day 5. Nuclear parameters measured utilizing QuPath in each sample: E, nuclear area; F, nuclear max caliper; G, nuclear perimeter; H, Nuclear min caliper; I, nuclear circularity; J, nuclear eccentricity. Data were analyzed with a Student's unpaired t-test for each separate parameter. Significance is indicated within the figures using the following scale: ns, not significant; *, $p<0.05$; **, $p<0.01$; ***, $p<0.001$; ****, $p<0.0001$. Bars represent mean ± SD.

Nuclear DAPI staining showed significant enlargement and variability in size and shape of nuclei in aged fibroblasts compared to healthy cells (Figures 2.7, 2.8). Nuclei of fibroblasts exposed to the H_2O_2 displayed more elongated morphology compared to untreated cells in the CCD-1064Sk cell line, while some remaining cells retained a round architecture. We noticed the appearance of gigantic nuclei with irregular shapes (Figure 2.7, C, D). In contrast, prematurely senescent BJ-5ta fibroblasts exhibited predominantly round irregular size nuclei (Figure 2.8, C, D). Other nuclear parameters, such as perimeter, max caliper, and min caliper as well as the nuclear area, significantly increased in CCD-1064Sk senescent fibroblast (Figure 2.7, E-H). Similar trend with minor differences was found in BJ-5ta fibroblasts (Figure 2.8). In contrast, nuclear circularity and eccentricity remained almost unchanged between untreated and senescence CCD-1064Sk fibroblast (Figure 2.7, I-J). In BJ-5ta, noticeable elevation in nuclear circularity and declined eccentricity was found in prematurely aged fibroblasts (Figure 2.8, I-J).

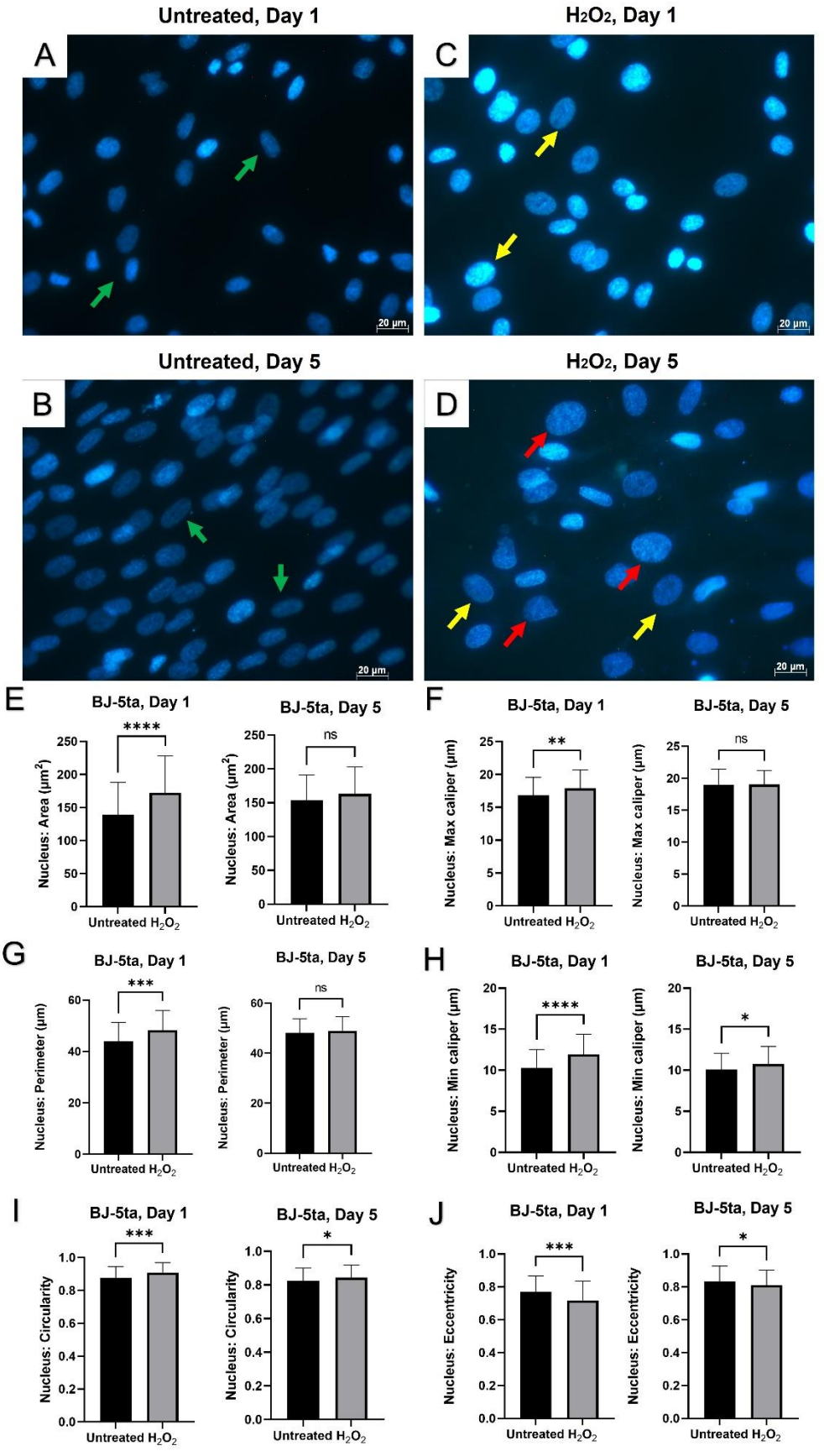
Untreated, Day 1
H2O2, Day 1
A
C
20 µm
Untreated, Day 5
H2O2, Day 5
B
D
20 µm
E
BJ-5ta, Day 1
BJ-5ta, Day 5
****
ns
Nucleus: Area (µm²)
Untreated H2O2
F
**
ns
Nucleus: Max caliper (µm)
G
***
ns
Nucleus: Perimeter (µm)
H
****
*
Nucleus: Min caliper (µm)
I
***
*
Nucleus: Circularity
J
***
*
Nucleus: Eccentricity

Figure 2.8. DAPI stained nuclei of dermal fibroblasts (BJ-5ta), 90 PDL (one-step senescence model). Pictures A-D represent nuclear changes observed by immunofluorescence microscopy on days 1 and 5 after single 25 µM H_2O_2 exposure. Arrows depict changes in nuclear shapes: yellow – round, green – elongated, and red - gigantic/irregular. A, Untreated cells on day 1; B, prematurely aged fibroblasts after H_2O_2 exposure on day 1; C, Untreated cells on day 5; D, senescent fibroblasts on day 5. Nuclear parameters measured utilizing QuPath in each sample: E, nuclear area; F, nuclear max caliper; G, Nuclear perimeter; H, Nuclear min caliper; I, nuclear circularity; J, nuclear eccentricity. Data were analyzed with a Student's unpaired t-test for each separate parameter. Significance is indicated within the figures using the following scale: ns, not significant; *, $p<0.05$; **, $p<0.01$; ***, $p<0.001$; ****, $p<0.0001$. Bars represent mean ± SD.

2.4.5. Senescence-related changes to gene expression profiles are accompanied by elevation in the expression of cell-cycle regulators

Based on morphological studies, it was hypothesized that cellular shape changes would result in nuclear reorganization through alterations in cell cycle regulators inducing cytoskeleton changes followed by functional and metabolic deterioration. Hence, it was decided to test the expression levels of p16, p21, and p53, cell-cycle progression regulators, senescence-associated markers and corresponding genes in CCD-1135Sk, CCD-1064Sk, and BJ-5ta cultures. This analysis would also show the reliability of our cellular senescence model (see Chapter 3 and Chapter 4).

The Western blot image shown in Figure 2.9 B indicates that the p16 protein levels were increased in cells with RS (CCD-1135Sk, 40 PDL and CCD-1064Sk, 48 PDL), significantly reduced in untreated healthy fibroblasts (CCD-1064Sk, 24 PDL), and were surprisingly low in the 25 µM of H_2O_2 exposed fibroblast. p16 modulates growth inhibitory state by keeping retinoblastoma protein (Rb) hypophosphorylated via targeting CDK4 and CDK6 complexes, ensuing repression of E2F target genes required for S-phase onset. Similar repressive effects of E2F target genes is achieved by cyclin-dependent

kinase inhibitor p21, which inhibits the action of CDK2 activity arresting the cell cycle in G1. The analysis of p21 expression levels indicates that they were almost absent in CCD-1135Sk 40 PDL compared with their CCD-1064Sk 48 PDL counterparts, where the p21 levels were prominent (Figure 2.9, C). A slightly opposite tendency was observed for p53. The expression of this protein was elevated in CCD-1064Sk 48 PDL and 25 µM H_2O_2 treated fibroblast compared with CCD-1135Sk 40 PDL and untreated fibroblast (Figure 2.9, D). Original Western blot images were included in Supplementary Figures 1-11.

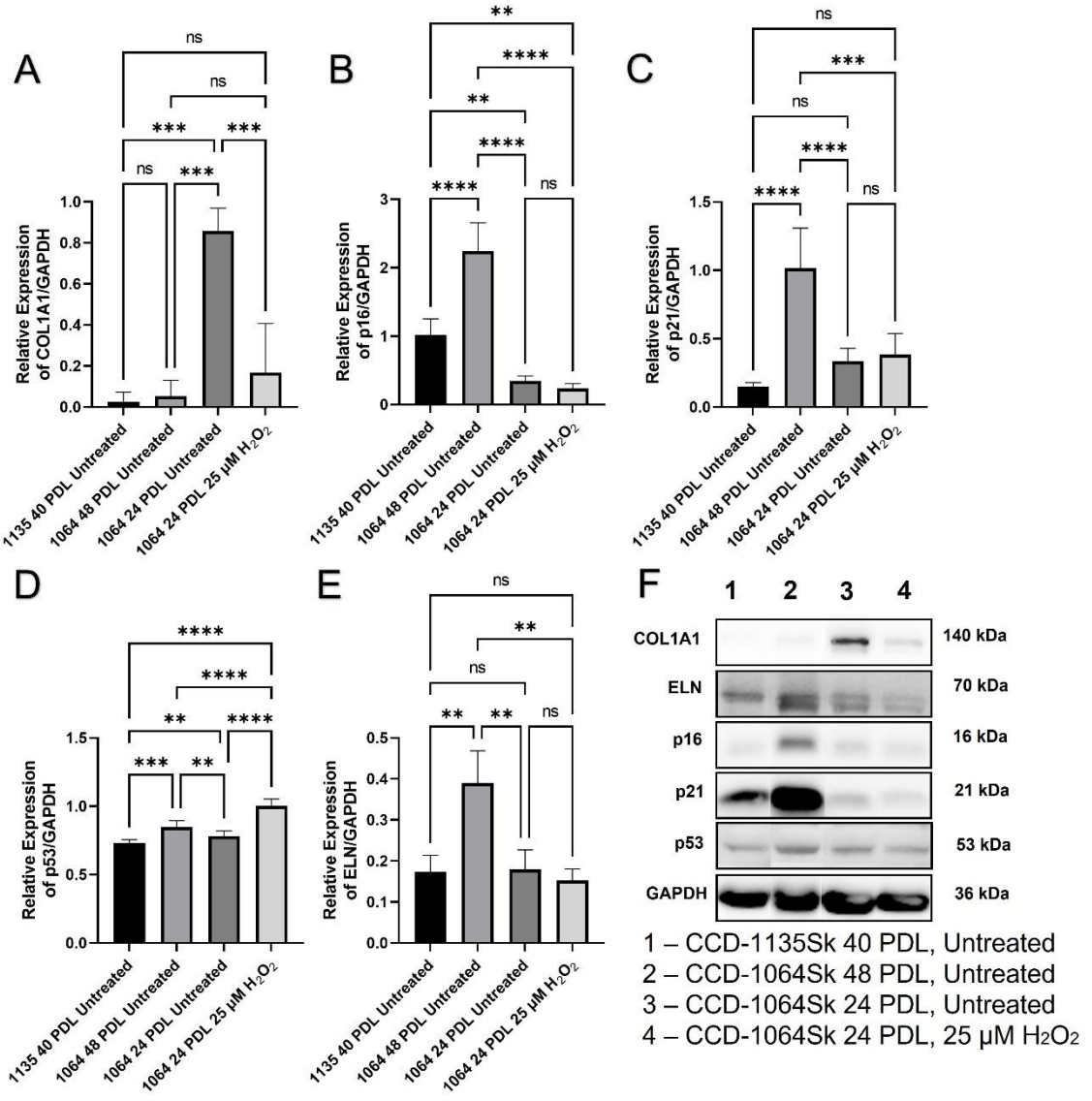

Figure 2.9. The expression of cellular checkpoint regulators and collagen in aged fibroblasts from different cell lines. Fibroblast's cell-lines CCD-1135Sk (40 PDL) and CCD-1064Sk (48 PDL) aged naturally by replicative senescence, and CCD-1064Sk (24 PDL) was aged by one-step H_2O_2 senescence model. Figures A-E show protein expression levels for selected genes measured by Western blot. A, COL1A1 expression; B, p16 expression; C, p21 expression; D, p53 expression; E, Elastin expression; F, Levels of protein expression detected in Western blots. Western blot analysis was performed using 30-50 µg of protein extracts. Glyceraldehyde-3-phosphate dehydrogenase (GAPDH) was used as a loading control. Relative densitometry was presented as a ratio of target protein to GAPDH. Data were analyzed with an ANOVA test (Tukey post-hoc multiple comparison test). Significance is indicated within the figures using the following scale: ns, not significant; *, $p<0.05$; **, $p<0.01$; ***, $p<0.001$; ****, $p<0.0001$. Bars represent mean ± SD.

Western blot analysis of BJ-5ta foreskin fibroblasts showed an exponential rise in p16 and p21 expression levels in a dose-dependent manner (Figure 2.10, A and C respectively). However, the p53 protein levels did not show significant differences, albeit showed a tendency to decrease in response to increasing doses of H_2O_2 (Figure 2.10, E).

One of the typical features of SIPS is lost functional activity. It is well-known that fibroblasts are the main generators of extracellular matrix (ECM) components such as elastin and various types of collagens. Western blots showed significant reduction in type I collagen (COL1A1) expression in senescent CCD-1135Sk 40 PDL, CCD-1064Sk 48 PDL and aged CCD-1064Sk 24 PDL fibroblasts (Figure 2.9, A, F), but not in the prematurely aged BJ-5ta treated with 25 µM H_2O_2 or 50 µM H_2O_2 (Figure 2.11, A). The expression level of type III collagen (COL3A1) was significantly reduced compared to healthy cells (Figure 2.11, C).

Another key protein of the ECM is elastin, encoded by the *ELN* gene. It maintains elasticity and helps cells to regain their shape after stretching or contracting. Increased expression of elastin protein observed in old fibroblasts CCD-1064Sk 48 PDL was unexpected. At the same time, elastin expression was slightly lower in old CCD-1135Sk

40 PDL and prematurely aged CCD-1064Sk compared to the young cells ($p<0.01$, Figure 2.9, E, F).

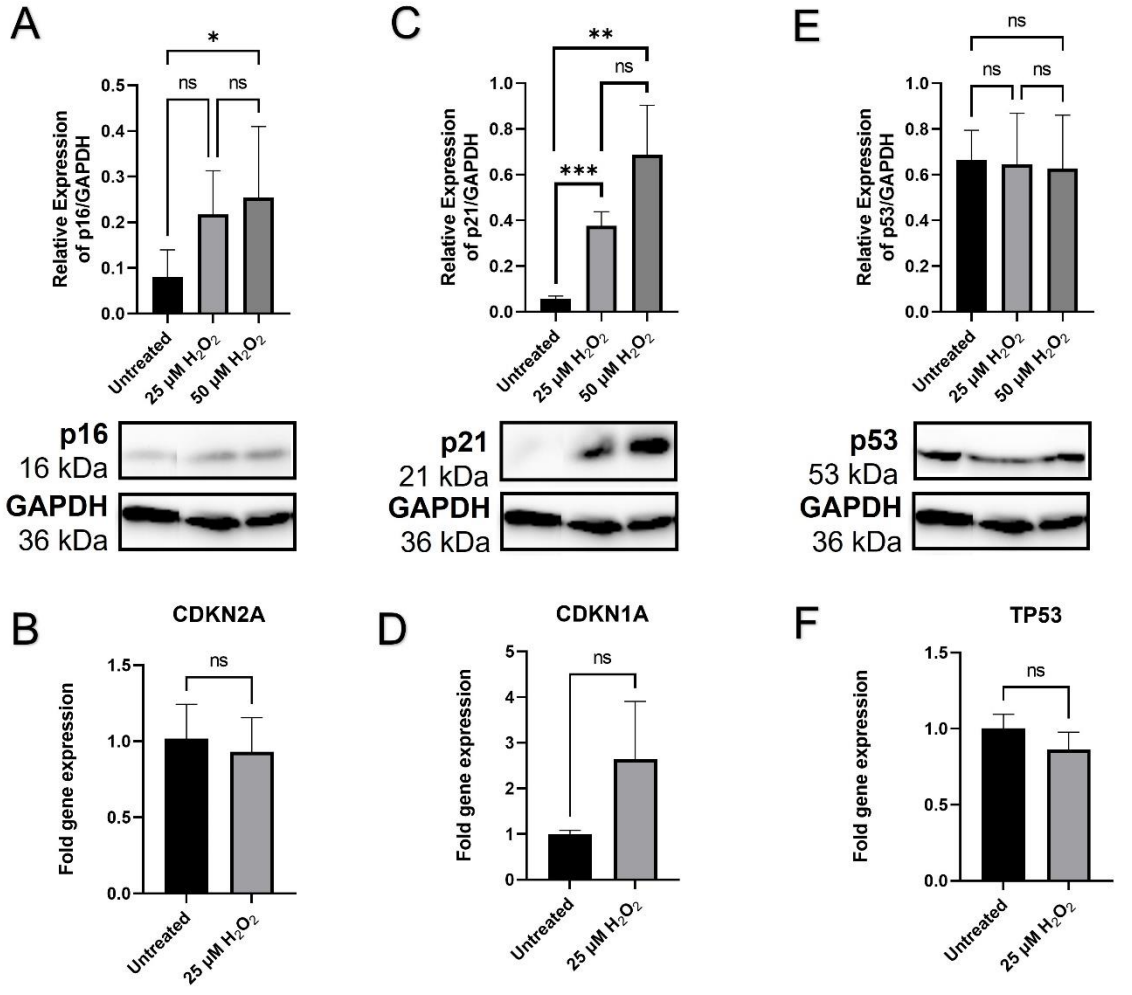

Figure 2.10. The effects of age on cell cycle checkpoint regulators in BJ-5ta fibroblasts. Western blots showing protein levels of p16 (A), p21 (C), and p53 (E). Relative densitometry was presented as a ratio of target protein to GAPDH. Changes of mRNA expression as measured by RT-PCR for *CDKN2A (p16)*, *CDKN1 (p21)*, and *TP53* (B, D, and F, – respectively). Data were analyzed with an ANOVA test (Tukey post-hoc multiple comparison test) (A, C, and E), and an unpaired Student's t-test was used for analysis with two groups (B, D, and F). Significance (p) is indicated within the figures using the following scale: ns, not significant; *, $p<0.05$; **, $p<0.01$; ***, $p<0.001$; ****, $p<0.0001$. Bars represent mean ± SD.

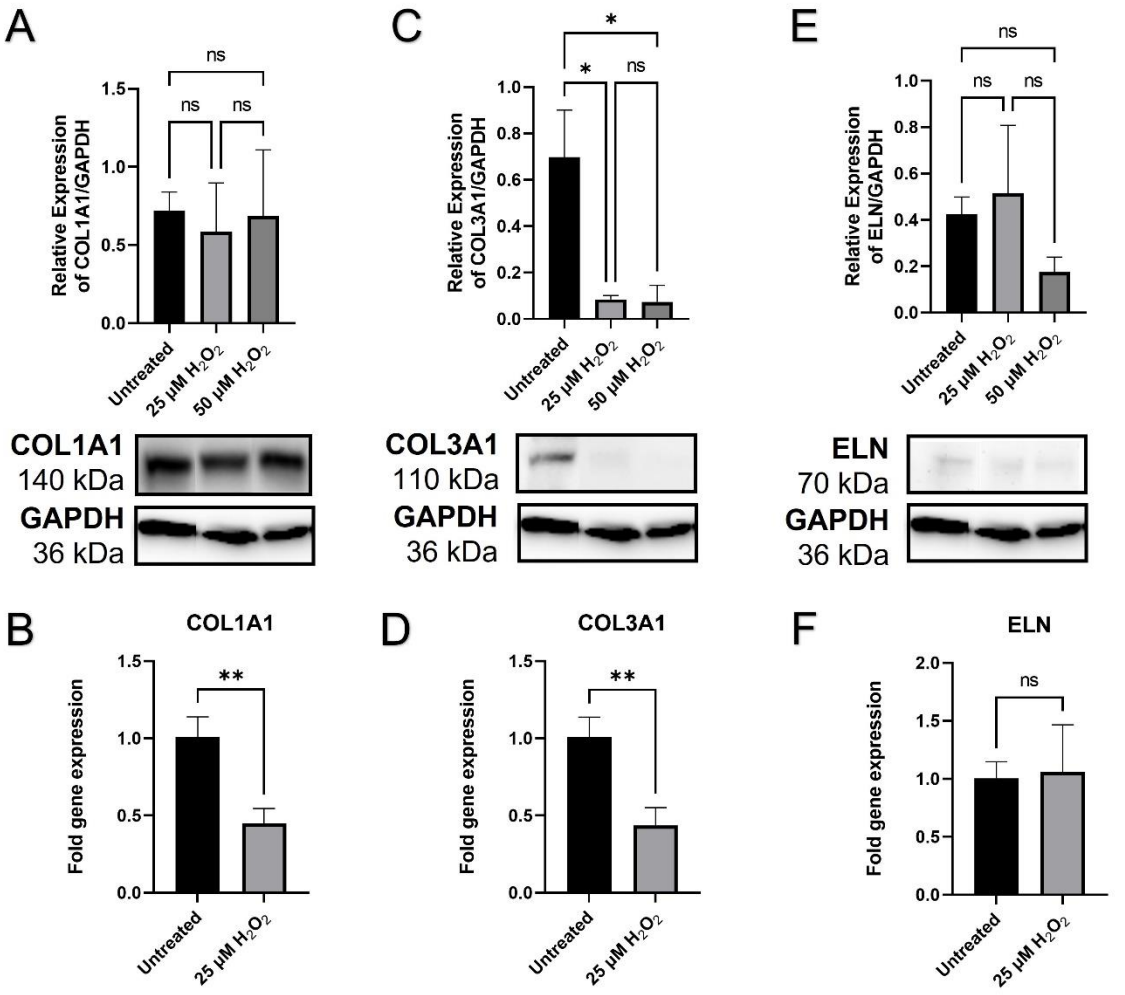

Figure 2.11. The effects of age on production of extracellular matrix components in BJ-5ta fibroblasts. Western blots showing protein levels of COL1A1 (A), COL3A1 (C), and ELN (E). Relative densitometry was presented as a ratio of target protein to GAPDH. Changes of mRNA expression as measured by RT-PCR for *COL1A1*, *COL3A1*, and *ELN* (B, D, and F, – respectively). Data were analyzed with an ANOVA test (Tukey post-hoc multiple comparison test) (A, C, and E), and an unpaired Student's t-test was used for analysis with two groups (B, D, and F). Significance (p) is indicated within the figures using the following scale: ns, not significant; *, $p<0.05$; **, $p<0.01$; ***, $p<0.001$; ****, $p<0.0001$. Bars represent mean ± SD.

Next, mRNA was isolated from dermal fibroblasts and analyzed via RT-PCR. To some extent, the mRNA expression of cell cycle progression regulators quantified with RT-PCR corresponded to the protein expression data seen via Western blot. The expression of important developmental transcriptional regulators and signaling molecules

implicated in fibroblasts' growth, proliferation, and ECM production were quantified. Cell proliferation inhibitor *CDKN2A*, encoding p16 was downregulated in aged CCD-1064Sk ($p<0.01$, Figure 2.12, M), but not BJ-5ta ($p>0.05$, Figure 2.10, B). Although, *TP53* appeared to have lower expression in BJ-5ta senescent cells ($p>0.05$, Figure 2.10, F) and elevated in CCD-1064Sk ($p>0.05$, Figure 2.12, O), it was not statistically significant. In contrast, *CDKN1A*, also known as coding gene for protein p21, was insignificantly upregulated in prematurely aged BJ-5ta ($p>0.05$, Figure 2.10, D) and CCD-1064Sk cells ($p>0.05$, Figure 2.12, N) compared to untreated ones. The senescence-associated abatement in transcript levels of ECM genes *COL1A1* and *COL3A1* was detected ($p<0.01$, Figure 2.11, B and D respectively), while *ELN* expression was slightly elevated compared to untreated cells ($p>0.05$, Figure 2.11, F), which corresponds to the Western blot findings (Figure 2.11, A, C, E). Interestingly, the *MMP1* (matrix metalloproteinase 1) gene, whose protein is known to degrade collagens and other components of ECM was downregulated in aged cells ($p<0.05$, Figure 2.12, R). Similar alterations in gene expression were detected in prematurely aged CCD-1064Sk fibroblasts ($p<0.05$, Figure 2.12). The results for the main dermal scaffold genes *COL3A1* and *ELN* matched BJ-5ta results. Another important gene associated with maintenance of ECM and known to preserve components of the extracellular matrix from damaging activity of MMPs is *TIMP1* (tissue inhibitor of metalloproteinases 1). In addition, the encoded protein can promote cell proliferation exhibit an anti-apoptotic function. As expected, *TIMP1* was downregulated in senescent fibroblasts ($p<0.01$, Figure 2.12, E). *MMP2*, like *MMP1* in BJ-5ta aged fibroblasts, was also downregulated ($p<0.001$, Figure 2.12, D). Furthermore, *HAS1* (Hyaluronan synthase 1 or hyaluronic acid), a vital component of ECM that provides skin hydration and supports

a matrix which enables cells to migrate through (Skandalis, 2019), showed an unexpected rise in senescent cells ($p>0.05$, Figure 2.12, C) but was not statistically significant.

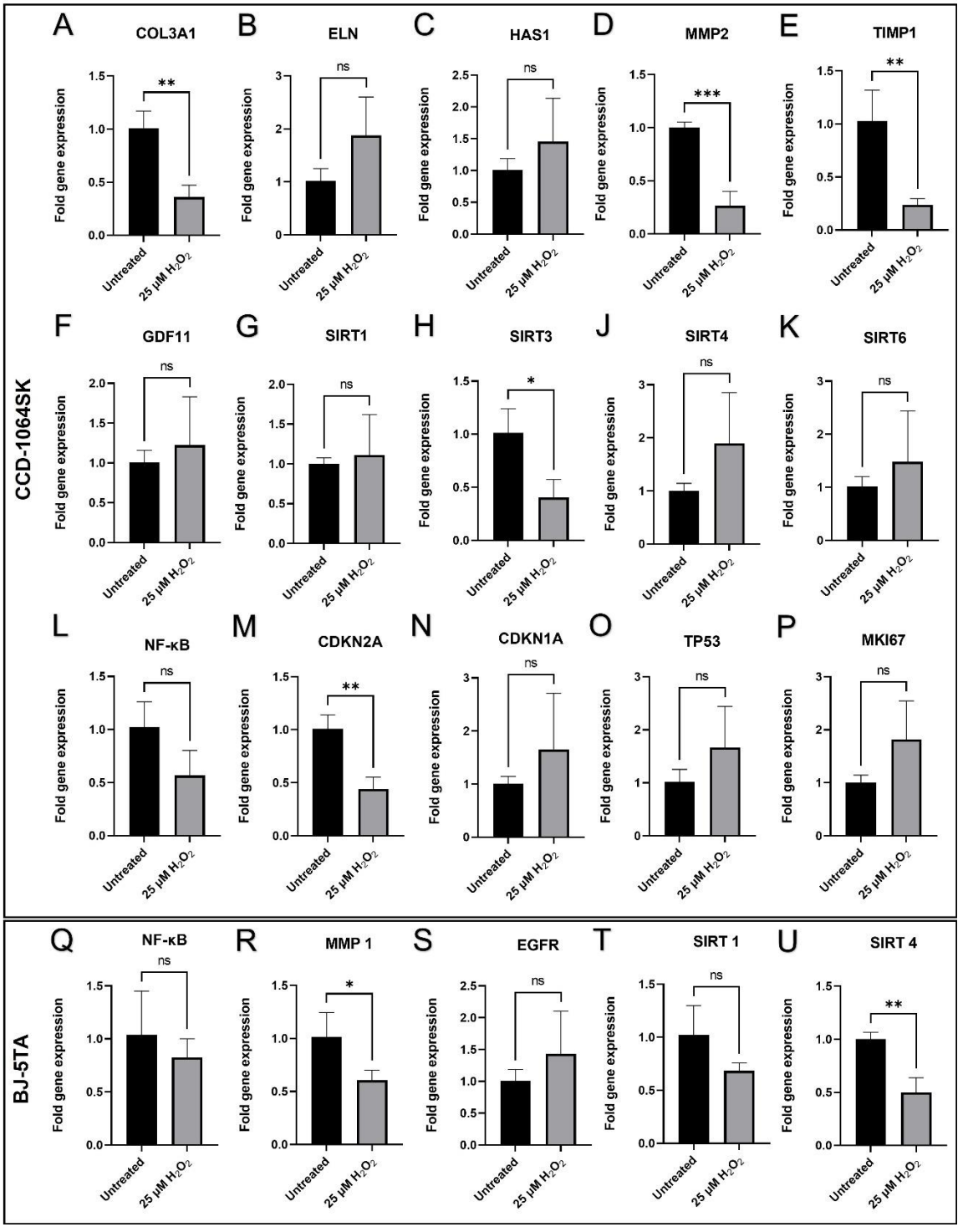

Figure 2.12. Senescence-associated gene expression in CCD-1064Sk and BJ-5ta dermal fibroblasts (one-step senescence model). Changes in mRNA expression levels for selected genes measured by RT-PCR in **CCD-1064Sk** cells: A, *COL3A1*; B, *ELN*; C, *HAS1*; D, *MMP2*; E, *TIMP1*; F, *GDF11*; G, *SIRT1*; H, *SIRT3*; J, *SIRT4*; K, *SIRT6*; L, *NF-κB*; M, *CDKN2A*; N, *CDKN1A*; O, *TP53*; P, *MKI67*; in **BJ-5ta**: Q, *NF-κB*; R, *MMP1*; S, *EGFR*; T, *SIRT1*; U, *SIRT4*. Data were analyzed with an unpaired Student's t-test. Significance is indicated within the figures using the following scale: ns, not significant; *, $p<0.05$; **, $p<0.01$; ***, $p<0.001$. Bars represent mean ± SD.

Taken together, there was a change in the expression of a large number of genes when comparing young to old passages of untreated cells and prematurely aged fibroblasts. Specifically, altered expression of p16, p21 and collagens were demonstrated and are indicators of SIPS.

2.4.6. Senescence-related changes in the expression of genes and proteins involved in cell cycle regulation, cellular replication, and metabolic responses

To obtain an understanding of what molecular pathways were involved in the progression of senescence or may be abnormally regulated during senescence, we analyzed the gene expression by RT-PCR analysis of mRNA and at the protein level by Western blot in dermal fibroblasts.

The expression of *NF-κB* (Nuclear factor-kappa B) was moderately downregulated in both CCD-106Sk and BJ-5ta prematurely aged fibroblasts ($p>0.05$, Figures 2.12, L and Q respectively). Similar trends were seen in Western blot analysis (Figure 2.13, D). NF-κB is a protein transcription factor that controls transcription of DNA, cytokine production, and regulation of expression of multiple genes associated with cell survival, proliferation, and differentiation. Another critical gene, which protein is involved in cell signaling pathways that control cell division and survival, *EGFR* (epidermal growth factor

receptor), was mildly upregulated ($p>0.05$, Figure 2.12, S) and was poorly expressed on the protein level ($p<0.001$, Figure 2.13, G) after the H_2O_2 exposure.

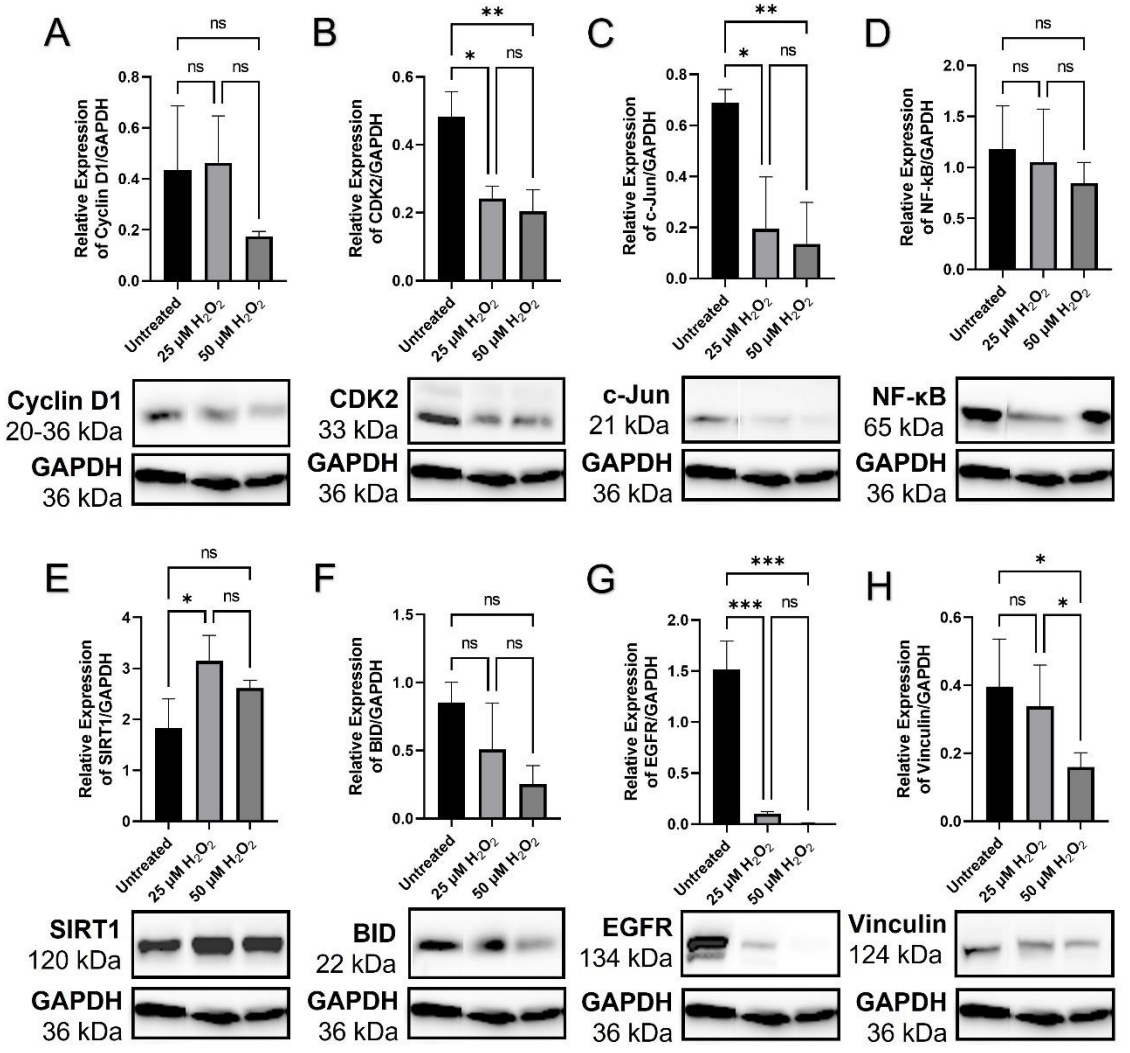

Figure 2.13. The expression of cell-cycle regulators, functional, and regulatory proteins in aged fibroblasts of BJ-5ta cell line. Fibroblasts were aged by the one-step H_2O_2 senescence model. Figures represents changed protein expression levels for selected genes measured by Western blot. A, Cyclin D1 expression; B, CDK2 expression; C, c-Jun expression; D, NF-κB expression; E, SIRT1 expression; F, BID expression; G, EGFR expression; H, Vinculin expression. Western blot analysis was performed using 30-50 μg of protein extracts. Glyceraldehyde-3-phosphate dehydrogenase (GAPDH) was used as a loading control. Relative densitometry was presented as a ratio of target protein to GAPDH. Data were analyzed with an ANOVA test (Tukey post-hoc multiple comparison test). Significance is indicated within the figures using the following scale: ns, not significant; *, $p<0.05$; **, $p<0.01$; ***, $p<0.001$. Bars represent mean ± SD.

Besides the role in cell signaling pathways that control cell division and survival, NF-κB and EGFR are also involved in apoptosis pathways, hence, deviations in their regulation might influence the process of programmed cell death and potentially senescence. For this reason, we tested expression levels of the BH3 interacting-domain death agonist (BID), which is a pro-apoptotic member of the Bcl-2 protein family contributing to the mitochondrial pathway of apoptosis. Of note, BID expression demonstrated a dose-dependent decrease with exposure to increasing concentrations of H_2O_2 ($p>0.05$, Figure 2.13, F). Corresponding changes were found in the level of Vinculin expression (Figure 2.13, H); vinculin is a membrane-cytoskeletal protein associated with maintaining cell-cell and cell-matrix adhesion, emerging as a regulator of apoptosis, and found to be overexpressed in apoptotic cells (Propato et al., 2001). In addition to this, c-Jun is a part of the activator protein-1 (AP-1) complex, involved in regulation of proliferation, apoptosis, survival, tumorigenesis, and tissue morphogenesis (Meng & Xia, 2011) was significantly diminished in aged fibroblast (Figure 2.13, C). Moreover, c-Jun is required for progression through the G1 phase of the cell cycle which occurs by a mechanism that incorporates direct transcriptional control of the cyclin D1 gene, forming a molecular connection between growth factor signaling and cell cycle regulation (Wisdom et al., 1999). Cyclin D1 levels were almost identical to the untreated fibroblasts after treatment with 25 μM of H_2O_2 and insignificantly declined after treatment with 50 μM of H_2O_2 (Figure 2.13, A). In parallel, the levels of cyclin-dependent kinase 2 (CDK2), the protein required for the transition from G1 to S phase, decreased significantly ($p<0.05$, Figure 2.13, C).

Changes in the cell cycle progression typically affect other cellular functions like proliferation, differentiation, metabolic activity, etc. Recently ascertained growth differentiation factor 11 (GDF11), a key to progenitor proliferation and/or differentiation, was also considered to be important for the preservation of youthful phenotypes in different human tissues, and, in the skin, to inhibit inflammatory responses (Rochette et al., 2020). The expression of *GDF11* in prematurely aged fibroblasts tends to increase compared to untreated cells ($p>0.05$, Figure 2.12, L). One more essential nuclear protein associated with cellular proliferation is a marker of proliferation Ki-67 (MKI67). *MKI67* was insignificantly elevated in fibroblasts treated with H_2O_2 (Figure 2.12, P).

Sirtuins (SIRT1–7) are known to prevent diseases and even reverse aspects of aging. They are regulated at the level of transcription, translation, protein stability, and oxidation (Bonkowski & Sinclair, 2016). Thus, nuclear sirtuins SIRT1, SIRT6, and SIRT7 act as transcription regulators (Fernandez-Marcos & Auwerx, 2011; Toiber et al., 2011) and modulate energy metabolism, cell survival, DNA repair, tissue regeneration, inflammation, neuronal signaling, and even circadian rhythms (Chang & Guarente, 2014; Haigis & Sinclair, 2010). Cytosolic SIRT2 was also detected in the nucleus where it modulates cell cycle control (Dryden et al., 2003; L. Serrano et al., 2013). SIRT3 activity intersects with the mammalian target of rapamycin (mTOR) (Karnewar et al., 2018; Wu et al., 2018), AMPK signaling extracellular signal-regulated kinase (ERK) (Mihaylova & Shaw, 2011), and is also involved in mitochondrial biogenesis and activating autophagy (Choi, 2020; Kuang et al., 2020). Mitochondrial SIRT3-5 modulate the activities of metabolic enzymes and moderate oxidative stress in response to calorie restriction (CR), inducing stress tolerance by switching cells to favor mitochondrial oxidative metabolism (Chang & Guarente, 2014).

The results of RT-PCR analysis of Sirtuins, family of signaling proteins involved in metabolic regulation, showed that *SIRT1* was mildly upregulated in aged CCD-1064Sk cells ($p>0.05$, Figure 2.12, G), while in BJ-5ta fibroblasts it was downregulated ($p>0.05$, Figure 2.12, T). However, levels of protein expression of SIRT1 were significantly augmented in fibroblasts exposed to the 25 μM H_2O_2 (Figure 2.13, E). At the same time, *SIRT3* was strongly downregulated ($p<0.05$, Figure 2.12, H) in contrast to moderately upregulated *SIRT4* and *SIRT6* ($p>0.05$, Figures 2.12, J and K respectively).

In summary, changes in gene expression were observed when comparing young and senescent dermal fibroblasts. Along with the altered expression of numerous cell cycle regulators and genes with previously determined age-related expression changes, we found changes in the expression of proteins involved in metabolic regulation and the ECM.

2.4.7. Aspects of senescence-associated cellular viability

Results of the cellular viability assay showed a significant reduction in number of prematurely senescent fibroblasts (Figure 2.14). The growth of CCD-1064Sk cells was three times of that of untreated newborn fibroblasts. At the same time, in prematurely senescent cells a 33.6% elevation in cellular growth was observed five days after single H_2O_2 exposure (Figure 2.14, A). In comparison, lysosomal absorption of neutral red (NR) was slightly higher in the senescent fibroblasts than in untreated cells at the beginning of the experiment (Figure 2.15, A). However, NR absorbance gradually declined within the next five days.

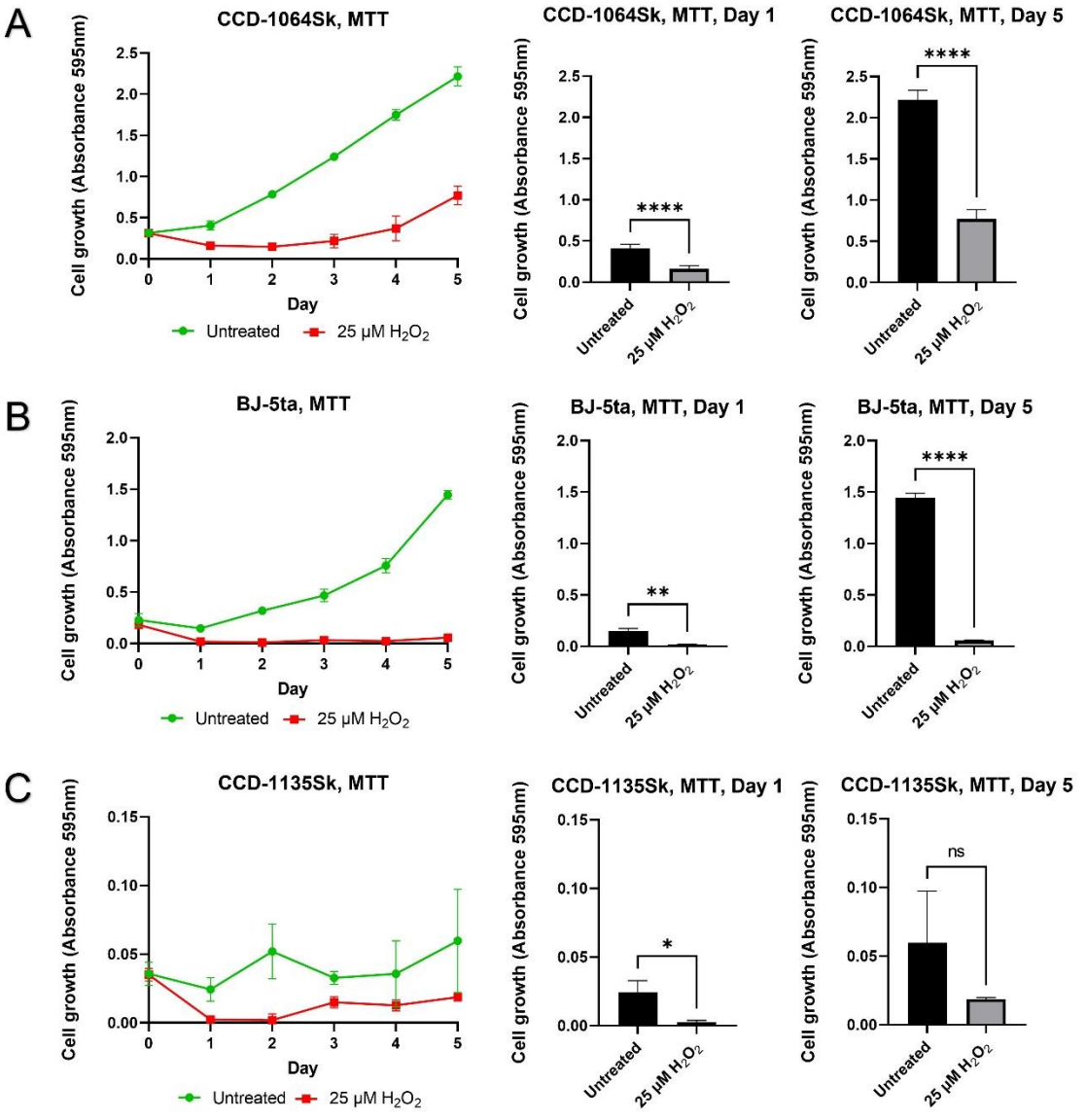

Figure 2.14. Viability of dermal fibroblasts estimated by MTT assay five days after single treatment of 25 μM of H_2O_2 (one-step senescence model). A, CCD-1064Sk, 24 PDL; B, BJ-5ta, 90 PDL; C, CCD-1135Sk, 36 PDL. Data were analyzed with a Student's unpaired t-test for each separate parameter. Bars represent mean ± SD. ns, not significant; *, $p<0.05$; **, $p<0.01$; ***, $p<0.001$; ****, $p<0.0001$.

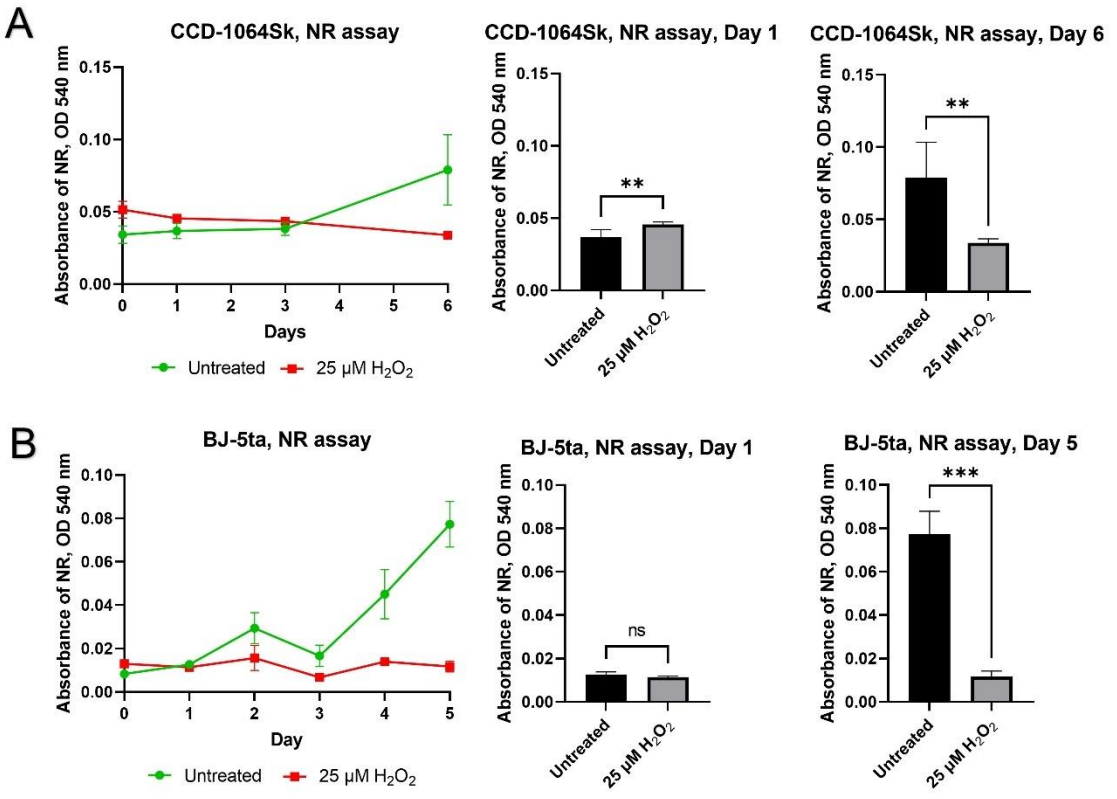

Figure 2.15. Viability of dermal fibroblasts estimated by Neutral red assay (one-step senescence model). A, CCD-1064Sk 32 PDL in six days after a single treatment of H_2O_2; B, BJ-5ta 48 PDL within five days after a single treatment of H_2O_2. Data were analyzed with a Student's unpaired t-test for each separate parameter. Bars represent mean ± SD. ns, not significant; *, $p<0.05$; **, $p<0.01$; ***, $p<0.001$.

Significantly less growth was detected in the prematurely senescent cells by approximately ten-fold compared to the untreated fibroblasts of the BJ-5ta cell line (Figure 2.14, B). The development of senescent BJ-5ta fibroblasts was stopped. Only 3% increase in cell number was noticed five days after the H_2O_2 exposure. Like the CCD-1064Sk cell line, prematurely senescent BJ-5ta fibroblast showed slightly higher NR absorbance than untreated cells (Figure 2.15, B).

In the adult dermal fibroblasts (CCD-1135Sk, 36 PDL) we found decreased cellular viability (Figure 2.14, C). Interestingly, one day after H_2O_2 exposure, the growth of the untreated cells was higher ($p<0.05$) than in senescent cells, although, growth was substantially lower in CCD-1135Sk, as compared to two other cell lines. Mycoplasma contamination of cell cultures has been ruled out (data not shown). Albeit until day five, the untreated skin fibroblasts demonstrated increased rate of growth compared to the prematurely senescent cells, but this difference was not significant (Figure 2.14). This interesting finding showed that adult dermal fibroblasts at 36 PDL, which according to the manufacturer, are almost in a senescent state (Dimri et al., 1995).

2.4.8. Senescent fibroblasts showed reduced ability in the healing process

To determine if senescent dermal fibroblasts have a similar ability to fully participate in the healing process, we performed the wound healing assay in the adherent cellular monolayer. Images of the wound healing assay were taken at the following time points: 1 h, 6 h, 24 h, 48 h, and 72 h after scratching.

The most prominent findings were detected on 24 h and 72 h from the beginning of the experiment. Thus, in both untreated cell lines, the wound was more than 50% closed after 24 h (Figure 2.16, E, G). In contrast, the wound surface in the H_2O_2-exposed cell cultures was moderately increased (Figure 2.16, F) or slightly narrowed (Figure 2.16, H) at the same time point. Complete closure of the scratch line was observed 48 h after the beginning of the experiment in the BJ-5ta cell line (data not shown). Whereas after 72 h, about 3% of the wound area in the untreated CCD-1164Sk fibroblasts and 23% ($p<0.01$) in prematurely senescent fibroblasts were still uncovered (Figure 2.16, M). In the case of

BJ-5ta cells treated with H_2O_2, after 72 h, 12.5% of the wound area remained unhealed ($p<0.01$, Figure 2.16, N).

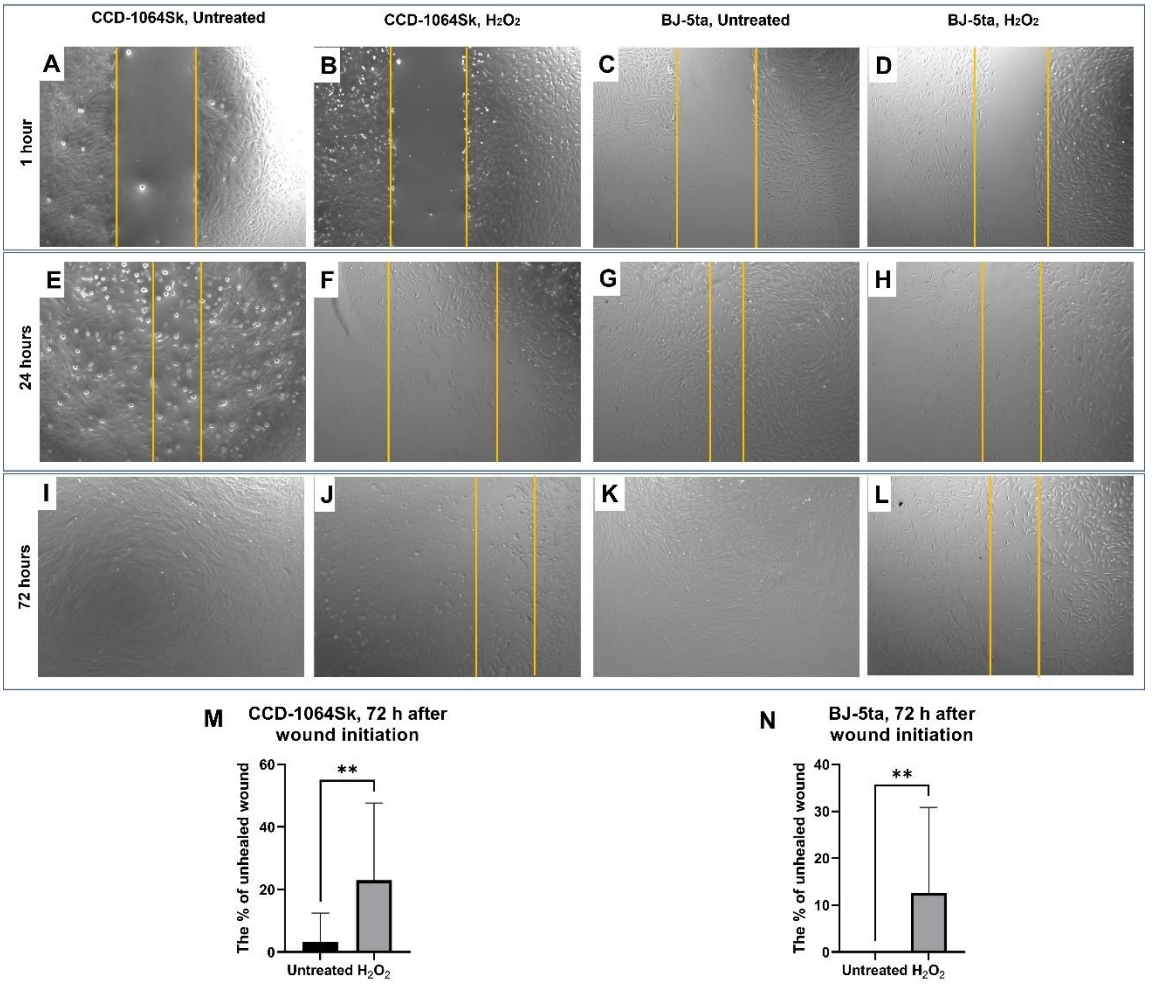

Figure 2.16. Regenerative ability of dermal fibroblasts estimated by wound-healing assay (one-step senescence model). Wound area in CCD-1064Sk, 24 PDL (A-B) and BJ-5ta, 90 PDL (C-D) one hour after single-time H_2O_2 exposure. Decreased wound area in CCD-1064Sk, 24 PDL (E-F) and BJ-5ta, 90 PDL (G-H) 24 hours after a single treatment of H_2O_2. Wound closure in CCD-1064Sk, 24 PDL (I-J) and BJ-5ta, 90 PDL (K-L) 72 hours after a single treatment of H_2O_2. The percentage of the area of the wound that is not healed in CCD-1064Sk, 24 PDL (M) and BJ-5ta, 90 PDL (N) 72 hours after single-time H_2O_2 exposure. Data were analyzed with a Student's unpaired t-test for each separate parameter. Bars represent mean ± SD. **, $p<0.01$.

The wound-healing assay results demonstrated delayed regenerative capabilities of the senescent dermal fibroblasts, resulting in a decline in the healing process.

Based on the significant increase in the senescence biomarkers of the CCD-1135Sk, CCD-1064Sk, and BJ-5ta cultures, along with the reduced functional and metabolic activity, the one-step senescence model was chosen for all further experiments and will be hereafter referred to as the senescence model.

2.5. DISCUSSION

Senescence has been studied for many decades, and still, there are more questions than answers. The main breakthroughs in cellular senescence were made after the Hayflick limit discovery. To date, we accumulated knowledge about cell-cycle life span, gene function, regulation, editing, and molecular mechanisms of various pathways for multiple physiological and pathological processes, i.e., immune response, inflammation, senescence, and cancer regulation. However, we cannot stop senescence and have not even come close to understanding mechanisms that might allow us to delay it.

In our research, we focused on establishing a reliable model of cellular senescence. It is a well-known fact that the number of senescent cells increases with age. Considering that skin is the largest organ in the body and represents the main line of defense, it also expresses the first visible aging features. Accordingly, the most suitable cells for senescence studies *in vitro* are dermal fibroblasts, dominant in the skin structure and important for maintaining the skin's microenvironment.

The three different fibroblasts cell lines used herein were selected for senescence model reproduction induced by H_2O_2 exposure. After H_2O_2 exposure, dermal fibroblasts exhibited senescent-like morphology, significantly higher β-gal expression, decreased PD levels, and proliferation (Figures 2.4-2.8). These findings are in line with previous reports, which show that SIPS is associated with growth arrest, elevation in the proportion of β-

gal-positive cells, and typical structural changes (Chen et al., 1998; Chhunchha et al., 2017; Frippiat et al., 2001; Ott et al., 2018; De Magalhães, 2004; Sasaki et al., 2014; Sidler, Woycicki, et al., 2014; Toussaint et al., 2000). It is important to note that β-gal is a lysosomal enzyme that is typically active at pH 4, but in RS and SIPS cells becomes detectable at pH 6 mirroring to some extent the increase in lysosomal mass (Ott et al., 2018). It has been confirmed that lysosomes increase in number and size in senescent cells (Robbins et al., 1970). In 1995, Debacq-Chainiaux and colleagues found that an increase in β-galactosidase activity was strongly associated with senescent cells, as a function of replicative age both in the absence and presence of lysosomal inhibitors; β-Gal activity was not detected in quiescent or terminally differentiated cells (Debacq-Chainiaux et al., 2009). Later on, Lee et al. confirmed the lysosomal origin of β-gal activity when showed that it resulted from an increased expression of *GLB1*, the gene encoding lysosomal β-D-galactosidase, the activity of which is typically measured at acidic pH 4.5 (Lee et al., 2006).

With that in mind, another interesting observation came out after analyzing the NR assay results. This assay is based on the ability of viable cells to incorporate and bind the supravital dye neutral red in the lysosomes (Repetto et al., 2008). Our results demonstrated an increase in neutral red lysosomal absorption after one day of H_2O_2 exposure compared to untreated cells ($p<0.01$, Figure 2.15, A). That might be explained by the compensatory response to sudden stress-related senescent changes in the cellular microenvironment. As mentioned above, the number of lysosomes increases proportionally to the age (Robbins et al., 1970). Simultaneously, images taken 24 h since the beginning of exposure of H_2O_2 (Figure 2.5, I-L) indicated a dose-dependent decline in the number of viable lysosomes containing NR dye. These findings potentially explain the gradual decrease in NR

absorbance levels within the next five days of exposure. It might also be related to the elevated degradation processes inside the prematurely aged fibroblasts and consequent reduction in the total number of viable cells. The latter is in line with the MTT results, which showed significant diminishing in viability and rate of fibroblasts growth (Figure 2.14), which is also supported by the data from other research groups (Burova et al., 2013; Dudonné et al., 2011; Ho et al., 2021; Lee et al., 2022).

Apart from reduced growth and viability, morphological changes in senescent dermal fibroblasts were also detected. Increased cellular size and changes in the cell shape were observed parallel to the changes in nucleus. The analysis of the prematurely aged fibroblasts nuclei reflected morphological alterations of an entire cell. Nuclei of senescent fibroblasts displayed wide-scale deformations and lobulations, whereas young cells had smooth disk-shaped nuclei. Interestingly, nuclei from aged cells showed an increased area in both cell lines and significant busting of circularity that represents roundness (Figures 2.7, 2.8). At the same time, the gene expression and protein levels of ECM components, mainly collagens, which externally affect the cellular shape, were decreased.

Furthermore, such deviations in cellular shape might be caused by decreased expression of membrane-cytoskeletal protein vinculin in senescent cells, associated with maintaining cell-cell and cell-matrix connections (Figure 2.13, H). We can speculate that fibroblasts enlargement was a compensatory response to a decline in vinculin level to prevent cellular detachment and increase the surface of adhesion. Other publications partially support these assumptions. Aifuwa and colleagues recently determined that prematurely senescent cells were considerably softer and less elastic than control cells (Aifuwa et al., 2015). The authors emphasized diminished focal adhesion (vinculin) and

decreased expression of cytoskeletal proteins (lamin A/C, F-actin, myosin II, Rho A), as well as a significant reduction in root mean square traction forces and the cytoskeletal contractility of senescent cells that eventually result in the loss of cellular tension that correlated with shape changes of the cells and their nuclei. Altogether, these results may suggest that intercellular contractility and traction inhibition are sufficient to recapitulate the nuclear phenotype induced by H_2O_2 and potentiated by alterations in cell-cycle regulation followed by metabolic changes.

Table 2.3. Summary of the investigated characteristics of prematurely aged skin fibroblasts compared to untreated fibroblasts

Characteristic	H_2O_2-Induced SIPS Fibroblasts
Shape and size of the cell	Enlarged, flattened, irregular
Nuclear circularity (roundness)	Increased
β-Gal level	High
BID	No change detected
CDK2	Low
c-Jun	Low
Collagens (type I, III)	Low
Cyclin D1	No change detected
EGFR	No change detected
Elastin	Increased
Hyaluronan	Increased
MMP 1, 2	Low
MKI67	High
NF-kB	No change detected
P16	Moderate
P21	High
P53	No change detected
SIRT 1	No change detected
SIRT 3, 4	Low
SIRT 6	No change detected
TIMP 1	Low
Vinculin	Low
Cell viability	Low
Wound healing	Decreased

We observed increased transcriptional abundance from p21, deviations in p16, p53, decreased CDK2, and c-Jun, suggesting that the H_2O_2-dependent SIPS contribute to growth arrest typical for senescent cells (Table 2.3). Indeed, SIPS-triggered senescence is directly maintained by p53, which promotes the cyclin-dependant kinase inhibitor p21 upregulation, which in turn inhibits the action of CDK2 kinase activity arresting the cell cycle in G1. Additionally, p21 blocks the cyclin D1/CDK4/6-mediated hyperphosphorylation of Rb protein. The hypophosphorylated state of Rb leads to the inhibition of the transcription factor gene *E2F* and subsequent transcription machinery required for S-phase onset (Ott et al., 2018). Besides, p16 may mediate the initiation of H_2O_2-induced cell cycle arrest by inhibiting the activation of CDK4 and CDK6 that contribute to cell cycle phase progression ensuing repression of E2F target genes forcing a G1 cell-cycle arrest (Burova et al., 2013).

Our results indicated a significant reduction in CDK2, c-Jun protein levels, accompanied by decline of cyclin D1 (Figures 2.13, A-B), suggesting potential growth arrest. Interestingly, Morris and coworkers found that reduced cyclin D1 levels and enhanced association of p27kip1 with CDK2 causes G1 arrest in NIH 3T3 cells (Morris et al., 1998). Another research group showed that in contrast to young cells, senescent fibroblasts contained mainly underphosphorylated cyclin E and proportionally more unphosphorylated and inactive CDK2. Moreover, in the predominant part of senescent cells, the CDK2 was complexed with cyclin D1. It is worth mentioning that cyclin D1-CDK2 complexes were severalfold higher in senescent cells and contained exclusively unphosphorylated CDK2, perhaps accounting for the low kinase activity (Dulić et al., 1993).

A critical step in the cell-cycle regulation is associated with c-Jun-mediated G1 progression, directly controlling cyclin D1 gene transcription (Wisdom et al., 1999). Our experimental model showed a substantial reduction of c-Jun expression in SISP-induced fibroblasts (Figure 2.13, C), which also explains the consequent alterations in CDK2 and cyclin D1 expression. Apart from the fact that c-Jun is involved in multiple molecular pathways, it also protects cells from various SIPS associated stressors and their effects (i.e., UV-induced cell death) and cooperates with NF-κB to prevent apoptosis induced by tumor necrosis factor alpha (TNFα) (Wisdom et al., 1999). At the same time, our data indicated that expression of *NF-κB* has been moderately downregulated in prematurely aged dermal fibroblasts (Figure 2.12, L, Q). This might be an additional factor leading to delayed cell cycle progression as NF-κB, apart from controlling multiple genes associated with cell survival, proliferation, apoptosis, and differentiation, also activates the expression of cyclin D1.

Aside from the findings related to the alterated cell-cycle regulators in SIPS-induced cells, changes in the proteins associated with apoptosis pathways (BID), metabolic regulation (sirtuins), and components of ECM (collagens, elastin, hialuronan) were also found (Table 2.3). These results are widely supported by various research by similar findings in various cell types and tissues (Chiang et al., 2014; di Martino et al., 2017; Lago & Puzzi, 2019; Lämmermann et al., 2018; Lee et al., 2022; Skandalis et al., 2020; Soydas et al., 2018, 2021).

Dermal fibroblasts are mesenchymal cells considered to maintain skin integrity and functionality via ECM production. They also orchestrate tissue repair by interacting with and controlling other cell types, including immune cells, myocytes, and keratinocytes in the wound microenvironment. Decreased expression of *COL1A1*, *COL3A1*, *TIMP1*, and

elevation of elastin suggests degradation of ECM and explains delayed healing process and corresponds to literature data (di Martino et al., 2017; Lago & Puzzi, 2019). Moreover, collagen fibrils and elastin are responsible for the strength and resiliency of skin. It is a known fact that ECM components degeneration with aging causes skin to become fragile and easily bruised. On the histological level, connective tissue damage (e.g., skin) induced by ultraviolet irradiation manifests as a disorganization of collagen fibrils resembling wavy worm-like appearance of the fibers, massive aggregation of abnormal, amorphous and elastin containing material. Such accumulation of elastotic material (i.e., increased deposition of degraded elastin material) is accompanied by degeneration of the surrounding collagen matrix (Taihao, 2016). In support of the previous statements, we observed increased expression of elastin (Figures 2.11, 2.12) accompanied by a delayed wound healing process in the monolayer of cultured fibroblasts exposed to H_2O_2 (Figure 2.16). These data showed significant deterioration in regenerative capabilities of the prematurely aged fibroblasts that reflected the morphological, biomolecular, and functional changes in naturally old cells (Ott et al., 2018; Kang, 2019).

To summarize, both H_2O_2-induced senescence models designed in our lab demonstrated clearly visible changes in fibroblasts morphology typical for SIPS corresponding to other research groups (Frippiat et al., 2001; Ott et al., 2018; Serrano et al., 1997; Toussaint et al., 2010). Moreover, both SIPS models showed the evidence of fibroblasts developing similar aging characteristics as the RS cells, compared to the respective young and untreated controls. Among the most noticeable senescent biomarkers were the increased β-gal and *MKI67* expression, accompanied by high p21 protein levels, altered levels of cell-cycle regulators (i.e., CDK2 and c-Jun) and ECM components, reduced cellular viability, and delayed wound healing properties (Table 2.3). This suggests

that although replicative and H_2O_2-induced senescence present very similar phenotypic traits, pathogenetic factors in the SIPS model led to more transcriptional changes.

The results of our research uncovered some potential mechanisms of cellular senescence and might help find possible anti-aging remedies. The one-step cellular senescence model developed here should be suitable to test effects of potential anti-aging compounds.

2.6. REFERENCES

Aifuwa, I., Giri, A., Longe, N., Lee, S. H., An, S. S., & Wirtz, D. (2015). Senescent stromal cells induce cancer cell migration via inhibition of RhoA/ROCK/myosin-based cell contractility. *Oncotarget*, *6*(31), 30516–30531. www.impactjournals.com/oncotarget/

Ashcroft, G. S., Horan, M. A., Herrick, S. E., Tarnuzzer, R. W., Schultz, G. S., & Ferguson, M. W. J. (1997). Age-related differences in the temporal and spatial regulation of matrix metalloproteinases (MMPs) in normal skin and acute cutaneous wounds of healthy humans. *Cell and Tissue Research*, *290*(3), 581–591. https://doi.org/10.1007/s004410050963

Bayreuther, K., Peter Rodemann, H., Hommel, R., Dittmann, K., Albiez, M., & Francz, P. I. (1988). Human skin fibroblasts in vitro differentiate along a terminal cell lineage. *Proc. Nail. Acad. Sci. USA*, *85*(14), 5112–5116.

Berneburg, M., Plettenberg, H., Medve-König, K., Pfahlberg, A., Gers-Barlag, H., Gefeller, O., & Krutmann, J. (2004). Induction of the photoaging-associated mitochondrial common deletion in vivo in normal human skin. *Journal of Investigative Dermatology*, *122*(5), 1277–1283. https://doi.org/10.1111/j.0022-202X.2004.22502.x

Bertschmann, J., Thalappilly, S., & Riabowol, K. (2019). The ING1a model of rapid cell senescence. *Mechanisms of Ageing and Development*, *177*, 109–117. Elsevier Ireland Ltd. https://doi.org/10.1016/j.mad.2018.06.004

Bonkowski, M. S., & Sinclair, D. A. (2016). Slowing ageing by design: The rise of NAD+ and sirtuin-activating compounds. *Nature Reviews Molecular Cell Biology*, *17*(11), 679–690). Nature Publishing Group. https://doi.org/10.1038/nrm.2016.93

Boraldi, F., Annovi, G., Tiozzo, R., Sommer, P., & Quaglino, D. (2010). Comparison of ex vivo and in vitro human fibroblast ageing models. *Mechanisms of Ageing and Development*, *131*(10), 625–635. https://doi.org/10.1016/j.mad.2010.08.008

Brack Christine, Lithgow Gordon, Osiewacz Heinz, & Toussaint Olivier. (2000). EMBO WORKSHOP REPORT: Molecular and cellular gerontology Serpiano, Switzerland, September 18-22, 1999. *The EMBO Journal*, *19*(9), 1929–1934. https://doi.org/10.1093/emboj/19.9.1929

Burova, E., Borodkina, A., Shatrova, A., & Nikolsky, N. (2013). Sublethal oxidative stress induces the premature senescence of human mesenchymal stem cells derived from endometrium. *Oxidative Medicine and Cellular Longevity*, *2013*, 1–12. https://doi.org/10.1155/2013/474931

Caldini, R., Chevanne, M., Mocali, A., Tombaccini, D., & Paoletti, F. (1998). Premature induction of aging in sublethally H_2O_2-treated young MRC5 fibroblasts correlates with increased glutathione peroxidase levels and resistance to DNA breakage. *Mechanisms of Ageing and Development*, *105*(1–2), 137–150. https://doi.org/10.1016/S0047-6374(98)00085-2

Campisi, J., & D'Adda Di Fagagna, F. (2007). Cellular senescence: When bad things happen to good cells. *Nature Reviews Molecular Cell Biology*, *8*(9), 729–740. https://doi.org/10.1038/nrm2233

Chang, H. C., & Guarente, L. (2014). SIRT1 and other sirtuins in metabolism. *Trends in Endocrinology and Metabolism*, *25*(3), 138–145. https://doi.org/10.1016/j.tem.2013.12.001

Chen, Q., & Ames, B. N. (1994). Senescence-like growth arrest induced by hydrogen peroxide in human diploid fibroblast F65 cells. *PNAS*, *91*(May), 4130–4134. https://doi.org/10.1073/pnas.91.10.4130

Chen, Q., Fischer, A., Reagan, J. D., Yan, L.-J., Ames, B. N., & Hall, B. (1995). Oxidative DNA damage and senescence of human diploid fibroblast cells (8-oxoguanine/protein oxidation/oxygen tension/a-phenyl-t-butyl nitrone/replicative life span). *Cell Biology*, *92*(10), 4337–4341. https://doi.org/10.1073/pnas.92.10.4337

Chen, Q. M., Bartolomew, J. C., Campisi, J., Acosta, M., Reagan, J. D., & Ames, B. N. (1998). Molecular analysis of H2O2-induced senescent-like growth arrest in normal human fibroblasts: p53 and Rb control G1 arrest but not cell replication. *Biochemical Journal*, *332*(1), 43–50. https://doi.org/10.1042/bj3320043

Chhunchha, B., Singh, P., Stamer, W. D., & Singh, D. P. (2017). Prdx6 retards senescence and restores trabecular meshwork cell health by regulating reactive oxygen species. *Cell Death Discovery*, *3*(1), 17060. https://doi.org/10.1038/cddiscovery.2017.60

Chiang, H. M., Chen, C. W., Lin, T. Y., & Kuo, Y. H. (2014). N-phenethyl caffeamide and photodamage: Protecting skin by inhibiting type I procollagen degradation and stimulating collagen synthesis. *Food and Chemical Toxicology*, *72*, 154–161. https://doi.org/10.1016/j.fct.2014.07.007

Choi, Y. J. (2020). Shedding light on the effects of calorie restriction and its mimetics on skin biology. *Nutrients*, *12*(5), 1529. MDPI AG. https://doi.org/10.3390/nu12051529

Debacq-Chainiaux, F., Erusalimsky, J. D., Campisi, J., & Toussaint, O. (2009). Protocols to detect senescence-associated beta-galactosidase (SA-βgal) activity, a biomarker of senescent cells in culture and in vivo. *Nature Protocols*, *4*(12), 1798–1806. https://doi.org/10.1038/nprot.2009.191

Debacq-Chainiaux, F., Leduc, C., Verbeke, A., & Toussaint, O. (2012). UV, stress and aging. *Dermato-Endocrinology*, *4*(3), 236–240. https://doi.org/10.4161/derm.23652

di Martino, O., Tito, A., de Lucia, A., Cimmino, A., Cicotti, F., Apone, F., Colucci, G., & Calabrò, V. (2017). *Hibiscus syriacus* extract from an established cell culture stimulates skin wound healing. *BioMed Research International*, *2017*, 7932019. https://doi.org/10.1155/2017/7932019

Dickey, J. S., Zemp, F. J., Martin, O. A., & Kovalchuk, O. (2011). The role of miRNA in the direct and indirect effects of ionizing radiation. *Radiation and Environmental Biophysics*, *50*(4), 491–499. https://doi.org/10.1007/s00411-011-0386-5

Dimri, G. P., Leet, X., Basile, G., Acosta, M., Scorrt, G., Roskelley, C., Medrano, E. E., Linskensi, M., Rubeljii, I., Pereira-Smithii, O., Peacocket, M., Campisi, J., & Pardee, B. (1995). A biomarker that identifies senescent human cells in culture and in aging skin *in vivo*. *Cell Biology*, *92*, 9363–9367.

Douki, T., Reynaud-Angelin, A., Cadet, J., & Sage, E. (2003). Bipyrimidine photoproducts rather than oxidative lesions are the main type of DNA damage involved in the genotoxic effect of solar UVA radiation. *Biochemistry*, *42*(30), 9221–9226. https://doi.org/10.1021/bi034593c

Dryden, S. C., Nahhas, F. A., Nowak, J. E., Goustin, A.-S., & Tainsky, M. A. (2003). Role for human SIRT2 NAD-dependent deacetylase activity in control of mitotic exit in the cell cycle. *Molecular and Cellular Biology*, *23*(9), 3173–3185. https://doi.org/10.1128/mcb.23.9.3173-3185.2003

Dudonné, S., Coutière, P., Woillez, M., Mérillon, J.-M., & Vitrac, X. (2011). DNA macroarray study of skin aging-related genes expression modulation by antioxidant plant extracts on a replicative senescence model of human dermal fibroblasts. *Phytotherapy Research: PTR*, *25*(5), 686–693. https://doi.org/10.1002/ptr.3308

Dulić, V., Drullingert, L. F., Leest, E., Reed, S. I., & Steint, G. H. (1993). Altered regulation of G1 cyclins in senescent human diploid fibroblasts: Accumulation of inactive cyclin E-Cdk2 and cyclin D1-Cdk2 complexes. *Proc. Natl. Acad. Sci. USA*, *90*, 11034–11038. https://doi.org/10.1073/pnas.90.23.11034

Elder, D. E., Elenitsas, R., Rosenbach, M., Murphy, G. F., Rubin, A. I., & Xu, X. (2015). *Lever's Histopathology of the Skin* (R. E. editor in chief, David E. Elder; associate editors & X. X. Misha Rosenbach, George F. Murphy, Adam I. Rubin, Eds.; 11th ed.). Wolters Kluwer.

Eyden, B. (2001). The myofibroblast: An assessment of controversial issues and a definition useful in diagnosis and research. *Ultrastructural Pathology*, *25*(1), 39–50. https://doi.org/10.1080/019131201300004672

Farage, M. A., Miller, K. W., & Maibach, H. I. (2017). Degenerative changes in aging skin. In M. A. Farage, K. W. Miller, & H. I. Maibach (Eds.), *Textbook of Aging Skin* (2nd ed., pp. 15–30). Springer, Berlin, Heidelberg. https://doi.org/10.1007/978-3-662-47398-6

Feoktistova, M., Geserick, P., & Leverkus, M. (2016). Crystal violet assay for determining viability of cultured cells. *Cold Spring Harbor Protocols*, *2016*(4), 343–346. https://doi.org/10.1101/pdb.prot087379

Fernandez-Marcos, P. J., & Auwerx, J. (2011). Regulation of PGC-1α, a nodal regulator of mitochondrial biogenesis. *American Journal of Clinical Nutrition*, *93*(4), 884S–90. https://doi.org/10.3945/ajcn.110.001917

Frippiat, C., Chen, Q. M., Zdanov, S., Magalhaes, J. P., Remacle, J., & Toussaint, O. (2001). Subcytotoxic H2O2 stress triggers a release of transforming growth factor-β1, which Induces biomarkers of cellular senescence of human diploid fibroblasts. *Journal of Biological Chemistry*, *276*(4), 2531–2537. https://doi.org/10.1074/jbc.M006809200

Gebhard, D., Matt, K., Burger, K., & Bergemann, J. (2014). Shortwave UV-induced damage as part of the solar damage spectrum is not a major contributor to mitochondrial dysfunction. *Journal of Biochemical and Molecular Toxicology*, *28*(6), 256–262. https://doi.org/10.1002/jbt.21561

Greussing, R., Hackl, M., Charoentong, P., Pauck, A., Monteforte, R., Cavinato, M., Hofer, E., Scheideler, M., Neuhaus, M., Micutkova, L., Mueck, C., Trajanoski, Z., Grillari, J., & Jansen-Dürr, P. (2013). Identification of microRNA-mRNA functional interactions in UVB-induced senescence of human diploid fibroblasts. *BMC Genomics*, *14*(1), 1–19. https://doi.org/10.1186/1471-2164-14-224

Haigis, M. C., & Sinclair, D. A. (2010). Mammalian sirtuins: Biological insights and disease relevance. *Annual Review of Pathology: Mechanisms of Disease*, *5*, 253–295. https://doi.org/10.1146/annurev.pathol.4.110807.092250

Hayflick, L. (1965). The limited *in vitro* lifetime of human diploid cell strains. *Experimental Cell Research*, *37*(3), 614–636. https://doi.org/10.1016/0014-4827(65)90211-9

Hayflick, L., & Moorhead, P. S. (1961). The serial cultivation of human cell strains. *Experimental Cell Research*, *25*(3), 585–621. https://doi.org/10.1016/0014-4827(61)90192-6

Ho, C. C., Ng, S. C., Chuang, H. L., Wen, S. Y., Kuo, C. H., Mahalakshmi, B., Huang, C. Y., & Kuo, W. W. (2021). Extracts of *Jasminum sambac* flowers fermented by *Lactobacillus rhamnosus* inhibit H_2O_2- and UVB-induced aging in human dermal fibroblasts. *Environmental Toxicology*, *36*(4), 607–619. https://doi.org/10.1002/tox.23065

Huang, H. C., Chang, T. M., Chang, Y. J., & Wen, H. Y. (2013). UVB irradiation regulates ERK1/2- and p53-dependent thrombomodulin expression in human keratinocytes. *PLoS ONE*, *8*(7), 1–10. https://doi.org/10.1371/journal.pone.0067632

Ikehata, H. (2018). Mechanistic considerations on the wavelength-dependent variations of UVR genotoxicity and mutagenesis in skin: The discrimination of UVA-signature from UV-signature mutation. *Photochemical & Photobiological Sciences*, *17*(12), 1861–1871. https://doi.org/10.1039/C7PP00360A

Ilnytskyy, Y., Koturbash, I., & Kovalchuk, O. (2009). Radiation-induced bystander effects *in vivo* are epigenetically regulated in a tissue-specific manner. *Environmental and Molecular Mutagenesis*, *50*(2), 105–113. https://doi.org/10.1002/em.20440

Kalfalah, F., Sobek, S., Bornholz, B., Götz-Rösch, C., Tigges, J., Fritsche, E., Krutmann, J., Köhrer, K., Deenen, R., Ohse, S., Boerries, M., Busch, H., & Boege, F. (2014). Inadequate mito-biogenesis in primary dermal fibroblasts from old humans is associated with impairment of PGC1A-independent stimulation. *Experimental Gerontology*, *56*, 59–68. https://doi.org/10.1016/j.exger.2014.03.017

Kang, S. M., Han, S., Oh, J. H., Lee, Y. M., Park, C. H., Shin, C. Y., Lee, D. H., & Chung, J. H. (2017). A synthetic peptide blocking TRPV1 activation inhibits UV-induced skin responses. *Journal of Dermatological Science*, *88*(1), 126–133. https://doi.org/10.1016/j.jdermsci.2017.05.009

Karnewar, S., Neeli, P. K., Panuganti, D., Kotagiri, S., Mallappa, S., Jain, N., Jerald, M. K., & Kotamraju, S. (2018). Metformin regulates mitochondrial biogenesis and senescence through AMPK mediated H3K79 methylation: Relevance in age-associated vascular dysfunction. *Biochimica et Biophysica Acta - Molecular Basis of Disease*, *1864*(4), 1115–1128. https://doi.org/10.1016/j.bbadis.2018.01.018

Kemp, M. G., Spandau, D. F., & Travers, J. B. (2017). Impact of age and insulin-like growth factor-1 on DNA damage responses in UV-irradiated human skin. *Molecules*, *22*(3), 1–20. https://doi.org/10.3390/molecules22030356

Kierszenbaum, L. A., & Tres, L. (2019). *Histology and Cell Biology: An Introduction to Pathology E-Book*.

Kim, K. S., Kim, J. E., Choi, K. J., Bae, S., & Kim, D. H. (2014). Characterization of DNA damage-induced cellular senescence by ionizing radiation in endothelial cells. *International Journal of Radiation Biology*, *90*(1), 71–80. https://doi.org/10.3109/09553002.2014.859763

Kirkland, J. B. (1991). Lipid peroxidation, protein thiol oxidation and DNA damage in hydrogen peroxide-induced injury to endothelial cells: Role of activation of poly(ADP-ribose)polymerase. *Biochimica et Biophysica Acta*, *1092*(3), 319–325. https://doi.org/10.1016/s0167-4889(97)90007-0

Kovalchuk, O., Burke, P., Besplug, J., Slovack, M., Filkowski, J., & Pogribny, I. (2004). Methylation changes in muscle and liver tissues of male and female mice exposed to acute and chronic low-dose X-ray-irradiation. *Mutation Research - Fundamental and Molecular Mechanisms of Mutagenesis*, *548*(1–2), 75–84. https://doi.org/10.1016/j.mrfmmm.2003.12.016

Kuang, Y., Hu, B., Feng, G., Xiang, M., Deng, Y., Tan, M., Li, J., & Song, J. (2020). Metformin prevents against oxidative stress-induced senescence in human periodontal ligament cells. *Biogerontology*, *21*(1), 13–27. https://doi.org/10.1007/s10522-019-09838-x

Lago, J. C., & Puzzi, M. B. (2019). The effect of aging in primary human dermal fibroblasts. *PLoS ONE, 14*(7), e0219165. https://doi.org/10.1371/journal.pone.0219165

Lämmermann, I., Terlecki-Zaniewicz, L., Weinmüllner, R., Schosserer, M., Dellago, H., de Matos Branco, A. D., Autheried, D., Sevcnikar, B., Kleissl, L., Berlin, I., Morizot, F., Lejeune, F., Fuzzati, N., Forestier, S., Toribio, A., Tromeur, A., Weinberg, L., Higareda Almaraz, J. C., Scheideler, M., … Grillari, J. (2018). Blocking negative effects of senescence in human skin fibroblasts with a plant extract. *NPJ Aging and Mechanisms of Disease*, *4*(4), e-Collection. https://doi.org/10.1038/s41514-018-0023-5

Lee, B. Y., Han, J. A., Im, J. S., Morrone, A., Johung, K., Goodwin, E. C., Kleijer, W. J., DiMaio, D., & Hwang, E. S. (2006). Senescence-associated β-galactosidase is lysosomal β-galactosidase. *Aging Cell*, *5*(2), 187–195. https://doi.org/10.1111/j.1474-9726.2006.00199.x

Lee, J. J., Ng, S. C., Hsu, J. Y., Liu, H., Chen, C. J., Huang, C. Y., & Kuo, W. W. (2022). Galangin reverses H2O2-induced dermal fibroblast senescence via SIRT1-PGC-1α/Nrf2 signaling. *International Journal of Molecular Sciences*, *23*(3), 1387. https://doi.org/10.3390/ijms23031387

Lin'kova, N. S., Drobintseva, A. O., Orlova, O. A., Kuznetsova, E. P., Polyakova, V. O., Kvetnoy, I. M., & Khavinson, V. K. (2016). Peptide regulation of skin fibroblast functions during their aging *in vitro*. *Bulletin of Experimental Biology and Medicine*, *161*(1), 175–175. https://doi.org/10.1007/s10517-016-3370-x

Marionnet, C., Pierrard, C., Lejeune, F., Sok, J., Thomas, M., & Bernerd, F. (2010). Different oxidative stress response in keratinocytes and fibroblasts of reconstructed skin exposed to non extreme daily-ultraviolet radiation. *PLoS ONE, 5*(8), e12059. https://doi.org/10.1371/journal.pone.0012059

Meng, Q., & Xia, Y. (2011). c-Jun, at the crossroad of the signaling network. *Protein and Cell, 2*(11), 889–898). Higher Education Press. https://doi.org/10.1007/s13238-011-1113-3

Mihaylova, M. M., & Shaw, R. J. (2011). The AMPK signalling pathway coordinates cell growth, autophagy and metabolism. *Nature Cell Biology, 13*(9), 1016–1023. https://doi.org/10.1038/ncb2329

Morris, T. A., Delorenzo, R. J., & Tombes, R. M. (1998). CaMK-II inhibition reduces Cyclin D1 levels and enhances the association of p27 kip1 with Cdk2 to cause G1 arrest in NIH 3T3 cells. *Experimental Cell Research*, *240*, 218-227.

Ott, C., Jung, T., Grune, T., & Höhn, A. (2018). SIPS as a model to study age-related changes in proteolysis and aggregate formation. *Mechanisms of Ageing and Development*, *170*(July 2017), 72–81. https://doi.org/10.1016/j.mad.2017.07.007

Pedro De Magalhães, J. (2004). From cells to ageing: A review of models and mechanisms of cellular senescence and their impact on human ageing. *Experimental Cell Research*, *300*(1), 1–10. https://doi.org/10.1016/j.yexcr.2004.07.006

Propato A., Cutrona G., Francavilla V., Ulivi M., Schiaffella E., Landt O., Dunbar R., Cerundolo V., Ferrarini M., & Barnaba V. (2001). Apoptotic cells overexpress vinculin and induce vinculin-specific cytotoxic T-cell cross-priming. *Nature Medicine*, *7*(7), 807–813. https://doi.org/10.1038/89930

Taihao Q. (2016). *Molecular mechanisms of skin aging and age-related diseases*. 1st Ed. *E-Book.* https://doi.org/10.1201/b21370

Rattan, S. I. S. (2016). Origins of the Hayflick system, the phenomenon and the limit. In Suresh I.S. Rattan & L. Hayflick (Eds.), *Cellular Ageing and Replicative Senescence. Healthy Ageing and Longevity* (pp. 3–14). Springer, Cham. https://doi.org/10.1007/978-3-319-26239-0_1

Repetto, G., del Peso, A., & Zurita, J. L. (2008). Neutral red uptake assay for the estimation of cell viability/cytotoxicity. *Nature Protocols*, *3*(7), 1125–1131. https://doi.org/10.1038/nprot.2008.75

Rittié, L., & Fisher, G. J. (2015). Natural and sun-induced aging of human skin. *Cold Spring Harbor Perspectives in Medicine*, *5*(1), a015370. https://doi.org/10.1101/cshperspect.a015370

Robbins, E., Levine, E. M., & Eagle, H. (1970). Morphologic changes accompanying senescence of cultured human diploid cells. *Senescence Of Cultured Diploid Cells*, *131* (6), 1211–1222. https://doi.org/10.1084/jem.131.6.1211

Robles, S. J., & Adami, G. R. (1998). Agents that cause DNA double strand breaks lead to p16 INK4a enrichment and the premature senescence of normal fibroblasts. *Oncogene*, *16*(9), 1113–1123.

Rochette, L., Mazini, L., Meloux, A., Zeller, M., Cottin, Y., Vergely, C., & Malka, G. (2020). Anti-aging effects of GDF11 on skin. *International Journal of Molecular Sciences*, *21*(7), 2598. MDPI AG. https://doi.org/10.3390/ijms21072598

Rodemann, H. P. (1989). Differential degradation of intracellular proteins in human skin fibroblasts of mitotic and mitomycin-C (MMC)-induced postmitotic differentiation states *in vitro*. *Differentiation*, *42*(1), 37–43. https://doi.org/10.1111/j.1432-0436.1989.tb00605.x

Sanders, Y. Y., Liu, H., Zhang, X., Hecker, L., Bernard, K., Desai, L., Liu, G., & Thannickal, V. J. (2013). Histone modifications in senescence-associated resistance to apoptosis by oxidative stress. *Redox Biology*, *1*(1), 8–16. https://doi.org/10.1016/j.redox.2012.11.004

Sasaki, M., Kajiya, H., Ozeki, S., Okabe, K., & Ikebe, T. (2014). Reactive oxygen species promotes cellular senescence in normal human epidermal keratinocytes through

epigenetic regulation of p16INK4a. *Biochemical and Biophysical Research Communications*, *452*(3), 622–628. https://doi.org/10.1016/j.bbrc.2014.08.123

Serrano, L., Martínez-Redondo, P., Marazuela-Duque, A., Vazquez, B. N., Dooley, S. J., Voigt, P., Beck, D. B., Kane-Goldsmith, N., Tong, Q., Rabanal, R. M., Fondevila, D., Muñoz, P., Krüger, M., Tischfield, J. A., & Vaquero, A. (2013). The tumor suppressor SirT2 regulates cell cycle progression and genome stability by modulating the mitotic deposition of H4K20 methylation. *Genes and Development*, *27*(6), 639–653. https://doi.org/10.1101/gad.211342.112

Serrano, M., Lin, A. W., Mccurrach, M. E., Beach, D., & Lowe, S. W. (1997). Oncogenic ras provokes premature pell penescence pssociated with accumulation of p53 and p16 INK4a. *Cell*, *88*, 593–602.

Sewon Kang. (2019). *Fitzpatrick's Dermatology* (S. Kang, M. Amagai, A. H. E. Anna L. Bruckner, D. J. Margolis, A. J. McMichael, & J. S. Orringer, Eds.; 9th ed.). McGraw-Hill Education.

Shlush, L. I., Itzkovitz, S., Cohen, A., Rutenberg, A., Berkovitz, R., Yehezkel, S., Shahar, H., Selig, S., & Skorecki, K. (2011). Quantitative digital in situ senescence-associated β-galactosidase assay. *BMC Cell Biology*, *12*, 16. https://doi.org/10.1186/1471-2121-12-16

Sidler, C., Li, D., Wang, B., Kovalchuk, I., & Kovalchuk, O. (2014). SUV39H1 downregulation induces deheterochromatinization of satellite regions and senescence after exposure to ionizing radiation. *Frontiers in Genetics*, *5*(NOV), 411. https://doi.org/10.3389/fgene.2014.00411

Sidler, C., Woycicki, R., Kovalchuk, I., & Kovalchuk, O. (2014). WI-38 senescence is associated with global and site-specific hypomethylation. *Aging*, *6*(7), 564–574. https://doi.org/10.18632/aging.100679

Silasi, G., Diaz-Heijtz, R., Besplug, J., Rodriguez-Juarez, R., Titov, V., Kolb, B., & Kovalchuk, O. (2004). Selective brain responses to acute and chronic low-dose X-ray irradiation in males and females. *Biochemical and Biophysical Research Communications*, *325*(4), 1223–1235. https://doi.org/10.1016/j.bbrc.2004.10.166

Skandalis, S. S., Karalis, T., & Heldin, P. (2020). Intracellular hyaluronan: Importance for cellular functions. *Seminars in Cancer Biology*, *62*, 20–30. Academic Press. https://doi.org/10.1016/j.semcancer.2019.07.002

Soydas, T., Sayitoglu, M., Sarac, E. Y., Cınar, S., Solakoglu, S., Tiryaki, T., & Sultuybek, G. K. (2021). Metformin reverses the effects of high glucose on human dermal fibroblasts of aged skin via downregulating RELA/p65 expression. *Journal of Physiology and Biochemistry*, *77*(3), 443–450. https://doi.org/10.1007/s13105-021-00823-y

Soydas, T., Yaprak Sarac, E., Cinar, S., Dogan, S., Solakoglu, S., Tuncdemir, M., & Kanigur Sultuybek, G. (2018). The protective effects of metformin in an in vitro model of aging

3T3 fibroblast under the high glucose conditions. *Journal of Physiology and Biochemistry*, *74*(2), 273–281. https://doi.org/10.1007/s13105-018-0613-5

Tobin, D. J. (2017). Introduction to skin aging. *Journal of Tissue Viability*, *26*(1), 37–46. https://doi.org/10.1016/j.jtv.2016.03.002

Toiber, D., Sebastian, C., & Mostoslavsky, R. (2011). Characterization of nuclear sirtuins: Molecular mechanisms and physiological relevance. *Handbook of Experimental Pharmacology*, *206*, 189–224. https://doi.org/10.1007/978-3-642-21631-2_9

Toussaint, O., Dumont, P., Dierick, J.-F., Pascal, T., Frippiat, C., Chainiaux, F., Sluse, F., Eliaers, F., & Remacle, J. (2010). Stress-induced premature senescence: essence of life, evolution, stress, and aging. *Annals of the New York Academy of Sciences*, *908*(1), 85–98. https://doi.org/10.1111/j.1749-6632.2000.tb06638.x

Toussaint, O., Medrano, E. E., & von Zglinicki, T. (2000). Cellular and molecular mechanisms of stress-induced premature senescence (SIPS) of human diploid fibroblasts and melanocytes. *Experimental Gerontology*, *35*(8), 927–945. https://doi.org/10.1016/s0531-5565(00)00180-7

Toussaint, O., Michiels, C., Raes, M., & Remacle, J. (1995). Cellular aging and the importance of energetic factors. *Experimental Gerontology*, *30*(1), 1–22.

Toutfaire, M., Bauwens, E., & Debacq-Chainiaux, F. (2017). The impact of cellular senescence in skin ageing: A notion of mosaic and therapeutic strategies. *Biochemical Pharmacology*, *142*, 1–12. https://doi.org/10.1016/j.bcp.2017.04.011

Vandesompele, J., de Preter, K., Pattyn, F., Poppe, B., van Roy, N., de Paepe, A., & Speleman, F. (2002). Accurate normalization of real-time quantitative RT-PCR data by geometric averaging of multiple internal control genes. *Genome Biology*, *3*(7), research0034.1-0034.11. https://doi.org/10.1186/gb-2002-3-7-research0034

Varani, J., Dame, M. K., Rittie, L., Fligiel, S. E. G., Kang, S., Fisher, G. J., & Voorhees, J. J. (2006). Decreased collagen production in chronologically aged skin: Roles of age-dependent alteration in fibroblast function and defective mechanical stimulation. *American Journal of Pathology*, *168*(6), 1861–1868. https://doi.org/10.2353/ajpath.2006.051302

Wisdom, R., Johnson, R. S., & Moore, C. (1999). c-Jun regulates cell cycle progression and apoptosis by distinct mechanisms. *The EMBO Journal*, *18*(1), 188–197.

Wu, K., Tian, R., Huang, J., Yang, Y., Dai, J., Jiang, R., & Zhang, L. (2018). Metformin alleviated endotoxemia-induced acute lung injury via restoring AMPK-dependent suppression of mTOR. *Chemico-Biological Interactions*, *291*, 1–6. https://doi.org/10.1016/j.cbi.2018.05.018

CHAPTER 3: EFFECT OF CANNABINOID TREATMENT ON THE SKIN FIBROBLASTS' SENESCENCE-ASSOCIATED PHENOTYPE

3.1. ABSTRACT

Cannabis sativa produces over 100 active medical ingredients called phytocannabinoids (pCBs), and the most abundant are Δ-9-tetrahydrocannabinol (Δ9-THC or THC) and cannabidiol (CBD). THC works primarily as a weak partial agonist on cannabinoid 1 (CB1) and cannabinoid 2 (CB2) receptors with well-known psychoactive effects, antiemetic, neuroprotective, anticancer, and anti-inflammatory properties. In contrast to THC, CBD has little direct affinity to CB1 and CB2 receptors; it acts as a negative allosteric modulator of CB1 and demonstrates neuroprotective, and anti-inflammatory properties, and improves common skin disorders such as psoriasis, eczema, dermatitis, lupus, acne, and nail-patella syndrome. Currently, cannabis compounds are popular ingredients in modern beauty products available on the general market. However, reliable information about the possible anti-aging and rejuvenation properties of pCBs is absent. The results indicate that: (i) there is a specific dose range of phytocannabinoids (2 µM – 5 µM) that has a protective effect in the SIPS model on dermal fibroblasts; (ii) pCBs stimulate fibroblasts' functional ability to close the damaged area in different skin cell lines via upregulation of the proliferative biomarkers, and (iii) overall pCBs inhibit dermal aging via reduction of morphological alterations in skin cells, potentiated cellular viability, and extracellular matrix components production through preserving cell-cycle regulators and metabolic maintenance. Our data help fill knowledge gaps regarding the potential role of THC/CBD in the regulation of cell proliferation, anti-aging, and rejuvenation aspects.

3.2. INTRODUCTION

3.2.1. Cannabis pharmacology and main clinical effects

Cannabis sativa, also known as marijuana (Figure 3.1), has been used for spiritual, medical, and industrial purposes for millennia. Products include rope, textiles, clothing, shoes, food, paper, bioplastics, insulation, and biofuel. The cannabis plant produces over 100 active medical ingredients called phytocannabinoids (pCBs). The most abundant phytocannabinoids are Δ-9-tetrahydrocannabinol (Δ9-THC or THC) and cannabidiol (CBD) (Lim & Kirchhof, 2018). THC works primarily as a weak partial agonist on cannabinoid 1 (CB1) and cannabinoid 2 (CB2) receptors with well-known psychoactive, antiemetic, neuroprotective, anticancer, and anti-inflammatory properties. It also can reduce certain forms of neuropathic and chronic pain, stimulate appetite, digestion, emotions, and thought processes mediated through the endocannabinoid system (Dhadwal & Kirchhof, 2018). CBD is another important cannabinoid and in contrast to THC, has little direct affinity to CB1 and CB2 receptors. Rather, it is a negative allosteric modulator of CB1, with protean pharmacological effects on various other receptor systems including vanilloid receptor 1, adenosine A2A, and non-receptor mechanisms (MacCallum & Russo, 2018). CBD demonstrates neuroprotective, anti-inflammatory, antipsychotic, and antiseizure properties without the THC-like intoxicating and psychoactive effects. Additionally, it improves blood circulation, provides antioxidant and antimicrobial activity, relieves diabetes, neurofibromatosis, and common skin disorders such as psoriasis, eczema, dermatitis, lupus, acne, and nail-patella syndrome (Lim & Kirchhof, 2018). Other minor phytocannabinoids, such as cannabigerol (CBG), cannabichromene

(CBC), and Δ9-tetrahydrocannabivarin (THCV), also exhibit interesting pharmacological properties and usually potentiate the effects of THC and/or CBD.

Thus far, current medicine more often uses cannabis plant and its products based on empirical and scientific evidence of its effectiveness. Most of the cannabis-related studies concentrated on the treatment of neurological and neurodegenerative disorders such as multiple sclerosis (Strouse, 2016), Huntington chorea (MacCallum & Russo, 2018) and Parkinsonism (Zuardi et al., 2009), and Alzheimer (Zuardi et al., 2006). Phytocannabinoids demonstrate potential in cancer treatment (Massi et al., 2013). Their anti-inflammatory, analgesic, and anti-allergic effects were also shown (Husni et al., 2014). Moreover, cannabinoids are recognized as transcriptional repressors that can control cell proliferation and differentiation (Ramot et al., 2013).

Few studies have been performed in the dermatological field despite the aforementioned activities of cannabinoids. Phytocannabinoids have been shown to be beneficial in treating psoriasis, eczema, and fibrosis (Oláh et al., 2017; Ramot et al., 2013; Tóth et al., 2011; Vincenzi & Tosti, 2020). Nevertheless, little attention has been given to the use of cannabis and cannabinoids in testing anti-aging properties on human skin (Lim & Kirchhof, 2018). Most cannabis-containing beauty products recently appeared on the market, are based primarily on empirical knowledge from various users and on the occasional practical positive customer experience. Current but limited scientific data suggests cannabis could have beneficial properties for use in anti-aging or rejuvenation products, however the extent of these benefits is unknown.

Figure 3.1. The *Cannabis sativa*, also known as marijuana.

3.2.2 Modern therapeutic strategies of cannabinoids

Thus far, current medicine uses *Cannabis sativa* and its products more often based on scientific evidence of its effectiveness. Numerous published data encompass multifaceted regulatory aspects of the endocannabinoid system (ECS) activity and demonstrate the remarkable potential in the therapy of various pathological conditions and diseases affecting humankind. There are numerous promising results of therapeutic benefits of cannabinoids in the broad spectrum of neurodegenerative disorders (MacCallum & Russo, 2018; Strouse, 2016; Zuardi et al., 2006, 2009), gastrointestinal and liver diseases (Izzo & Camilleri, 2008), cancer (Guzmán, 2003; MacCallum & Russo, 2018; Massi et al., 2013), cardiovascular disorders (Pacher et al., 2008), inflammatory processes and obesity (Pellati et al., 2018; Scherer & Buettner, 2009), musculoskeletal disorders (Xing et al., 2020), ischemia/reperfusion injury (Pacher & Haskó, 2008), pain (Baron, 2018; Bíró et al., 2009; MacCallum & Russo, 2018), and anti-allergic effects (Husni et al., 2014).

Cannabinoids can be broadly divided into three main classes: i) pCBs that are derived from the *C. sativa* plant (e.g., THC, CBD), ii) endocannabinoids (eCBs), which are endogenously produced in the human body (2-AG and AEA, lipid mediators such as N-PEA), and iii) synthetic cannabinoids (sCBs), which are synthesized molecules that bind to the endogenous CB receptors. For example, WIN 55 is a drug that produces effects similar to THC, AM-1221 is a drug that acts as a potent and selective agonist for CB2; Dronabinol and Nabilone are synthetic analogs of THC that acts as an agonist of CB1 and CB2 receptors (Eagelston et al., 2018; Sivesind et al., 2022). Cannabinoids (CBs) are lipophilic components that could easily pass through biological barriers such as skin. Interestingly, CB1 and CB2 receptors are expressed in epidermal keratinocytes, cutaneous

nerves, sebaceous cells, eccrine sweat glands, mast cells, and macrophages (Lim & Kirchhof, 2018). Moreover, CBs are recognized as transcriptional repressors that can control cell proliferation and differentiation (Ramot et al., 2013). Collectively, all findings suggest that cannabinoids might be worthwhile for treating dermatological pathologies.

3.2.3. Cannabinoids in the treatment of dermatological diseases

Within the last decade, CBs gained popularity among the general public and are widely present in skincare products in several countries. Also, CBs piqued the attention of researchers and clinicians because of their anti-inflammatory, neuroprotective and immunomodulatory effects in association with multiple pathologies.

In addition to other medical applications, CBs represent promising avenues in dermatology for the therapy of inflammatory and autoimmune skin disorders (Nagasai & Friedman, 2021). Positive findings in pre-clinical research are rapidly leading to randomized controlled trials needed to support positive experiences from the use of commercially available cannabinoid preparations (Table 3.1). Currently, there are several approved medical indications for cannabis use, including psoriasis, lupus, nail-patella syndrome, and severe pain. Studies have suggested CBs might also have a therapeutic effect on acne, dermatitis, pruritus, wound healing, and skin cancer (melanoma) (Dhadwal & Kirchhof, 2018). For instance, a recent study demonstrated that topical administration of palmitoylethanolamide (PEA), which stimulated anandamide (AEA) activity on CB1 receptors, reduced itch by 86.4%, and was well-tolerated by patients (Liszewski & Farah, 2017).

Table 3.1. Treatments of skin disorders based on the targeting cutaneous endocannabinoid system

Disease or pathologic condition	Target receptor(s) / components of ECS	Treatment	Tested object / type of study	References
Acne vulgaris	TRPV4	CBD	*In vitro* (human immortalized SZ95 sebocytes)	Oláh, Markovics, et al., 2016
Allergic contact dermatitis	CB1, CB2, FAAH	WOBE440, WOBE479	*In vitro* (primary normal human epidermal keratinocytes and immortalized (HPV-KER) human epidermal keratinocytes); *In vivo* (NC/Tnd mice)	Karsak et al., 2007; Oláh, Ambrus, et al., 2016
Asteatotic eczema (dermatitis)	PPAR-α	PEA/AEA	*Clinical trial* (double-blind, randomized study – 66 participants)	Yuan et al., 2014
Atopic dermatitis	CB1, CB2	Ec. Extract, CBD	*In vitro* (HaCaT keratinocytes); *Clinical trial (*pre-post observational study)	Maghfour et al., 2021; Oláh et al., 2017
Cutaneous Lupus Erythematosus	CB1, CB2	AEA-np	*In vivo* (MRL-Lpr/Lpr mice)	Chalmers, 2018
Chronic pruritus	PPAR-α	PEA	*Clinical trials*: 1) open application observation – 22 participants; 2) multinational, multicentre,	Ardigò et al., 2020; Eberlein et al., 2008; Ständer et al., 2006

			observational, non-controlled, prospective cohort study – 2456 participants	
Dermatomyositis	CB2	ajulemic acid/lenabasum, a CB2R agonist	*In vitro* (peripheral blood mononuclear cells)	Robinson et al., 2017
Epidermolysis bullosa	CB2, TRPV1	Cannabidiol oil	*3 clinical case-reports*	Chelliah et al., 2018
Kaposi Sarcoma	CB1, CB2	CB1/CB2 agonist WIN-55,212-2	*In vitro* (human Kaposi's sarcoma cell line KS-IMM*)*	Luca et al., 2009
Melanoma	CB1, CB2	Sativex (1:1 ratio of THC and CBD)	*In vitro (*melanoma cell lines CHL-1, A375, and SK-MEL-28)	Armstrong et al., 2015
Photodamage	CB1, CB2, HSP90	CBD, 17AAG	*In vitro* (human epidermal keratinocytes, CDD 1102 KERTr); *In vivo* (SKH-1 hairless mice)	Gęgotek et al., 2021; Singh et al., 2015
Psoriasis	CB1, CB2	THC distillate, CBD shampoo	*Clinical case report* of 33-year-old male patient; *Clinical trial* (50 – participants)	Friedman et al., 2020; Vincenzi & Tosti, 2020
Systemic sclerosis (SSc)	CB2	Oral lenabasum (agonist of cannabinoid receptor 2 (CB_2)	*Clinical trial* (randomized, double-blind, placebo-controlled,	Spiera et al., 2020

			phase II study – 42 participants)	
Trichotillomania	CB1, CB2	dronabinol (2.5–15 mg/day	*Clinical trial* (pilot study – 14 subjects)	Grant et al., 2011

CB1, cannabinoid receptor 1; CB2, cannabinoid receptor 2; CBD, cannabidiol; Ec. Extract, Echinacea purpurea-derived alkylamides; FAAH, fatty acid amide hydrolase; HSP90, heat shock protein 90; 17AAG, HSP90 inhibitor; PEA, *N*-Palmitoylethanolamine; PPAR-α, peroxisome-proliferative-activated receptor-α; THC, tetrahydrocannabinol; WOBE440 and WOBE479, FAAH inhibitors; TRPV1, transient receptor potential channels of the vanilloid subtype 1, TRPV4, transient receptor potential channels of the vanilloid subtype 4.

Among the wide variety of CBs, the most abundant are THC and CBD applications, which show promise in treating different skin diseases.

Cocchiara and coworkers reported that CBD oil had improved the symptoms of systemic sclerosis, reduced cutaneous ulcers, and significantly improved pain management (Cocchiara et al., 2019; Sivesind et al., 2022). Maida and Corban (2017) reported that topical application of combined CBD-THC appears to be effective for pain relief in patients with pyoderma gangrenosum, which are rapidly enlarging, painful pustules or nodules progressively transforming into ulcers, typically on the legs (Maida & Corban, 2017). Topical THC and CBD have been found (at 0.1–5 μM) to suppress the production and secretion of proinflammatory cytokines in a dose-dependent manner (e.g., IL-6 and IL-17). In contrast, pretreatment with CBD has resulted in an upregulation of IL-10, an anti-inflammatory cytokine (Kozela et al., 2013).

Severe itching or pruritus is a common dermatological condition, albeit it might also be a symptom of different internal diseases. Oral application of THC was efficacious for treating recalcitrant pruritus secondary to cholestatic liver disease (Neff et al., 2002).

Interestingly, all three reported patients who experienced severe and debilitating pruritus that resulted in impaired quality of life, depression, and suicidal thoughts were unresponsive to doxepin, naltrexone, cholestyramine, UV therapy, and plasmapheresis that is provided according to current protocols. The decrease of pruritus, improvements in sleep, and functional activities were experienced with 5 mg of THC therapy at bedtime with effects lasting 4 to 6 hours (Neff et al., 2002).

Calciphylaxis is a rare disease associated with calcium aggregation in small blood vessels of the fat and skin tissues and manifested with blood clots, painful dermal ulcers, may be complicated by serious infections that can lead to death. Results of a multicohort open-label trial showed that 32 patients with calciphylaxis, not caused by uremia, received topical CBD (3.75 mg/ml) and THC (<1 mg per day), which was applied to wound beds and peri-wound tissues. After 1 year of treatment wound closure was achieved in 90% of cases (Maida et al., 2020).

Epidermolysis bullosa, another rare pathology caused by mutations in at least one of 16 different genes, manifested fragile, blistering skin and mucous membranes in response to a minor injury, even from heat, rubbing, scratching, or adhesive tape. There is no cure for this disease; the disease may be complicated by esophageal narrowing, squamous cell skin cancer, and the need for amputations without proper management. Two different studies showed that topical application of CBD was associated with a reduction in blisters by at least 50%, with improved wound healing and decreased use of opioid analgesics in six pediatric patients aged 6 months to 10 years (Chelliah et al., 2018; Eberlein et al., 2008). Moreover, lower doses of CBD were shown to be more effective than vitamin C and E as a neuroprotective antioxidant and, in addition to its combined

lipostatic, antiproliferative, and anti-inflammatory effects, can alleviate skin conditions such as acne (Hampson et al., 1998; Oláh et al., 2014).

Nevertheless, currently we have limited research data in the dermatological field. A positive effect of phytocannabinoids in treating psoriasis, eczema, and fibrosis have been shown (Ramot et al., 2013; Tóth et al., 2011; Tóth et al., 2019). At the same time, little attention has been given to the role of cannabis and cannabinoids as anti-aging compounds for human skin (Lim & Kirchhof, 2018). Most of the cannabis-containing beauty products recently appeared in the market, are based primarily on empirical knowledge and on the occasional positive experience of the customers. Thus, a limited scientific background concerning the skin anti-aging or rejuvenation aspects sparked the interest of our team to start addressing these knowledge gaps.

Aging is associated with gradual damage of the cells and tissues with subsequent accumulation of their degraded components due to the inhibition of elimination of cell debris accompanied by progressive inflammatory responses and general deterioration. It is worth noting that CBs have demonstrated CB1 and CB2 receptor dependent and independent anti-inflammatory effects (CBD/THC). Thus, cannabinoids might possess anti-aging and rejuvenation properties on the skin.

3.3. METHODS AND MATERIALS

3.3.1. Main reagents

1. Cannabinoids: Δ9-THC (Cat#T4764) and CBD (Cat#C-045) were purchased from Sigma. 1.0 mg/ml stock solutions were prepared by dissolving cannabinoids in 1 ml DMSO (Dimethyl sulfoxide anhydrous, Life Technologies) and stored at -20 ℃.

2. Hydrogen peroxide 30% (Merck®, Cat#: 1072091000)

3. D-PBS (*MULTICELL*, Cat#: 311-425-CL)

3.3.2. Cell culture and maintenance

Normal human neonatal foreskin fibroblasts CCD-1064Sk (ATCC® CRL-2076™), normal human adult skin fibroblasts CCD-1135Sk (ATCC® CRL-2691™), and human foreskin normal BJ-5ta hTERT-immortalized cell lines (CRL-4001™) were obtained from the American Type Culture Collection (Rockville, MD, USA). Cells were cultivated in ISCOVE's Modified Dulbecco's Medium (IMDM) 1X (MULTICELL, Cat# 319-106-CL) containing 10% heat-inactivated Premium Grade Fetal Bovine Serum (Cat# 97068-085, VWR International LLC, Radnor, USA) and 1% Penicillin-Streptomycin (10,000 IU Penicillin and 10 mg/ml Streptomycin, Cat# 450-201-EL, WISENT INC., Quebec, Canada). All cells were grown and harvested in our Biosafety Level 2 laboratory. Experimental cell lines were incubated in a Forma Steri-Cycle CO_2 Incubator (Thermo Scientific) at 37°C in a humidified atmosphere of 5% CO_2. Complete media renewals were performed every three days subcultured every six or seven days. The replication speed or population doubling (PD) numbers of the cell lines were determined for each subculture as $\Delta PD = \log_2(n_f/n_i)$, where n_i is the number of cells initially seeded and n_f is the final number of cells in a culture. Cells for the senescence model were not older than 24-30 population doublings when employed in the experiments.

3.3.3. Senescence-associated phenotype modelling

Skin fibroblasts (CCD-1064Sk) in 70% confluency were treated 1 hour with 25 µM concentration of hydrogen peroxide solution (H_2O_2 dissolved in D-PBS) in 100 x 15 mm

Petri plates in aseptic conditions (Figure 2.3). Petri plates with skin fibroblasts were maintained in a humidified incubator at 37°C with 5% CO_2.

After 1-hour single treatment, H_2O_2 solution was poured out and substituted with cell culture medium. Thereafter, SIPS features, and biomarkers were determined microscopically and by β-galactosidase senescence assay, MTT and Neutral red colorimetric cell viability assays, Crystal violet cytotoxicity assay, western immunoblotting, reverse transcription-polymerase chain reaction, wound-healing assay (WHA), and nuclear DAPI staining.

3.3.4. Cannabinoid treatments

Fibroblast cell cultures were treated with cannabinoids THC and CBD in the following doses: 0.25 µM, 0.5 µM, 1 µM, 2 µM, 5 µM, 7.5 µM, and 10 µM (Figure 3.2). THC and CBD were dissolved in DMSO. Next, THC/CBD or a vehicle (DMSO) were dissolved in media and applied to the media surrounding the cell cultures (n=3 for each condition). Following one-hour of exposure to H_2O_2, the H_2O_2 solution was poured out, washed once with cell culture medium, substituted with designated treatment, and incubated for 2 h daily for 5 days. After that, the media was replaced without any additional treatment amendments. Healthy fibroblasts, which were not exposed to the H_2O_2, were treated with cannabinoids at the previously described concentrations.

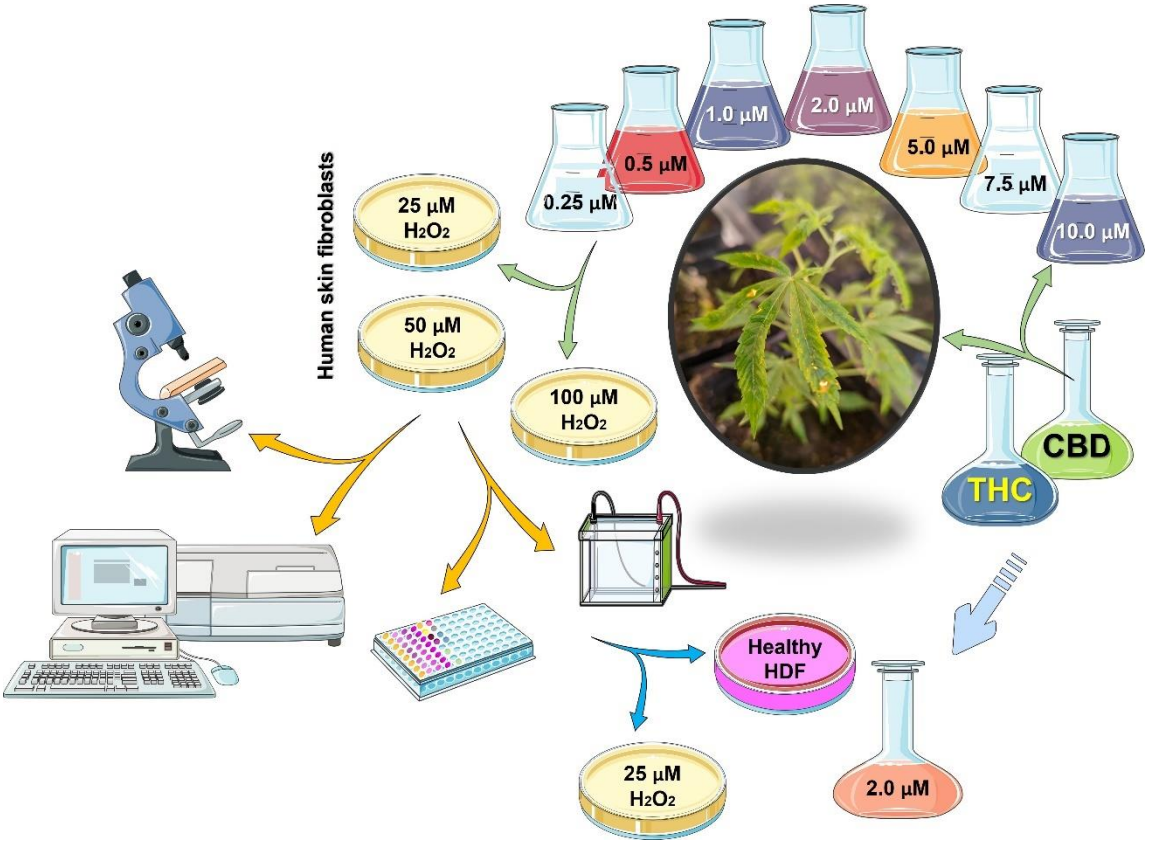

Figure 3.2. Testing of different concentrations of cannabinoids on young and prematurely senescent dermal fibroblasts. CBD, cannabidiol; HDF, human dermal fibroblasts; H_2O_2, hydrogen peroxide; THC, Δ-9-tetrahydrocannabinol. This figure was created using images from Servier Medical Art Commons Attribution 3.0 Unported License (http://smart.servier.com).

3.3.5. β-galactosidase analysis

See Chapter 2 Methods

3.3.6. Cell viability/cytotoxicity assays

3.3.6.1. The micro-culture tetrazolium assay (MTT)

See Chapter 2 Methods.

3.3.6.2. Neutral red assay and microscopy

See Chapter 2 Methods

3.3.6.3. Crystal violet assay

See Chapter 2 Methods.

3.3.7. Protein extraction and quantification

See Chapter 2 Methods.

3.3.8. Western immunoblotting

See Chapter 2 Methods.

3.3.9. RNA isolation

See Chapter 2 Methods.

3.3.10. Reverse transcription polymerase chain reaction (RT-PCR)

See Chapter 2 Methods.

3.3.11. Wound-healing assay

See Chapter 2 Methods.

3.3.12. Immunocytochemistry

See Chapter 2 Methods.

3.3.13. QuPath Analysis

See Chapter 2 Methods.

3.3.14. Statistical analysis

See Chapter 2 Methods.

3.4. RESULTS

3.4.1. Testing of cannabinoids using senescence model

To identify the optimal "safe" concentration of cannabinoids, healthy fibroblasts (not exposed to the H_2O_2) were treated with cannabinoids THC and CBD in the following doses: 0.25 µM, 0.5 µM, 1 µM, 2 µM, 5 µM, 7.5 µM, and 10 µM (Figure 3.2), DMSO was used as a vehicle. Dermal fibroblasts were incubated in THC or CBD for 2 h daily for 5 days.

Phase-contrast imaging was used to characterize quantitative and qualitative changes in dermal fibroblasts simultaneously with assessment of cell viability (Figure 3.3). Our observations showed that low doses of THC and CBD (i.e., 0.25 µM, 0.5 µM, 1 µM) have a cytostatic effect as the number of cells in the culture remained almost unchanged. Morphologically fibroblasts treated with low concentrations of cannabinoids were similar to the untreated fibroblasts. At the same time, a cytotoxic effect was observed in response to 7.5 µM & 10 µM concentrations of CBD and 10 µM THC. We detected substantial quantitative reduction of cells after five days of cannabinoid treatments. The cellular architecture was drastically affected: fibroblasts were decreased in size with a coin-like round shape or visible degradation surrounded by remnants of debris (Figure 3.3). While low and high doses of CBD and THC demonstrated adverse effects, 2 µM and 5 µM exert no effect or even resulted in an increase in cell number without morphological changes.

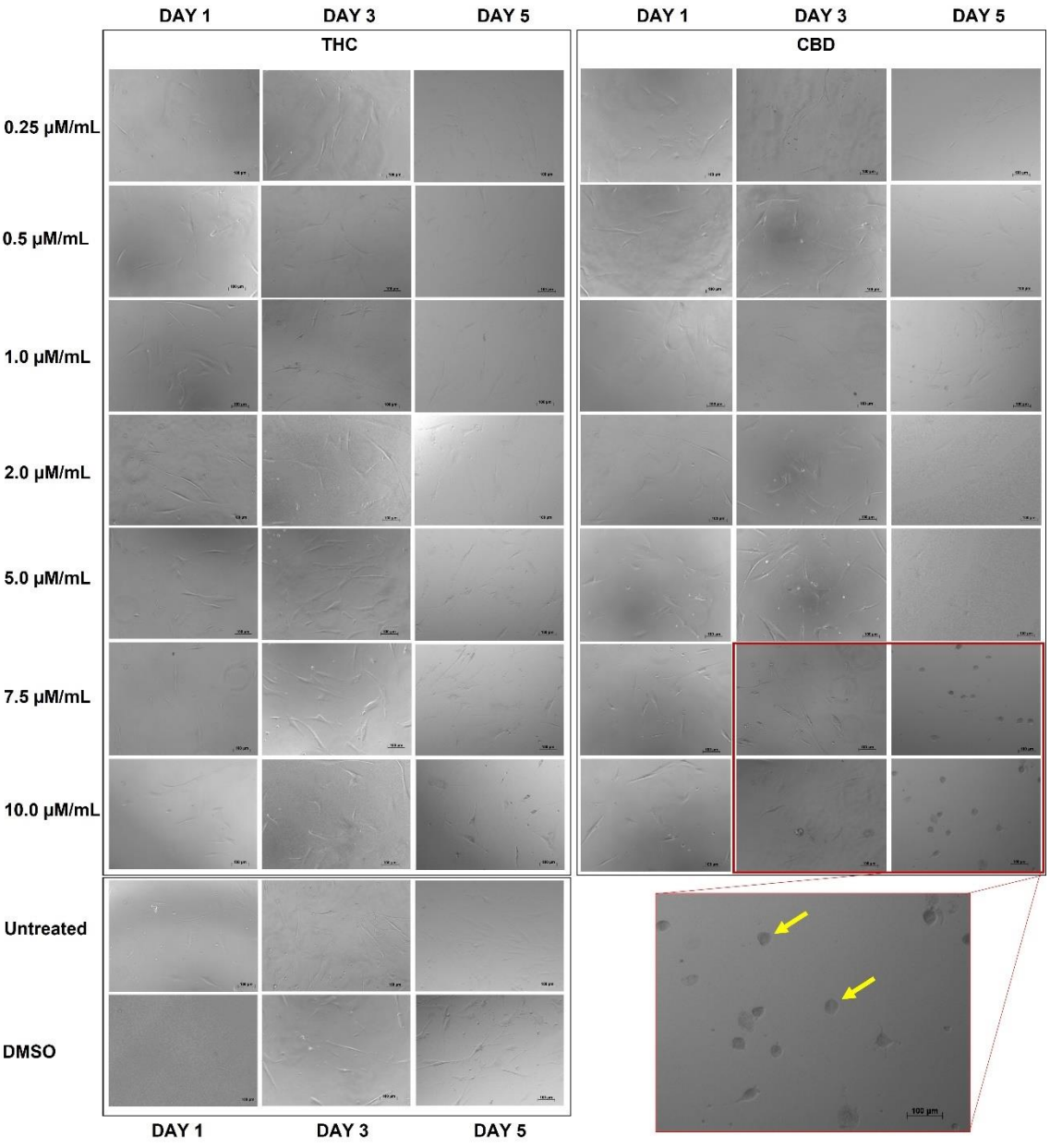

Figure 3.3. Human skin fibroblasts (CCD-1064Sk), 24 PDL exposed to different concentrations of THC and CBD. The figure represents gradual changes in cell quality and quantity on the 1st, 3rd and 5th day of treatment. Arrows depict changes in nuclear shapes – coin-like round fibroblasts. DMSO, dimethyl sulfoxide (vehicle).

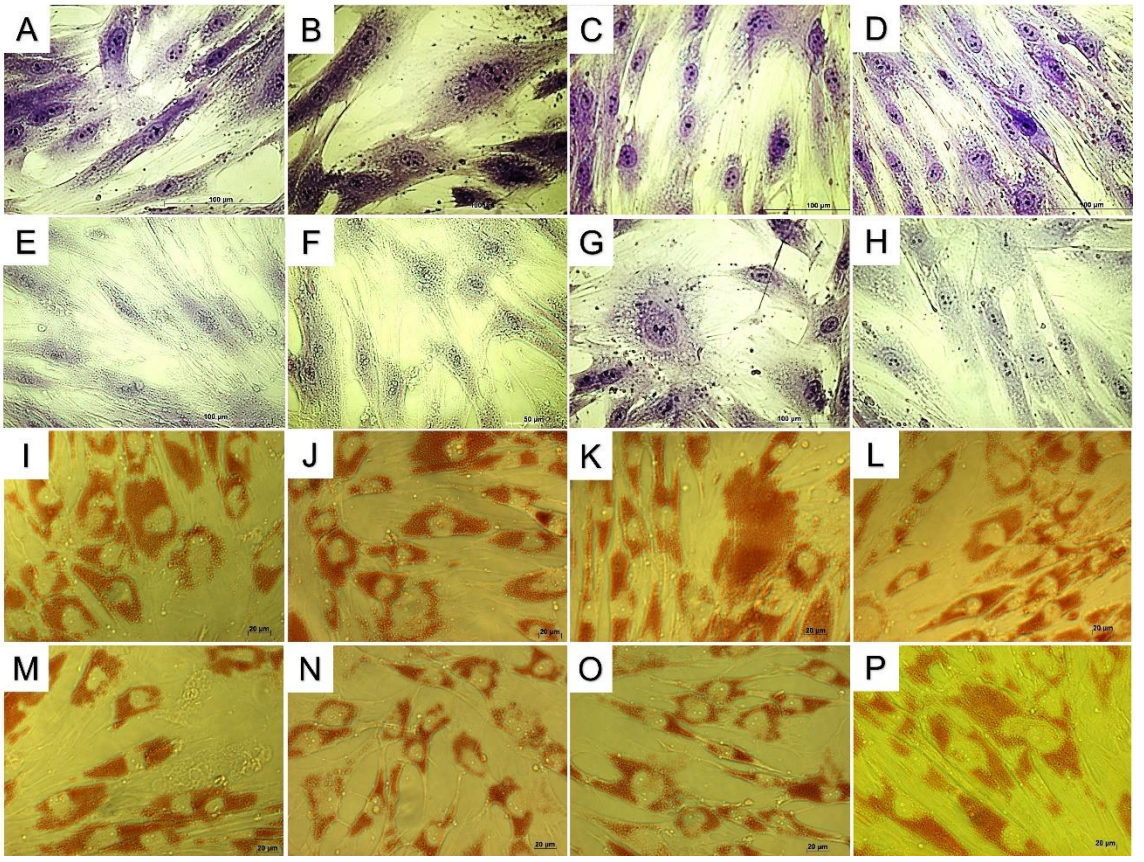

Figure 3.4. Human skin fibroblasts (CCD-1064Sk), 27 PDL after 24 hours phytocannabinoids treatment. A-H, Crystal violet staining; I-P, Neutral red staining. A and I represents untreated fibroblasts; B and J, vehicle (DMSO); C and K, THC 2.0 µM treatment; D and H, CBD, 2.0 µM treatment; E and M, 25 µM H_2O_2; F and N, H_2O_2+DMSO; G and O, H_2O_2+THC; H and P, H_2O_2+CBD.

To better visualize morphological results, healthy and senescent skin fibroblasts were stained with crystal violet (binds to proteins and DNA) and neutral red (accumulates in the lysosomes of viable cells). Significant structural alterations were detected in senescent cells as compared to healthy ones or those treated with pCBs (Figure 3.4). Prematurely aged cells treated with THC and CBD exerted mild modifications of shape and size, unlike aged fibroblasts.

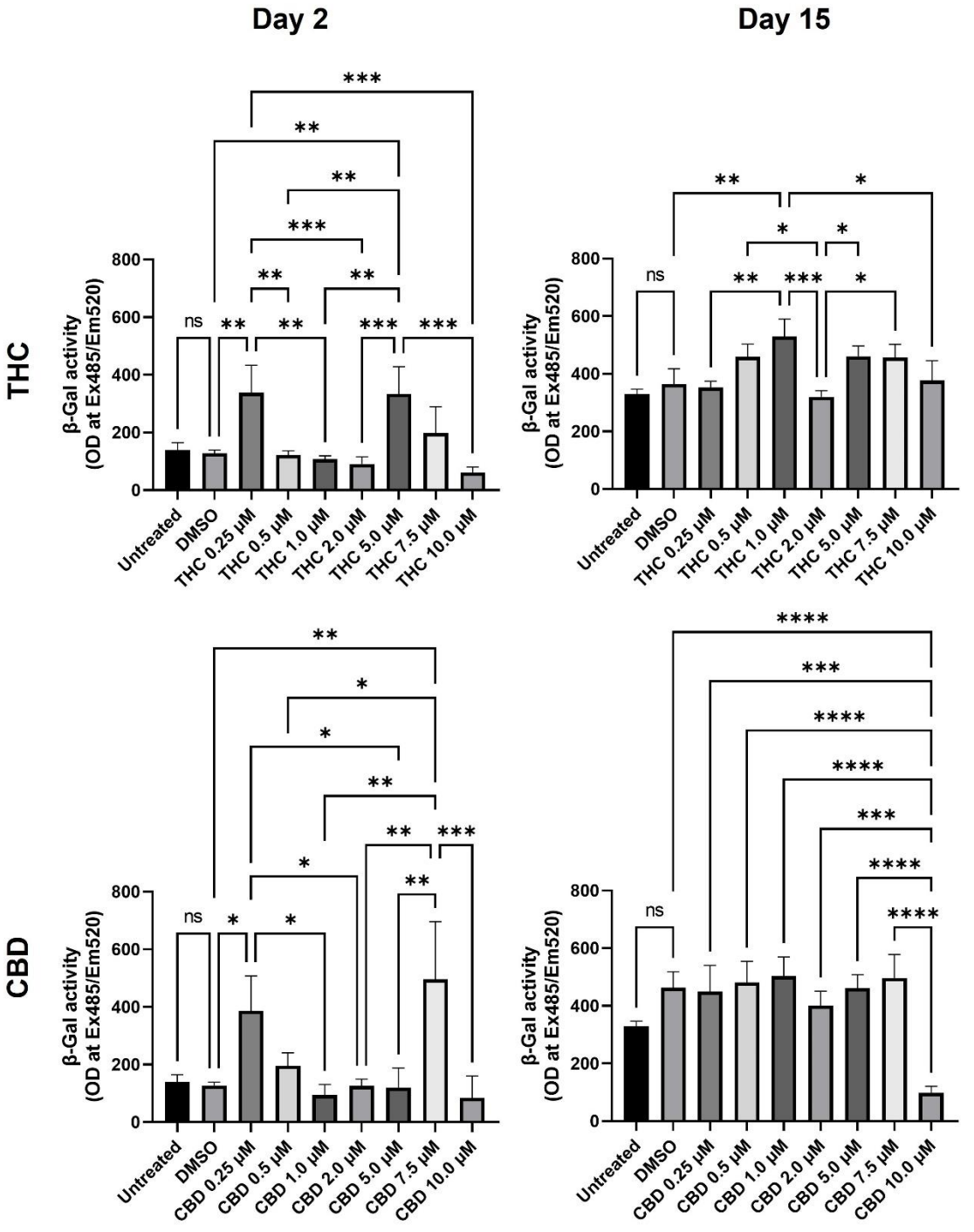

Figure 3.5. β-Gal levels in human skin fibroblasts (CCD-1064Sk), 48 PDL exposed to different concentrations of THC and CBD. The figure represents gradual changes in β-Gal levels within 15 days period shown for the 2nd and 15th day of CBs treatment. DMSO, dimethyl sulfoxide (vehicle). Data were analyzed with an ANOVA test (Tukey post-hoc multiple comparison test). Bars represent mean ± SD. Significance is indicated within the figures using the following scale: *, $p<0.05$; **, $p<0.01$; ***, $p<0.001$; ****, $p<0.0001$.

To determine efficacy and potential cytotoxicity of cannabinoid treatment, fibroblasts of CCD-1064Sk 48 PDL in replicative senescence (RS) were treated with 0.25 µM, 0.5 µM, 1 µM, 2 µM, 5 µM, 7.5 µM, and 10 µM concentrations of THC and CBD for 15 days, 2 h daily (Figure 3.5). Treatment length was chosen because cellular senescence status is associated with slowing down of metabolic activities and complete stop of growth. β-Gal assay was used on day 2 and 15 (Dimri et al., 1995). Two days after the start of CBs treatment β-Gal level was significantly higher in the fibroblasts treated with 0.25 µM, 5.0 µM, 7.5 µM of THC and 0.25 µM, 0.5 µM, and 7.5 µM of CBD as compared to vehicle (DMSO). Following two weeks of treatments with CBs, β-Gal levels in fibroblasts compared to the vehicle were elevated after 1 µM THC ($p<0.01$) and 1 µM CBD ($p>0.05$), while reduced levels of β-Gal were linked to the 2 µM THC ($p<0.05$) and 10 µM CBD ($p<0.0001$) in RS fibroblasts (Figure 3.5).

Next, 2.0 µM THC and 2.0 µM CBD concentrations, which showed favorable results (potentiated of cellular viability, decreased b-Gal levels, preserved cellular morphology), were tested on the prematurely senescent fibroblasts. After 5 days of 2 µM THC application, the elevation of β-Gal levels ($p<0.05$, Figure 3.6, A) was noticed in healthy cells. In contrast, β-Gal levels in H_2O_2 senescent dermal fibroblasts were significantly lower after CBD ($p<0.01$) and THC ($p<0.001$) treatments (Figure 3.6, B).

Results of cellular viability MTT assay suggested no difference after CBs treatments and vehicle control, while untreated dermal fibroblasts showed higher viability (Figure 3.7, A, B). At the same time, prematurely senescent fibroblasts showed a significant reduction in viability compared to those treated with CBs. Moreover, cell growth was boosted substantially after 2 µM CBD and 2 µM THC treatment, whereas 0.5 µM CBD and 0.5 µM THC were less effective (Figures 3.7, C, and D, respectively). Besides, a

similar tendency in CBs treatment was found after induction of senescence with 50 µM H_2O_2 (Figure 3.7, E and F). Interestingly, similarly to what was reported in Figure 3.3, CBD in concentration of 10 µM showed a strong detrimental effect on cell viability (Figure 3.7, E). THC in concentration 10 µM showed similar results as 0.5 µM and 2 µM THC in senescent fibroblasts (Figure 3.7, F). Similar results were received when the experiment was repeated (Suppl. Figure 12).

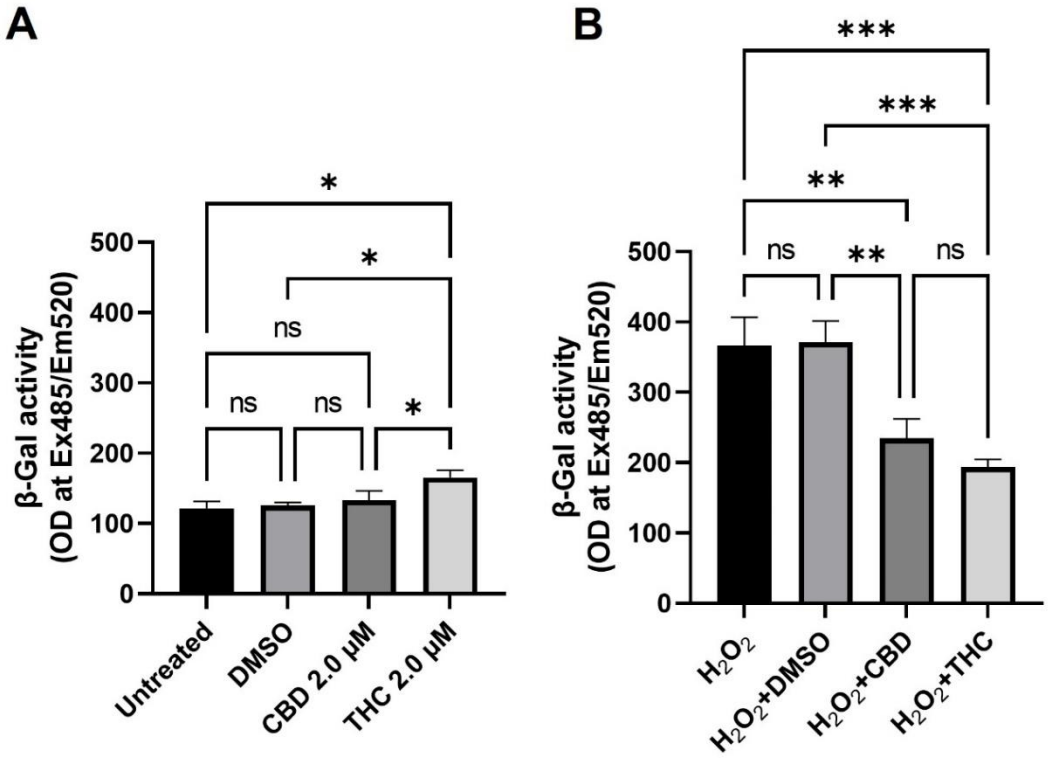

Figure 3.6. β-Gal levels in human skin fibroblasts (CCD-1064Sk), 24 PDL exposed to 2.0 µM THC and 2.0 µM CBD. The figure represents gradual changes in cell β-Gal levels in healthy and prematurely aged fibroblasts after cannabinoid treatments. DMSO, dimethyl sulfoxide (vehicle). Data were analyzed with an ANOVA test (Tukey post-hoc multiple comparison test). Bars represent mean ± SD. Significance is indicated within the figures using the following scale: *, $p<0.05$; **, $p<0.01$; ***, $p<0.001$.

Based on our findings, 2 µM concentration of CBD and THC were chosen as optimal for all subsequent experiments.

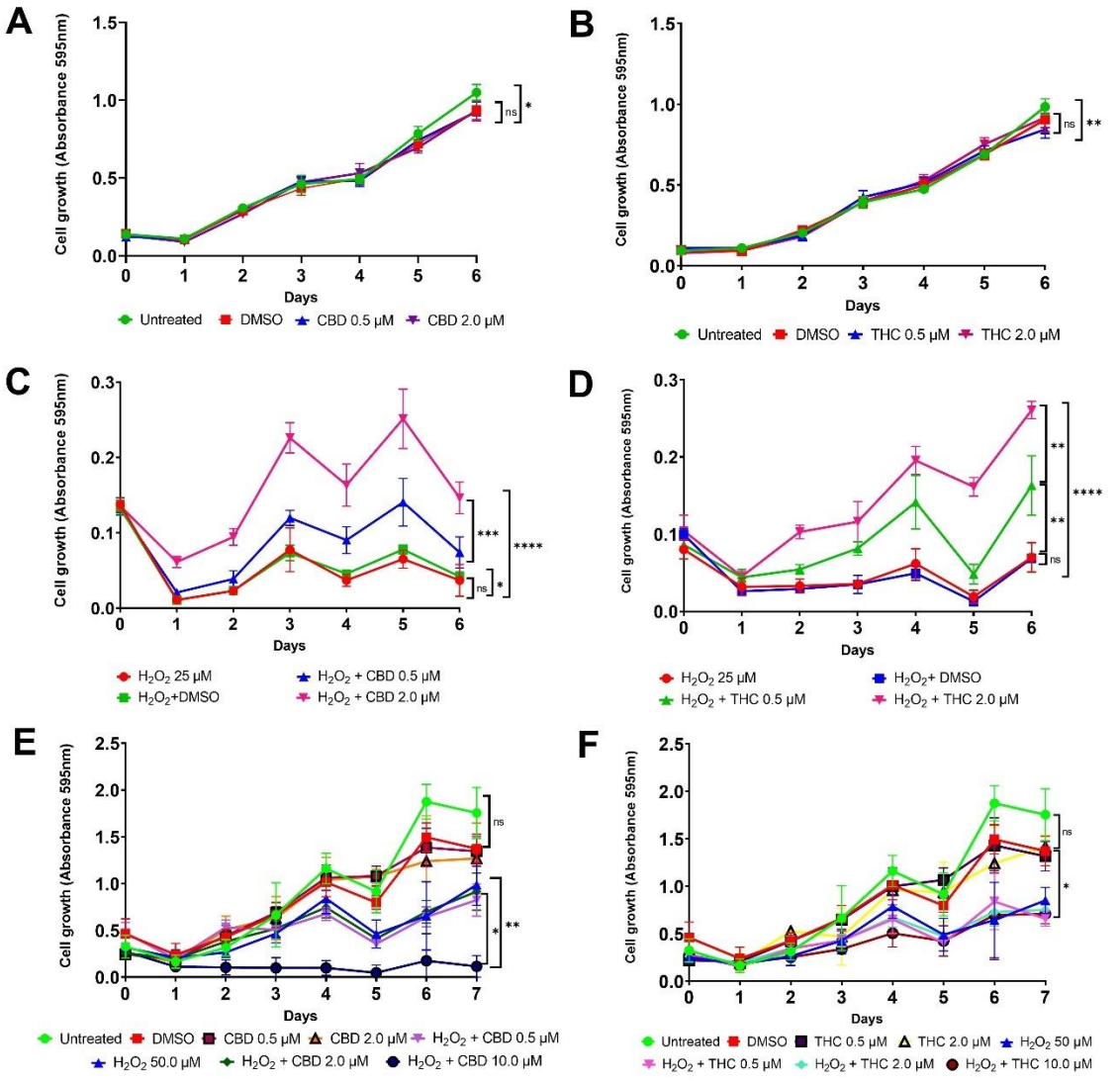

Figure 3.7. Viability of human skin fibroblasts (CCD-1064Sk), 24 PDL treated by different concentrations of THC and CBD. The figure represents gradual changes in cell viability: A, B, healthy HDF treated with 0.5 µM and 2 µM concentrations of CBD and THC respectively; C, D, 25 µM H_2O_2 -induced senescent fibroblasts treated with 0.5 µM and 2 µM concentrations of CBD and THC, respectively; E, F, 50 µM H_2O_2-induced senescent fibroblasts treated with 0.5 µM, 2 µM, and 10 µM concentrations of CBD and THC, respectively. DMSO, dimethyl sulfoxide (vehicle), HDF, human dermal fibroblasts. Data were analyzed with an ANOVA test (Tukey post-hoc multiple comparison test). Bars represent mean ± SD. Significance is indicated within the figures using the following scale: ns, not significant; *, $p<0.05$; **, $p<0.01$; ***, $p<0.001$; ****, $p<0.0001$.

3.4.2. Effect of cannabinoids on the nuclear morphology

In line with previous findings (Figures 2.7, 2.8), nuclear DAPI staining showed significant enlargement and variability in size and shape of nuclei in aged fibroblasts compared to healthy cells. Nuclei of fibroblasts exposed to the H_2O_2 displayed more elongated morphology than untreated cells in the CCD-1064Sk cell line, while some retained round architecture. The gigantic nuclei with irregular shapes were detected in prematurely senescent cells (Figure 3.8, C, D). The nuclear architecture of healthy dermal fibroblasts treated with both CBs remained almost unchanged (Figure 3.8, I-J, M-N). The nuclei area was slightly lower after CBD application on day one compared to the vehicle but normalized on day 5 (Figure 3.8, Q-R). THC effect on healthy cells was opposite: area of nuclei in fibroblasts tended to increase after a single treatment and reduced by day five. Regardless, senescent cells treated with THC and CBD exhibited reduction in circularity (Figure 3.8, S-T); in addition, some nuclei had reduced size compared to the vehicle control (DMSO) and there was a smaller number of gigantic or minuscule irregular nuclei (Figure 3.8, K-L, O-P). Other nuclear parameters, such as perimeter, max caliper, and min caliper, were decreased, while nuclear eccentricity tended to increase in CCD-1064Sk senescent fibroblast treated with CBs (Suppl. Figure 13).

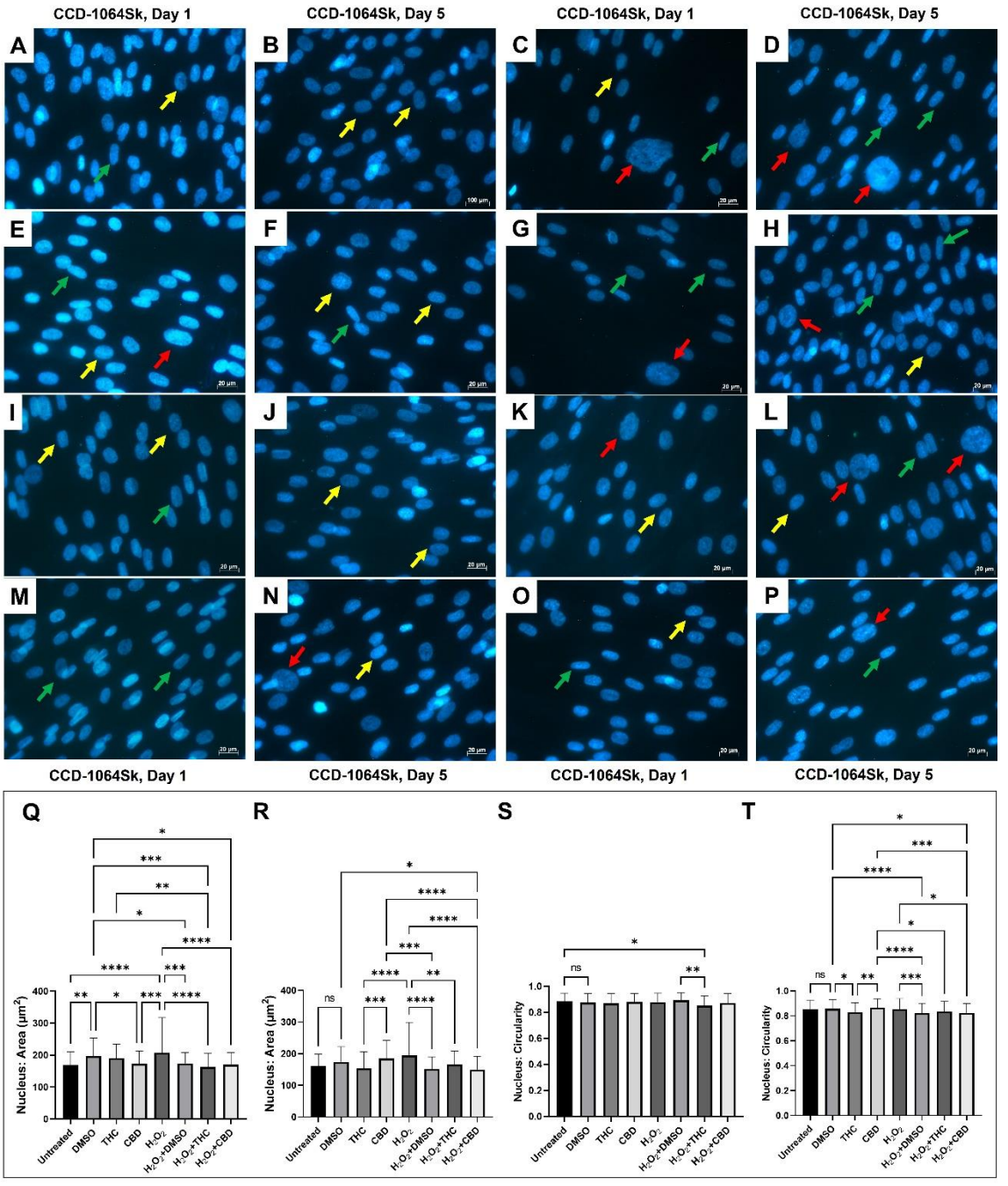

Figure 3.8. DAPI stained nuclei of dermal fibroblasts (CCD-1064Sk), 24 PDL treated with cannabinoids. Pictures A-P represent nuclear changes observed by immunofluorescence microscopy in healthy and senescent fibroblasts treated with cannabinoids on days 1 and 5. Arrows depict changes in nuclear shapes: yellow – round, green – elongated, and red – gigantic/irregular. A and B, Untreated; C and D, 25 µM H_2O_2; E and F, DMSO (vehicle); G and H, 25 µM H_2O_2+DMSO; I and J, THC; K and L, 25 µM H_2O_2+THC; M and N, CBD; O and P, 25 µM H_2O_2+CBD. Graphic representation of nuclear changes on day 1 and day 5 of the experiment, respectively: Q and R, nuclear area; S and T, nuclear circularity. Data were analyzed with an ANOVA test (Tukey post-hoc

multiple comparison test). Bars represent mean ± SD. Significance is indicated within the figures using the following scale: ns, not significant; *, $p<0.05$; **, $p<0.01$; ***, $p<0.001$; ****, $p<0.0001$.

Nuclei of healthy skin fibroblasts BJ-5ta appeared predominantly rounded at the beginning of the experiment and became more elongated on day 5 (Figure 3.9, A-B, E-F). These changes possibly could have been related to the increased cellular confluency, causing changes in cellular and nuclear morphology (Micah et al., 2009). Cannabinoid treatment did not detect significant deviations in the nuclear parameters compared to the vehicle (Figure 3.9, Q-R). As previously described in Chapter 2, prematurely senescent BJ-5ta fibroblasts exhibited predominantly enlarged variable size nuclei (Figure 3.9, C-D, G-H). Significant enlargement of the nuclear area was detected after THC treatment (Figure 3.9, R, L). Other nuclear parameters, such as perimeter, max caliper, min caliper, and the nuclear area, were slightly different in BJ-5ta senescent fibroblast after THC and CBD treatment (Suppl. Figure 14).

3.4.3. Favorable effects of cannabinoids on the expression of senescence-related genes

Our earlier findings suggested that senescent skin fibroblasts demonstrate detrimental changes in the expression of genes involved in cell-cycle regulation, cytoskeletal and metabolic maintenance in addition to changes in cell and nuclear morphology (Chapter 2). We hypothesized that CBD and THC would induce a decrease in aging biomarkers and a reduction of cytoskeleton changes, which were induced by alterations in cell cycle regulation, thus reducing functional and metabolic deterioration associated with progression of senescence.

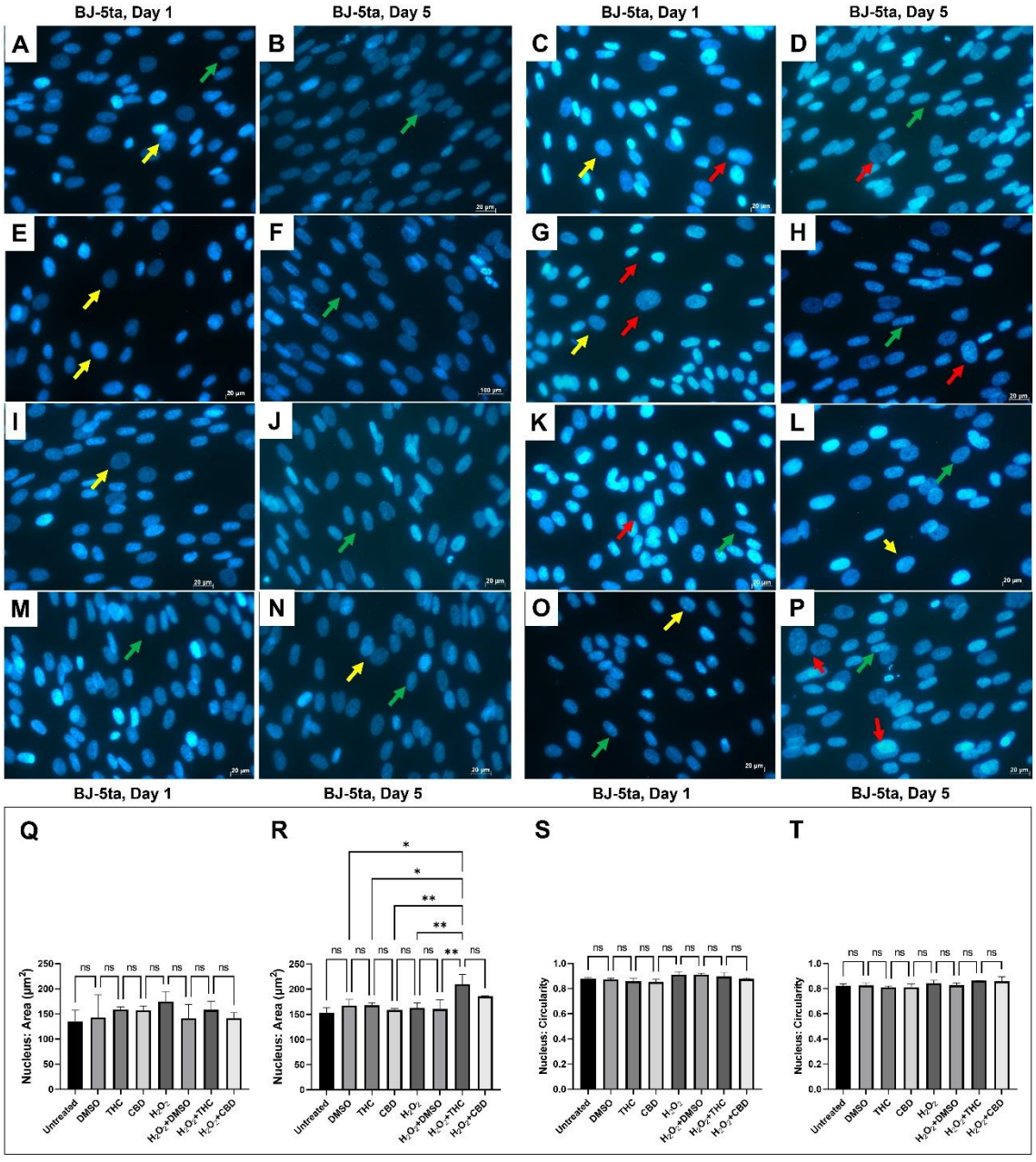

Figure 3.9. DAPI stained nuclei of dermal fibroblasts (BJ-5ta), 90 PDL treated with cannabinoids. Pictures A-P represent nuclear changes observed by immunofluorescence microscopy in healthy and senescent fibroblasts treated with cannabinoids on days 1 and 5. Arrows depict changes in nuclear shapes: yellow – round, green – elongated, and red – gigantic/irregular. A and B, Untreated; C and D, 25 µM H_2O_2; E and F, DMSO (vehicle); G and H, 25 µM H_2O_2+DMSO; I and J, THC; K and L, 25 µM H_2O_2+THC; M and N, CBD; O and P, 25 µM H_2O_2+CBD. Graphic representation of nuclear changes on day 1 and day 5 of the experiment respectively: Q and R, nuclear area; S and T, nuclear circularity. Data were analyzed with an ANOVA test (Tukey post-hoc multiple comparison test). Bars represent mean ± SD. Significance is indicated within the figures using the following scale: ns, not significant; *, $p<0.05$; **, $p<0.01$.

Considering the effects of CBD and THC on senescent fibroblasts based on the reduced β-Gal levels, preserved morphological characteristics cells and nuclear architecture, potentiated viability, we decided first to test the expression of cell-cycle progression regulators p16, p21, and p53, known as senescence-associated markers, in CCD-1135Sk and CCD-1064Sk cultures.

Western blot analysis of different cell lines treated with cannabinoids noted the deviations in the expression of p16, p21, and p53. The expression of p16, a tumor-suppressing protein, was found to be upregulated in RS cells of CCD-1135Sk 40 PDL after 5 days of CBD treatment ($p<0.0001$, Figure 3.10, A). In another RS fibroblasts, CCD-1064Sk 48 PDL, we observed an increase in p16 after CBD ($p<0.01$) and decrease after THC ($p>0.05$) application compared to vehicle (Figure 3.10, B). Senescent fibroblasts exposed to THC and CBD demonstrated the lowest level of p16 expression ($p<0.0001$, Figure 3.10, C). Original Western blot images were included in Supplementary Figures 1-11 (Appendix). Interestingly, in BJ-5ta foreskin fibroblasts, we noticed that the expression of p16 tended to decrease in healthy cells after pCBs application, while expression of *CDKN2A* was not changed (Figure 3.11, A, E). At the same time, senescent fibroblasts expressed CBD-induced suppression ($p<0.05$) of p16 compared to the vehicle, while *CDKN2A* expression in response to pCBs remained almost the same (Figure 3.11, B, F). Slightly opposite results were detected in healthy fibroblasts of the CCD-1064Sk cell line, where CBD ($p<0.05$) and THC ($p>0.05$) tended to increase *CDKN2A* expression but haven't significantly affected senescent cells (Suppl. Figure 15, E).

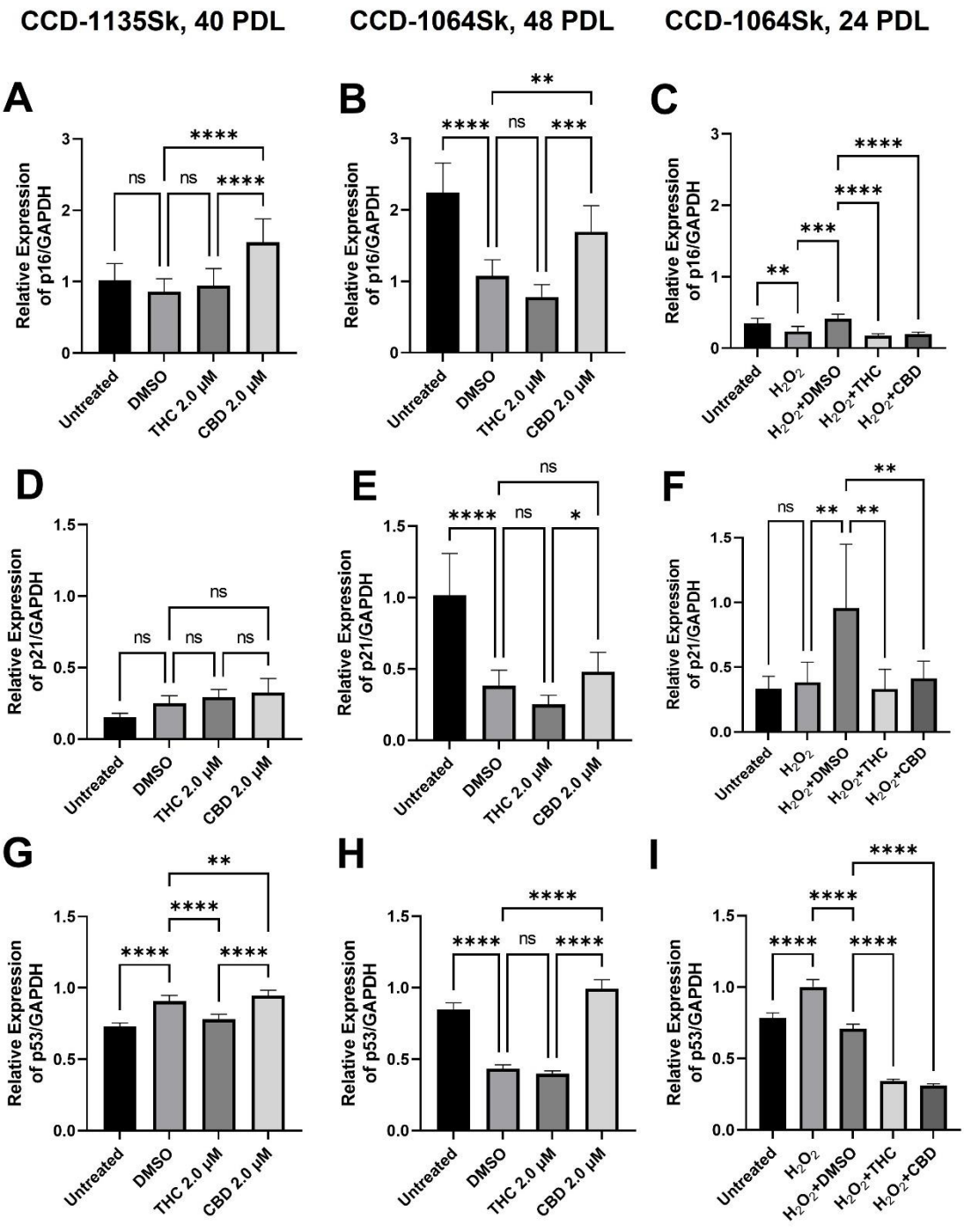

Figure 3.10. The expression of cellular checkpoint regulators in aged fibroblasts from different cell lines treated with cannabinoids. Fibroblast's cell-lines CCD-1135Sk (40 PDL) and CCD-1064Sk (48 PDL) aged naturally by replicative senescence, while CCD-1064Sk (24 PDL) was aged by the one-step H_2O_2 senescence model. Figures represent changed protein expression levels for selected genes measured by Western blot in three different cell lines. A-C, p16 expression; D-F, p21 expression; G-I, p53 expression. Western blot analysis was performed using 30-50 µg of protein

extracts. Glyceraldehyde-3-phosphate dehydrogenase (GAPDH) was used as a loading control. Relative densitometry was presented as a ratio of target protein to GAPDH. Data were analyzed with an ANOVA test (Tukey post-hoc multiple comparison test). Bars represent mean ± SD. Significance is indicated within the figures using the following scale: ns, not significant; *, $p<0.05$; **, $p<0.01$; ***, $p<0.001$; ****, $p<0.0001$.

The analysis of cell proliferation inhibitor p21 expression levels indicates that they were almost unchanged in CCD-1135Sk 40 PDL and CCD-1064Sk 48 PDL compared with H_2O_2 treated CCD-1064Sk 24 PDL (Figure 3.10 D-F). The p21 levels were prominent in the untreated old fibroblasts and significantly decreased in groups treated with pCBs ($p<0.01$, Figure 3.10, E). In parallel, in the H_2O_2-aged cells of CCD-1064Sk 24 PDL, was noticed substantial suppression of p21 followed THC and CBD applications ($p<0.01$, Figure 3.10, F). In BJ-5ta prematurely senescent fibroblasts, a significant rise in p21 expression was observed compared to healthy cells (Figure 3.11, C-D). Simultaneously, *CDKN1A* transcript levels were measured via RT-PCR; however, no significant differences were detected in *CDKN1A* expression between treatment groups (Figure 3.11, G-H). Nevertheless, *CDKN1A* and p21 protein expression were substantially higher in senescent fibroblasts compared to healthy groups with and without pCBs treatment (Figure 3.11, C-D, G-H). Concomitantly, in CCD-1064Sk, it was detected THC-induced *CDKN1A* overexpression ($p<0.05$), while in the senescent treatment groups, pCBs did not affect *CDKN1A* expression compared to vehicle (Suppl. Figure 15, F).

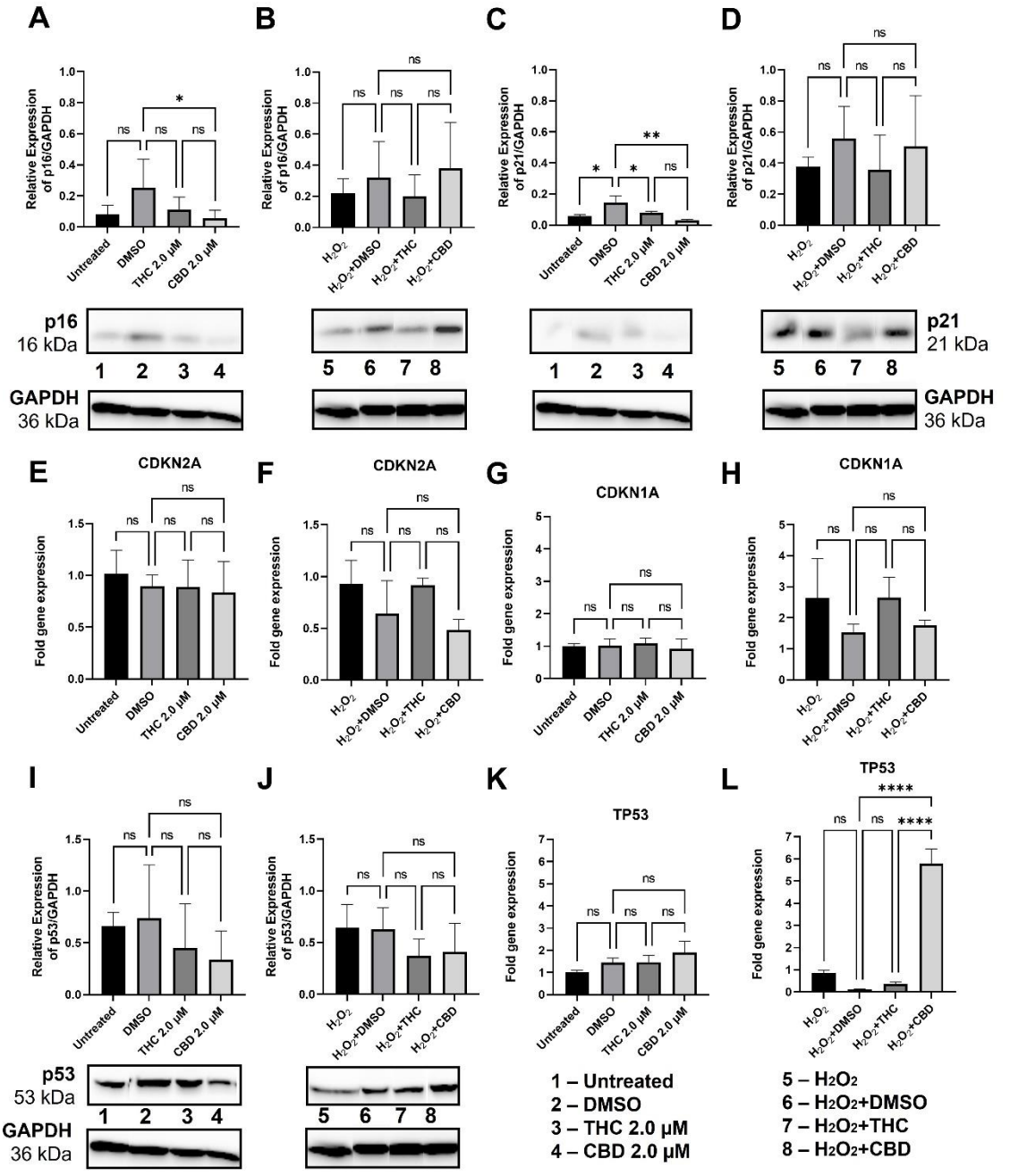

Figure 3.11. Effects of phytocannabinoids on cell cycle checkpoint regulators in BJ-5ta fibroblasts. Western blots showing protein levels of p16 (A-B), p21 (C-D), and p53 (I-J) in healthy and prematurely senescent foreskin fibroblasts. Relative densitometry was presented as a ratio of a target protein to GAPDH. Changes of mRNA expression as measured by RT-PCR for *CDKN2A (p16)* (E-F), *CDKN1 (p21)* (G-H), and *TP53* (K-L). Data were analyzed with an ANOVA test (Tukey post-hoc multiple comparison test). Bars represent mean ± SD. Significance is indicated within the figures using the following scale: ns, not significant; *, p<0.05; **, p<0.01; ***, p<0.001; ****, p<0.0001.

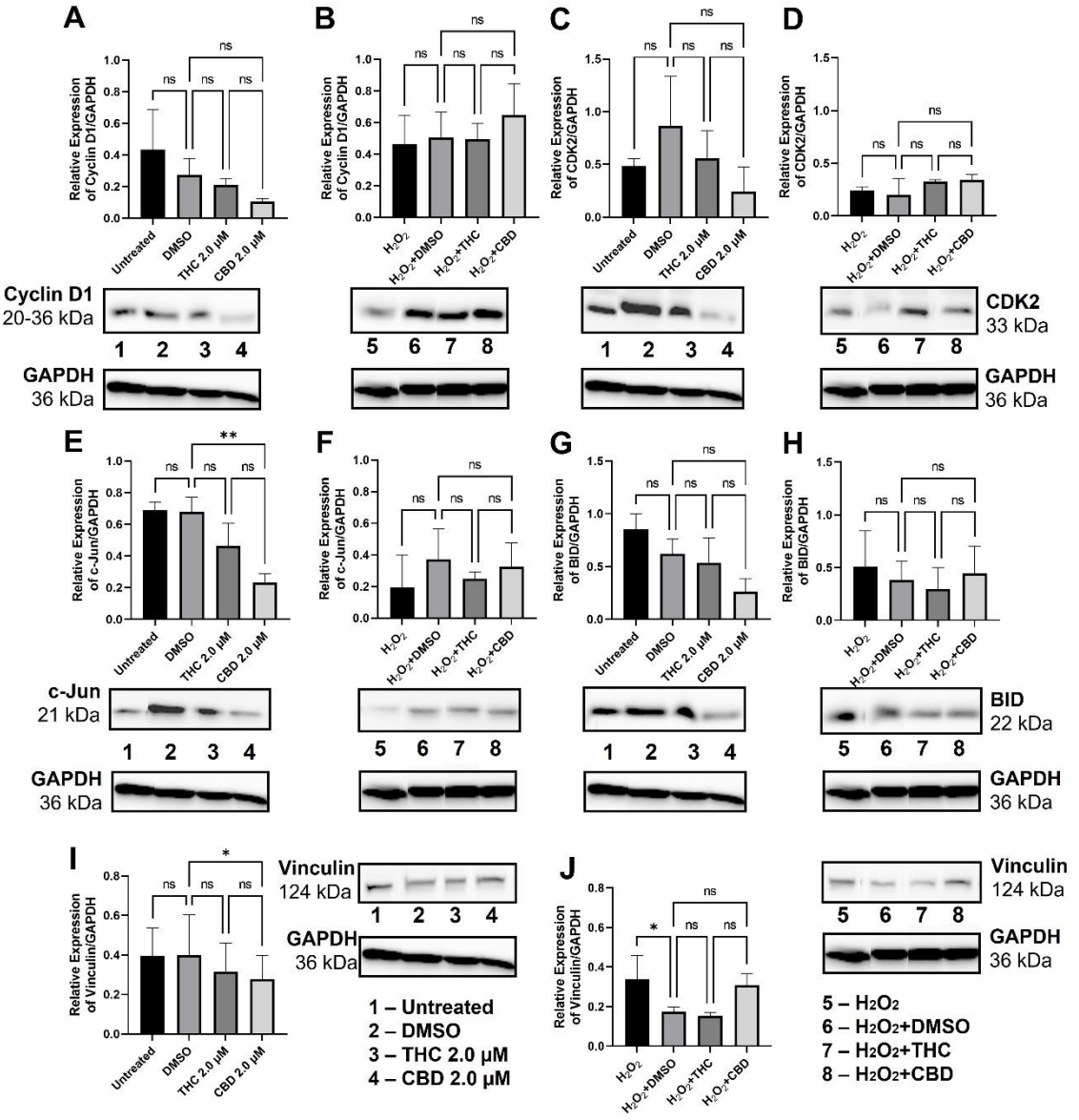

Figure 3.12. The expression of cell-cycle regulators, functional, and regulatory proteins in healthy and aged fibroblasts of BJ-5ta cell line. Fibroblasts were aged by the one-step H_2O_2 senescence model. Figures represent changed protein expression levels for selected genes measured by Western blot. A-B, Cyclin D1 expression; C-D, CDK2 expression; E-F, c-Jun expression; G-H, BID expression; I-J, Vinculin expression. Western blot analysis was performed using 30-50 µg of protein extracts. Glyceraldehyde-3-phosphate dehydrogenase (GAPDH) was used as a loading control. Relative densitometry was presented as a ratio of the target protein to GAPDH. Data were analyzed with an ANOVA test (Tukey post-hoc multiple comparison test). Bars represent mean ± SD. Significance is indicated within the figures using the following scale: ns, not significant; *, $p<0.05$; **, $p<0.01$; ***, $p<0.001$; ****, $p<0.0001$.

p53 expression was somewhat similar to p21; in both naturally aged fibroblast cultures were detected THC-induced downregulation of p53, CCD-1135Sk 40 PDL ($p<0.0001$) and CCD-1064Sk 48 PDL ($p>0.05$) (Figure 3.10, G-H). However, in CCD-1135Sk 40 PDL ($p<0.01$) and in CCD-1064Sk 48 PDL ($p<0.0001$) p53 upregulation after CBD treatment was observed. In contrast, the principal "gatekeeper" expression was significantly reduced in prematurely senescent cells following pCBs treatment ($p<0.0001$, Figure 3.10, I). The expression levels of p53 in the BJ-5ta cell line were similar to the aged CCD-1064Sk fibroblasts (Figure 3.11, I-J). Besides, in the group of healthy fibroblasts, there was a tendency to increase ($p>0.05$) in the expression of mRNA levels of *TP53* after pCBs treatment. Furthermore, senescent BJ-5ta cells exhibited significantly boosted *TP53* expression after CBD 2 μM application ($p<0.0001$). At the same time, vehicle and THC groups demonstrated low *TP53* expression (Figure 3.11, K-L). Besides, in the CCD-1064Sk 24 PDL healthy cells was noted THC-induced elevation ($p<0.05$) of *TP53* mRNA transcripts, whereas in prematurely aged ones *TP53* remained unchanged compared to the vehicle and slightly lower ($p>0.05$) than in healthy counterparts (Suppl. Figure 15, G).

We can speculate that CBD potentiates cell growth inhibition in naturally senescent cells. At the same time, in the case of SIPS, both pCBs tended to reduce tumor suppressor proteins and promote cellular activity except for CBD-induced mRNA *TP53* upregulation in prematurely aged BJ-5ta dermal fibroblasts ($p<0.0001$, Figure 3.11, L).

In parallel, in senescent fibroblasts compared to the healthy counterparts, Cyclin D1 tended to increase, to more extent, following CBD usage and vice versa in the healthy group of fibroblasts ($p>0.05$, Figure 3.12, A-B). Typically for the senescent cells, CDK2 decreased as compared to a healthy group of fibroblasts, with a trend to increase in

response to THC and CBD compared to the vehicle ($p>0.05$, Figure 3.12, C-D). Moreover, c-Jun, necessary for progression through the G1 phase of the cell cycle via direct transcriptional control of the cyclin D1 gene (Wisdom et al., 1999), was also moderately reduced in prematurely aged fibroblasts compared to the healthy group with similar treatments (Figure 3.12, E-F). Surprisingly, CBD downregulated c-Jun in healthy dermal fibroblasts ($p<0.01$, Figure 3.12, E). Together, these data suggest pCBs have the potential to stimulate increased proliferation by modulation of cell cycle progression.

3.4.4. Protective effects of phytocannabinoids on the expression of age-related genes involved in extracellular matrix maintenance and metabolic response

Fibroblasts are the main generator of extracellular matrix components (ECM) (i.e., collagens, elastin, and hyaluronan) necessary to maintain the proper functioning of not just skin but all tissues and organs in the body. Our previous data showed significant deterioration of ECM elements in senescent cells (Chapter 2). Subsequently, it was hypothesized that phytocannabinoids have rejuvenation properties by restoring collagen, elastin, and hyaluronic acid production.

Western blot results showed a significant increase in type I collagen (COL1A1) expression in healthy fibroblasts treated with THC ($p<0.0001$, Figure 3.13, A), while CBD showed no change in protein levels. In prematurely aged BJ-5ta fibroblasts, we detected a significant reduction in COL1A1 compared to healthy ones regardless of treatment (Figure 3.13, A-B). Moreover, THC was noted to inhibit COL1A1 production in senescent cells ($p<0.01$, Figure 3.13, B). In addition, pCBs did not affect *COL1A* expression in healthy and senescent fibroblasts (Figure 3.13, E-F). Similar changes were detected in the CCD-1064Sk fibroblasts after pCBs treatment (Suppl. Figure 15, A).

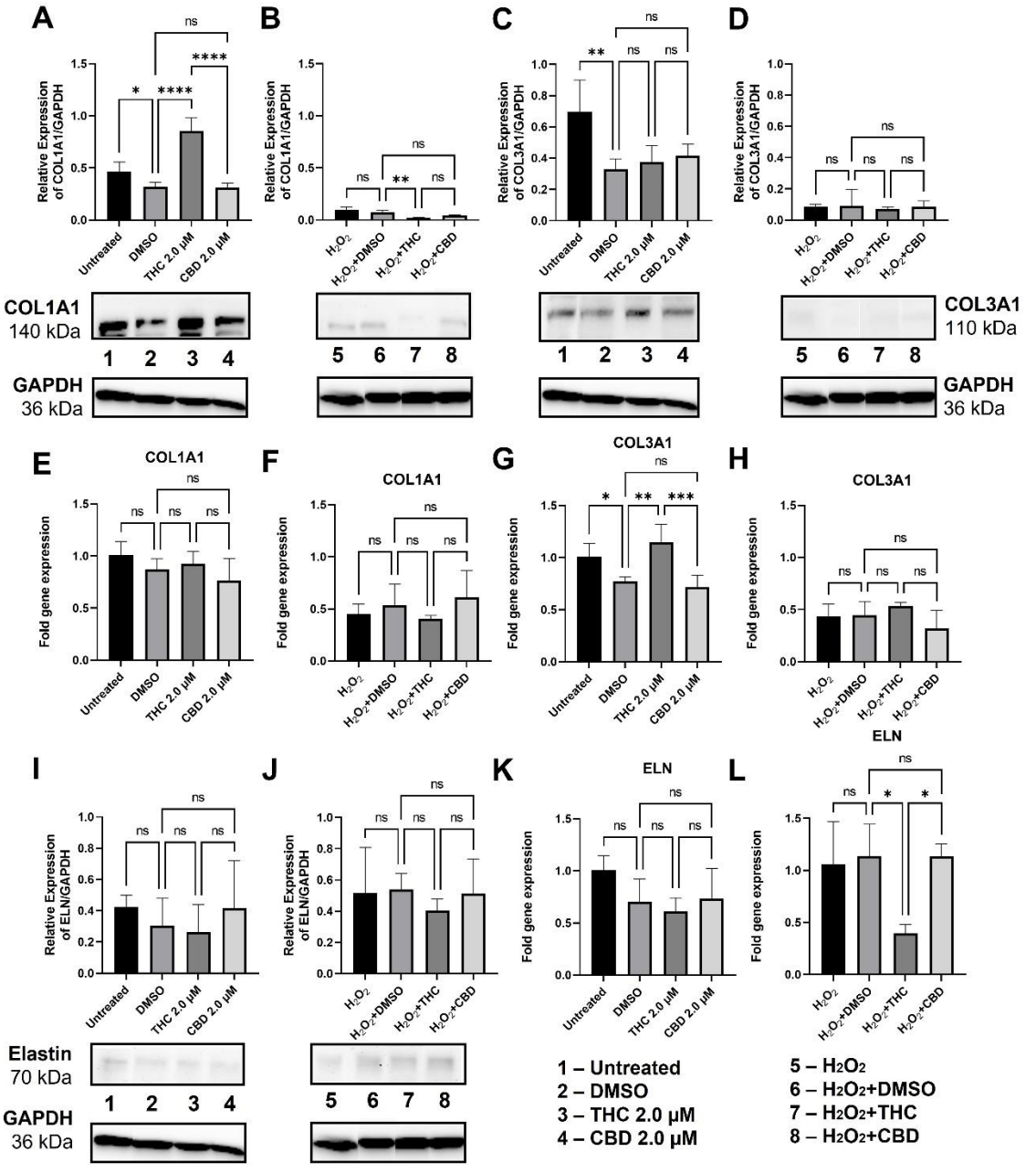

Figure 3.13. Effects of phytocannabinoids on extracellular matrix producers in BJ-5ta fibroblasts. Western blots showing protein levels of COL1A1 (A-B), COL3A1 (C-D), and Elastin (I-J) in healthy and prematurely senescent foreskin fibroblasts. Relative densitometry was presented as a ratio of the target protein to GAPDH. Changes of mRNA expression as measured by RT-PCR for *COL1A1* (E-F), *COL3A1* (G-H), and *ELN* (K-L). Data were analyzed with an ANOVA test (Tukey post-hoc multiple comparison test). Bars represent mean ± SD. Significance is indicated within the figures using the following scale: ns, not significant; *, $p<0.05$; **, $p<0.01$; ***, $p<0.001$; ****, $p<0.0001$.

Type III collagen is another abundant protein in the skin. Protein levels of COL3A1 in healthy BJ-5ta foreskin fibroblasts were slightly elevated compared to the vehicle ($p>0.05$, Figure 3.13, C). At the same time, no significant change was observed in prematurely aged cells ($p>0.05$, Figure 3.13, D). Interestingly, in healthy fibroblasts, *COL3A1* expression was upregulated after THC ($p<0.01$); however, it was lowered in senescent ones and had a similar trend (Figure 3.13, G-H). These findings directly corresponded to *COL3A1* expression in CCD-1064Sk (Suppl. Figure 15, B).

After stretching or contracting, elastin reinstates skin and other tissues. It was found almost unchanged in all experimental groups after pCBs treatment in BJ-5ta culture, except THC-induced suppression ($p<0.05$) of *ELN* mRNA transcripts (Figure 3.13, I-L). At the same time, we noticed a slight elevation of elastin expression in senescent fibroblasts on protein and mRNA levels. Nevertheless, in the healthy CCD-1064Sk cells, THC ($p<0.0001$) and, to less extent, CBD ($p<0.05$) stimulated *ELN* expression. Albeit in the SIPS cells, *ELN* mRNA levels were decreased compared to the healthy treatment groups and were not affected by pCBs treatment (Suppl. Figure 15, C). Simultaneously, were detected pCBs-stimulated upregulation of *TIMP1* (tissue inhibitor of metalloproteinases 1) ($p>0.05$) and *HAS1* (hyaluronan) ($p<0.01$) in healthy fibroblasts, albeit it was lowered in all senescent fibroblasts regardless of treatment compared to their healthy counterparts (Suppl. Figure 15, L and D, respectively). Important, *MMP2*, known to degrade ECM constituents, was significantly upregulated followed THC ($p<0.01$) application in the healthy group, while it was tended to decline in senescent cells treated with pCBs (Suppl. Figure 15, H). One more exciting finding showed decreased expression of vinculin, an adhesive protein involved in the nexus of integrin adhesion molecules to the actin cytoskeleton, after CBD ($p<0.05$) and THC ($p>0.05$) application in healthy cells

(Figure 3.12, I). Vinculin levels remained lower in the senescent group with a CBD-induced trend to increase ($p>0.05$, Figure 3.12, J).

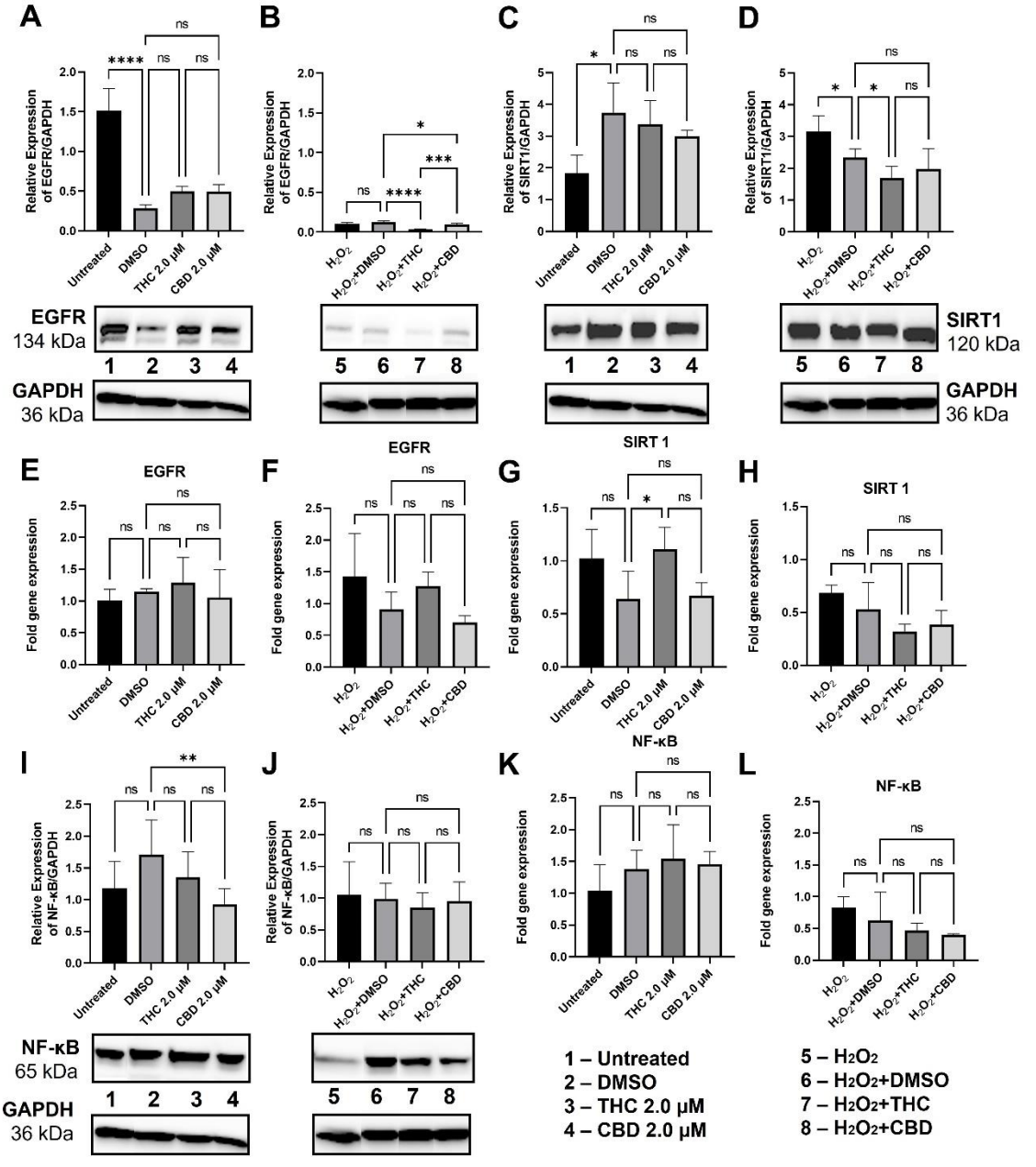

Figure 3.14. The effect of THC and CBD treatments on expression of cell-cycle and metabolic regulators in healthy and aged fibroblasts of BJ-5ta cell line. Western blots showing protein levels of EGFR (A-B), SIRT1 (C-D), and NF-κB (I-J) in healthy and prematurely senescent foreskin fibroblasts. Relative densitometry was presented as a ratio of the target protein to GAPDH. Changes of mRNA expression as measured by RT-PCR for *EGFR* (E-F), *SIRT1* (G-H), and *NF-κB* (K-L). Data were analyzed with an

ANOVA test (Tukey post-hoc multiple comparison test). Bars represent mean ± SD. Significance is indicated within the figures using the following scale: ns, not significant; *, $p<0.05$; **, $p<0.01$; ***, $p<0.001$; ****, $p<0.0001$.

EGFR, known to be involved in a variety of cell signaling pathways that control cell division and survival, was unchanged after pCBs application in healthy BJ-5ta fibroblast compared to vehicle, albeit it was higher than in senescent group (Figure 3.14, A). EGFR expression was reduced in senescent cells in response to THC ($p<0.0001$) and CBD ($p<0.05$) (Figure 3.14, B). In contrast, *EGFR* mRNA transcripts were not affected by pCBs usage (Figure 3.14, E-F). Concurrently, the expression of *NF-κB* was not significantly affected by THC or CBD in both BJ-5ta and CCD-106Sk healthy fibroblasts (Figure 3.14, K and Suppl. Figure 15, J respectively). Western blot analysis did not validate these data as CBD caused a reduction in NF-κB protein levels ($p<0.01$, Figure 3.14, I). In both cell lines of prematurely aged fibroblasts, no significant change in *NF-κB* expression was observed in response to pCBs; still, they were lower than the healthy group (Figure 3.14, K-L and Suppl. Figure 15, J, respectively). NF-κB protein regulates the expression of numerous genes associated with cell survival, proliferation, and differentiation. *MKI67*, one of the proliferative biomarkers, was upregulated in healthy fibroblasts following THC ($p<0.01$) and CBD ($p>0.05$) usage, while in senescent ones in response to CBD ($p<0.05$) (Suppl. Figure 15, I). In addition, another NF-κB influence is associated with apoptosis. As a result, BID protein, a pro-apoptotic member of the Bcl-2 protein family involved in the mitochondrial pathway of programmed cell death, was almost unchanged in both healthy and senescent groups, except for a slight tendency to decline in healthy fibroblasts after CBD treatment (Figure 3.12, G).

To determine the effects of pCBs on changes in metabolic regulation, we tested the expression of sirtuins such as SIRT1 (nuclear), SIRT3 (mitochondrial), SIRT4 (mitochondrial), and SIRT 6 (nuclear). The expression of "longevity" *SIRT1* was increased in the THC group ($p<0.05$) and unaffected in the CBD group of healthy BJ-5ta fibroblasts (Figure 3.14, G). Interestingly, Western blot data did not detect significant alterations in levels of SIRT1 after pCBs application in healthy cells (Figure 3.14, C). Similarly, healthy CCD-1064Sk fibroblasts treated with THC ($p<0.05$) and CBD ($p>0.05$) showed elevated *SIRT1* expression (Suppl. Figure 15, M). At the same time, pCBs treatment of senescent cells was associated with decreased SIRT1 protein levels followed by THC exposure ($p<0.01$) and pCBs-induced tendency to decline in *SIRT1* gene expression in BJ5-ta culture (Figures 3.14, D, and H, respectively). Correspondingly *SIRT1* was unchanged compared to the vehicle in CCD-1064Sk prematurely aged fibroblasts, albeit it was lower than in healthy experimental groups (Suppl. Figure 15, M).

Our findings showed that expression of other sirtuins, *SIRT3* and *SIRT4*, located on mitochondrial matrix and widely implicated in regulating metabolic processes, and nuclear *SIRT6* was insignificantly potentiated by THC and CBD in the CCD-1064Sk healthy fibroblasts ($p>0.05$, Suppl. Figure 15, N-P). At the same time, in pCBs treated BJ-5ta healthy cells, *SIRT4* expression was moderately downregulated ($p>0.05$, Figure 3.15, A). Of note, in the senescent cells, the expression of *SIRT3*, *SIRT4*, and *SIRT6* was almost unchanged with a mild tendency for upregulation after CBD treatment ($p>0.05$) in CCD-1064Sk fibroblasts (Suppl. Figure 15, M-P). At the same time, in the BJ-5ta culture, CBD decreased *SIRT4* expression in prematurely aged fibroblasts ($p<0.01$, Figure 3.15, B).

To check whether CB receptors are also changed in response to senescence, the expression of CB receptors was also tested. *CB2* was not found to significantly deviate

from the vehicle in healthy and senescent fibroblasts after pCBs treatment in BJ-5ta culture (Figure 3.15, C-D). In contrast, *CB1* was upregulated after CBD exposure in healthy fibroblasts and also upregulated in senescent cells after THC and CBD treatment (data not shown). However, we did not detect significant changes in CB1 and CB2 protein levels (Figure 3.15, E-F).

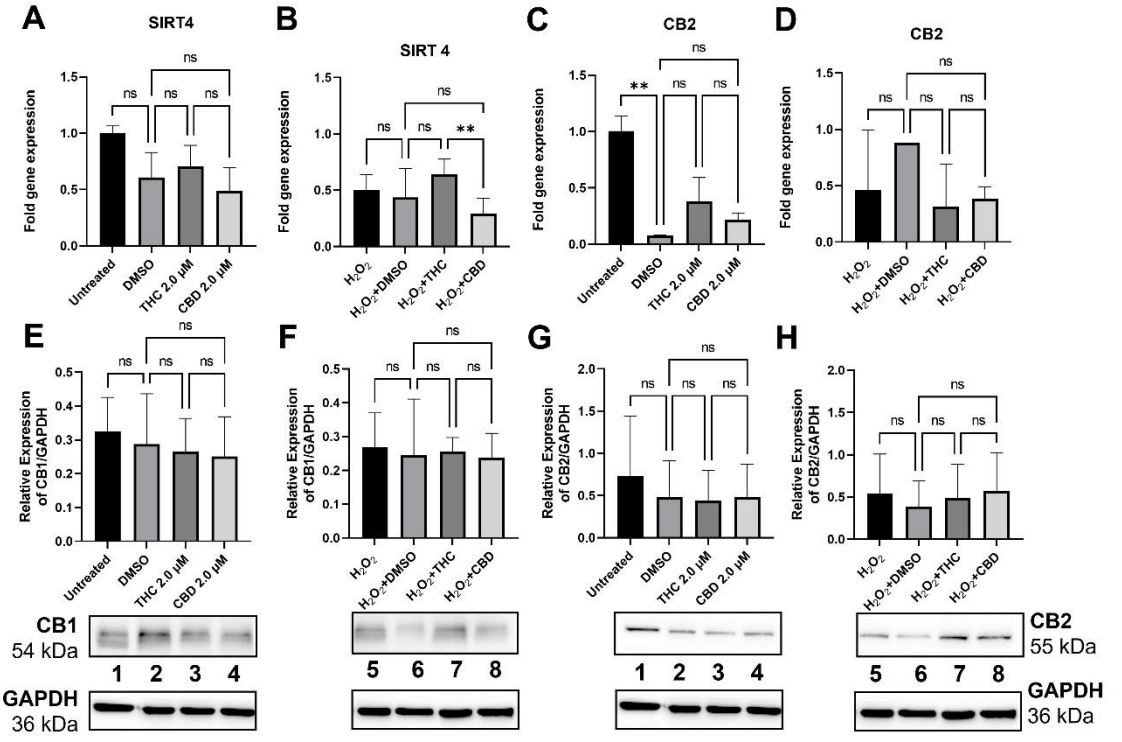

Figure 3.15. Effects of phytocannabinoids on SIRT4 and cannabinoid receptors expression in BJ-5ta dermal fibroblasts. Changes of mRNA expression levels for selected genes as measured by RT-PCR. A. *SIRT4* expression in healthy fibroblasts; B. *SIRT4* expression in senescent fibroblasts; C. *CB2* expression in healthy fibroblasts; D. *CB2* expression in senescent fibroblasts. Western blots showing protein levels of E, CB1 in healthy cells; F, CB1 in senescent fibroblasts; G, CB2 in healthy cells; H, CB2 in prematurely senescent foreskin fibroblasts, respectively. Relative densitometry was presented as a ratio of the target protein to GAPDH. Data were analyzed with an ANOVA test (Tukey post-hoc multiple comparison test). Bars represent mean ± SD. Significance is indicated within the figures using the following scale: ns, not significant; *, $p<0.05$; **, $p<0.01$.

Based on these findings, it is possible to suggest that pCBs mildly preserve ECM components and potentiate metabolic activity in senescent dermal fibroblasts via endocannabinoid regulation.

3.4.5. Phytocannabinoids preserve cellular viability in SIPS fibroblasts

In the previous experiment, we have shown the beneficial effects of different concentrations of phytocannabinoids on senescent fibroblasts (Figure 3.7). Here we tested fibroblasts viability after pCBs exposure as analyzed by MTT, Neutral red (NR), and Crystal violet (CV) assays.

Interestingly, the MTT assay detected unchanged viability of healthy fibroblasts subsequent to pCBs exposure, while in senescent cells, THC ($p<0.01$) and CBD ($p<0.001$) boosted cellular growth (Figure 3.16, A-B). Compared to the MTT assay results, the NR assay did not detect significant alterations in the viability of healthy and senescent experimental groups after pCBs treatments (Figure 3.16, C-D). Likewise, CV assay results, based on a 48/24 hour ratio, did not represent significant deviations in healthy cells (Figure 3.16, E). In contrast, in SIPS fibroblasts, an increased ratio of CV-positive cells was detected following THC ($p<0.05$) and CBD ($p<0.01$) usage (Figure 3.16, F) that resembled MTT data.

Our results showed that the influence of pCBs treatment exerted a significant positive effect on the preservation of senescent cell viability.

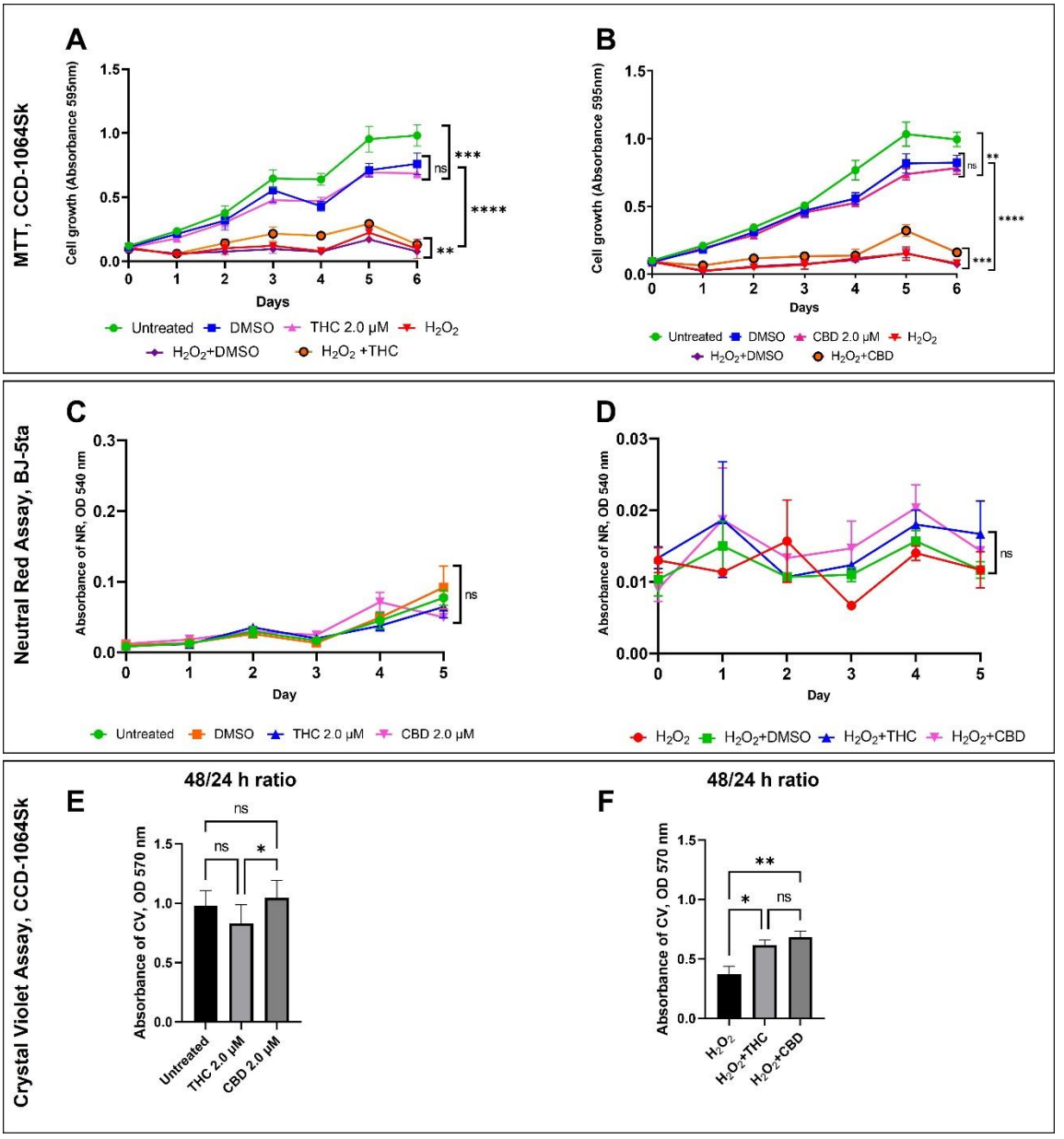

Figure 3.16. Viability of dermal fibroblasts treated with phytocannabinoids. The graphs represent the cell viability of CCD-1064Sk fibroblasts estimated by MTT assay after THC and CBD treatment (A and B, respectively). The graphs represent the cell viability of BJ-5ta fibroblasts estimated by Neutral Red assay after phytocannabinoids treatment in healthy and senescent fibroblasts (C and D, respectively). The graphs represent cell viability shown as 48/24 hours ratio in CCD-1064Sk fibroblasts estimated by Crystal violet assay after phytocannabinoids treatment in healthy and prematurely aged skin cells (E and F, respectively). Data were analyzed with an ANOVA test (Tukey post-hoc multiple comparison test). Bars represent mean ± SD. Significance is indicated within the figures using the following scale: ns, not significant; *, $p<0.05$; **, $p<0.01$; ***, $p<0.001$; ****, $p<0.0001$.

3.4.6. Influence of THC and CBD on the speed of the healing process

One of the prominent roles of fibroblasts is maintaining a proper healing process by repair and regeneration of tissues, which is also based on the generation of ECM components. Figure 3.17 shows the wound healing assay results (WHA), also known as a scratch assay done on three different dermal fibroblast cell lines: matured CCD-1064Sk 24 PDL, hTERT-immortalized BJ-5ta, and CCD-1135Sk 40 PDL in the replicative senescence state. Wound healing was similar in response to phytocannabinoids in healthy cells of both CCD-1064Sk and BJ-5ta cell lines (Figure 3.17, A-B, E-F, respectively). pCBs treatment of the senescent cells resulted in 50% of wound closure on 48 h of the experiment and complete closure on the 72 h compared to the vehicle ($p<0.001$, Figure 3.17, D). In the prematurely senescent fibroblasts of BJ-5ta, the vehicle group exhibited faster healing (Figure 3.17, G-H). CBD usage showed delayed ($p<0.01$) wound closure in H2O2-induced senescent BJ-5ta cells, THC treatment also tended to prolong healing speed ($p>0.05$, Figure 3.17, H). At the same time, visual wound enlargement after 24 h of experiment in the prematurely aged group in both CCD-1064 and BJ-5ta cell lines was noted (Figures 3.17, C and G, respectively). Interestingly, almost complete wound closure was detected after 48 hours of THC treatment ($p<0.01$) in the naturally senescent fibroblast group (Figure 3.17, I). At the 72 h time point, 28% of unhealed wound area was detected in untreated old fibroblasts, while vehicle and CBD groups showed nearly complete wound closure (Figure 3.17, J).

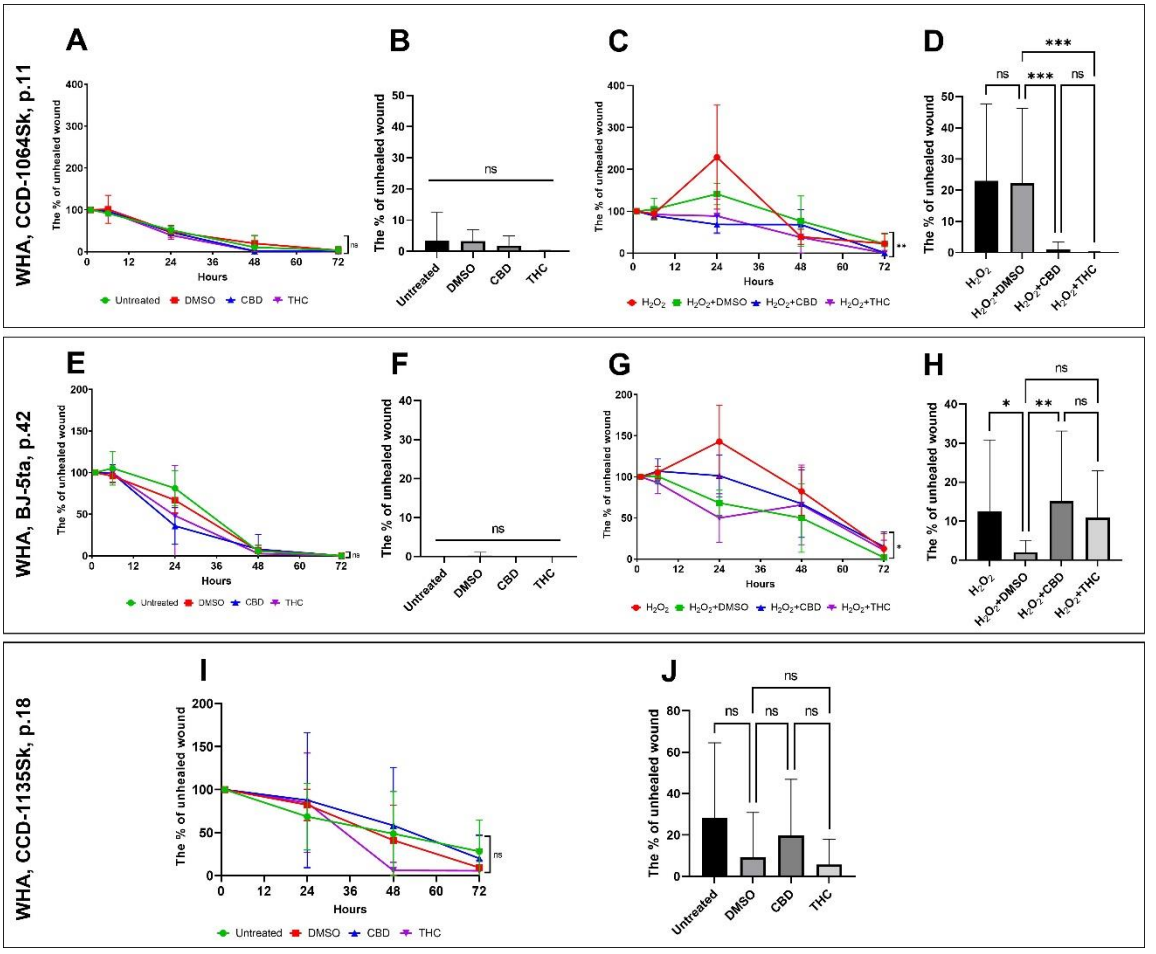

Figure 3.17. Phytocannabinoids effect on wound healing. Wound healing assay (WHA) results in CCD-1064Sk 24 PDL dermal fibroblasts, BJ-5ta 90 PDL foreskin fibroblasts, and naturally aged CCD-1135Sk 40 PDL skin fibroblasts. A. The percentage of an unhealed wound in healthy CCD-1064Sk, 24 PDL; B. The percentage of the unhealed wound after 72 hours of pCBs exposure; C. The percentage of the unhealed wound in senescent fibroblasts treated with pCBs; D. The percentage of the unhealed wound after 72 hours of pCBs exposure in prematurely aged fibroblasts; E. The percentage of the unhealed wound in healthy BJ-5ta, 90 PDL; F. The percentage of the unhealed wound after 72 hours of pCBs exposure; G. The percentage of the unhealed wound in senescent fibroblasts treated with pCBs; H. The percentage of the unhealed wound after 72 hours of pCBs exposure in prematurely aged fibroblasts; I. The percentage of the unhealed wound in naturally senescent CCD-1135Sk 40 PDL fibroblasts after pCBs exposure; J. The percentage of the unhealed wound after 72 hours of pCBs exposure in fibroblasts aged by replicative senescence. Data were analyzed with an ANOVA test (Tukey post-hoc multiple comparison test). Bars represent mean ± SD. Significance is indicated within the figures using the following scale: ns, not significant; *, $p<0.05$; **, $p<0.01$; ***, $p<0.001$.

One key biomarker of senescence is growth arrest: after exposure to H_2O_2, human dermal fibroblasts (HDF) show a decrease in cellular viability, ECM components production, and the healing process. Our findings suggest that both pCBs, CBD and THC, potentially improve dermal fibroblasts' functional capacity and speed up the restoration of damaged areas.

3.5. DISCUSSION

Cannabis sativa has been known to humankind for millennia and reported as a remedy by the Emperor of China, Shen Nung (ben Amar, 2006). He is recognized as the first to have described the properties and therapeutic uses of Cannabis in his compendium of Chinese medicinal herbs, the world's oldest pharmacopeia, written in 2737 BC (Li, 1974). In those days, Cannabis was prescribed to treat disorders of the female reproductive system, rheumatic pain, constipation, malaria, and others. Later, it was combined with wine to anesthetize patients during surgeries (Zuardi, 2006). From ancient China, Cannabis spread to India, Tibet, the Middle East, Europe and eventually reached all continents. For all that time, it was used as a remedy for multiple conditions such as eczema and psoriasis, atherosclerosis, osteoporosis, rheumatoid arthritis, and other inflammatory disorders (China); headache, neuralgia, toothache (as analgetic), epilepsy, tetanus, rabies (anticonvulsant), skin infections, erysipelas, tuberculosis (as anti-inflammatory and antibiotic) (India); in case of snakebite, to facilitate childbirth, malaria, fever, blood poisoning, anthrax, asthma, dysentery (Africa), and many others. Nevertheless, there is almost no data about the anti-aging or rejuvenation properties of Cannabis. Based on empirical and modern scientific data, Cannabis has shown multiple beneficial effects that might be used in the treatment of age-related conditions, skin

disorders and had a great potential to delay senescence and age-related changes (Zuardi, 2006).

Here, we tested phytocannabinoids THC and CBD effects on the healthy and senescent fibroblasts. We established a new SIPS model to study *in vitro* effects of potential anti-aging compounds. Using this model, we showed that both THC and CBD have dose-dependent effects on cellular viability, reduction or increase in senescence biomarkers, and changes in cell morphology. A summary of THC and CBD effects on healthy and senescent fibroblasts is presented in Table 3.2.

Table 3.2. Summary of the investigated characteristics of healthy and prematurely aged skin fibroblasts after phytocannabinoid treatment

Characteristic	Young fibroblasts			Senescent fibroblasts		
	DMSO	CBD	THC	H_2O_2+DMSO	CBD	THC
Shape and size of the cell	Elongated, small	Elongated, small	Elongated, small	Enlarged, flattened, irregular	Enlarged, flattened	Enlarged, flattened
Nuclear circularity (roundness)	↔	↑	↓	↓	↔	↔
β-Gal level	↓	↔	↑	↑	↓	↓
BID	↔↓	↔↓	↔↓	↔↓	↔	↔
CB1	↔	↔	↔	↔	↔	↔
CB2	↓	↔	↔↑	↑	↔↓	↔↓
CDK2	↑	↔↓	↔↓	↔↓	↔↑	↔↑
c-Jun	↔	↓	↔↓	↓	↔	↔
Collagen (type I)	↔↓	↔	↑	↓	↔	↓
Collagen (type III)	↓	↔	↔	↓	↔	↔
Cyclin D1	↔↓	↔↓	↔↓	↔	↔↑	↔↑
EGFR	↓	↔↑	↔↑	↓	↓	↓
Elastin	↔↓	↔↑	↔	↔↑	↔	↔↓

Hyaluronan	↔	↑	↑	↔	↔	↔
MMP 2	↔	↑	↑	↓	↓	↓
MKI67	↔	↔↑	↑	↔↓	↑	↔
NF-kB	↔↑	↓	↔	↔↓	↔	↔
P16	↔↑	↔	↓	↔↑	↔	↔
P21	↑	↓	↓	↑	↔	↔
P53	↔↑	↔↓	↔↓	↔	↔↑	↔
SIRT 1	↑	↔	↔	↓	↔	↓
SIRT 3, 4	↔	↔↑	↔↑	↔	↔	↔
SIRT 6	↔	↔↑	↔↑	↔↓	↔	↔↓
TIMP 1	↔	↔↑	↔↑	↔↓	↔	↔
Vinculin	↔	↓	↔↓	↓	↔↑	↔
Cell viability	↔	↔	↔	↓	↑	↑
Wound healing	↔	↔	↔	↓	↑	↑

↓, Decreased/low; ↑, Increased/high; ↔, no change detected; ↔↓, tendency to decrease; ↔↑, tendency to increase.

The results of morphological analysis of senescent fibroblasts treated with pCBs demonstrate preservation of typical features and architecture of the healthy cells. Structural deviations in prematurely aged groups exposed to THC and CBD were associated with slight deformations, increased transparency, accompanied by quantitative reduction (Figure 3. 4). No significant changes were observed in the pCBs-treated healthy fibroblasts. Merve and colleagues (2022) also reported no changes in cardiomyocyte morphology or viability in response to THC in the low doses (100 ng/ml), whereas treatment with primary THC metabolites 11-hydroxy-D9-THC (THC-OH) and 11-nor-9-carboxy-D9-tetrahydrocannabinol (THC-COOH) in higher doses (250–100 ng/mL) resulted in increased cell death and significant deterioration in cellular architecture (Merve et al., 2022). Recent studies have shown that cannabinoids affect the actin cytoskeleton and other components involved in cellular motility, proliferation, and many biological

functions in glioblastoma cell lines (Hohmann et al., 2019; Tahir et al., 1991). Moreover, a cannabinoid-induced reduction in cell growth and a delay in cell division has been observed in protozoan *Tetrahymena pyriformis* following THC (3.2-24 µM) exposure (McClean & Zimmerman, 1976). This data aligns with our findings that 7.5 µM and higher concentrations of THC and CBD exert cytotoxic effects on the healthy dermal fibroblasts.

Analysis of nuclear changes showed a reduction in altered nuclei architecture followed pCBs treatment. Almost identical nuclear architecture was exhibited in healthy dermal fibroblasts treated with both CBs (Figure 3.8, I-N). Parameters of the nuclear area after CBD application were normalized by day 5 of the experiment (Figure 3.8, Q-R). At the same time, aged nuclei were predominantly elongated with irregular shape and increased area (Figure 3.8, C, D). Senescent cells treated with THC and CBD exhibited a reduction in circularity (Figure 3.8, S-T), accompanied by a reduced number of gigantic or minuscule irregular nuclei (Figure 3.8, K-P). Interestingly, THC tests on microbial (i.e., *Salmonella typhimurium* strains TA 98 and TA 100) and eukaryotic *in vitro* test systems (i.e., fibroblasts from healthy individuals and DNA repair-deficient *Xeroderma pigmentosum* patients) displayed similar survival activity without indication of elevation in the number of chromosome breaks or chromatid exchanges following exposure to THC or THC plus S9 microsomal fraction. Furthermore, it was reported that THC, 11-OHΔ9-THC, cannabinol, and cannabidiol did not induce unscheduled DNA repair synthesis in cultured human fibroblasts and did not suppress UV-induced DNA repair synthesis (Zimmerman et al., 1978).

To elucidate the underlying mechanisms involved in the aging process and identify potential targets for pCBs, the expression of genes involved in the cell-cycle regulation,

ECM maintenance, and metabolic response of senescent cells was compared with that of young cells followed THC and CBD application. We observed a cannabinoid-induced reduction in main cellular senescence biomarkers like β-galactosidase, p16, and p21 in naturally aged fibroblasts and SIPS (Figure 3.10). Besides, a mild elevation in the *CDKN2A* and *CDKN1A* expression was detected in senescent cells. In parallel, we noticed that expression of p16 and p21 tended to decrease in healthy cells after pCBs application, while *CDKN2A* and *CDKN1A* expressions were not changed (Figure 3.11). Concomitantly, p53 levels were slightly reduced in healthy and senescent CBD and THC treated groups, while *TP53* expression was highly increased in aged cells followed CBD ($p<0.0001$) application (Table 3.2). This correlates with previous reports describing the effects of CBD and THC upon the treatment of aged pancreatic islets cells; reduced β-Gal activity and decrease in expression of p53, p38, p21 with a consequent significant ROS decline were found (Baeeri et al., 2020). Senescent activation is not solely dependent on p53, p21, or p16, suggesting the presence of separate, independent regulatory networks in the aging process (Ngoi et al., 2021). It was earlier stated that decline in the cyclin D1- and cyclin-dependent kinases (CDKs) resulted in inefficient G1-to-S-phase progression. Meanwhile, c-Jun is also required for progression through the G1 phase of the cell cycle and directly affects transcriptional control of the cyclin D1 (Wisdom et al., 1999). Besides, c-Jun acts as a negative regulator of *p53* and *p21* expressions and establish a mechanistic link between c-Jun-dependent mitogenic signaling and cell-cycle regulation (Schreiber et al., 1999). Our experiments showed inhibition of c-Jun and CDK2 in the senescent cells as compared to healthy cells, while after pCBs treatment, both slightly increased ($p>0.05$). At the same time, Cyclin D1 was elevated in SIPS fibroblasts with the tendency to rise followed by THC and CBD exposure. This may explain preserved fibroblasts' viability

supported by MTT, NR, and CV assays, and maintenance of functional and proliferative activity (upregulated *MKI67*) in groups exposed to the THC and CBD treatments.

The main functional activity of fibroblasts is to produce and maintain ECM such as collagen, elastin, and hyaluronan. With age, their functional capacity declines leading to the appearance of wrinkles, sagging, and dull skin (Gerasymchuk et al., 2020). One of the key features of senescent cells is a phenotypic change into a secretory state represented by the release of various inflammatory cytokines, growth factors, enzymes, and ECM proteins known as the senescence-associated secretory phenotype (SASP). To that end, numerous pathways have been shown to regulate SASP: NF-κB, mammalian target of rapamycin (mTOR), p38, mitogen-activated protein kinase (MAPK), sirtuin 3/5 (SIRT3/5), transforming growth factor-beta (TGF-β), H2A histone family member X (γH2AX), ATM induced in response to DNA damage response (DDR), macroH2A1 histone variants, janus kinases 1/2 (JAK1/2), IL-1α, etc. (Birch & Gil, 2020; Guarente, 2011; Turan & Oktay, 2019; Vaziri et al., 1997). Almost all of these signaling pathways converge at NF-κB, which in turn modulates numerous genes associated with cell survival, proliferation, and differentiation (Liu et al., 2017; Ngoi et al., 2021; Yo & Rünger, 2018). We determined moderately upregulated ($p>0.05$) expression of *NF-κB* in healthy fibroblasts treated with CBD and THC (Figures 3.14, K and Suppl. Figure 15, J respectively) that was partially validated by Western blot analysis (Figure 3.14, I). Simultaneously, *NF-κB* was mildly ($p>0.05$) downregulated in senescent fibroblasts exposed to pCBs (Figure 3.14, L and Suppl. Figure 15, J, respectively) and which was in line with Western blot data (Figure 3.14, J). Recent reviews stated that activation of NF-κB transcription factor is vital for host defense through innate or adaptive immune system

activation. As soon as a harmful agent is eradicated, NF-κB signaling needs to be downregulated to maintain tissue homeostasis required to prevent inflammation, autoimmune disease, and oncogenesis (Liu et al., 2017; Ruland, 2011).

Based on numerous literature and research data, another critical component in cell wellbeing is metabolic regulation, which was altered in senescent fibroblasts (Chapter 2). One of the potent metabolic regulators is the family of nicotinamide dinucleotide (NAD+)-dependent protein deacetylases termed sirtuins (Guarente, 2011). Sirtuins are involved in the regulation of DNA repair, glucose output, insulin sensitivity, fatty acid oxidation, fat differentiation, neurogenesis, inflammation, and aging. In our research, we focused on changes in the expression of *SIRT1*, *SIRT3*, *SIRT4*, and *SIRT6*, which are in mitochondria and nuclei and tightly associated with maintaining cellular homeostasis and reversing some aspects of aging (Lee et al., 2019). Thus, SIRT1 is known to deacetylate transcription factors contributing to cellular regulation (reaction to stressors, longevity). Nuclear SIRT1 and SIRT6 regulate cellular responses to energy demands in most tissues through the activity of key transcription factors and cofactors, whereas mitochondrial sirtuins, SIRT3, SIRT4, and SIRT5, control the functioning of mitochondrial enzymes in response to fasting and calorie restriction (Bonkowski & Sinclair, 2016). It's worth noting that SIRT4 and SIRT7 repress fatty acids oxidation, insulin secretion, and mitochondrial biogenesis, increasing lipogenesis and liver lipids accumulation. On the contrary, SIRT2, SIRT3, and SIRT6 are positive regulators (Song et al., 2018).

We observed no changes in *SIRT1* expression in the pCBs treatments in healthy BJ-5ta fibroblasts (Figure 3.14, G), while in CCD-1064Sk fibroblasts, THC induced elevation of *SIRT1* ($p<0.05$, Suppl. Figure 15, M). The latter was validated by Western blot data,

where increased levels of SIRT1 after THC application in healthy cells were found ($p<0.05$, Figure 3.14, C). In cultured cells, embryonic and neonatal tissues, SIRT1 was demonstrated to deacetylate and thereby deactivate the p53 protein, stimulating autophagy by preventing acetylation of proteins and thereby reducing the risk of age-related diseases (Baur, 2010; Yessenkyzy et al., 2020). Unfortunately, pCBs were ineffective in senescent groups. THC decreased SIRT1 protein levels in BJ-5ta prematurely aged fibroblasts ($p<0.05$, Figure 3.14, D). CBD and THC tended to downregulate *SIRT1* gene expression in BJ-5ta and CCD-1064Sk senescent fibroblast cultures (Figures 3.14, H, and Suppl. Figure 15, M, respectively). We can speculate that pCBs efficacy depends on the cell type or tissue and the expression of cannabinoid receptors or perhaps the expression of enzymes metabolizing cannabinoids. For instance, CBD was shown to induce SH-SY5Y human neuroblastoma cell line autophagy to protect cells from mitochondrial dysfunction by upregulating SIRT1 via inhibition of NF-κB and NOTCH pathways and therefore was considered as a protector in Parkinson's disease (Pengyue et al., 2021). Moreover, activation of CB2 receptors promotes fatty acid oxidation through the stimulation of SIRT1 deacetylase activity by augmenting the phosphorylation of cAMP response element-binding protein (CREB), thereby leading to elevated levels of PGC-1α deacetylation in C2C12 skeletal muscle cells (Zheng et al., 2013). However, CB2 was also tended to be downregulated following pCBs treatments (Figure 3.15, D).

The expression of other mitochondrial (*SIRT3*, *SIRT4*) and nuclear (*SIRT6*) sirtuins in healthy fibroblasts was upregulated by THC and CBD ($p>0.05$, Suppl. Figure 15, N-P), whereas the expression of a negative regulator of lipid metabolism *SIRT4* following pCBs exposure was unchanged (Figure 3.15, A). These findings may provide therapeutic

possibilities to prevent metabolic diseases associated with lipid dysregulation in the potential risk groups for diabetes and cardiovascular pathology. In the case of the senescent cells, *SIRT3*, *SIRT4*, and *SIRT6* transcripts were moderately downregulated, while CBD showed a slight tendency to increase *SIRT6* expression in CCD-1064Sk fibroblasts ($p>0.05$, Suppl. Figure 15, M-P). In contrast, THC tended to upregulate *SIRT4* expression in the BJ-5ta cell line, while CBD downregulated it ($p>0.05$, Figure 3.15, B).

Previous work shows that SIRT4 is upregulated in various cell lines following senescence and increases with age (Betsinger & Cristea, 2019). Also, SIRT4 transcript levels were decreased in old mouse spermatogonia stem cells after treatment with the lifespan-enhancing drug rapamycin (Kofman et al., 2013). In normal human epidermal keratinocytes, SIRT4 was expressed inversely to SIRT3, and they both followed a temporal cycle of expression, whereas after UVB and H_2O_2 exposure, *SIRT4* and *SIRT3* mRNA levels both increased, and the temporal cycle of expression was lost (Dong et al., 2012). In human dermal fibroblasts undergoing replicative or stress-induced senescence triggered by UVB or γ-irradiation, *SIRT4* mRNA and protein levels were also increased (Lang et al., 2016). Furthermore, SIRT4 has been shown to prevent the binding of manganese superoxide dismutase, leading to elevated ROS accumulation following UV damage that could contribute to aging-related phenotypes by promoting increased ROS generation (Luo et al., 2017).

As a first step to study the potential role of phytocannabinoids in the rejuvenation properties of collagen restoration, elastin, and hyaluronic acid production in senescent fibroblasts, we tested mRNA transcripts and protein levels of main ECM components and used WHA (Table 3.2).

In healthy fibroblasts of both cell lines, THC to a greater degree upregulated *COL1A1* expression ($p<0.01$, Suppl. Figure 15, A and $p>0.05$, Figure 3.13, E). COL1A1 protein level also increased in response to THC (Figure 3.13, A), while CBD showed no effect on protein generation. Concomitantly, type III collagen production was not significantly affected by pCBs exposure ($p>0.05$, Figure 3.13, C), while THC elevated mRNA transcripts in healthy fibroblasts ($p<0.01$, Figure 3.13, G and $p<0.05$, Suppl. Figure 15, B). A recent study reported no effect of 1% CBD topical application on the mice's skin mRNA expression levels of *Col1a1*, *Col1a2*, hyaluronic acid degrading enzyme, *Has2*, loricrin, filaggrin ceramide degrading enzyme, and ceramide synthase except a significant increase in dermal water presented by cutaneous aquaporin 3 (Ikarashi et al., 2021). Another study reported decreased collagen deposition by CB2 receptor-selective agonist, GP1α, accompanied by reduced levels of TGF-β1 and its receptor TβRI and phosphorylated small mothers against decapentaplegic homolog 3 (P-Smad3), but increased the expression of its inhibitor, Smad7 during skin wound repair in the mouse (S. S. Li et al., 2016). In addition, the expression of crucial ECM proteins α-SMA and collagen was found to be up-regulated in response to primary THC metabolites THC-OH and THC-COOH treatments with simultaneous modulation of PI3K and MAPK signaling in cardiomyocytes (Merve et al., 2022).

As expected, collagen expression in prematurely aged dermal fibroblasts compared to healthy ones was reduced regardless of treatment (Figure 3.13, B, D). Despite this, it was noted that CBD tended to increase *COL1A1* expression levels, while THC was more effective on *COL3A1* ($p>0.05$, Figure 3.13 F, H, respectively). Analogous trends in collagen expression were detected in both prematurely aged skin fibroblasts cultures.

These findings agree with the available literature (Lago & Puzzi, 2019), confirming the downregulation of *COL1A1*, *COL3A1*, *TIMP1* in senescent HDFs.

In BJ-5ta fibroblasts, elastin levels in healthy and senescent groups were not significantly altered, except THC-induced suppression of *ELN* expression in SIPS-fibroblasts ($p<0.05$, Figure 3.13, L). In contrast, in the healthy CCD-1064Sk, THC stimulated *ELN* expression stronger ($p<0.0001$) than CBD ($p<0.05$) (Suppl. Figure 15, C). However, pCBs did not significantly affect *ELN* mRNA transcripts in prematurely aged fibroblasts (Suppl. Figure 15, C). At the same time, healthy fibroblasts exerted pCBs-stimulated upregulation of *TIMP1* ($p>0.05$) and *HAS1* ($p<0.01$), albeit they were downregulated in all senescent cells regardless of treatment (Suppl. Figure 15, L and D, respectively). Interestingly, HDF from elderly donors were different from the HDF from the replicative senescence model in the expression of only 3 genes (*LMNA*, *TIMP1*, *TIMP2*) (Lago & Puzzi, 2019). Hence, other aging study models might reveal variations in gene expression that explain discrepancies in the observed results. Surprisingly, *MMP2*, responsible for ECM breakdown, was significantly upregulated in response to THC treatment in the healthy cells and downregulated in the entire senescent group despite treatment (Suppl. Figure 15, H). We suggest that such changes might be related to the excessive degradation of the ECM environment based on the excessive generation of ROS in response to the H_2O_2 induction followed by depletion in the metabolic maintenance and dissociation of other regulatory mechanisms.

We then compared pCBs effect on wound healing. Interestingly, after 24 h of experiment in the H_2O_2-induced senescent group, visual wound enlargement in both CCD-1064Sk and BJ-5ta cell lines was found (Figures 3.16, C, and G, respectively). This might be related to the diminished adhesive protein vinculin levels and explained by increased

cellular detachment resulting in levered adhesive forces potentiated by injury (i.e., scratch). In contrast, pCBs expressed stimulatory effects toward fibroblasts' ability to close the damaged zone in different skin cell lines, which is in line with upregulation of the proliferative biomarkers (i.e., *MKI67*) in senescent cells in the CBD group ($p<0.05$, Suppl. Figure 15, I). Moreover, a pro-apoptotic BID protein tended to decline in healthy fibroblasts after pCBs treatment, primarily CBD ($p>0.05$, Figure 3.11, G), while in H_2O_2-exposed dermal fibroblasts were not detected significant deviations in BID expression levels (Figure 3.11, H).

Recently, THC was reported to promote wound healing by inducing periodontal fibroblast cell adhesion and migration in a CB2-dependent manner via activation of focal adhesion kinase and its modulation of MAPK activities (Liu et al., 2019). The authors showed that the effect of cannabinoids on periodontal fibroblast cell adhesion and migration was mainly dependent on the CB2. However, the results of our investigation showed that *CB2* was downregulated in healthy and senescent fibroblasts after pCBs treatment ($p>0.05$, Figure 3.15, C-D) and almost unchanged CB1 and CB2 protein levels (Figure 3.15, E-H).

Thus, the data gathered here are not sufficient to definitively answer whether cannabinoids have anti-aging properties; however, cannabinoids may still be useful as they can partially reduce senescent-associated morphological changes (e.g., structural prevention changes of nuclei and scaffolding proteins of ECM such as collagen and elastin, regulation of cell cycle, and conserving cellular functions).

The key findings of our study are: (i) there are a certain dose range of phytocannabinoids (2 μM – 5 μM) that has a protective effect in the SIPS model on dermal fibroblasts; (ii) pCBs stimulated fibroblasts' ability to close the damaged area in different

skin cell lines via upregulation of the proliferative biomarkers, and (iii) overall pCBs reduced morphological alterations in skin cells, potentiated cellular viability via preserving cell-cycle regulators, and boosted ECM production by metabolic maintenance. Our data help fill knowledge gaps regarding the potential role of THC/CBD in the regulation of cell proliferation.

3.6. REFERENCES

Adusumilli Nagasai C, & Friedman Adam J. (2021). An updated therapeutic strategy for chronic idiopathic urticaria. *Journal of Drugs in Drmatology*, *20*(3), 354–355. https://doi.org/10.36849/JDD.0421

Ardigò, M., Franceschini, C., Campione, E., Cosio, T., Lanna, C., Bianchi, L., & Milani, M. (2020). Efficacy of a topical product containing purified omental lipids and three anti-itching compounds in the treatment of chronic pruritus/ prurigo nodularis in elderly subjects: A prospective, assessor-blinded, 4-week trial with transepidermal water loss and optical coherence tomography assessments. *Clinical, Cosmetic and Investigational Dermatology*, *13*, 1051–1058. https://doi.org/10.2147/CCID.S292636

Armstrong, J. L., Hill, D. S., McKee, C. S., Hernandez-Tiedra, S., Lorente, M., Lopez-Valero, I., Anagnostou, M. E., Babatunde, F., Corazzari, M., Redfern, C. P. F., Velasco, G., & Lovat, P. E. (2015). Exploiting cannabinoid-induced cytotoxic autophagy to drive melanoma cell death. *Journal of Investigative Dermatology*, *135*(6), 1629–1637. https://doi.org/10.1038/jid.2015.45

Baeeri, M., Rahimifard, M., Daghighi, S. M., Khan, F., Salami, S. A., Moini-Nodeh, S., Haghi-Aminjan, H., Bayrami, Z., Rezaee, F., & Abdollahi, M. (2020). Cannabinoids as anti-ROS in aged pancreatic islet cells. *Life Sciences*, *256*, 117969. https://doi.org/10.1016/j.lfs.2020.117969

Baron, E. P. (2018). Medicinal properties of cannabinoids, terpenes, and flavonoids in cannabis, and benefits in migraine, headache, and pain: an update on current evidence and cannabis science. *Headache*, *58*(7), 1139–1186. https://doi.org/10.1111/head.13345

Baur, J. A. (2010). Biochemical effects of SIRT1 activators. *Biochimica et Biophysica Acta - Proteins and Proteomics*, *1804*(8), 1626–1634. https://doi.org/10.1016/j.bbapap.2009.10.025

ben Amar, M. (2006). Cannabinoids in medicine: A review of their therapeutic potential. *Journal of Ethnopharmacology*, *105*(1–2), 1–25. https://doi.org/10.1016/j.jep.2006.02.001

Betsinger, C. N., & Cristea, I. M. (2019). Mitochondrial function, metabolic regulation, and human disease viewed through the prism of Sirtuin 4 (SIRT4) functions. *Journal of Proteome Research*, *18*(5), 1929–1938. American Chemical Society. https://doi.org/10.1021/acs.jproteome.9b00086

Birch, J., & Gil, J. (2020). Senescence and the SASP: many therapeutic avenues. *Genes & Development*, *34*, 1565–1576. https://doi.org/10.1101/gad.343129

Bíró, T., Tóth, B. I., Haskó, G., Paus, R., & Pacher, P. (2009). The endocannabinoid system of the skin in health and disease: novel perspectives and therapeutic opportunities. *Trends in Pharmacological Sciences*, *30*(8), 411–420. https://doi.org/10.1016/j.tips.2009.05.004

Bonkowski, M. S., & Sinclair, D. A. (2016). Slowing ageing by design: The rise of NAD+ and sirtuin-activating compounds. *Nature Reviews Molecular Cell Biology*, *17*(11), 679–690. Nature Publishing Group. https://doi.org/10.1038/nrm.2016.93

Chalmers S., G. S. D. A. D. J. A. F. J. F. C. P. (2018). Topical endocannabinoid administration protects MRL-Lpr/Lpr mice from cutaneous lupus erythematosus. *[Abstract]. Arthritis Rheumatol. 2018; 70* (Suppl 10). https://acrabstracts.org/abstract/topical-endocannabinoid-administration-protects-mrl-lpr-lpr-mice-from-cutaneous-lupus-erythematosus/

Chelliah, M. P., Zinn, Z., Khuu, P., & Teng, J. M. C. (2018). Self-initiated use of topical cannabidiol oil for epidermolysis bullosa. *Pediatric Dermatology*, *35*(4), e224–e227. https://doi.org/10.1111/pde.13545

Cocchiara E., Spinella A., Magnani L., Lumetti Federica, Palermo A., Baiocchi G., Salvarani C., & Giuggioli D. (2019). AB0645 Cannabinoids in the treatment of pain related to systemic sclerosis skin ulcers: our experience. *Annals of the Rheumatic Diseases, 78*, 1784. https://doi.org/10.1136/annrheumdis-2019-eular.6609

Dhadwal, G., & Kirchhof, M. G. (2018). The risks and benefits of cannabis in the dermatology clinic. *Journal of Cutaneous Medicine and Surgery*, *22*(2), 194–199. https://doi.org/10.1177/1203475417738971

Dimri, G. P., Leet, X., Basile, G., Acosta, M., Scorrt, G., Roskelley, C., Medrano, E. E., Linskensi, M., Rubeljii, I., Pereira-Smithii, O., Peacocket, M., Campisi, J., & Pardee, B. (1995). A biomarker that identifies senescent human cells in culture and in aging skin in vivo. *Cell Biology, 92*, 9363–9367.

Dong, K., Pelle, E., Yarosh, D. B., & Pernodet, N. (2012). Sirtuin 4 identification in normal human epidermal keratinocytes and its relation to sirtuin 3 and energy metabolism under normal conditions and UVB-induced stress. *Experimental Dermatology*, *21*(3), 231–233. https://doi.org/10.1111/j.1600-0625.2011.01439.x

Eagelston, L. R. M., Yazd, N. K. K., Patel, R. R., Flaten, H. K., Dunnick, C. A., & Dellavalle, R. P. (2018). Cannabinoids in dermatology: A scoping review. *Dermatology Online Journal*, *24*(6), 13030. Dermatology Online Journal. https://doi.org/10.5070/d3246040706

Eberlein, B., Eicke, C., Reinhardt, H. W., & Ring, J. (2008). Adjuvant treatment of atopic eczema: Assessment of an emollient containing N-palmitoylethanolamine (ATOPA study). *Journal of the European Academy of Dermatology and Venereology*, *22*(1), 73–82. https://doi.org/10.1111/j.1468-3083.2007.02351.x

Friedman, A. J., Momeni, K., & Kogan, M. (2020). Topical cannabinoids for the management of *Psoriasis Vulgaris*: Report of a case and review of the literature. *Journal of Drugs in Dermatology, 19*(8), 795. https://doi.org/10.36849/JDD.2020.5229

Gęgotek, A., Atalay, S., Rogowska-Wrzesińska, A., & Skrzydlewska, E. (2021). The effect of cannabidiol on UV-induced changes in intracellular signaling of 3D-cultured skin keratinocytes. *International Journal of Molecular Sciences, 22*(3), 1–17. https://doi.org/10.3390/ijms22031501

Gerasymchuk, M., Cherkasova, V., Kovalchuk, O., & Kovalchuk, I. (2020). The role of microRNAs in organismal and skin aging. *International Journal of Molecular Sciences, 21*(15), 5281. https://doi.org/10.3390/ijms21155281

Grant, J. E., Odlaug, B. L., Chamberlain, S. R., & Kim, S. W. (2011). Dronabinol, a cannabinoid agonist, reduces hair pulling in trichotillomania: A pilot study. *Psychopharmacology, 218*(3), 493–502. https://doi.org/10.1007/s00213-011-2347-8

Guarente, L. (2011). Sirtuins, aging, and medicine. *The New England Journal of Medicine, 364*, 2235–2244. https://doi.org/10.1101/sqb.2011.76.010629

Guzmán, M. (2003). Cannabinoids: Potential anticancer agents. *Nature Reviews Cancer, 3*(10), 745–755. European Association for Cardio-Thoracic Surgery. https://doi.org/10.1038/nrc1188

Hampson, A. J., Grimaldi, M., Axelrod, J., & Wink, D. (1998). Cannabidiol and (-) delta9-tetrahydrocannabinol are neuroprotective antioxidants. *Medical Sciences, 95*(14), 8268–8273. https://doi.org/10.1073/pnas.95.14.8268.

Hohmann, T., Feese, K., Ghadban, C., Dehghani, F., & Grabiec, U. (2019). On the influence of cannabinoids on cell morphology and motility of glioblastoma cells. *PLoS ONE, 14*(2), e0212037. https://doi.org/10.1371/journal.pone.0212037

Husni, A. S., McCurdy, C. R., Radwan, M. M., Ahmed, S. A., Slade, D., Ross, S. A., Elsohly, M. A., & Cutler, S. J. (2014). Evaluation of phytocannabinoids from high-potency Cannabis sativa using in vitro bioassays to determine structure-activity relationships for cannabinoid receptor 1 and cannabinoid receptor 2. *Medicinal Chemistry Research, 23*(9), 4295–4300. https://doi.org/10.1007/s00044-014-0972-6

Ikarashi, N., Shiseki, M., Yoshida, R., Tabata, K., Kimura, R., Watanabe, T., Kon, R., Sakai, H., & Kamei, J. (2021). Cannabidiol application increases cutaneous aquaporin-3 and exerts a skin moisturizing effect. *Pharmaceuticals, 14*(9), 879. https://doi.org/10.3390/ph14090879

Izzo, A. A., & Camilleri, M. (2008). Emerging role of cannabinoids in gastrointestinal and liver diseases: Basic and clinical aspects. *Gut, 57*(8), 1140–1155. https://doi.org/10.1136/gut.2008.148791

Karsak, M., Gaffal, E., Date, R., Wang-Eckhardt, L., Rehnelt, J., Petrosino, S., Starowicz, K., Steuder, R., Schlicker, E., Cravatt, B., Mechoulam, R., Buettner, R., Werner, S., di Marzo, V., Tüting, T., & Zimmer, A. (2007). Attenuation of allergic contact dermatitis through the endocannabinoid system. *Science, 316*(5830), 1494–1497. https://doi.org/10.1126/science.1142265

Kofman, A. E., Huszar, J. M., & Payne, C. J. (2013). Transcriptional analysis of histone deacetylase family members reveal similarities between differentiating and aging spermatogonial stem cells. *Stem Cell Reviews and Reports*, *9*(1), 59–64. https://doi.org/10.1007/s12015-012-9392-5

Kozela, E., Juknat, A., Kaushansky, N., Rimmerman, N., Ben-Nun, A., & Vogel, Z. (2013). Cannabinoids decrease the Th17 inflammatory autoimmune phenotype. *Journal of Neuroimmune Pharmacology*, *8*(5), 1265–1276. https://doi.org/10.1007/s11481-013-9493-1

Lago, J. C., & Puzzi, M. B. (2019). The effect of aging in primary human dermal fibroblasts. *PLoS ONE*, *14*(7), e0219165. https://doi.org/10.1371/journal.pone.0219165

Lang, A., Grether-Beck, S., Singh, M., Kuck, F., Jakob, S., Kefalas, A., Altinoluk-Hambüchen, S., Graffmann, N., Schneider, M., Lindecke, A., Brenden, H., Felsner, I., Ezzahoini, H., Marini, A., Weinhold, S., Vierkötter, A., Tigges, J., Schmidt, S., Stühler, K., … Piekorz, R. P. (2016). MicroRNA-15b regulates mitochondrial ROS production and the senescence-associated secretory phenotype through sirtuin 4/SIRT4. *Aging*, *8*(3), 484–505. www.impactaging.com

Lee, S. H., Lee, J. H., Lee, H. Y., & Min, K. J. (2019). Sirtuin signaling in cellular senescence and aging. *BMB Reports*, *52*(1), 24–34. The Biochemical Society of the Republic of Korea. https://doi.org/10.5483/BMBRep.2019.52.1.290

Li, H.-L. (1974). An archaeological and historical account of cannabis in China. *Economic Botany*, *28*, 437–448.

Li, S. S., Wang, L. L., Liu, M., Jiang, S. K., Zhang, M., Tian, Z. L., Wang, M., Li, J. Y., Zhao, R., & Guan, D. W. (2016). Cannabinoid CB2 receptors are involved in the regulation of fibrogenesis during skin wound repair in mice. *Molecular Medicine Reports*, *13*(4), 3441–3450. https://doi.org/10.3892/mmr.2016.4961

Lim, M., & Kirchhof, M. (2018). Dermatology-related uses of medical cannabis promoted by dispensaries in Canada, Europe, and the United States. *Journal of Cutaneous Medicine and Surgery*, *23*(2), 178–184. https://doi.org/10.1177/1203475418808761

Liszewski, W., & Farah, R. S. (2017). The role of cannabinoids in dermatology". *Journal of the American Academy of Dermatology*, *77*(3), e87–e88. https://doi.org/10.1016/j.jaad.2017.05.023

Liu, C., Qi, X., Alhabeil, J., Lu, H., & Zhou, Z. (2019). Activation of cannabinoid receptors promote periodontal cell adhesion and migration. *Journal of Clinical Periodontology*, *46*(12), 1264–1272. https://doi.org/10.1111/jcpe.13190

Liu, T., Zhang, L., Joo, D., & Sun, S. C. (2017). NF-κB signaling in inflammation. *Signal Transduction and Targeted Therapy*, *2*, e17023. https://doi.org/10.1038/sigtrans.2017.23

Luca, T., di Benedetto, G., Scuderi, M. R., Palumbo, M., Clementi, S., Bernardini, R., & Cantarella, G. (2009). The CB1/CB2 receptor agonist WIN-55,212-2 reduces viability of human Kaposi's sarcoma cells in vitro. *European Journal of Pharmacology*, *616*(1–3), 16–21. https://doi.org/10.1016/j.ejphar.2009.06.004

Luo, Y. X., Tang, X., An, X. Z., Xie, X. M., Chen, X. F., Zhao, X., Hao, D. L., Chen, H. Z., & Liu, D. P. (2017). SIRT4 accelerates Ang II-induced pathological cardiac hypertrophy by inhibiting manganese superoxide dismutase activity. *European Heart Journal*, *38*(18), 1389–1398. https://doi.org/10.1093/eurheartj/ehw138

MacCallum, C. A., & Russo, E. B. (2018). Practical considerations in medical cannabis administration and dosing. *European Journal of Internal Medicine*, *49*(October 2017), 12–19. https://doi.org/10.1016/j.ejim.2018.01.004

Maghfour, J., Rundle, C. W., Rietcheck, H. R., Dercon, S., Lio, P., Mamo, A., Runion, T. M., Fernandez, J., Kahn, J., Dellavalle, R. P., & Yardley, H. (2021). Assessing the effects of topical cannabidiol in patients with atopic dermatitis. *Dermatology Online Journal*, *27* (2), 15. https://doi.org/10.5070/d3272052393

Maida, V., & Corban, J. (2017). Topical medical cannabis: A new treatment for wound pain—three cases of *Pyoderma Gangrenosum*. *Journal of Pain and Symptom Management*, *54*(5), 732–736. https://doi.org/10.1016/j.jpainsymman.2017.06.005

Maida, V., Shi, R. B., Fazzari, F. G. T., & Zomparelli, L. (2020). Promoting wound healing of uremic calciphylaxis leg ulcers using topical cannabis-based medicines. *Dermatologic Therapy*, *33*(6), e14419. Blackwell Publishing Inc. https://doi.org/10.1111/dth.14419

Massi, P., Solinas, M., Cinquina, V., & Parolaro, D. (2013). Cannabidiol as potential anticancer drug. *British Journal of Clinical Pharmacology*, *75*(2), 303–312. https://doi.org/10.1111/j.1365-2125.2012.04298.x

McClean Daniel, & Zimmerman M. Arthur. (1976). Action of Δ9-tetrahydrocannabinol on cell division and macromolecular synthesis in division-synchronized protozoa. *Pharmacology*, *14*, 307–321.

Merve, A. O., Sobiecka, P., Remeškevičius, V., Taylor, L., Saskoy, L., Lawton, S., Jones, B. P., Elwakeel, A., Mackenzie, F. E., Polycarpou, E., Bennett, J., & Rooney, B. (2022). Metabolites of Cannabis induce cardiac toxicity and morphological alterations in cardiac myocytes. *International Journal of Molecular Sciences*, *23*(3), 1401. https://doi.org/10.3390/ijms23031401

Neff, G. W., O'brien, C. B., Reddy, K. R., Bergasa, N. v, Regev, A., Molina, E., Amaro, R., Rodriguez, M. J., Chase, V., Jeffers, L., & Schiff, E. (2002). Preliminary observation with Dronabinol in patients with intractable pruritus secondary to cholestatic liver disease. *The American Journal of Gastroenterology*, *97*(8), 2117–2119. https://doi.org/10.1111/j.1572-0241.2002.05852.x.

Ngoi, N. Y., Liew, A. Q., Chong, S. J. F., Davids, M. S., Clement, M. V., & Pervaiz, S. (2021). The redox-senescence axis and its therapeutic targeting. *Redox Biology*, *45*, 102032. Elsevier B.V. https://doi.org/10.1016/j.redox.2021.102032

Oláh, A., Ambrus, L., Nicolussi, S., Gertsch, J., Tubak, V., Kemény, L., Soeberdt, M., Abels, C., & Bíró, T. (2016). Inhibition of fatty acid amide hydrolase exerts cutaneous anti-inflammatory effects both *in vitro* and *in vivo*. *Experimental Dermatology*, *25*(4), 328–330. Blackwell Publishing Ltd. https://doi.org/10.1111/exd.12930

Oláh, A., Markovics, A., Szabó-Papp, J., Szabó, P. T., Stott, C., Zouboulis, C. C., & Bíró, T. (2016). Differential effectiveness of selected non-psychotropic phytocannabinoids on human sebocyte functions implicates their introduction in dry/seborrhoeic skin and acne treatment. *Experimental Dermatology*, *25*(9), 701–707. https://doi.org/10.1111/exd.13042

Oláh, A., Szabó-Papp, J., Soeberdt, M., Knie, U., Dähnhardt-Pfeiffer, S., Abels, C., & Bíró, T. (2017). Echinacea purpurea-derived alkylamides exhibit potent anti-inflammatory effects and alleviate clinical symptoms of atopic eczema. *Journal of Dermatological Science*, *88*(1), 67–77. https://doi.org/10.1016/j.jdermsci.2017.05.015

Oláh, A., Tóth, B. I., Borbíró, I., Sugawara, K., Szöllõsi, A. G., Czifra, G., Pál, B., Ambrus, L., Kloepper, J., Camera, E., Ludovici, M., Picardo, M., Voets, T., Zouboulis, C. C., Paus, R., & Bíró, T. (2014). Cannabidiol exerts sebostatic and anti-inflammatory effects on human sebocytes. *Journal of Clinical Investigation*, *124*(9), 3713–3724. https://doi.org/10.1172/JCI64628

Pacher, P., & Haskó, G. (2008). Endocannabinoids and cannabinoid receptors in ischaemia-reperfusion injury and preconditioning. *British Journal of Pharmacology*, *153*(2), 252–262. https://doi.org/10.1038/sj.bjp.0707582

Pacher, P., Mukhopadhyay, P., Mohanraj, R., Godlewski, G., Bátkai, S., & Kunos, G. (2008). Modulation of the endocannabinoid system in cardiovascular disease: Therapeutic potential and limitations. *Hypertension*, *52*(4), 601–607. https://doi.org/10.1161/HYPERTENSIONAHA.105.063651

Pellati, F., Borgonetti, V., Brighenti, V., Biagi, M., Benvenuti, S., & Corsi, L. (2018). *Cannabis sativa L.* and nonpsychoactive cannabinoids: their chemistry and role against oxidative stress, inflammation, and cancer. *BioMed Research International*, *2018*, 1691428. https://doi.org/10.1155/2018/1691428

Pengyue, Z., Zhang, J., Li, D., Liu, J., Kang, S., Li, J., & Yao, Z. (2021). Cannabidiol induces autophagy to protects neural cells from mitochondrial dysfunction by upregulating SIRT1 to inhibits NF-κB and NOTCH pathways. *Frontiers in Cellular Neuroscience*, *15*, 654340. https://doi.org/10.3389/fncel.2021.654340

Ramot, Y., Sugawara, K., Zákány, N., Tóth, B. I., Bíró, T., & Paus, R. (2013). A novel control of human keratin expression: cannabinoid receptor 1-mediated signaling down-

regulates the expression of keratins K6 and K16 in human keratinocytes *in vitro* and *in situ*. *PeerJ*, *1*, e40. https://doi.org/10.7717/peerj.40

Robinson, E. S., Alves, P., Bashir, M. M., Zeidi, M., Feng, R., & Werth, V. P. (2017). Cannabinoid reduces inflammatory cytokines, tumor necrosis factor-α, and Type I interferons in dermatomyositis *In Vitro*. *Journal of Investigative Dermatology*, *137*(11), 2445–2447. https://doi.org/10.1016/j.jid.2017.05.035

Ruland, J. (2011). Return to homeostasis: Downregulation of NF-κB responses. *Nature Immunology*, *12*(8), 709–714. https://doi.org/10.1038/ni.2055

Scherer, T., & Buettner, C. (2009). The dysregulation of the endocannabinoid system in diabesity-a tricky problem. *Journal of Molecular Medicine, 87*(7), 663–668. https://doi.org/10.1007/s00109-009-0459-y

Schreiber, M., Kolbus, A., Piu, F., Szabowski, A., Mö Hle-Steinlein, U., Tian, J., Karin, M., Angel, P., & Wagner, E. F. (1999). Control of cell cycle progression by c-Jun is p53 dependent. *Genes & Development*, *13*, 607–619. www.genesdev.org

Singh, A., Singh, A., Sand, J. M., Bauer, S. J., bin Hafeez, B., Meske, L., & Verma, A. K. (2015). Topically applied Hsp90 inhibitor 17AAG inhibits UVR-induced cutaneous squamous cell carcinomas. *Journal of Investigative Dermatology*, *135*(4), 1098–1107. https://doi.org/10.1038/jid.2014.460

Sivesind, T. E., Maghfour, J., Rietcheck, H., Kamel, K., Malik, A. S., & Dellavalle, R. P. (2022). Cannabinoids for the treatment of dermatologic conditions. *JID Innovations*, *2*(2), 100095. https://doi.org/10.1016/j.xjidi.2022.100095

Song, J., Yang, B., Jia, X., Li, M., Tan, W., Ma, S., & Shi, X. (2018). Distinctive roles of sirtuins on diabetes, protective or detrimental? *Frontiers in Endocrinology*, *9*(November), 724. https://doi.org/10.3389/fendo.2018.00724

Spiera, R., Hummers, L., Chung, L., Frech, T. M., Domsic, R., Hsu, V., Furst, D. E., Gordon, J., Mayes, M., Simms, R., Lafyatis, R., Martyanov, V., Wood, T., Whitfield, M. L., Constantine, S., Lee, E., Dgetluck, N., & White, B. (2020). Safety and Efficacy of Lenabasum in a Phase II, Randomized, Placebo-Controlled Trial in Adults With Systemic Sclerosis. *Arthritis and Rheumatology*, *72*(8), 1350–1360. https://doi.org/10.1002/art.41294

Ständer, S., Reinhardt, H. W., & Luger, T. A. (2006). Topische cannabinoidagonisten. Eine effektive, neue möglichkeit zur behandlung von chronischem pruritus. *Hautarzt*, *57*(9), 801–807. https://doi.org/10.1007/s00105-006-1180-1

Strouse, T. B. (2016). Cannabinoids in medical practice. *Cannabis and Cannabinoid Research*, *1*(1), 38–43. https://doi.org/10.1089/can.2015.0010

Tahir, S. K., Zimmerman, A. M., & Zimmerman, A. M. (1991). Influence of Marihuana on cellular structures and biochemical activities. *Pharmacology Biochemistry & Behavior*, *40*, 617–623.

Tóth, B. I., Dobrosi, N., Dajnoki, A., Czifra, G., Oláh, A., Szöllsi, A. G., Juhász, I., Sugawara, K., Paus, R., & Bíró, T. (2011). Endocannabinoids modulate human epidermal keratinocyte proliferation and survival via the sequential engagement of cannabinoid receptor-1 and transient receptor potential vanilloid-1. *Journal of Investigative Dermatology*, *131*(5), 1095–1104. https://doi.org/10.1038/jid.2010.421

Tóth, K. F., Ádám, D., Bíró, T., & Oláh, A. (2019). Cannabinoid signaling in the skin: Therapeutic potential of the "c(ut)annabinoid" system. *Molecules*, *24*(5), 1–56. https://doi.org/10.3390/molecules24050918

Turan, V., & Oktay, K. (2019). BRCA-related ATM-mediated DNA double-strand break repair and ovarian aging. *Human Reproduction Update*, *26*(1), 43–57. https://doi.org/10.1093/humupd/dmz043

Vaziri, H., West, M. D., Allsopp, R. C., Davison, T. S., Wu, Y., Arrowsmith, C. H., Poirier, G. G., & Benchimol, S. (1997). ATM-dependent telomere loss in aging human diploid fibroblasts and DNA damage lead to the post-translational activation of p53 protein involving poly (ADP-ribose) polymerase. *The EMBO Journal*, *16*(19), 6018–6033.

Vincenzi, C., & Tosti, A. (2020). Efficacy and tolerability of a shampoo containing broad-spectrum cannabidiol in the treatment of scalp inflammation in patients with mild to moderate scalp psoriasis or seborrheic dermatitis. *Skin Appendage Disorders*, *6*(6), 355–361. https://doi.org/10.1159/000510896

Webster Micah, Witkin Keren L. Witkin, & Cohen-Fix Orna. (2009). Sizing up the nucleus: nuclear shape, size and nuclear-envelope assembly. *Journal of Cell Science*, *122*(10), 1477–1486. https://doi.org/10.1242/jcs.037333

Wisdom, R., Johnson, R. S., & Moore, C. (1999). c-Jun regulates cell cycle progression and apoptosis by distinct mechanisms. *The EMBO Journal*, *18*(1), 188–197.

Xing, C., Zhuang, Y., Xu, T. H., Feng, Z., Zhou, X. E., Chen, M., Wang, L., Meng, X., Xue, Y., Wang, J., Liu, H., McGuire, T. F., Zhao, G., Melcher, K., Zhang, C., Xu, H. E., & Xie, X. Q. (2020). Cryo-EM structure of the human cannabinoid receptor CB2-Gi signaling complex. *Cell*, *180*(4), 645-654.e13. https://doi.org/10.1016/j.cell.2020.01.007

Yessenkyzy, A., Saliev, T., Zhanaliyeva, M., Masoud, A. R., Umbayev, B., Sergazy, S., Krivykh, E., Gulyayev, A., & Nurgozhin, T. (2020). Polyphenols as caloric-restriction mimetics and autophagy inducers in aging research. *Nutrients*, *12*(5), 1344. MDPI AG. https://doi.org/10.3390/nu12051344

Yo, K., & Rünger, T. M. (2018). The long non-coding RNA FLJ46906 binds to the transcription factors NF-κB and AP-1 and regulates expression of aging-associated genes. *Aging*, *10*(8), 2037–2050. https://doi.org/10.18632/aging.101528

Yuan, C., Wang, X. M., Guichard, A., Tan, Y. M., Qian, C. Y., Yang, L. J., & Humbert, P. (2014). N-palmitoylethanolamine and N-acetylethanolamine are effective in asteatotic eczema: Results of a randomized, double-blind, controlled study in 60 patients. *Clinical Interventions in Aging*, *9*, 1163–1169. https://doi.org/10.2147/CIA.S65448

Zheng, X., Sun, T., & Wang, X. (2013). Activation of type 2 cannabinoid receptors (CB2R) promotes fatty acid oxidation through the SIRT1/PGC-1α pathway. *Biochemical and Biophysical Research Communications*, *436*(3), 377–381. https://doi.org/10.1016/j.bbrc.2013.05.108

Zimmerman A. M., Stich H., & San R. (1978). Nonmutagenic action of cannabinoids *in vitro*. *Pharmacology*, *16*, 333–343.

Zuardi, A. W. (2006). History of cannabis as a medicine: A review. *Revista Brasileira de Psiquiatria*, *28*(2), 153–157. https://doi.org/10.1590/S1516-44462006000200015

Zuardi, A. W., Crippa, J. A. S., Hallak, J. E. C., Moreira, F. A., & Guimarães, F. S. (2006). Cannabidiol, a *Cannabis sativa* constituent, as an antipsychotic drug. *Brazilian Journal of Medical and Biological Research*, *39*(3), 421–429. https://doi.org/10.1590/S0100-879X2006000400001

Zuardi, A. W., Crippa, J. A. S., Hallak, J. E. C., Pinto, J. P., Chagas, M. H. N., Rodrigues, G. G. R., Dursun, S. M., & Tumas, V. (2009). Cannabidiol for the treatment of psychosis in Parkinsons disease. *Journal of Psychopharmacology*, *23*(8), 979–983. https://doi.org/10.1177/0269881108096519

CHAPTER 4: EFFECT OF CANNABINOIDS AND POPULAR ANTI-AGING DRUGS ON THE SKIN FIBROBLASTS' SENESCENCE-ASSOCIATED PHENOTYPE

4.1. ABSTRACT

Identifying effective anti-aging compounds is a cornerstone of modern longevity, aging and skin health research. There are numerous experimental data on the ability of certain drugs and natural compounds to prevent, delay, or alleviate the development of age-related diseases, their symptoms, cellular senescence, and rejuvenation activity. There is considerable evidence of the effectiveness of natural signaling regulators (NSRs) such as metformin, triacetylresveratrol (TRSV), and rapamycin in longevity and anti-aging studies. Concomitantly, there is controversial information regarding their potential protective role against skin aging. Moreover, in the light of the increased popularity of phytocannabinoids (pCBs) and their appearance in multiple beauty products without rigorous research data on their rejuvenation efficacy, we decided to investigate the potential role of pCBs in skin rejuvenation. In addition, no information exists about the combined effects of NSRs and pCBs on dermal aging and potential rejuvenation properties.

Here we tested the efficacy of metformin, TRSV, and rapamycin combined with pCBs as anti-aging compounds on the CCD-1064Sk, CCD-1135Sk, and BJ-5ta skin fibroblasts cell lines. The nuclear alterations based on the DAPI staining were analyzed. The cellular viability was determined using the MTT and Neutral red assays. The ability

of NRS combined with pCBs to potentiate the functional and metabolic activity of the senescent fibroblasts was assessed based on the RT-PCR data and wound healing assay. We found that metformin and TRSV combined with pCBs reduced the adverse influence of oxidative stress, lowered expression of senescence markers, and in turn, stimulated metabolic and functional activity, inhibited dermal aging processes, and positively affected the viability of skin fibroblasts. Therefore, pCBs can be a valuable source of biologically active substances used in aging. Concurrently, the data obtained from three different dermal fibroblasts cell lines demonstrated rapamycin's adverse effects on the speed of wound healing in senescent cultures. The analysis also showed that cannabinoids alone and combined with TRSV positively affected the wound healing process. Thus, TRSV alone or combined with pCBs have a potential for enhancing regeneration and repair in injured tissues. More studies are needed, especially those using 3D tissues and animals, to confirm the efficacy of pCBs combined with metformin or TRSV on various processes associated with aging.

4.2. INTRODUCTION

4.2.1. Anti-aging and rejuvenation strategies

The life expectancy in most developed countries almost doubled within the last century. This tendency goes hand in hand with improved healthcare, effective antibiotics against infectious diseases, the development of vital technologies, better nutrition, and an increased aging population in the world (Shetty et al., 2018). Longevity is a double-edged sword – people live longer, but life quality might be adversely affected by age-related

diseases (ARDs) (Gerasymchuk et al., 2020). That is why research teams around the globe are focusing on investigating aging and treatment strategies to delay or prevent the development of ARDs (Zhu et al., 2020). A significant challenge of aging research is distinguishing the pathogenesis of cell and tissue senescence from the myriad of changes that accompany it. Substantial data exist describing causes and mechanisms of the aging process and potential ways to delay or prevent it. So far, we can not stop aging, but there are opportunities to delay it, and cure or alleviate some ARDs and their symptoms.

A few big groups of drugs and nutrients directed at the elimination of detrimental effects of aging have been discovered, like (i) senolytics and senomorphics, (ii) senescence-associated secretory phenotype (SASP) inhibitors, and (iii) nutrient signaling regulators (Thoppil & Riabowol, 2020; Zhu et al., 2020).

4.2.1.1. Senolytics and senomorphics

Senolytics are drugs that selectively kill senescent cells; they are widely presented on the pharmaceutical market as Dasatinib, Navitoclax, Quercetin (also found in many fruits and vegetables), and Fisetin (found in strawberries) (Blagosklonny, 2021; Khan et al., 2013; Kirkland & Tchkonia, 2020). At the same time senomorphics which modulate senescent cells by blocking SASP, without induction of their apoptosis (Kim & Kim, 2019). The development of senolytic compounds was based on the targeting of pathways related to SASP expression, such as the p38MAPK, PI3k/Akt, mTOR (epigallocatechin gallate – mTOR signaling inhibitor, SIRT1/SIRT3 inducer) and JAK/STAT pathways (JAK inhibitor – ruxolitinib) and transcription factors, such as NF-κB (kaempferol and apigenin - NF-κB pathway inhibitors), C/EBP β and STAT3 (Lagoumtzi & Chondrogianni, 2021).

The development of senolytic compounds was based on a bioinformatics approach to identify Senescent-Cell Anti-Apoptotic Pathways, including inter-related Bcl-2/Bcl-XL, p53/p21, PI3K/AKT, and serpine anti-apoptotic pathways, which are highly upregulated in senescent cells because they resist apoptosis despite the production of pro-apoptotic SASP factors (Fuhrmann-Stroissnigg et al., 2018; Kirkland & Tchkonia, 2020). Senolytics stimulate the death of senescent cells and concomitantly decrease accumulation of mutations and possibilities of malignant transformation. In addition to those mentioned above, there are Bcl family inhibitors (e.g., Panobinostat, is a post-chemotherapy senolytic with the potential to kill persistent senescent cells that accumulate during standard chemotherapy) (Samaraweera et al., 2017), PI3K/AKT inhibitors, and forkhead box O (FOXO) regulators, which alleviate senescence in skin-derived precursors (Liu et al., 2011), and HSP90 inhibitors (e.g., geldanamycin) (Fuhrmann-Stroissnigg et al., 2018), catechins (found in green tea) (Bae et al., 2020; Zhu et al., 2020).

Senolytics contribute to healthy aging by clearing senescent cells and, based on the numerous studies, effectively alleviate symptoms of aging, improve symptoms of ARDs, are efficient in anti-cancer therapy, and extend median lifespan (Zhu et al., 2020). Nevertheless, since they may target different types of senescent cells, they may have significant adverse effects. That is why they should be selected according to distinct senescent cell types and cautious assessment of possible risks. More research is necessary to confirm the safety and efficacy of senolytics and senomorphics drugs.

4.2.1.2. SASP inhibitors

SASP inhibitors inhibit the release of inflammation-promoting molecules, immune suppressors, and protein-digesting enzymes that drive sterile inflammation,

correspondingly negatively affecting neighboring healthy cells, and eventually speeding up aging (Zhu et al., 2020). They are also called senomorphics and are directed to extend healthspan and potential lifespan without induction of cell death. This group includes Wnt/β-catenin inhibitors (e.g., Klotho, ICG-001) (Kawarazaki et al., 2020; Miao et al., 2019), JAK1/2 inhibitors (e.g., ruxolitinib) (Griveau et al., 2020), NF-κB and p38 inhibitors (Robbins et al., 2011; Salminen et al., 2012), IL-1α blockers (Dinarello et al., 2012; Rea et al., 2018), glucocorticoids as potent suppressors of selected components of the SASP (Hasan et al., 2012; Poulsen et al., 2014), mitochondrial depleters (i.e., in the case of impaired mitophagy by either mTORC1 inhibition or PGC-1β deletion) (Chen et al., 2020; Correia-Melo et al., 2016; Sun et al., 2016), various antioxidants (e.g., MitoQ, SS31, SKQ1, melatonin, astaxhantin, and equol, *Ganoderma lucidum* Chinese plant) (Zhu et al., 2020) and statins (e.g., simvastatin, decrease the expression of pro-inflammatory cytokines IL-6, IL-8, and MCP-1) (Liu et al., 2015; Olivieri et al., 2012).

In general, SASP inhibitors contribute to healthy aging by abating oxidative-stress damage, augmenting mitochondrial function, and suppressing the bystander effect of senescent cells, spreading senescence towards their neighbor cells *in vitro* and *in vivo* (Ilnytskyy et al., 2009; Koturbash et al., 2008; Nelson et al., 2012; Widel et al., 2014). Some SASP drugs may simultaneously contribute to healthy aging by targeting different mechanisms. For instance, melatonin is a hormone that follows a circadian light-dependent rhythm of secretion. It maintains immune defense responses, body weight, reproduction, serves as a direct, receptor-independent potent antioxidant, chemotoxicity-reducing agent, a putative general anti-aging substance, exerts anti-jet lag and tumor growth-inhibitory effects (Kleszczynski & Fischer, 2012). Melatonin alleviates oxidative

stress via reducing ROS production and protects mitochondria through both the Keap1/Nrf2/ARE pathway and SIRT1 activation (Manchester et al., 2015; Ramis et al., 2015).

Even if SASP inhibitors demonstrated beneficial effects, their prescription must be carefully considered (Zhu et al., 2020). For instance, most SAPS inhibitors exert significant antioxidant potential that might affect the internal defensive mechanism by diminishing immune response in certain conditions (e.g., immunodeficiency, cancer) (Kim & Kim, 2019; Lagoumtzi & Chondrogianni, 2021). In addition, alteration in oxidative-antioxidative homeostasis is accompanied by a reduction in regeneration and repair, which are components of the third stage of inflammation, resulting in delayed wound healing and an increased risk of recurrent infections. Thus, though SASP inhibitors have health benefits, they might turn into poison and harm the organism in excessive doses or uncontrolled consumption.

4.2.1.3. Nutrient signaling regulators

Nutrient signaling regulators (NSRs) maintain nutrient-sensitive signaling pathways and are vital for biological processes (Zhu et al., 2020). They were shown to regulate pathways responsible for organismal survival, growth, metabolism, signaling systems, including Sirtuin, mTOR, AMP-activated protein kinase (AMPK), and therefore can be used as novel therapeutic approaches to age-related diseases (Cummings & Lamming, 2017; Ramis et al., 2015). Among the most studied in this group are Sirtuin regulators (e.g., resveratrol and its metabolite piceatannol, Selisistat, selective SIRT1 inhibitor) (Curry et al., 2021; Mayack et al., 2020; Yessenkyzy et al., 2020), mTOR inhibitors (e.g., rapamycin) (Bai et al., 2021; Fletcher et al., 2013; Qin et al., 2018; Yoshizaki et al., 2010),

spermidine (Madeo et al., 2019; Shetty et al., 2018), AMPK activators (e.g., Metformin) (Barzilai et al., 2016; Shetty et al., 2018; Soydas et al., 2018, 2021), curcumin (Dudás et al., 2013; Mandrol et al., 2016; Shetty et al., 2018; Shishodia, 2013; Silvia Loebsch, 2014; Singh et al., 2012; Yang et al., 2012; Zhu et al., 2020), and *Lycium barbarum* (a traditional Chinese medicine) (Gao et al., 2017; Zhou et al., 2022). The abovementioned NSRs were tested on eukaryotic organisms from yeast to humans. Observed results demonstrate positive effects of nutrient-sensing signaling mainly targeting the master regulators of aging such as mTOR, FOXO, and PGC1α, affecting autophagy, inflammation, and oxidative stress leading to the extension of lifespan in model organisms. In clinical trials, these drugs have been shown to prevent cardiovascular diseases (CVD), reduce inflammation, and potentially inhibit cancerogenesis, interfering with molecular mechanisms of cellular metabolism, proliferation, angiogenesis, and apoptosis (Piskovatska et al., 2019).

Most NSRs have strong capacity to support healthy aging and longevity. However, there are still many uncertainties related to the adverse effects, and correspondingly more clinical trials are required.

4.2.2. Rapamycin, metformin, and resveratrol as a cornerstone in anti-aging studies

Numerous current age-related studies are focused on the anti-aging aspects of rapamycin, metformin, resveratrol, aspirin, statins, etc. Most of them can target one or several mechanisms by blocking different signaling pathways associated with age-related

cellular and molecular dysfunctions. Nevertheless, there are multiple gaps in the understanding of the mechanisms mediating the anti-aging properties of medications that remain essentially unknown and need to be elucidated. Let's take a more detailed look into the most promising pharmaceutical anti-aging tools available nowadays.

4.2.2.1. Rapamycin

Rapamycin was initially extracted from a soil sample of Easter Island (also known as Rapa Nui) (Li et al., 2014). It is also named sirolimus, and represents a macrolide produced from *Streptomyces hygroscopicus* to inhibit fungal growth (Benedetti et al., 2020). Subsequently, immunosuppressive, anti-proliferative properties of rapamycin with defined “anti-aging” effects in cells and tissues were discovered in mammalian cells (Li et al., 2014).

Rapamycin is a central modulator of the mammalian target of the rapamycin (mTOR) pathway; it regulates transcription and protein synthesis by integrating various signal stimulation, and finally controls apoptosis, growth, and autophagy in cells (Zou et al., 2020). mTOR includes two structurally and functionally discrete complexes termed the mammalian target of rapamycin complex 1 (mTORC1) and mammalian target of rapamycin complex 2 (mTORC2) (Zou et al., 2020). mTORC1 is composed of mTOR, mammalian lethal with sec-13 protein 8 (mLST8) and regulatory associated protein of TOR (raptor), GβL, DEP-domain containing mTOR interacting protein (deptor), and Proline-rich Akt substrate 40kDa (PRAS40). In contrast, mTOR complex 2 (mTORC2) is comprised of a rapamycin-insensitive companion of mTOR (rictor), stress-activated protein kinase-interacting protein 1 (SIN1), mLST8, GβL, PRR5, and deptor (Li et al., 2014). mTORC1 incorporates signals from numerous growth factors, nutrients, and

energy supplies to stimulate cell growth when energy is sufficient and to induce catabolism when the body lacks energy. mTORC1 also facilitates lipid biosynthesis, inhibit degradation through the autophagy pathway, actively promotes mitochondrial biogenesis and metabolism through the peroxisome-proliferator-activated receptor coactivator PGC-1α, regulates glucose metabolism through the upregulation of hypoxic response transcription factor HIF-1α and c-Myc (Johnson et al., 2013), and positively controls glutamine metabolism by SIRT4 repression (Li et al., 2014). That is why mTORC1 is highly susceptible to inhibition by rapamycin compared to mTORC2. Nevertheless, long-term exposure to rapamycin represses mTORC2 in distinct cell types by sequestering newly synthesized mTOR molecules (Laplante & Sabatini, 2012). Thus, mTORC1 is primarily responsible for cell growth and metabolism regulation, while mTORC2 predominantly controls cell proliferation and survival (Unni & Arteaga, 2019). Interestingly, alterations in the mTORC1 pathway regulation are commonly involved in several genetic diseases and cancers.

The mTOR pathway is the crucial controller of growth (mass accumulation) in animals and is the fundamental link between the availability of nutrients in the environment and the control of most anabolic and catabolic processes (Sabatini, 2017). In response to the cell-cycle arrest by p16 or p21, mTOR drives growth-like conversion from reversible arrest (quiescence) to senescence (Blagosklonny, 2019). Besides, mTOR is one of the primary regulators of the cellular stress response following ischemia and reperfusion (Fletcher et al., 2013). Recent reports showed deregulation of mTOR signaling in ARDs, cancer, epilepsy, and aging in multiple model organisms (Cunningham et al., 2007; Sabatini, 2017; Squarize et al., 2010). Almost a decade ago, mTORC1 was

identified as a crucial modulator for aging and ARDs (Johnson et al., 2013). It was suggested that mTORC1 inhibition might be efficient to treat ARDs even when the treatment is initiated in middle-aged humans. On the other hand, mTORC2 contributes to cell survival via the Akt and SGK1 (Serum and glucocorticoid-induced kinase) activation (Castel et al., 2016). Besides, mTORC2 regulates the structure of the actin cytoskeleton through activation of paxillin, PKCα, and small GTPases, Rho and Rac (Laplante & Sabatini, 2012).

In 2012, Lamming et al. showed that rapamycin increased longevity and maintained normal glucose homeostasis via mTORC1 inhibition, while disruption of mTORC2 contributed to insulin resistance *in vivo* (Lamming et al., 2012). Moreover, intraperitoneal injection of rapamycin was associated with the development of diabetes-like syndrome by reducing β-cell mass and function, causing hyperlipidemia, severe insulin resistance, glucose intolerance, and promoting hepatic gluconeogenesis in mice and guinea pigs. Such detrimental changes in metabolic status are expressed mainly by reduction rather than an increase in life span (Aggarwal et al., 2006; Fraenkel et al., 2008; Houde et al., 2010). The reason for this paradox is unclear and could be related to either too little or too much biological availability of rapamycin; encapsulation and limited exposure to the tissues may lead to too little rapamycin being bioavailable, while intraperitoneal injection may lead to rapid and high absorption of rapamycin by the gut. Broadly, these findings support the idea that rapamycin dosing and administration methods have to be carefully adjusted to get beneficial effects on both longevity and metabolism (Laplante & Sabatini, 2012).

Nevertheless, rapamycin and its analogs are currently approved by the FDA for the treatment of a number of conditions, as they have been demonstrated, both *in vitro* and *in*

vivo, to slow aging and extend life span in different species (Johnson et al., 2013) and prevent ARDs, including diabetic complications such as retinopathy (Blagosklonny, 2019). Wilkinson et al. reported that age-dependent changes occur more slowly in rapamycin-treated mice, including heart alterations, liver, endometrium, adrenal gland, and tendon elasticity. They showed rapamycin treatment caused improvement in age-related decline in spontaneous activity of mice (Wilkinson et al., 2012). Recently rapamycin has been demonstrated as a preventive and therapeutic compound for UVA-induced dermal photoaging (Bai et al., 2021).

Apart from different diseases, rapamycin was also recommended in cosmetological practice for anti-aging and rejuvenation purposes. It was noted that rapamycin-containing cream was effective when applied to selected areas, like the hands and face, especially skin affected by age-related spots and dermatopathies. The topical usage is considered safer and might relieve the adverse effects of systemic treatment with rapamycin (Blagosklonny, 2021). However, there is some evidence that solely topical use of rapamycin may seem insufficient (Blagosklonny, 2019). For this reason, we believe that rapamycin combined with other anti-aging compounds or natural products like phytocannabinoids might open new perspectives in the aging abatement and rejuvenation strategies.

4.2.2.2. Metformin

Metformin (1,1-Dimethylbiguanide) is a widely used anti-hyperglycemic drug for treating type 2 diabetes by decreasing blood glucose levels via reduced hepatic gluconeogenesis and increased glucose uptake in skeletal muscles (Wu et al., 2011). Metformins' mechanisms of action are focused on different cellular targets; in particular,

it inhibits the respiratory complex I of the electron transport chain (Benedetti et al., 2020; Bridges et al., 2016), directly affecting reactions requiring ATP and indirectly acting on the activation of AMPK (Bridges et al., 2016; Madiraju et al., 2014). As a result, this leads to elevated accumulation of NADH compared to NAD+ and inhibited production of NADH-ubiquinone oxidoreductase, which is localized on the mitochondrial membrane, thus activating AMPK and suppressing gluconeogenesis (Benedetti et al., 2020; Rena et al., 2017). Subsequently, this leads to fatty acid synthesis and mTOR signaling network suppression (Howell et al., 2017), causing reduced cellular energy consumption. Indeed, it was found to activate AMPK in hepatocytes, inhibit mTOR signaling and protein synthesis, promote mitophagy in mononuclear cells (Bhansali et al., 2019), induce apoptosis in lung cancer cells by activating the JNK/p38 MAPK pathway and upregulating the expression of growth arrest and DNA damage-inducible gene 153 (Wu et al., 2011). Metformin demonstrated improved nematode health span, locomotor activity, and median lifespan via an AMPK, LKB1, and SKN-1 dependent pathway, but is independent of insulin signaling (Onken & Driscoll, 2010). Epidemiological studies have documented the vital role of metformin in dwindling cancer incidence and mortality (Heckman-Stoddard et al., 2017). Moreover, studies have shown that long-term use of metformin alleviates oxidative damage and chronic inflammation, reduces cognitive deterioration, improves cardiomyocyte functioning, reduces CVD risk, and prolongs health and life (Zhu et al., 2020). Interestingly, metformin has been shown as a possible coadjuvant treatment for COVID-19 patients (EL-Arabey & Abdalla, 2020; Esam, 2020) due to its potential to reduce levels of IL-6 (Blanco-Melo et al., 2020), stimulate cellular pH elevation, and subsequently minimize viral replication (Benedetti et al., 2020; Zhang et al., 2016).

As a biguanide, metformin acts in a dietary restriction manner and on oxidative stress pathways in a lifespan-extending effect (Wu et al., 2011). It reduces advanced glycation end product (AGEs) accumulation in response to massive ROS generation in high glucose conditions. Accelerated dermal aging is directly correlated with increased protein deterioration in the existing collagen due to crosslinking. The progressive increase in AGE affects cellular macromolecules during aging through oxidative damage and leads to NF-κB activation. Metformin has been shown to protect T3 fibroblasts in an *in vitro* aging model under high glucose conditions inducing cell proliferation, collagen I and III production, protection from apoptosis, and reducing NF-κB (p65) activity (Soydas et al., 2018). In response to the hypoglycemic condition, it inhibits SASP by repressing NF-κB pathway activation by preventing translocation of NF-κB to the nucleus and inhibiting the phosphorylation of IκB and IKKα/β in normal fibroblasts IMR90 (Moiseeva et al., 2013). This mechanism is suggested to be common for the anti-aging and antineoplastic effects of metformin reported in animal models and diabetic patients.

Thus, metformin may be a promising pharmacological dermal anti-aging remedy with a complex beneficial impact on the physiology of the skin and entire organism.

4.2.2.3. Resveratrol

Resveratrol (3,5,4′-trihydroxy-*trans*-stilbene) is a type of natural phenol and a phytoalexin that can be obtained from several sources, including red wine, grapes, a variety of berries, peanuts, and certain medicinal plants (Bastianetto et al., 2015; Liu et al., 2018; Salehi et al., 2018). Due to lipophilic characteristics, it is easily absorbed, metabolized, and excreted; however, its low bioavailability limits its use. Nevertheless, resveratrol is often used as a popular dietary supplement (Benedetti et al., 2020).

Resveratrol anti-aging characteristics were investigated in different species (Yessenkyzy et al., 2020). It was revealed that resveratrol could alleviate the inflammatory phenotype in senescent human fibroblasts treated by hydrogen peroxide through upregulation of autophagic pathways (Du et al., 2019). Moreover, autophagic flux in muscle cells after palmitate-induced cellular senescence was effectively restored by resveratrol (Chang et al., 2018). It has been shown that this effect was achieved partially through modulation of mitochondrial dynamics and upregulating autophagic flux via the mitogen-activated protein kinase/extracellular signal-regulated kinase (MEK/ERK) signaling pathway (Lin et al., 2018). Resveratrol mitigated the inflammatory phenotype detected in the gut of the fish *Nothobranchius guentheri*, causing down-regulation of SASP-associated proinflammatory cytokines IL-8 and TNFα, and up-regulation of anti-inflammatory cytokine IL-10 (Liu et al., 2018).

Resveratrol is known to extend the lifespans of nematodes and yeast, and prevent ARDs in the elderly through SIRT1 pathway modulation (Huo et al., 2019; Kim et al., 2007; Szkudelski & Szkudelska, 2015; Wang et al., 2017). SIRT1 is a NAD(+)-dependent deacetylase involved in gene silencing, anti-oxidative stress, anti-apoptosis, and inhibition of inflammation (Lee et al., 2022; Liu et al., 2018). Resveratrol can increase SIRT1 during aging and chronic inflammation, processes that are associated with reduced SIRT1 levels and activity in response to oxidative stress (Zhu et al., 2020). A recent study showed that resveratrol significantly elevates the SIRT1 activity, inhibits the NF-κB pathway, and prevents the loss of intestinal stem cells (Liu et al., 2018). Regardless of the increased longevity of nematodes and yeast, resveratrol and simvastatin have not been shown to prolong life expectancy of mice (Miller et al., 2011). Additionally, Luz et al. reported that

low resveratrol doses and red wine supplementation improved vascular function and aerobic capacity, reduced p53, p16 senescence biomarkers in rats, but did not extend their lifespan (da Luz et al., 2012). Furthermore, low resveratrol doses (0.1–1.0 μg/mL) enhance cell proliferation, whereas higher doses (10–100 μg/mL) reduce mitotic activity and induce apoptosis on human endothelial and cancer cell cultures (Szende et al., 2000). It is worth noting that at low concentrations (1 and 10 μmol/L), resveratrol increased HT-29 colon cancer cell number, while at higher doses (50 or 100 μmol/L), it reduced cellular quantity and augmented the percentage of apoptotic or necrotic cells (Hipólito-Luengo et al., 2017). In parallel, the authors observed increased levels of histone γH2AX, a marker of DNA damage, and NADPH oxidase activation caused by resveratrol cytotoxicity on HT-29 cells, which was accompanied by elevated SIRT6 levels, presumably as a repair mechanism.

There are numerous limitations in resveratrol effectiveness towards longevity and anti-aging due to its decreased bioavailability (Salehi et al., 2018; Hipólito-Luengo et al., 2017; Szende et al., 2000). Recently, it was found that its acetylated analog triacetylresveratrol (TRSV) has higher bioavailability (Duan et al., 2016; Liang et al., 2013). Due to its higher hydrophobic nature, TRSV, compared to resveratrol, has been shown to be more effective in interacting with and crossing phospholipid bilayers (Sarpietro et al., 2007). Moreover, findings revealed that TRSV might be a more potent anticancer agent than resveratrol and could block essential tumor-promoting effects of glioblastoma *in vitro* and *in vivo* (Sengupta et al., 2015). It was reported to exert an anti-cancer effect affecting proliferation and apoptosis by decreasing the phosphorylation of STAT3 and NF-κB, down-regulation of Mcl-1, and up-regulation of Bim and Puma in a

dose- and time-dependent manner in pancreatic cancer cells (Duan et al., 2016). TRSV was revealed to protect live cells after γ-irradiation and this effect was based on detected antioxidant-dependent radioprotection and longer half-life (Koide et al., 2011; Moyano-Mendez et al., 2014). In addition, it was found that TRSV stimulated lung tissue protection against LPS-induced ARDS by attenuating inflammation via the p38 MAPK/SIRT1 pathway (Ma et al., 2015). The anti-inflammatory effects of TRSV were associated with diminished LPS-induced histological changes, alleviated pulmonary edema, reduced vascular blood leakage, inhibited lungs' myeloperoxidase activity, and reduced secretion of TNF-α, IL-6, and IL-1β in lungs and NR8383 cells. Besides, TRSV relieved LPS-induced inhibition of SIRT1 expression and inhibited the activation effects of LPS on MAPKs and NF-κB *in vitro* and *in vivo* (Ma et al., 2015).

Although TRSV was revealed as a potent antioxidant, anti-inflammatory, radioprotector, and anticancer agent, there is a lack of data related to its other effects. As we could not find information about the anti-aging or rejuvenation properties of TRSV in the available literature, it piqued our interest.

4.2.3. Rejuvenation potential of metformin, triacetylresveratrol, and rapamycin in combination with phytocannabinoids

Living healthily with a long lifespan and looking young simultaneously is everyone's desire. NSRs such as rapamycin, metformin, and TRSV are the most popular anti-aging tools. They retard multiple aspects of aging in different species, in addition to any beneficial effects they may have on various diseases and pathological conditions

described earlier. Interestingly, all three compounds have been shown to delay cellular senescence by autophagy enhancement through the modulation of interconnected mechanisms. Specifically, metformin inhibits mTOR signaling, protein synthesis and activates AMPK (Sarkar, 2013; Shi et al., 2012), whereas resveratrol suppresses mTOR through ATP competition, promotes autophagy markers LC3-II and beclin-1 expression (Hu et al., 2017; Park et al., 2016; Sarkar, 2013), while rapamycin inhibits mTORC1 activity (Benjamin et al., 2011; Sarkar, 2013).

Some of the beneficial effects of rapamycin, metformin, and TRSV have been achieved through cutaneous application. It was revealed that locally applied metformin and TRSV, but not rapamycin, improved epidermis, hair follicles, and collagen deposition, resulted in amelioration of the wound beds vascularization, which were attributed to stimulation of the AMPK pathway, the key mediator of wound healing in both young and aged skin of the rodents (Zhao et al., 2017). Recent clinical studies have supported the efficacy of resveratrol and its analogs (i.e, resveratryl triacetate and resveratryl triglycolate) in human skin lightening and anti-aging due to its anti-inflammatory, anti-proliferative, and anti-pigmentation properties (Park et al., 2016). These characteristics were validated through antioxidative influence and modulation of nuclear factor erythroid 2-related factor 2 (Nrf2), inhibition of TNF-α–induced expression of inflammatory cytokines and MMPs by SIRT1-dependent mechanisms, and attenuation of cellular melanin synthesis effectively through the suppression of microphthalmia-associated transcription factor (MITF)-dependent expression of melanogenic enzymes (Boo, 2019; Park et al., 2016). Another recent clinical trial (ClinicalTrials.gov Identifier: NCT03103893) demonstrated that topical rapamycin application reduced senescence and

age-related features in human skin (Chung et al., 2019). The current study showed that the $p16^{INK4A}$ level, consistent with a reduction in cellular senescence and solar elastosis, was diminished in rapamycin-treated skin. This change was accompanied by the improvement of collagen VII, a critical component to the integrity of the basement membrane, and the restoration of degraded collagen (Chung et al., 2019).

Similar to TRSV, information on anti-aging properties of phytocannabinoids is also scarce. Recent studies showed that topical application of hydrogels based on cannabis extracts have a beneficial effect on skin hydration, inhibit the activity of matrix metalloproteinases (MMPs), collagenase, and elastase via reduction of oxidative stress markers; the extracts were shown to inhibit skin aging processes and positively affect the viability of skin cells (Zagórska-Dziok et al., 2021). Martinelli et al. noted photoprotective, antioxidant, and anti-inflammatory mechanisms of phytocannabinoids, emphasizing the possible impact of CBD on cell differentiation in the skin, especially in the case of dermatological disorders like psoriasis (Martinelli et al., 2021).

Our data reported in Chapter 2 demonstrated partial reduction of senescence-associated morphological changes accompanied by a reduction in senescence biomarkers and improvement of extracellular matrix (ECM) components in response to pCBs application. Thus, we hypothesized that the combination of NSRs and pCBs may have a beneficial anti-aging and potential rejuvenation effect. The idea of using metformin, rapamycin, or resveratrol is not novel. However, combining them with phytocannabinoids and using TRSV instead of resveratrol is a novel idea in anti-aging and rejuvenation strategies for aging skin.

The present chapter will describe molecular targets and the anti-aging effects of metformin, rapamycin, TRSV alone and in combination with phytocannabinoids. We will show the experimental data obtained in the stress-induced premature senescence (SIPS) model using human dermal fibroblasts, assess the results, address gaps, restrictions, and limitations of current research.

4.3. METHODS AND MATERIALS

4.3.1. Main reagents

1. Cannabinoids: Δ9-THC (Cat# T4764), CBD (Cat# C-045) were purchased from Sigma. 1.0 mg/ml stock solutions were prepared by dissolving cannabinoids in 1 ml DMSO (Dimethyl sulfoxide anhydrous, Life Technologies) and stored at -20 ℃.

2. Triacetylresveratrol (3,4',5-Triacetoxy-trans-stilbene) was purchased from Avantor-VWR (TCI America, USA, Cat# TCT3232-5G).

3. Metformin (Metformin Hydrochloride) was purchased from Cedarlane (Toronto Research Chemicals Inc., Canada, Cat#: M258815).

4. Rapamycin purchased from Fisher Scientific (Alfa Aesar™ J62473MF).

All products have ≥98% purity based on information provided by the manufacturer.

5. Hydrogen peroxide 30% (Merck®, Cat# 1072091000)

6. D-PBS (MULTICELL, Cat# 311-425-CL)

4.3.2. Cell culture and maintenance

The methodology is described in Chapter 2.

4.3.3. Senescence-associated phenotype modeling

Skin fibroblasts (CCD-1064Sk) in 70% confluency were treated 1 hour with 25 µM concentration of hydrogen peroxide solution (H_2O_2 dissolved in D-PBS) in 100 x 15 mm Petri plates in aseptic conditions (Chapter 2, Figure 2.3). Petri plates with skin fibroblasts were maintained in a humidified incubator at 37°C with 5% CO_2.

After 1-hour single treatment, H_2O_2 solution was poured out and substituted with cell culture medium. Thereafter, SIPS features, and biomarkers were determined microscopically and by β-galactosidase senescence assay, MTT and Neutral red colorimetric cell viability assays, Western immunoblotting, reverse transcription-polymerase chain reaction, wound-healing assay (WHA), and nuclear DAPI staining.

4.3.4. Experimental anti-aging treatments

Fibroblast cell cultures were treated with cannabinoids THC and CBD at 2.0 µM concentration (Chapter 3, Figure 3.2). In addition, CCD-1064Sk and BJ-5ta cell lines were treated with three popular anti-aging drugs: rapamycin, metformin, and TRSV. The concentrations of the anti-aging compounds were based on an accumulated body of literature that has demonstrated efficacy in anti-aging studies, for rapamycin 1 µM, 5 µM, 10 µM, 50 µM (Blagosklonny, 2019), for metformin 50 µM, 100 µM, 500 µM (Soydas et al., 2021), and for TRSV 5 µM, 10 µM, 50 µM (Duan et al., 2016; Salehi et al., 2018; Hipólito-Luengo et al., 2017; Vang, 2015) (Table 4.1). All anti-aging drugs like cannabinoids THC and CBD were dissolved in DMSO. Next, rapamycin, metformin,

TRSV or CBD, THC, and a vehicle (DMSO) were dissolved in media and applied to the media surrounding the cell cultures (n=3 for each condition) for 2 h daily for 5 days.

Table 4.1. Testing and identification of optimal anti-aging drugs concentrations on normal dermal fibroblasts

Anti-aging treatment	Tested concentrations (µM)				Final efficient concentration (µM)
Metformin	50	100	500	-	500
Rapamycin	1	5	10	50	5
Triacetylresveratrol	5	10	50	-	10

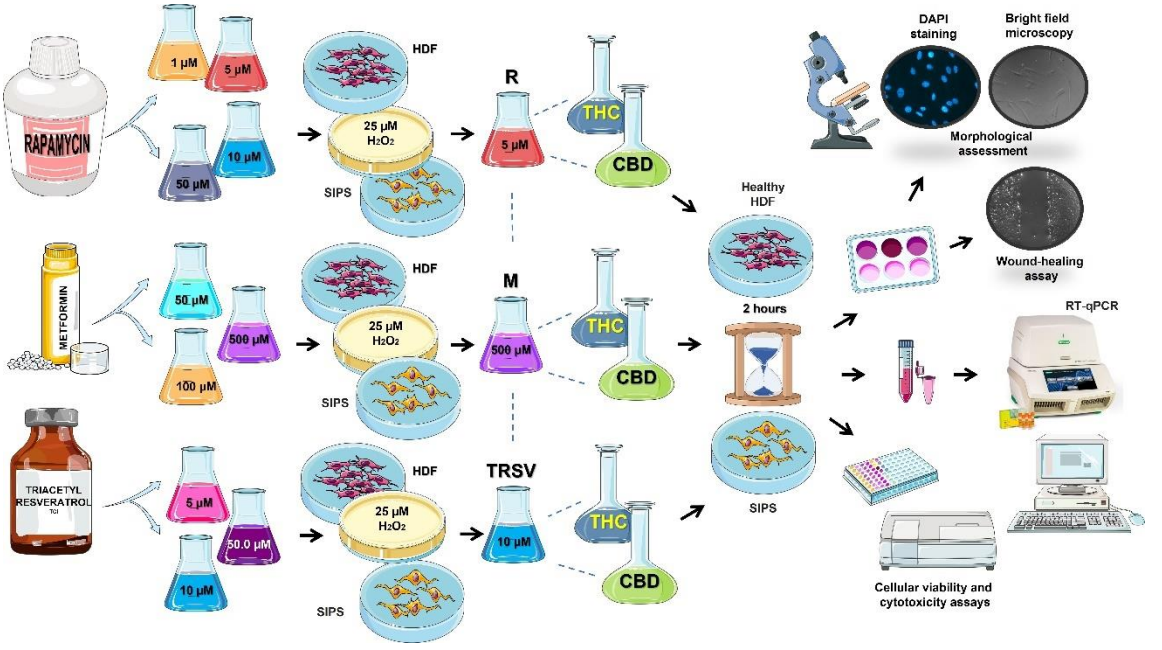

Figure 4.1. Testing of different concentrations of anti-aging drugs on prematurely senescent dermal fibroblasts. The figure shows steps to discover the efficient dose in treating senescent fibroblasts among three popular anti-aging drugs: rapamycin (R), metformin (M), and triacetylresveratrol (TRSV). CBD, cannabidiol; HDF,

human dermal fibroblasts; H_2O_2, hydrogen peroxide; SIPS, stress-induced premature senescence; THC, Δ-9-tetrahydrocannabinol. Dashed lines show a combination of treatments. This figure was created using images from Servier Medical Art Commons Attribution 3.0 Unported License (http://smart.servier.com).

After determining the optimal concentration of metformin, rapamycin, and TRSV, these drugs were applied alone or combined with phytocannabinoids (pCBs) CBD and THC and tested on healthy and senescent dermal fibroblasts (Table 4.2).

Table 4.2. Study groups of anti-aging drugs and their combination with phytocannabinoids that were used on human dermal fibroblasts

Treatment compounds	**CBD**	**THC**	**CBD+THC**	**Single compound**
Metformin (M)	+ CBD	+ THC	+ CBD+THC	M
Rapamycin (R)	+ CBD	+ THC	+ CBD+THC	R
Triacetylresveratrol (TRSV)	+ CBD	+ THC	+ CBD+THC	TRSV
Single compound	CDB	THC	-	-
Mixed	M+R+TRSV+THC+CBD			
Total	**15**			

CBD, cannabidiol; M, metformin; R, rapamycin; THC, Δ-9-tetrahydrocannabinol; TRSV, triacetylresveratrol.

4.3.5. Cell viability/cytotoxicity assays

4.3.5.1. The micro-culture tetrazolium assay (MTT)

The methodology is described in Chapter 2.

4.3.5.2. Neutral red assay and microscopy

The methodology is described in Chapter 2.

4.3.6. RNA isolation

The method is described in Chapter 2.

4.3.7. Reverse transcription polymerase chain reaction (RT-PCR)

The methodology is described in Chapter 2.

4.3.8. Wound-healing assay

The methodology is described in Chapter 2.

4.3.9. Immunohistochemistry

The methodology is described in Chapter 2.

4.3.10. QuPath Analysis

The methodology is described in Chapter 2.

4.3.11. Statistical analysis

The methodology is described in Chapter 2.

4.4. RESULTS

In this study, we analyzed anti-aging effects of NSRs metformin, rapamycin and TRSV, in combination with CBD, THC or CBD+THC using healthy and prematurely senescent dermal fibroblasts. The following aging-related characteristics were tested: cell senescence, cell growth rate and viability, gene expression profile, and functional activity based on ECM components production and speed of wound healing.

4.4.1. Identification of effective of metformin, rapamycin and triacetylresveratrol using fibroblasts senescence model system

The efficacy of NSRs was tested by cell viability MTT assay to identify the most effective and safest concentration of metformin, rapamycin, and TRSV.

In the previous chapter we have shown beneficial effects of different concentrations of phytocannabinoids on senescent fibroblasts (Figure 3.7). Here we tested cell viability after NSRs exposure as analyzed by MTT assay on different fibroblast culture lines.

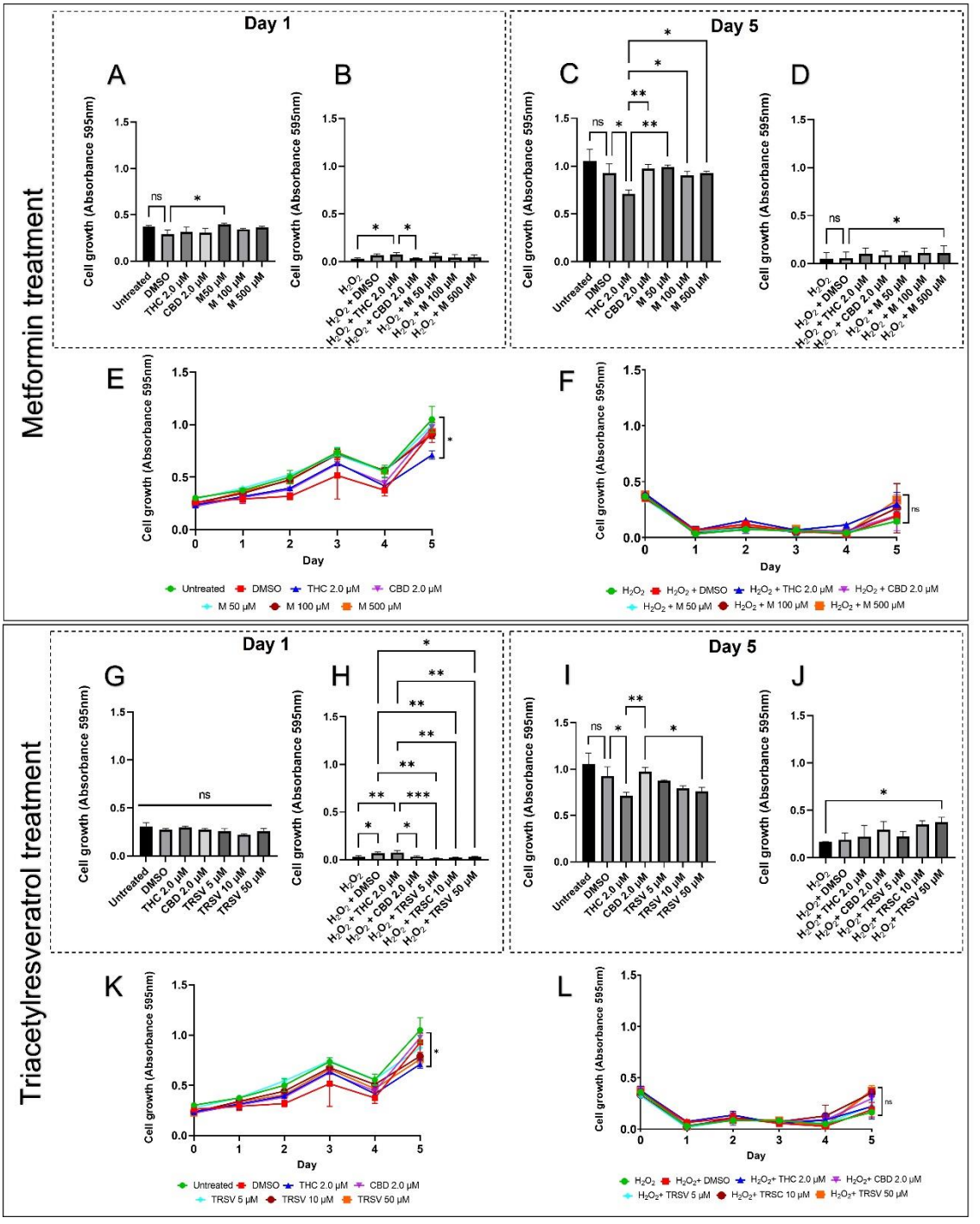

Figure 4.2. Viability of human skin fibroblasts (CCD-1064Sk), 24 PDL exposed to different concentrations of metformin and triacetylresveratrol compared to THC and CBD. The figure represents gradual changes in cell viability: A and B, day 1 after metformin treatment of healthy and senescent cells, respectively; C and D, day 5 after metformin treatment of healthy and senescent cells, respectively; E, cellular viability of healthy fibroblasts treated with metformin and pCBs; F, cellular viability of senescent

fibroblasts treated with metformin and pCBs; G and H, day 1 after TRSV treatment of healthy and senescent cells, respectively; I and J, day 5 after TRSV treatment of healthy and senescent cells, respectively; K, representation of healthy fibroblasts cellular viability treated with TRSV and pCBs; L, cellular viability of senescent fibroblasts treated with TRSV and pCBs. DMSO, dimethyl sulfoxide (vehicle), M, metformin, TRSV, triacetylresveratrol. Data were analyzed with an ANOVA test (Tukey post-hoc multiple comparison test). Bars represent mean ± SD. Significance is indicated within the figures using the following scale: ns, not significant; *, $p<0.05$; **, $p<0.01$; ***, $p<0.001$.

The MTT assay detected significant variability in treatment results depending on the dose, time of the exposure, fibroblasts condition (healthy or senescent), and type of the cell line. It was detected that a single 50 μM of metformin increased cellular viability in healthy CCD-1064Sk fibroblasts, while 10 μM TRSV showed the worst result on day one (Figure 4.2, A and G, respectively). At the same time, none of the rapamycin concentrations induced a significant effect compared to the vehicle, metformin, TRSV, or pCBs (Figure 4.3, A). The viability of senescent fibroblasts was reduced since the beginning of the experiment in all experimental groups following single treatment. On day 1 after treatments, THC and CBD showed better cell growth stimulation compared to best results of metformin (50 μM) or TRSV (50 μM) (Figure 4.2, B and H, respectively). At the same time, 50 μM of rapamycin tended to show better efficacy than pCBs ($p>0.05$, Figure 4.3, B).

Following 5 days of treatment of healthy CCD-1064Sk fibroblasts, it was found that 50 μM of metformin had the strongest effect on modulating cellular viability followed by CBD, 5 μM TRSV, and 1 μM rapamycin (Figures 4.2, C, I and 4.3, C). Simultaneously, the highest efficiency in the senescent fibroblasts was achieved by 50 μM of TRSV, 500 μM of metformin, and 10 μM rapamycin (Figures 4.2, D, J and 4.3, D). Among all NSRs

treatments, TRSV showed the best effect on senescent fibroblasts viability and was the only treatment with a significant increase in viability.

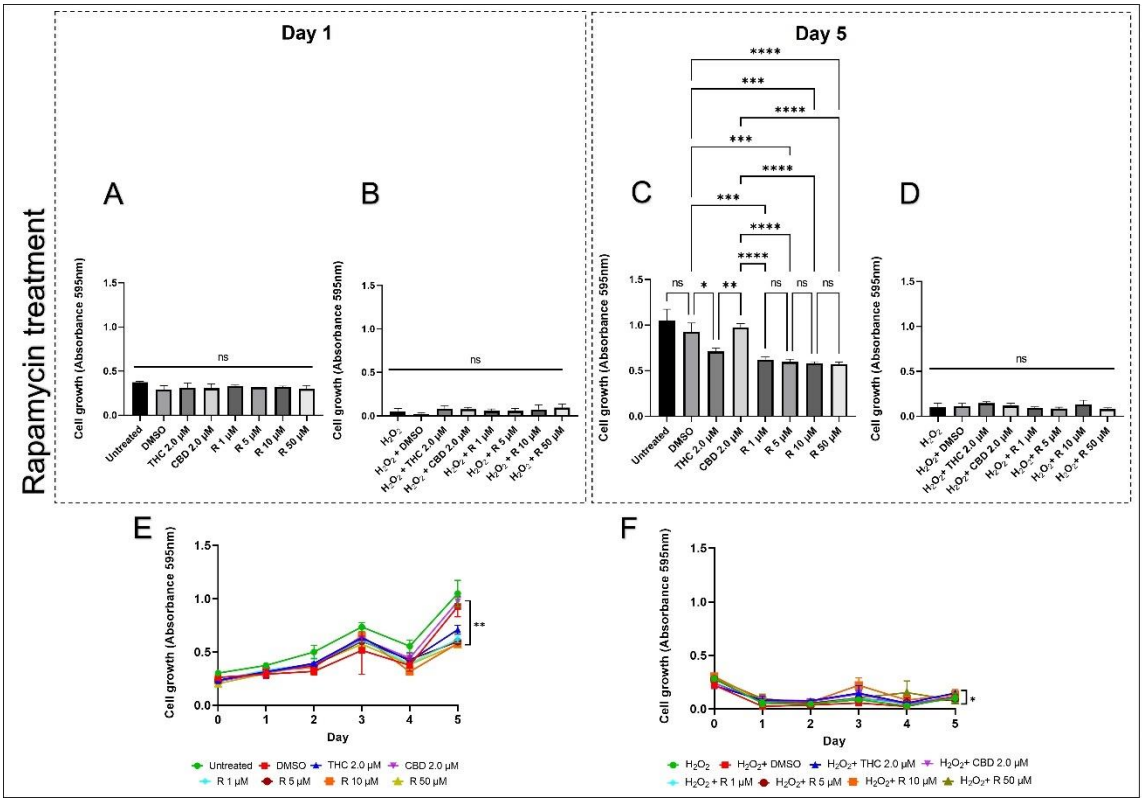

Figure 4.3. Viability of human skin fibroblasts (CCD-1064Sk), 24 PDL exposed to different concentrations of rapamycin compared to THC and CBD. The figure represents gradual changes in cell viability: A and B, day 1 after rapamycin treatment of healthy and senescent cells, respectively; C and D, day 5 after rapamycin treatment of healthy and senescent cells, respectively; E, cellular viability of healthy fibroblasts treated with rapamycin and pCBs; F, cellular viability of senescent fibroblasts treated with rapamycin and pCBs. DMSO, dimethyl sulfoxide (vehicle), R, rapamycin. Data were analyzed with an ANOVA test (Tukey post-hoc multiple comparison test). Bars represent mean ± SD. Significance is indicated within the figures using the following scale: ns, not significant; *, $p<0.05$; **, $p<0.01$; ***, $p<0.001$, ****, $p<0.0001$.

To confirm our findings, the same treatment groups were designed for treatment of BJ-5ta foreskin fibroblasts (Figure 4.4). Analysis of cell viability after single NSRs exposure revealed the most prominent results for 50 µM metformin, 5 µM TRSV, and 5 µM rapamycin in BJ-5ta 90 PDL (Figure 4.4, A, E and I, respectively), while in 93 PDL

results were slightly different: best results were achieved for 500 μM metformin, 50 μM TRSV, and 5 μM rapamycin (Suppl. Figure 16, A, C, and G, respectively). One day after NSRs application on BJ-5ta 90 PDL senescent fibroblasts, the highest cell viability was detected in 500 μM metformin, 10 μM TRSV and 50 μM rapamycin (Figure 4.4. B, F, and J). In the experiment on the BJ-5ta 93 PDL senescent cells, the highest cellular growth was in response to 100 μM metformin, 5 μM TRSV, and 1 μM rapamycin (Suppl. Figure 16, B, D, and F, respectively).

After 5 days of NSRs usage on BJ-5ta 90 PDL healthy fibroblasts, the following had the greatest effect: metformin – 100 μM, TRSV – 10 μM, and rapamycin – 5 μM (Figure 4.4. C, G, and K, respectively), while in BJ-5ta 93 PDL the most beneficial were 50 μM metformin, 5 μM TRSV, and 5 μM rapamycin (Suppl. Figure 16, C). In senescent fibroblasts, the viability was highest after 500 μM metformin, 50 μM TRSV, and 5 μM rapamycin treatments (Figure 4.4, D, H, and L, respectively). Almost identical results were detected in the older passage of fibroblasts culture: 500 μM metformin, 10 μM TRSV, and 5 μM rapamycin (Suppl. Figure 16, H, F, and D, respectively).

Because NSRs demonstrates significant variations in the concentration efficacy, it was decided to test them on an additional model, the adult skin fibroblast cell line CCD-1135Sk 36 PDL. Cellular viability results on the healthy cells showed 50 μM metformin, 5 μM TRSV, and 10 μM rapamycin treatments as beneficial doses after a single 2 h application (Figure 4.5, A, E, and I, respectively). In the senescent fibroblasts, analogues tendency was noted (Figure 4.5, B, F, and J).

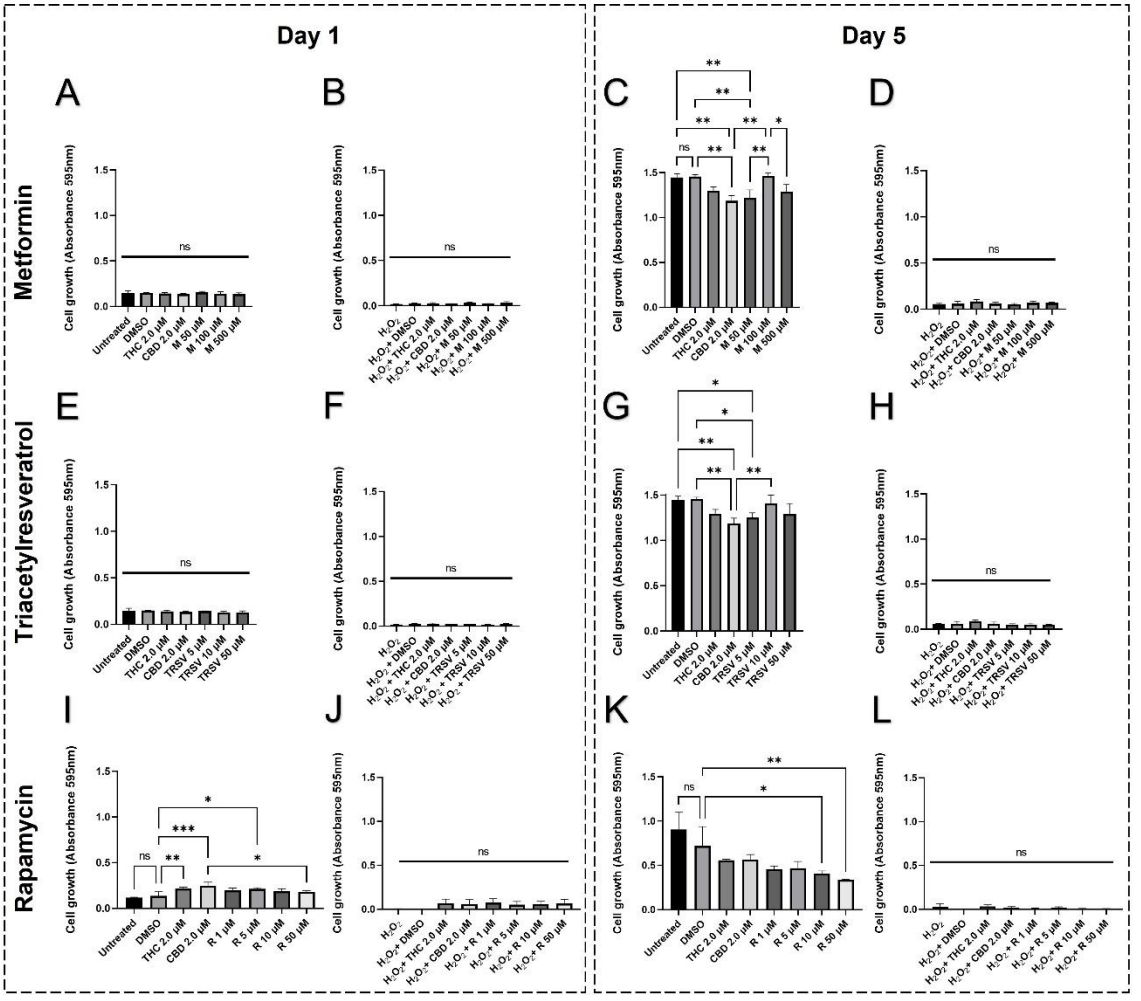

Figure 4.4. Viability of human skin fibroblasts (BJ-5ta), 90 PDL exposed to different concentrations of metformin, triacetylresveratrol, and rapamycin compared to THC and CBD. The figure represents gradual changes in cell viability: A and B, day 1 after metformin treatment of healthy and senescent cells, respectively; C and D, day 5 after metformin treatment of healthy and senescent cells, respectively; E and F, day 1 after TRSV treatment of healthy and senescent cells, respectively; G and H, day 5 after TRSV treatment of healthy and senescent cells, respectively; I and J, day 1 after rapamycin treatment of healthy and senescent cells, respectively; K and L, day 5 after rapamycin treatment of healthy and senescent cells, respectively. DMSO, dimethyl sulfoxide (vehicle); M, metformin; R, rapamycin; TRSV, triacetylresveratrol. Data were analyzed with an ANOVA test (Tukey post-hoc multiple comparison test). Bars represent mean ± SD. Significance is indicated within the figures using the following scale: ns, not significant; *, $p<0.05$; **, $p<0.01$, ***, $p<0.001$.

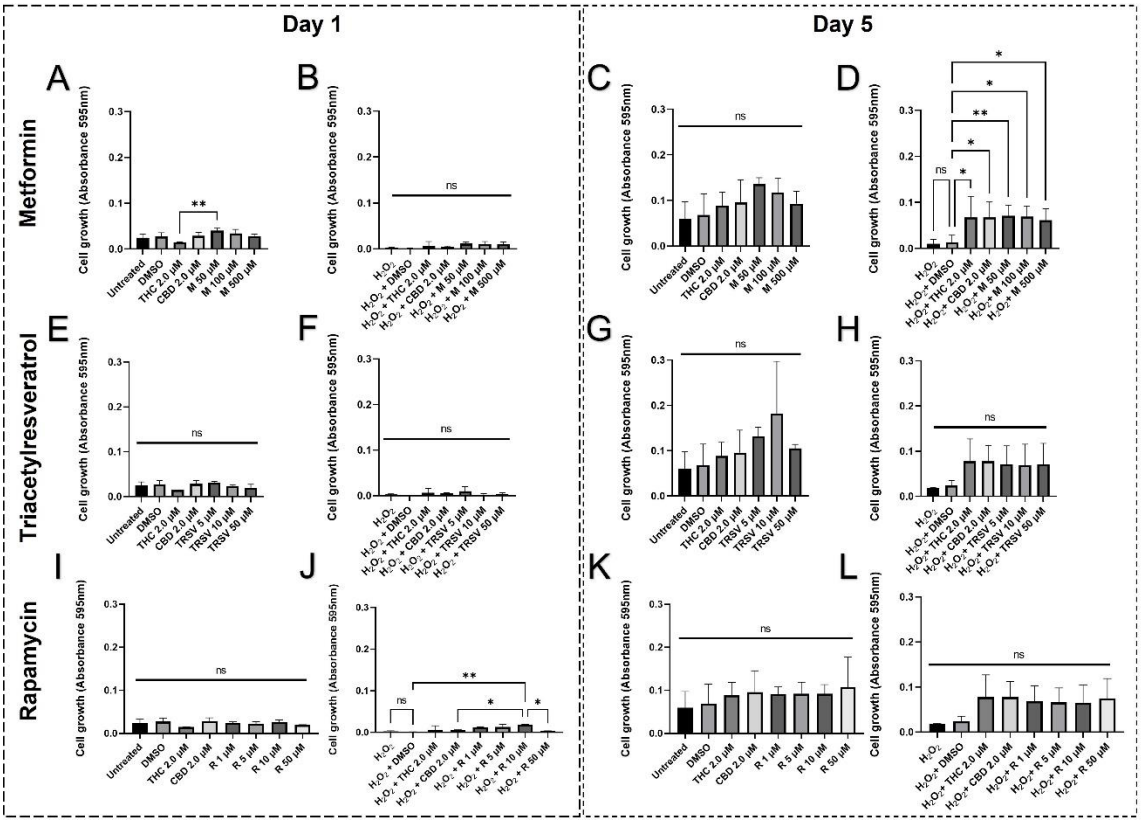

Figure 4.5. Viability of human skin fibroblasts (CCD-1135Sk), 36 PDL exposed to different concentrations of metformin, triacetylresveratrol, and rapamycin compared to THC and CBD. The figure represents gradual changes in cell viability: A and B, day 1 after metformin treatment of healthy and senescent cells, respectively; C and D, day 5 after metformin treatment of healthy and senescent cells, respectively; E and F, day 1 after TRSV treatment of healthy and senescent cells, respectively; G and H, day 5 after TRSV treatment of healthy and senescent cells, respectively; I and J, day 1 after rapamycin treatment of healthy and senescent cells, respectively; K and L, day 5 after rapamycin treatment of healthy and senescent cells, respectively. DMSO, dimethyl sulfoxide (vehicle); M, metformin; R, rapamycin; TRSV, triacetylresveratrol. Data were analyzed with an ANOVA test (Tukey post-hoc multiple comparison test). Bars represent mean ± SD. Significance is indicated within the figures using the following scale: ns, not significant; *, $p<0.05$; **, $p<0.01$.

At the end of the experiment on day 5 of treatment of healthy cells, metformin, TRSV, and rapamycin were maximally effective in doses 50 μM, 10 μM, and 50 μM respectively (Figure 4.5, C, G, and K). Concomitantly, in the group of senescent

fibroblasts, the most beneficial were 50 μM metformin, 5 μM TRSV, and 50 μM rapamycin treatments (Figure 4.5, D, H, and L, respectively).

Based on the data on all cells, it was decided to continue studies with the most effective doses: 500 μM metformin, 10 μM TRSV, and 5 μM rapamycin (Table 4.1).

4.4.2. Effects of nutrient signaling regulators and phytocannabinoids on the nuclear morphology

Based on the earlier discovered nuclear alterations in senescent fibroblasts described in the previous chapters (Figures 2.7, 2.8, 3.8) and the positive influence of phytocannabinoids on the nuclear structure preservation, it was decided to test NSRs alone and combined with pCBs. Dermal fibroblasts were treated with metformin (500 μM), TRSV (10 μM), rapamycin (5 μM), THC (2 μM) and CBD (2 μM).

In healthy dermal fibroblasts CCD-1064Sk, single treatment with metformin increased nuclear area and perimeter ($p<0.05$), while CBD ($p<0.001$) significantly lowered compared to vehicle (DMSO) and was not significantly different from untreated cells (Figure 4.6, A and C). Concomitantly, all treatments reduced nuclear circularity; however, the most significant decline was in response to TRSV ($p<0.0001$, Figure 4.6, B).

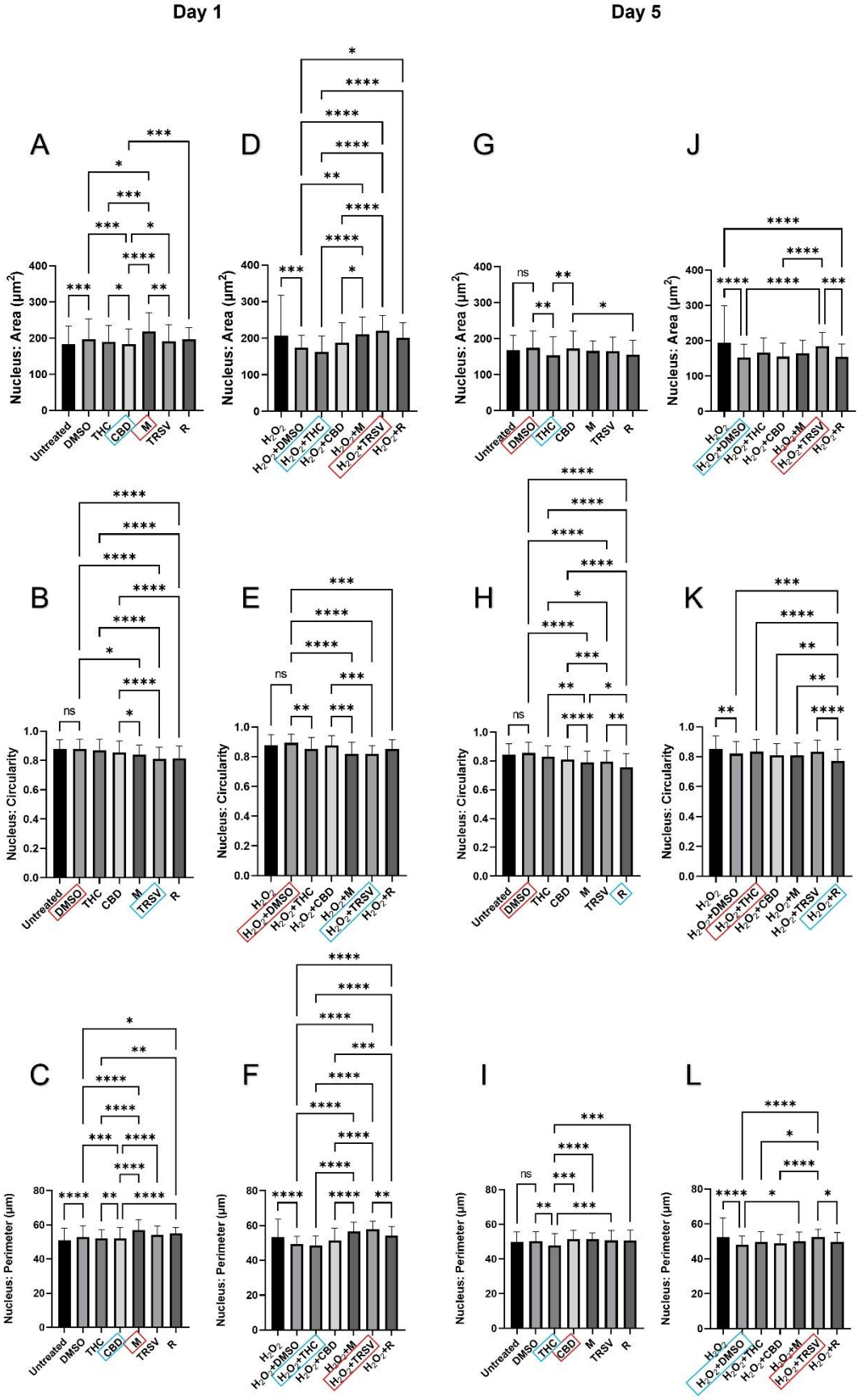
Day 1
Day 5
A
B
C
D
E
F
G
H
I
J
K
L
Nucleus: Area (µm²)
Nucleus: Circularity
Nucleus: Perimeter (µm)
Untreated
DMSO
THC
CBD
M
TRSV
R
H₂O₂
H₂O₂+DMSO
H₂O₂+THC
H₂O₂+CBD
H₂O₂+M
H₂O₂+TRSV
H₂O₂+R
ns

Figure 4.6. Parameters of DAPI stained nuclei of skin fibroblasts CCD-1064Sk, 24 PDL exposed to nutrient signaling regulators and cannabinoids. Figures A-C represent nuclear changes observed by immunofluorescence microscopy in healthy fibroblasts treated with 500 μM metformin (M), 10 μM triacetylresveratrol (TRSV), 5 μM rapamycin (R) and 2 μM of pCBs (THC and CBD) on the day 1; D-F, depict nuclear modifications in senescent fibroblasts on day 1; G-I, show treatment results in healthy fibroblasts on the day 5, while graphs J-L demonstrate data from senescent cells. Graphic representation of nuclear changes on day 1 and day 5 of the experiment, respectively: A, D, G, and J, Nuclear area; B, E, H, and K, nuclear circularity; C, F, I, and L, nuclear perimeter. Dimethyl sulfoxide (DMSO), vehicle. Rectangles depict changes in nuclei parameters: red, highest data; blue, lowest data. Data were analyzed with an ANOVA test (Tukey post-hoc multiple comparison test). Bars represent mean ± SD. Significance is indicated within the figures using the following scale: ns, not significant; *, $p<0.05$; **, $p<0.01$, ***, $p<0.001$, ****, $p<0.0001$.

One day after treatments in the senescent fibroblasts, TRSV increased the nuclear area and perimeter ($p<0.0001$), whereas THC ($p>0.05$) decreased it (Figure 4.6, D and F, respectively). TRSV also decreased nuclear circularity ($p<0.0001$) (Figure 4.6, E).

After 5 days of exposure to healthy fibroblasts, THC reduced the nuclear area and perimeter ($p<0.01$, Figure 4.6, G and I, respectively), while CBD increased nuclear perimeter ($p>0.05$, I), and rapamycin substantially decreased circularity ($p<0.0001$, H) (Figure 4.6). At the same time, the nuclear area and perimeter in senescent fibroblasts increased after TRSV ($p<0.0001$) application compared to vehicle and remained on the level of healthy cells (Figure 4.6, J and L). Besides, THC ($p>0.05$) increased nuclei circularity, whereas rapamycin significantly reduced it (Figure 4.6, K).

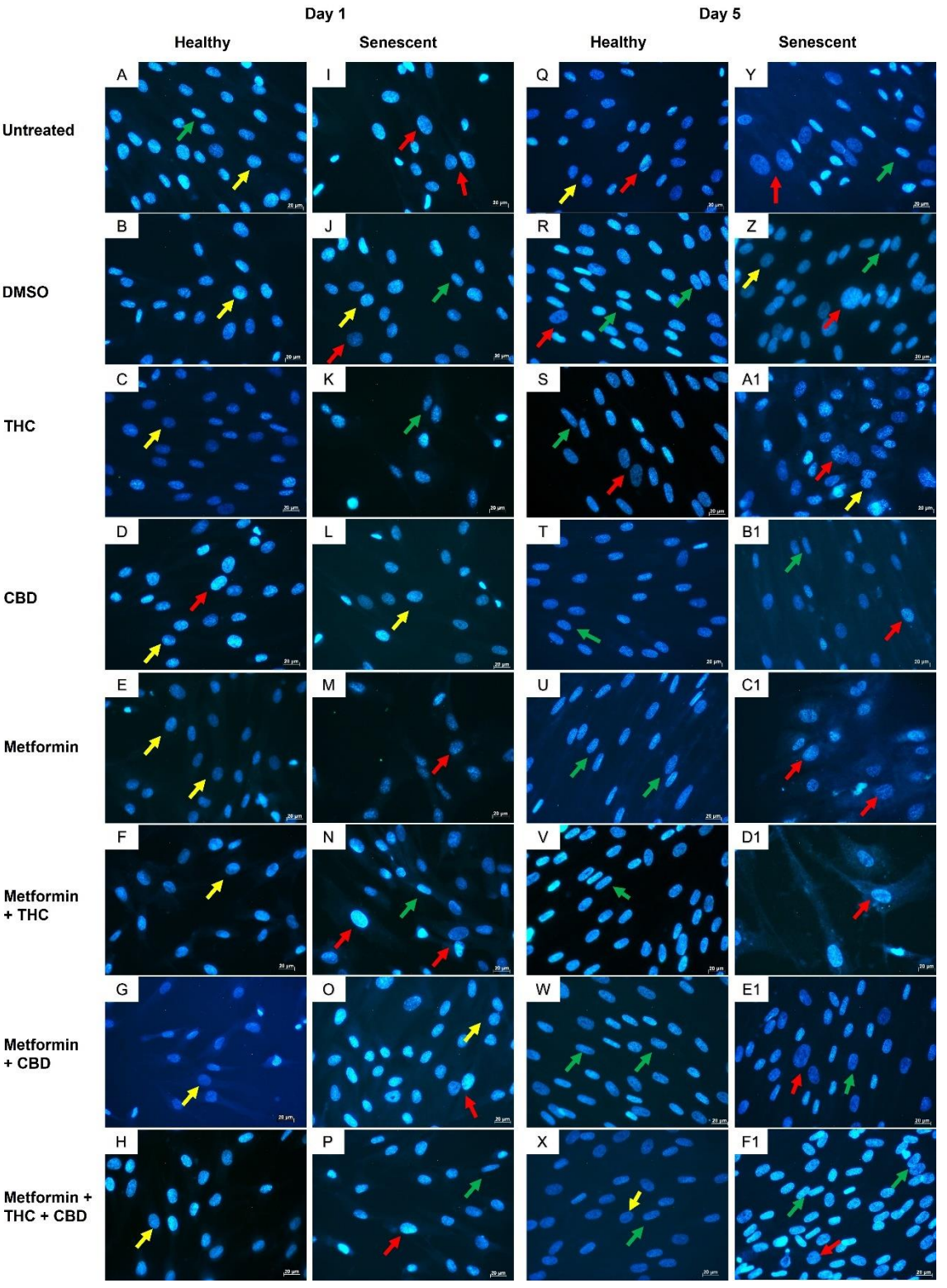

Figure 4.7. DAPI stained nuclei of dermal fibroblasts (CCD-1064Sk), 24 PDL treated with nutrient signaling regulators and cannabinoids. Pictures A-H represent nuclear changes observed by immunofluorescence microscopy in healthy fibroblasts

treated with cannabinoids and 500 µM metformin on day 1; I-P show nuclei of senescent fibroblasts treated with cannabinoids and metformin on day 1; Q-X demonstrate nuclear changes in healthy fibroblasts treated with cannabinoids and metformin on day 5; Y-F1 exhibit nuclear modifications after cannabinoids and metformin on day 5. Arrows depict changes in nuclear shapes: yellow – round, green – elongated, and red – gigantic/irregular.

Apart from testing the effect NSRs and cannabinoids on the dermal fibroblasts as separate compounds, we also decided to combine them (Table 4.2). Similar to our previous findings, nuclei of healthy CCD-1064Sk fibroblasts were round and equal in size. Combining metformin, TRSV, and rapamycin with either THC or CBD did not adversely affect healthy fibroblasts (Figures 4.7, 4.8, A-H, Q-X). The following combinations, however, resulted in changes of nuclear shape and size: metformin + TRSV + rapamycin + THC + CBD (Figure 4.8, D, T). Moreover, a drastic reduction in quantity of the cells was noticed after the combination of rapamycin with THC and CBD in all treatment groups (data not shown).

As in the case with our previous nuclear DAPI staining, we found an increased in size and change in shape of nuclei in aged fibroblasts compared to the CCD-1064Sk healthy cells (Figure 4.7). Compared to the vehicle, it was discovered that senescent fibroblasts treated with combinations of NSRs and pCBs showed fewer nuclear alterations. However, metformin-induced nuclear size irregularities, and nuclear enlargement was observed after metformin-THC (Figure 4.7, M, C1-D1) treatment. After TRSV+THC (Figure 4.8, D1) applications, there was a slight reduction in the cell number and corresponding nuclei.

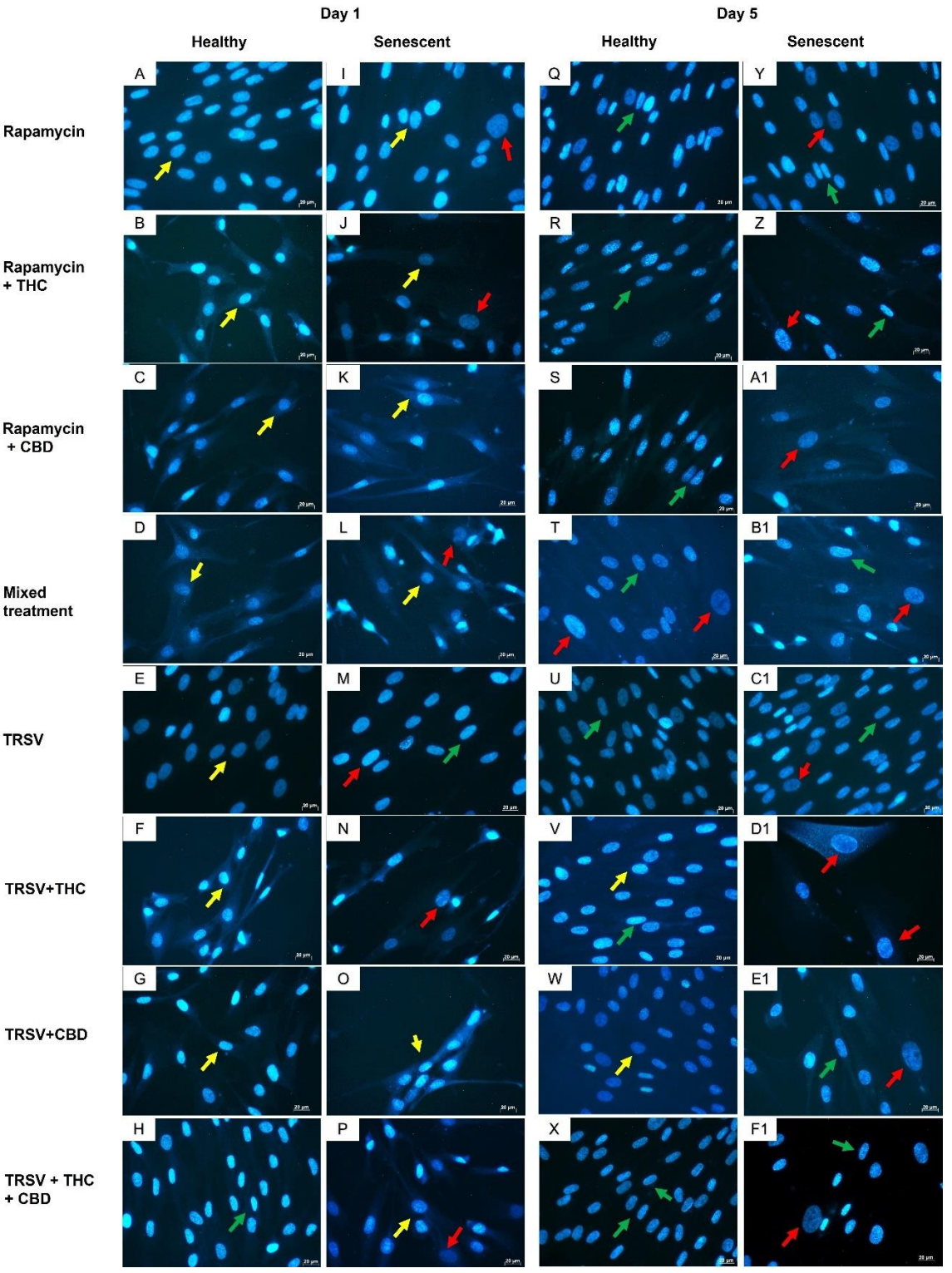

Figure 4.8. DAPI stained nuclei of dermal fibroblasts (CCD-1064Sk), 24 PDL treated with nutrient signaling regulators and cannabinoids. Pictures were taken on day 1 represent nuclear changes observed by immunofluorescence microscopy in healthy fibroblasts treated with: A-C cannabinoids and 5 µM rapamycin; D, mixed treatment,

which included metformin + TRSV + rapamycin + THC + CBD; E-H, 10 μM triacetylresveratrol (TRSV) and pCBs; subsequent photos show nuclei of senescent fibroblasts after 1 day of the treatment by: I-K, rapamycin, and pCBs; L, mixed treatment, which included metformin + TRSV + rapamycin + THC + CBD; M-P, TRSV; following images demonstrate nuclear modifications on day 5 in healthy fibroblasts exposed to: Q-S, rapamycin, and pCBs; T, mixed treatment, which included metformin + TRSV + rapamycin + THC + CBD; U-X, TRSV; next footages exhibit nuclear changes after 5 days of application with: Y-A1, rapamycin, and pCBS; B1, mixed treatment, which included metformin + TRSV + rapamycin + THC + CBD; C1-F1, TRSV. Arrows depict changes in nuclear shapes: yellow – round, green – elongated, and red – gigantic/irregular. DMSO (vehicle)

Most prominent effect on nuclear appearance of the senescent cells was observed in response to 5 days of treatment with metformin+THC+CBD, rapamycin, and TRSV (Figures 4.7 and 4.8).

Morphological observations partially mirrored the changes in the nuclear parameters. CBD, rapamycin, and TRSV increased nuclear area in healthy fibroblasts on day one of the experiments, while metformin+CBD, rapamycin+THC, and TRSV+THC substantially decreased it (Figure 4.9, A-C). In the case of senescent cells, nuclear area was increased in response to metformin ($p>0.05$, D), rapamycin ($p>0.05$, E), and TRSV ($p<0.001$, F), while decreased in response to THC ($p>0.05$, D), TRSV+THC ($p>0.05$, F), and metformin+TRSV+rapamycin+THC+CBD treatment, which included metformin + TRSV + rapamycin + THC + CBD ($p>0.05$, E) (Figure 4.9).

At day 5 after treatment, THC significantly increased nuclear area in healthy cells. In contrast, metformin ($p<0.01$, G), rapamycin+CBD ($p>0.05$, H), and TRSV+CBD ($p>0.05$, I) reduced nuclear area compared to vehicle (Figure 4.9). In senescent cells, metformin+THC ($p<0.0001$, J), rapamycin+THC ($p<0.0001$, K), and TRSV+CBD ($p<0.0001$, L) increased nuclear area (Figure 4.9).

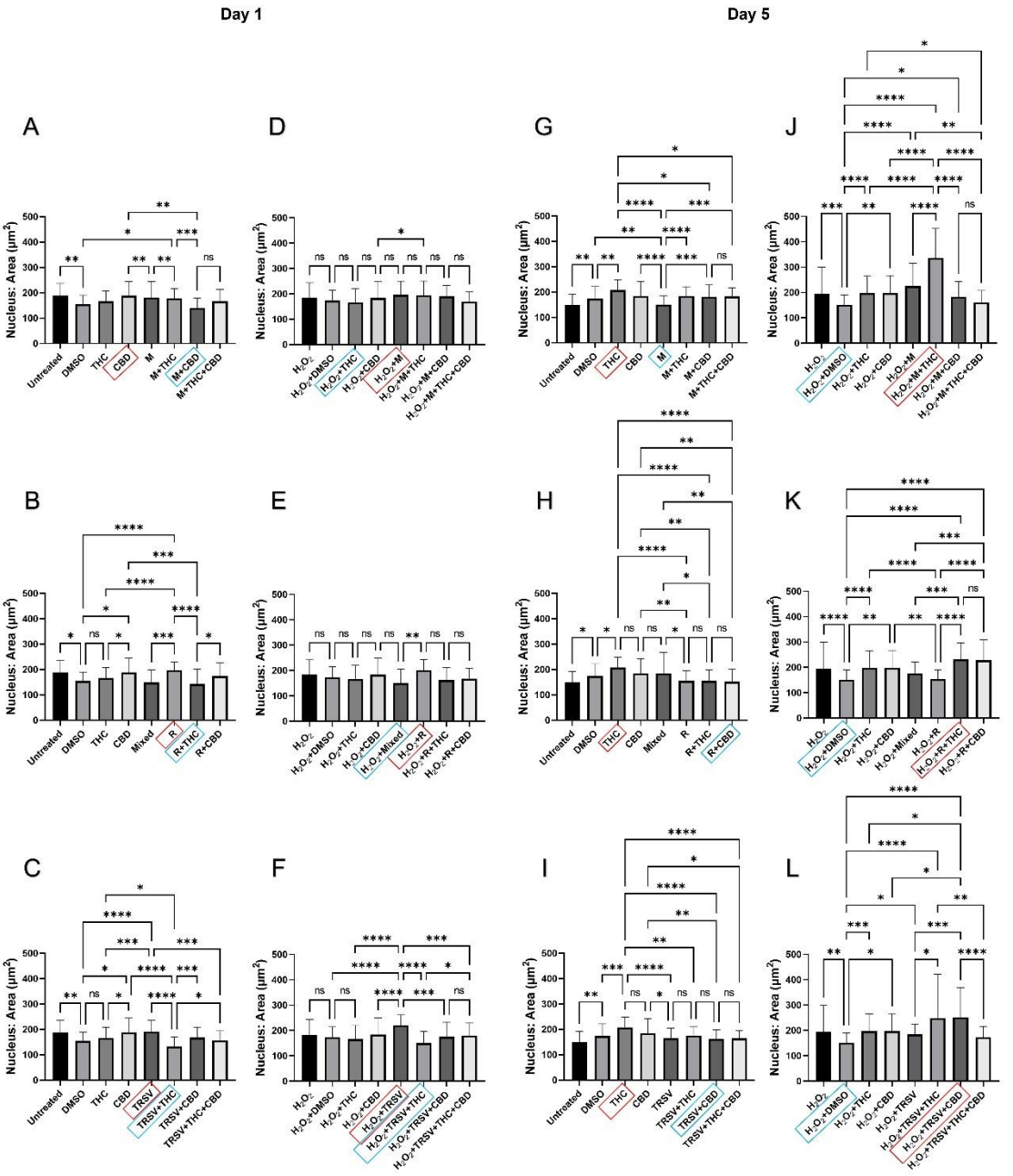

Figure 4.9. DAPI stained nuclei area parameters of skin fibroblasts CCD-1064Sk, 24 PDL exposed to metformin, triacetylresveratrol, and rapamycin combined with pCBs. Figures A-C represent nuclear area changes observed by immunofluorescence microscopy in healthy fibroblasts treated with 500 µM metformin (M), 10 µM triacetylresveratrol (TRSV), 5 µM rapamycin (R) and 2 µM of pCBs (THC and CBD) and their combinations on the day 1; D-F, nuclear area modifications in senescent fibroblasts on day 1; G-I, nuclei area in healthy fibroblasts on the day 5; J-L nuclei area in senescent cells on the day 5. Dimethyl sulfoxide (DMSO), vehicle. Rectangles depict changes in nuclei parameters: red, largest; blue, lowest. Data were analyzed with an ANOVA test (Tukey post-hoc multiple comparison test). Bars represent

mean ± SD. Significance is indicated within the figures using the following scale: ns, not significant; *, $p<0.05$; **, $p<0.01$, ***, $p<0.001$, ****, $p<0.0001$

Summary of the nuclear parameters in CCD-1064Sk and BJ-5ta cell lines after treatments with NSRs and cannabinoids is presented in Table 4.3.

Table 4.3. Nuclear parameters after fibroblast CCD-1064Sk and BJ-5ta cell line treatments with nutrient signaling regulators and cannabinoids

Day of experiment	Condition	Cell line	NA		NP		NC		MaxC		MinC		NE	
			Max	Min	Max	Min	Max	Min	Max	Min	Max	Min	Max	Min
DAY 1	Healthy	CCD-1064Sk, p.11	R	TRSV + THC	R	TRSV + THC	**CBD**	**R + CBD**	**R**	TRSV + THC	**M + THC**	**TRSV + THC**	**R**	Mixed
		BJ-5ta, p.42	R + CBD	TRSV + CBD	R + CBD	TRSV + CBD	**DMSO**	**R + CBD**	R + CBD	TRSV + CBD	M + THC + CBD	TRSV + CBD	Mixed	**M + THC**
	Senescent	CCD-1064Sk, p.11	TRSV	Mixed	TRSV	CBD	M + THC + CBD	Mixed	TRSV	CBD	**TRSV + THC + CBD**	**TRSV + THC**	TRSV	**TRSV + THC + CBD**
		BJ-5ta, p.42	**THSV + THC + CBD**	R + CBD	Mixed	**DMSO**	**DMSO**	TRSV + THC	Mixed	**DMSO**	**TRSV + THC + CBD**	CBD	R + CBD	**TRSV + THC + CBD**
DAY 5	Healthy	CCD-1064Sk, p.11	THC	M	THC	R + CBD	**CBD**	**R**	THC	R + CBD	CBD	M	**R**	CBD
		BJ-5ta, p.42	**TRSV + THC + CBD**	TRSV	TRSV + THC + CBD	TRSV	M + THC	**R**	**R**	**TRSV**	**M + THC**	TRSV	**R**	TRCV + CBD
	Senescent	CCD-1064Sk, p.11	M + THC	**DMSO**	M + THC	**DMSO**	TRSV + THC	**R**	M + THC	**DMSO**	**M + THC**	R	**R**	TRSV + THC
		BJ-5ta, p.42	TRSV + THC	**DMSO**	M	**DMSO**	THC	M	THSV + THC	**THSV**	THSV + THC	DMSO	DMSO	**M + THC**

CBD, cannabidiol; DMSO, dimethyl sulfoxide (vehicle); M, metformin; MaxC, max caliper; MinC, min caliper; Mixed, includes combination of metformin + TRSV + rapamycin + THC + CBD; NA, nuclear area; NC, nuclear circularity; NE, nuclear eccentricity; NP, nuclear perimeter; R, rapamycin; THC, Δ-9-tetrahydrocannabinol; TRSV, triacetylresveratrol. The bold blue text depicts data from several experiments.

4.4.3. Influence of nutrient signaling regulators and cannabinoids on the expression of senescence-related genes and metabolic response

Earlier, we have reported that senescent cells demonstrate adverse changes in the expression of genes involved in cell-cycle regulation paralleled by changes in cell morphology (Chapter 2). It was discovered that phytocannabinoids showed favorable effects on the expression of corresponding genes and partially improved cellular viability, functional and metabolic activity (Chapter 3). Based on these findings, together with data from nuclear DAPI staining after NSRs and cannabinoids treatments, it was decided to test whether metformin, TRSV, rapamycin, and their combinations with pCBs will affect gene expression in healthy and senescent fibroblasts.

The mRNA transcripts levels of cell-cycle progression regulators and senescence-associated markers *CDKN2A (p16)*, *CDKN1A (p21)*, and *TP53* were measured via RT-PCR after five days of the experimental treatments.

The *CDKN2A* levels were significantly upregulated in healthy fibroblasts compared to the vehicle after rapamycin ($p<0.0001$) and TRSV+CBD ($p<0.0001$); it also showed a tendency to increase following metformin, metformin+THC treatments, whereas in response to metformin+CBD, TRSV, and TRSV+THC it had a tendency to decrease ($p>0.05$, Figure 4.10, A).

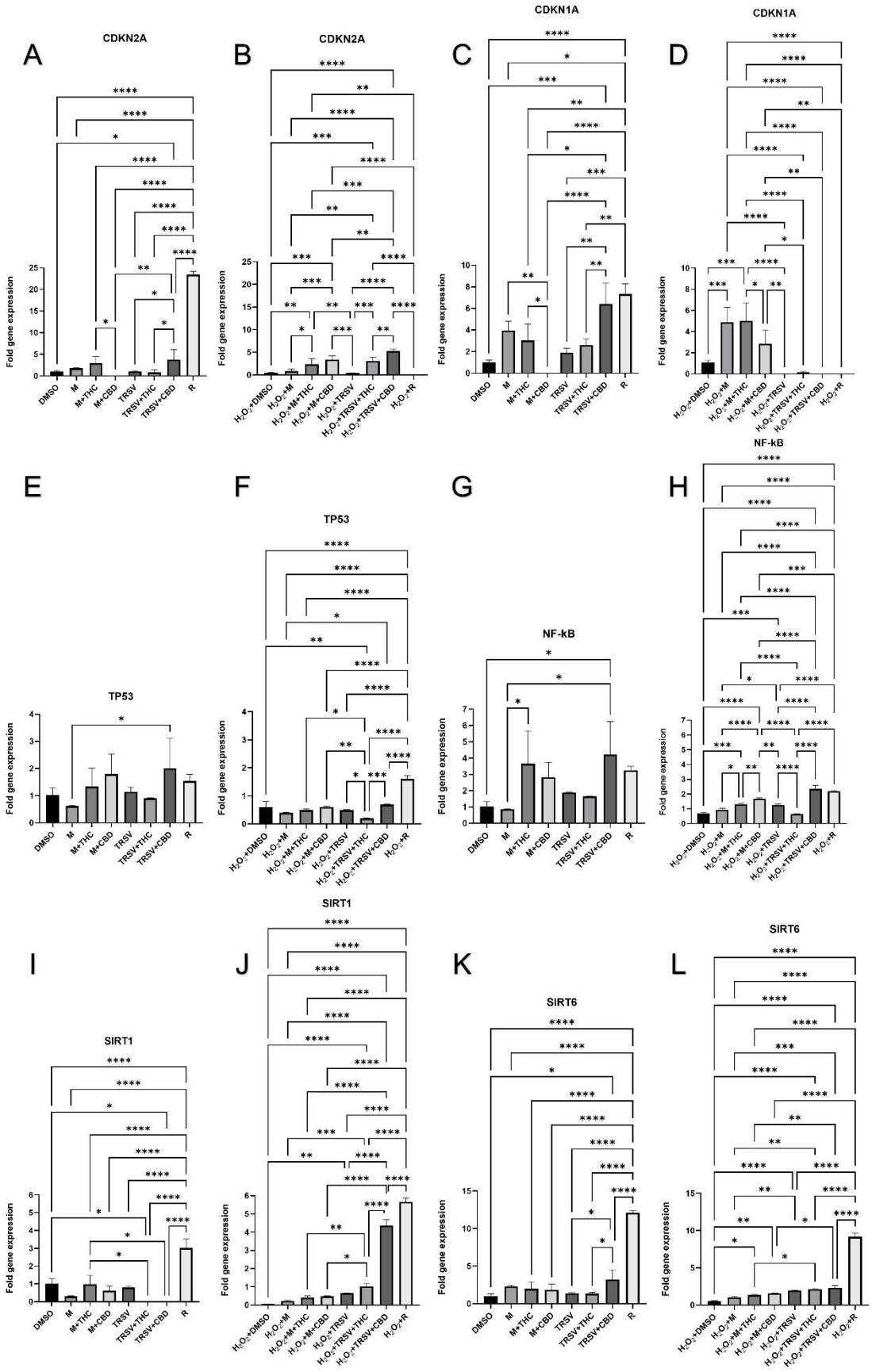
A
CDKN2A
B
CDKN2A
C
CDKN1A
D
CDKN1A
E
TP53
F
TP53
G
NF-kB
H
NF-kB
I
SIRT1
J
SIRT1
K
SIRT6
L
SIRT6
Fold gene expression
DMSO
M
M+THC
M+CBD
TRSV
TRSV+THC
TRSV+CBD
R
H2O2+DMSO
H2O2+M
H2O2+M+THC
H2O2+M+CBD
H2O2+TRSV
H2O2+TRSV+THC
H2O2+TRSV+CBD
H2O2+R

Figure 4.10. The expression of cellular checkpoint regulators in CCD-1064Sk fibroblasts treated with nutrient signaling regulators combined with cannabinoids. Changes of mRNA expression as measured by RT-PCR for *CDKN2A (p16)* in healthy (A) and senescent (B) fibroblasts: *CDKN1A (p21)* in healthy (C) and senescent (D); *TP53* in healthy (E) and senescent (F); *NF-κB* in healthy (G) and in senescent (H); *SIRT1* in healthy (I) and senescent (J); *SIRT6* in healthy (K) and senescent (L). CBD, cannabidiol; DMSO, dimethyl sulfoxide (vehicle), M, metformin; R, rapamycin; THC, Δ-9-tetrahydrocannabinol; TRSV, triacetylresveratrol. Data were analyzed with an ANOVA test (Tukey post-hoc multiple comparison test). Bars represent mean ± SD. Significance is indicated within the figures using the following scale: *, $p<0.05$; **, $p<0.01$; ***, $p<0.001$; ****, $p<0.0001$.

In the senescent cells, we observed *CDKN2A* upregulation induced by metformin ($p>0.05$), metformin+THC ($p<0.01$), metformin+CBD ($p<0.001$), TRSV+THC ($p<0.001$), and TRSV+CBD ($p<0.0001$), while TRSV ($p>0.05$) and rapamycin ($p>0.05$) alone downregulated it (Figure 4.10 B).

At the same time, the *CDKN1A* mRNA levels in healthy fibroblasts were reduced after metformin+CBD ($p<0.01$) application, whereas all other treatments increased expression (Figure 4.10, C). Like for *CDKN2A* in healthy cells, the significantly increased *CDKN1A* expression was associated with rapamycin ($p<0.0001$) and TRSV+CBD ($p<0.001$) exposure. In the senescent cells, *CDKN1A* expression decreased by rapamycin ($p>0.05$), TRSV ($p>0.05$), TRSV+THC ($p>0.05$), and TRSV+CBD ($p>0.05$), and increased by metformin alone ($p<0.001$) and in combinations with pCBs ($p<0.001$) (Figure 4.10, D).

Interestingly, the expression of the most critical cellular check-point regulator, "gatekeeper" *TP53*, slightly increased ($p>0.05$) after applications of metformin+THC, metformin+CBD, TRSV+CBD, and rapamycin, while it decreased in response to

metformin ($p>0.05$) and TRSV+THC ($p>0.05$) in the healthy dermal fibroblasts (Figure 4.10, E). At the same time, TRSV did not change *TP53* mRNA levels. Surprisingly, we also discovered rapamycin-induced upregulation ($p<0.0001$) in the senescent cells similar to the healthy ones. Significant decrease in *TP53* expression in response to the TRSV+THC treatment was observed ($p<0.01$), while there was no change in response to other treatments (Figure 4.10, F).

One of the prominent regulators of the numerous genes associated with cell survival, proliferation, and differentiation expression, *NF-κB*, was upregulated in healthy dermal fibroblasts in all treatment groups except metformin ($p>0.05$) following 5 days of treatment (Figure 4.10, G). In the senescent fibroblasts, we found increased *NF-κB* mRNA levels of in most of the treatment groups except TRSV+THC group, which remained slightly downregulated ($p>0.05$) compared to the vehicle (Figure 4.10, H). However, NF-κB transcripts in SIPS fibroblasts were lower than corresponding levels in the healthy cells.

Another essential role of NF-κB is associated with metabolic pathways and is directly related to sirtuin regulation (Ma et al., 2015). For this reason, we also tested the influence of pCBs combined with NSRs on the mRNA levels of *SIRT1* and *SIRT6* that have been negatively affected in senescent cells in our previous experiments (Chapters 2 and 3). The *SIRT1* and *SIRT6* expression remained almost unchanged in the healthy fibroblasts in all treatment groups except rapamycin ($p<0.0001$, Figure 4.10, I and K), which resulted in significantly upregulated expression of these genes. Besides, the "longevity" biomarker *SIRT1* was downregulated after TRSV+THC and TRSV+CBD application ($p<0.05$, Figure 4.10, I). Rapamycin, TRSV+CBD, and TRSV+THC increased *SIRT1* and *SIRT6* expression ($p<0.0001$), TRSV alone also increased *SIRT1* ($p<0.01$) and *SIRT6* ($p<0.0001$) in SIPS

fibroblasts. At the same time, a significant increase of the metformin alone and combined with pCBs was not significantly affected, albeit. it exerted a tendency to upregulate *SIRT1* ($p<0.05$, Figure 4.10, L). In contrast, *SIRT6* expression was found elevated in response to metformin+THC ($p<0.05$, L) and metformin+CBD ($p<0.01$, L) treatments, but to metformin alone (Figure 4.10, L).

Here, we can speculate that rapamycin and TRSV alone or combined with CBD or THC may restimulate cellular growth and metabolic activity in the senescent cells via reduction of cell growth inhibitors *p16, p21, TP53,* accompanied by potentiation of *NF-κB* expression and corresponding elevation of metabolic biomarkers *SIRT1* and *SIRT6.*

4.4.4. Protective effects of nutrient signaling regulators and phytocannabinoids on the expression of age-related genes involved in ECM maintenance

The results of our previous experiments (Chapters 2 and 3) are in line with literature data showing that ECM components and their production are adversely affected in the SIPS fibroblasts. It was revealed that functional and metabolic activity substantially deteriorated in the aged dermal cells, while pCBs showed a potential to preserve and stimulate ECM generation. These findings increased our curiosity on whether NSRs alone or in combination with pCBs have the potential to stimulate collagen and elastin production or preserve it from senescence-associated degradation. Moreover, we also tested whether those treatments changed the expression of cannabinoid receptors.

The mRNA level of the dermal collagen type I (*COL1A1*) was increased after experimental treatments except metformin+CBD ($p>0.05$) exposure in healthy fibroblasts

(Figure 4.11, A). Unfortunately, proposed "anti-aging" treatments were ineffective in the senescent fibroblasts. A significant reduction in *COL1A* expression was detected in response to metformin+THC ($p<0.01$), TRSV+THC ($p<0.01$), TRSV+CBD ($p<0.01$), and rapamycin ($p<0.01$) treatments (Figure 4.11, B).

Compared to the *COL1A1* data, the *COL3A1* expression was different in healthy and senescent fibroblasts. The mRNA levels of *COL3A1* in healthy fibroblasts were unchanged after metformin+CBD, TRSV, and rapamycin application, decreased after metformin ($p>0.05$), TRSV ($p>0.05$), and TRSV+CBD ($p>0.05$), while slightly increased in response to metformin+THC ($p>0.05$) (Figure 4.11, C). Meanwhile, in the senescent fibroblasts TRSV+CBD and rapamycin treatments induced significant ($p<0.0001$ for both) upregulation of *COL3A1*, while other treatments inhibited *COL3A1* expression (Figure 4.11, D).

In addition to collagens, skin integrity depends on the elastin activity, which is critical to the elasticity and resilience of many vertebrate tissues, including skin, large arteries, lung, ligament, tendon, and elastic cartilage (Mithieux & Weiss, 2005). In healthy fibroblasts, a substantially increased expression of *ELN* mRNA was noted in response to TRSV+CBD ($p<0.01$, Figure 4.11, G). In contrast, in the senescent cells, the most effective were rapamycin ($p<0.0001$), TRSV alone ($p<0.01$), TRSV combined with THC ($p<0.001$), and CBD ($p<0.05$) (Figure 4.11, H).

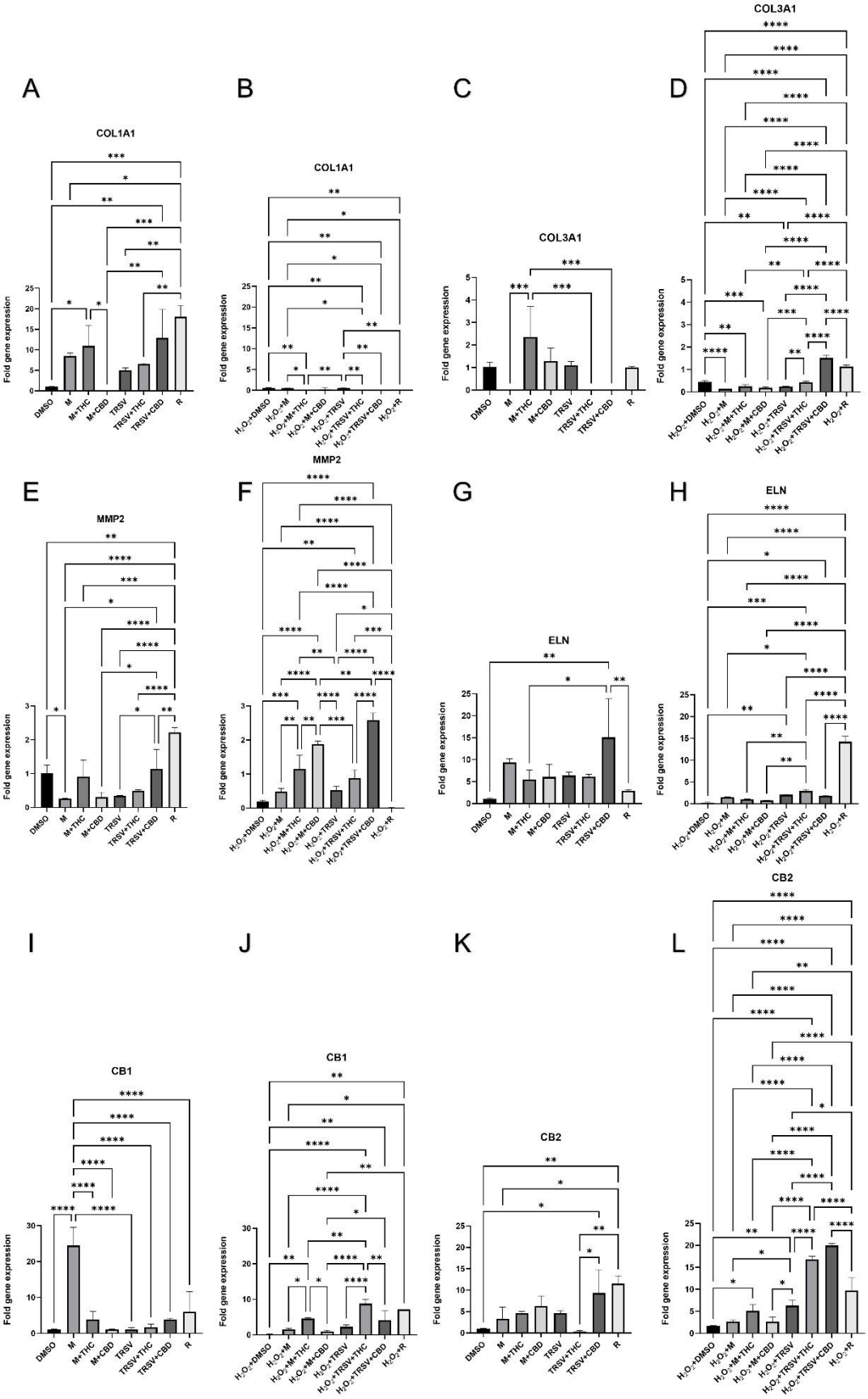
A
COL1A1
Fold gene expression
DMSO
M
M+THC
M+CBD
TRSV
TRSV+THC
TRSV+CBD
R
B
COL1A1
Fold gene expression
H2O2+DMSO
H2O2+M
H2O2+M+THC
H2O2+M+CBD
H2O2+TRSV
H2O2+TRSV+THC
H2O2+TRSV+CBD
H2O2+R
C
COL3A1
Fold gene expression
D
COL3A1
Fold gene expression
E
MMP2
Fold gene expression
F
MMP2
Fold gene expression
G
ELN
Fold gene expression
H
ELN
Fold gene expression
I
CB1
Fold gene expression
J
CB1
Fold gene expression
K
CB2
Fold gene expression
L
CB2
Fold gene expression

Figure 4.11. Effects of phytocannabinoids and nutrient signaling regulators on the expression of genes involved in the production of extracellular matrix in CCD-1064Sk. Changes of mRNA expression as measured by RT-PCR for A, *COL1A1* in healthy and B, senescent fibroblasts: C, *COL3A1* in healthy and D, senescent; E, *MMP2* in healthy and F, senescent; G, *ELN* (elastin) in healthy and H, in senescent; I, *CB1* in healthy and J, in senescent; K, *CB2* in healthy and L, in senescent. CBD, cannabidiol; DMSO, dimethyl sulfoxide (vehicle), M, metformin; R, rapamycin; THC, Δ-9-tetrahydrocannabinol; TRSV, triacetylresveratrol. Data were analyzed with an ANOVA test (Tukey post-hoc multiple comparison test). Bars represent mean ± SD. Significance is indicated within the figures using the following scale: *, $p<0.05$; **, $p<0.01$; ***, $p<0.001$; ****, $p<0.0001$.

In the healthy cells and tissues microenvironment, all components of ECM must stay in the equilibrium. Most ECM proteins during organogenesis, growth and normal tissue turnover are degraded by a group of metalloproteinases (MMPs). MMPs are enzymes that, in concert, are responsible for preventing excessive production and accumulation of healthy or damaged scaffold components. Typically, the expression and activity of MMPs in adult tissues usually are pretty low (Sorsa et al., 2004). However, the MMP level exponentially increases in an age-dependent manner, and is found in numerous pathological conditions that may lead to unwanted tissue destruction, such as inflammatory conditions, tumor enlargement, and metastasis (Ashcroft et al., 1997; Chiang et al., 2011).

We discovered significant metformin-induced ($p<0.05$) inhibition of *MMP2* in healthy fibroblast cells. *MMP2* expression was unchanged in response to metformin+THC and TRSV+CBD, while it increased in response to rapamycin ($p<0.01$) (Figure 4.11, E). Other treatments tended to decrease the level of *MMP2* transcripts. In senescent fibroblasts, all experimental groups except rapamycin ($p>0.05$) showed an increase in *MMP2* expression (Figure 4.11, F). It was significantly augmented after metformin+THC ($p<0.001$), metformin+CBD ($p<0.0001$), TRSV+THC ($p<0.01$), and TRSV+ CBD ($p<0.0001$) exposures.

Cannabinoid receptors CB1 and CB2 are part of the endocannabinoid system (ECS) and belong to the Class A (rhodopsin (Rho) family) of G-protein coupled receptors (GPCRs) and are known to interact with different phytocannabinoids (Morales et al., 2017; Morales & Reggio, 2017). These receptors are differentially expressed throughout the body, and the level of expression is correlated with time and dose of cannabinoids exposure (Ketcherside et al., 2017). CB1 receptors are mainly found in the neural system and less in other tissues, while CB2 is primarily associated with the immune and gastrointestinal systems (Caterina, 2014). Both CB1 and CB2 expression were identified in the normal human skin and its appendages: keratinocytes, hair follicles, sebaceous glands, melanocytes, fibroblasts, nerve fibers, adipocytes, sensory neurons, and immune cells (Scheau et al., 2020). However, information that discloses the response of CB1 and CB2 expression to the combined nuclear signaling regulator and pCBs treatments is absent.

We identified metformin-stimulated increased expression of *CB1* ($p<0.0001$), and slight elevation associated with metformin+THC, TRSV+CBD, and rapamycin ($p>0.05$ for all) exposure in healthy dermal fibroblasts (Figure 4.11, I). In contrast, metformin+THC ($p<0.01$), TRSV+THC ($p<0.0001$), TRSV+CBD ($p<0.01$), and rapamycin ($p<0.01$) significantly augmented *CB1* transcripts levels in prematurely aged cells (Figure 4.11, J).

At the same time, the mRNA expression of *CB2* was not affected by TRSV+THC application in healthy fibroblasts, while other treatments increased the expression, namely TRSV+CBD ($p<0.05$) and rapamycin ($p<0.01$) (Figure 4.11, K). In senescent cells, *CB2* expression increased in all treatment groups (Figure 4.11, L). The most efficient increase of *CB2* expression was in response to metformin+THC ($p<0.05$), rapamycin ($p<0.0001$), TRSV ($p<0.01$), and its combinations with THC or CBD ($p<0.0001$).

Endocannabinoids and their receptors are a constituent part of an adaptive system to regulate cutaneous inflammation, in turn, potentiation of inflammatory process is associated with decreased expression of *CB1/CB2* (Caterina, 2014). Besides, inflammation is an integral component of the aging process (Lago & Puzzi, 2019). Following these facts and our experimental data, we can speculate that the increase in the mRNA expression of *CB1* and *CB2* in senescent dermal fibroblasts in response to combined pCBs and NSRs treatment represents the initiation of the anti-aging protective mechanisms.

4.4.5. Phytocannabinoids combined with nutrient signaling regulators preserve cellular viability in SIPS fibroblasts

Our experiments tested different concentrations of NSRs (Table 4.1) to detect optimal safe doses with potential anti-aging properties (Figures 4.2 and 4.3). The present study tested cell viability after metformin, TRSV, and rapamycin treatments combined with THC and CBD as analyzed by MTT and Neutral red (NR) assays.

The viability of healthy fibroblasts exposed to metformin, TRSV, or rapamycin combined with pCBs was not significantly altered based on the MTT assay results on day one of the experiments ($p>0.05$, Figure 4.12, A, E, I). At the same time, metformin+TRSV+rapamycin+THC+CBD treatment, which included metformin, TRSV, rapamycin, THC, and CBD, significantly inhibited cellular growth ($p<0.001$, Figure 4.12, I). In addition, it was noted that CBD partially decreased fibroblasts viability. Compared to the healthy cells, the viability of senescent cells decreased. We also discovered significant CBD-induced inhibition of SIPS fibroblasts viability (Figure 4.12, B, F, and J).

Following five days of treatments, we found that NSRs combined with cannabinoids, such as metformin+THC ($p<0.05$), metformin+CBD ($p<0.05$), TRSV+THC ($p<0.01$), TRSV+CBD ($p<0.05$) tended to slow down cellular growth of healthy cells (Figure 4.12, C and G). Additionally, the viability of senescent dermal fibroblasts was not affected by metformin or TRSV combined with pCBs ($p>0.05$, Figure 4.12, D, and H). In parallel, we identified the significant reduction in cellular growth induced by rapamycin ($p<0.01$), rapamycin+THC ($p<0.05$), rapamycin+CBD ($p<0.01$), and metformin+TRSV+rapamycin+THC+CBD treatments ($p<0.01$) (Figure 4.12, L).

We also compared the efficacy of each treatment on cellular viability based on MTT assay in healthy and senescent dermal fibroblasts (Figure 4.13). Our study showed that rapamycin alone and combined with pCBs, as well as metformin+TRSV+rapamycin+THC+CBD had a detrimental effect on cellular viability in healthy and senescent dermal fibroblasts of the CCD-1064Sk cell line (Figure 4.13, E-H). In the CCD-1135Sk cell line, NSRs and pCBs treatments did not show significant differences (Suppl. Figure 17).

After MTT cell viability analysis, we additionally performed NR assay. NR assay results estimate cellular viability or potential cytotoxicity based upon the accumulation of the supravital dye neutral red in the lysosomes (Repetto et al., 2008). The skin fibroblasts viability was tested after 72 h of the NSRs combined with pCBs exposure. We found significant growth potentiation in healthy cells treated with THC and CBD ($p<0.0001$), and its inhibition was induced by metformin+THC ($p<0.0001$, Figure 4.14, A). Additionally, TRSV+CBD increased cellular viability in healthy fibroblasts ($p<0.0001$, Figure 4.14, B), while rapamycin+THC substantially inhibited cell growth ($p<0.05$, Figure 4.14, C).

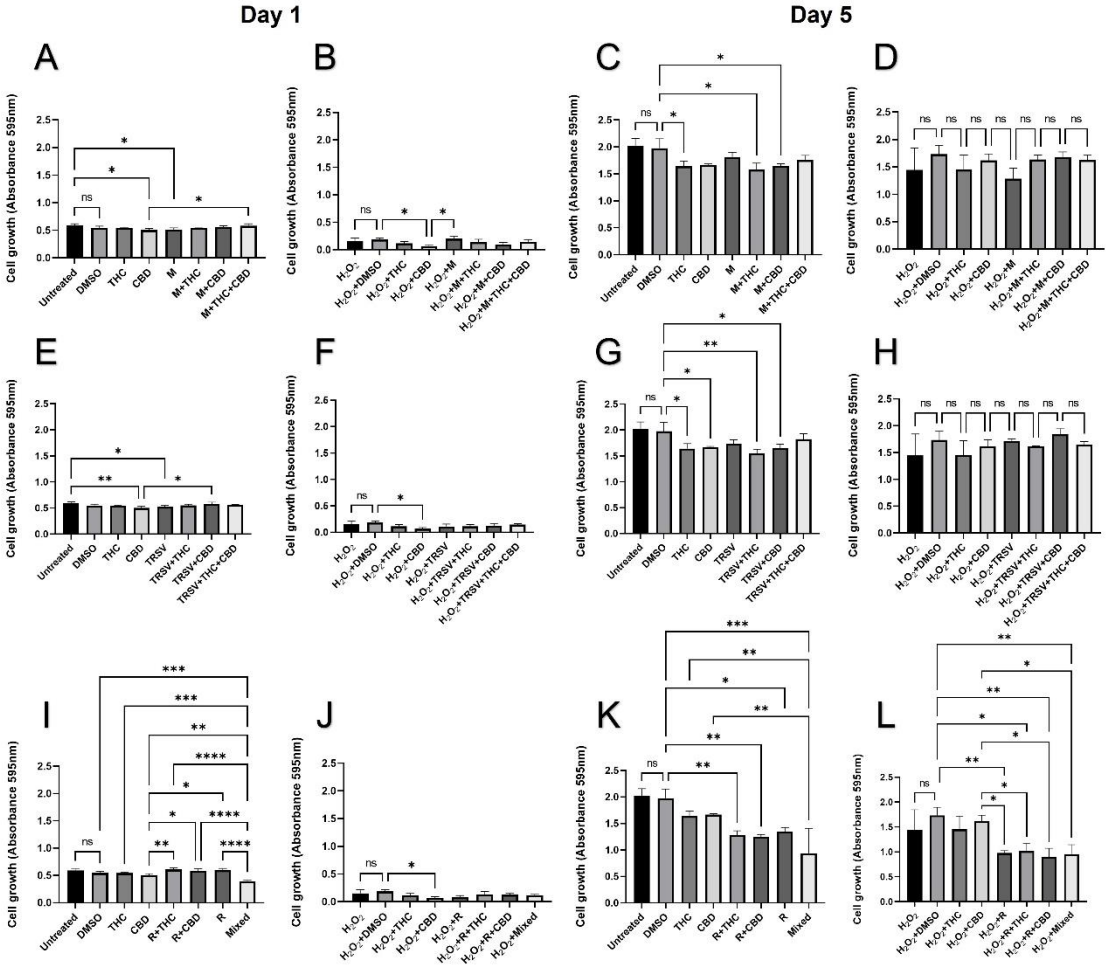

Figure 4.12. Viability of dermal fibroblasts CCD-1064Sk, 24 PDL, treated with nutrient signaling regulators combined with phytocannabinoids. The graphs represent cell viability of skin fibroblasts analyzed by MTT assay after experimental treatments with nutrient signaling regulators combined with THC and CBD. The day 1 results in healthy cells (A, E, and I) and senescent cells (B, F, and J). The day 5 data for healthy fibroblasts (B, F, and J) and senescent cells (D, H, L). CBD, cannabidiol; DMSO, dimethyl sulfoxide, M, metformin; Mixed, included metformin + TRSV + rapamycin + THC + CBD; R, rapamycin; THC, Δ-9-tetrahydrocannabinol; TRSV, triacetylresveratrol. Data were analyzed with an ANOVA test (Tukey post-hoc multiple comparison test). Bars represent mean ± SD. Significance is indicated within the figures using the following scale: ns, not significant; *, $p<0.05$; **, $p<0.01$; ***, $p<0.001$; ****, $p<0.0001$.

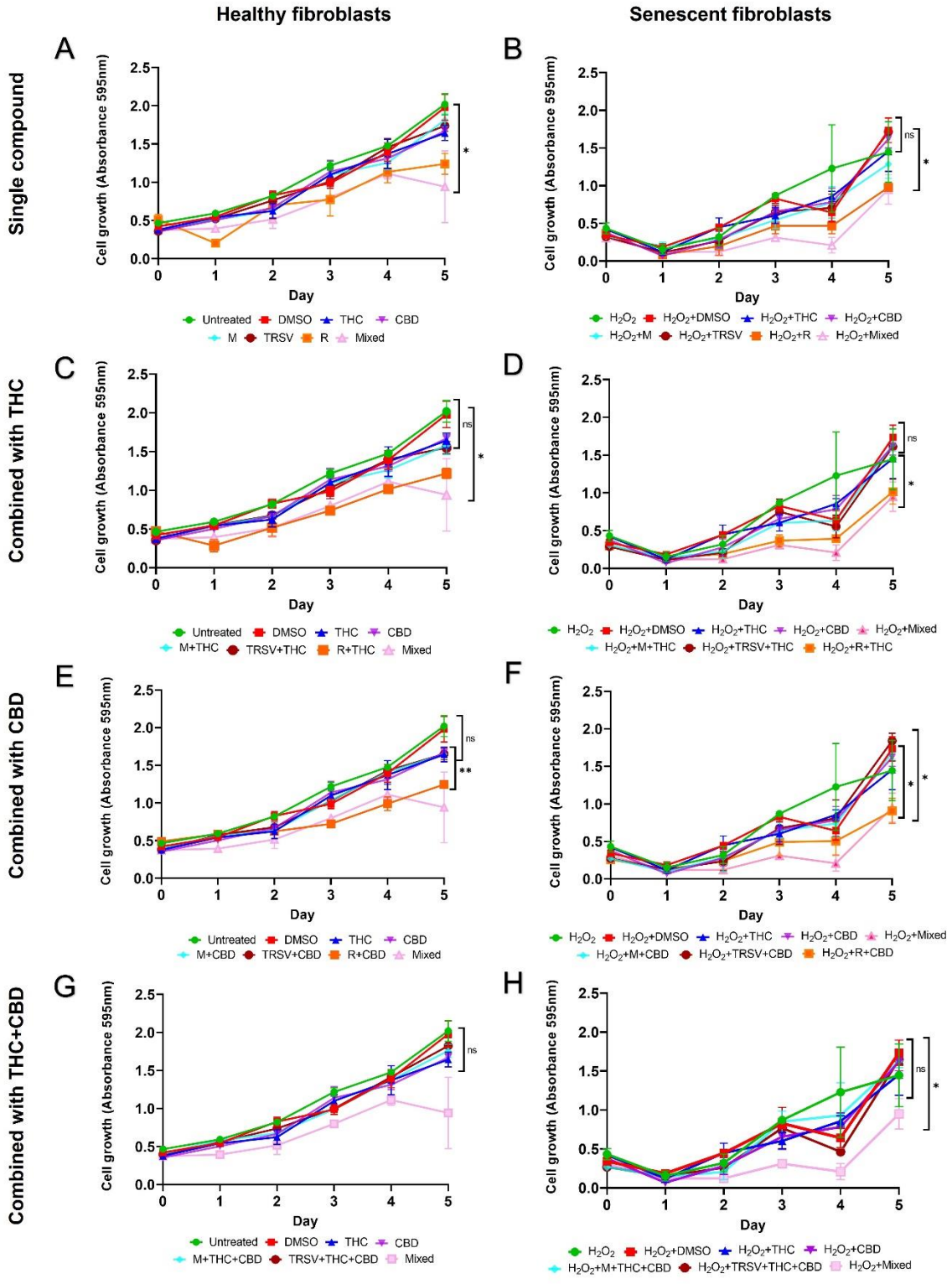

Figure 4.13. Viability of dermal fibroblasts CCD-1064Sk, 24 PDL, treated with potential anti-aging compounds combined with phytocannabinoids (MTT). The graphs show cell viability of skin fibroblasts estimated by MTT assay after experimental

treatments of healthy (A, C, E, and I) and senescent (B, D, F, and J) cells with nutrient signaling regulators combined with THC and CBD. CBD, cannabidiol; DMSO, dimethyl sulfoxide, M, metformin; Mixed, included metformin + TRSV + rapamycin + THC + CBD; R, rapamycin; THC, Δ-9-tetrahydrocannabinol; TRSV, triacetylresveratrol. Data were analyzed with an ANOVA test (Tukey post-hoc multiple comparison test). Bars represent mean ± SD. Significance is indicated within the figures using the following scale: ns, not significant; *, $p<0.05$; **, $p<0.01$.

The cellular viability in the prematurely aged dermal fibroblasts treated with metformin and pCBs compared was not significantly altered ($p>0.05$, Figure 4.14, D). Nevertheless, we detected increased viability of senescent fibroblasts in response CBD and TRSV+THC+CBD ($p<0.05$, Figure 4.14, E), and a decrease in response to rapamycin+THC ($p<0.001$), rapamycin+CBD ($p<0.05$), and metformin+TRSV+rapamycin+THC+CBD treatments ($p<0.05$) (Figure 4.14, F).

Interestingly, we noticed a higher level of incorporation of NR dye in the lysosomes of senescent cells compared to the healthy ones exposed to the same doses of metformin ($p<0.0001$), metformin+THC ($p<0.0001$), metformin+CBD ($p<0.0001$), metformin+THC+CBD ($p>0.05$) and, TRSV+CBD ($p<0.05$), whereas NR absorption was reduced after THC application (Figure 4.14).

The results obtained from the other cell lines revealed potentiation of cellular viability after the 3 days of application with NSRs combined with pCBs in healthy CCD-1135Sk and BJ-5ta fibroblasts, except in the case of mixed (metformin+TRSV+rapamycin+THC+CBD) treatment, rapamycin and its combinations with pCBs in BJ-5ta groups, where it was significantly decreased (Suppl. Figure 18, A-C, G-I). In both senescent fibroblast cell lines, NSRs combined with pCBs had no effect or

tended to reduce cellular viability, except in the case of metformin which increased growth in the BJ-5ta culture (Suppl. Figure 18, D-F, J-L).

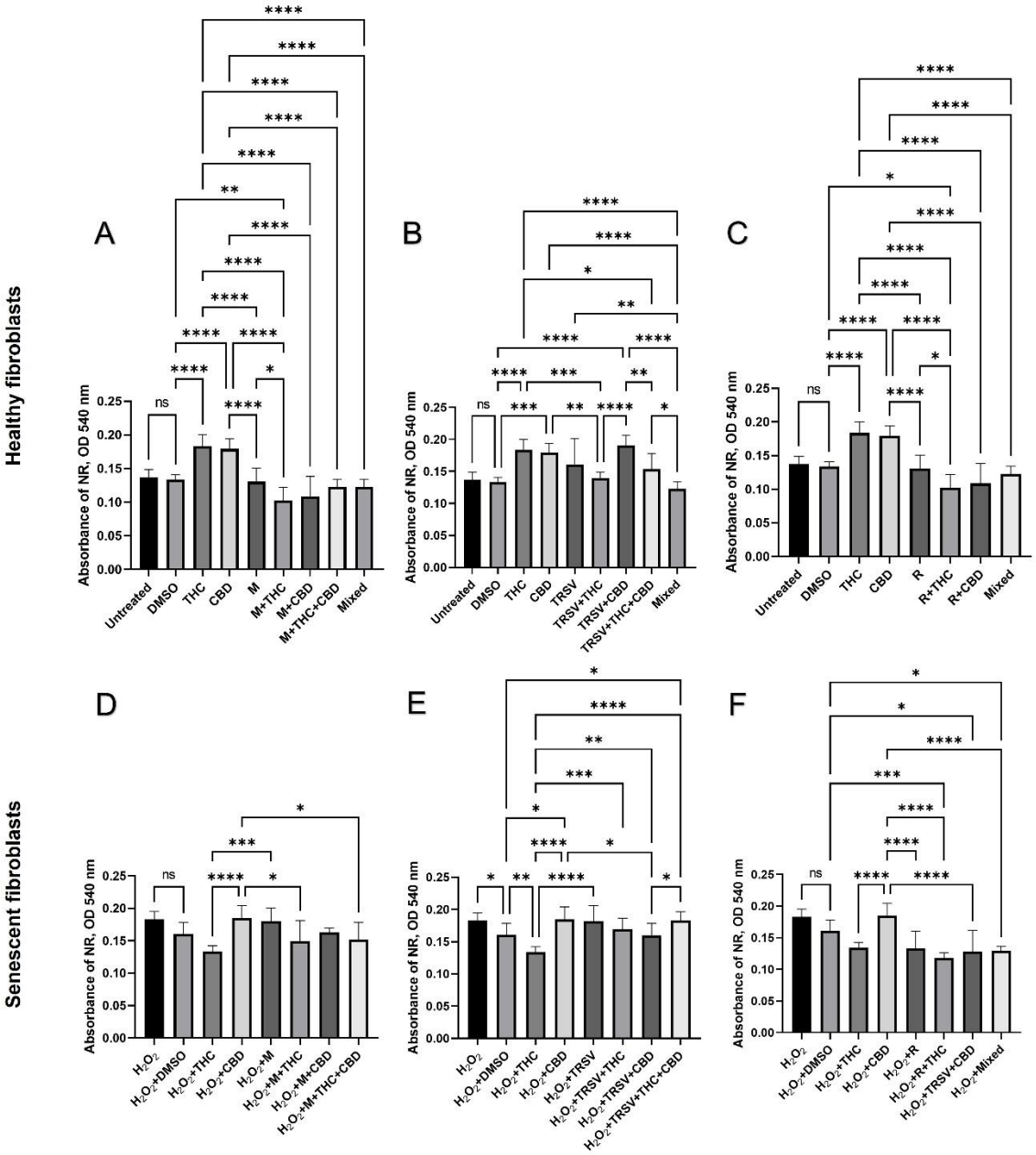

Figure 4.14. Viability of dermal fibroblasts CCD-1064Sk, 24 PDL, treated with potential anti-aging compounds combined with phytocannabinoids. The graphs represent cell viability of skin fibroblasts estimated by NR assay after experimental treatments of healthy (A, B, and C) and senescent (D, E, and F) cells with nutrient signaling regulators combined with THC and CBD. CBD, cannabidiol; DMSO, dimethyl sulfoxide (vehicle), M, metformin; Mixed, included metformin + TRSV + rapamycin + THC + CBD;

R, rapamycin; THC, Δ-9-tetrahydrocannabinol; TRSV, triacetylresveratrol. Data were analyzed with an ANOVA test (Tukey post-hoc multiple comparison test). Bars represent mean ± SD. Significance is indicated within the figures using the following scale: ns, not significant; *, $p<0.05$; **, $p<0.01$; ***, $p<0.001$; ****, $p<0.0001$.

These results revealed the potential of metformin and TRSV alone and in combination with pCBs to stimulate cellular viability of prematurely aged dermal fibroblasts. Although we noticed a positive anti-aging strategy of NSRs, it is necessary to test this on animal models.

4.4.6. The effect of phytocannabinoids combined with nutrient signaling regulators on wound healing

Apart from producing components of ECM, fibroblasts also constantly modulate the healing process by repairing and regenerating tissues. In this experiment, we tested the influence of NSRs combined with pCBs on the healing functionality of healthy and senescent dermal fibroblasts. For this purpose, scratch-lines were created in culture plates of the fibroblasts that represented a wound in the commonly used wound-healing assay (WHA). WHA was done on three different dermal fibroblast cell lines: matured CCD-1064Sk 24 PDL (Figure 4.15), hTERT-immortalized BJ-5ta 90 PDL (Suppl. Figure 19), and CCD-1135Sk 38 PDL (Suppl. Figure 20) in the healthy condition and replicative senescence state.

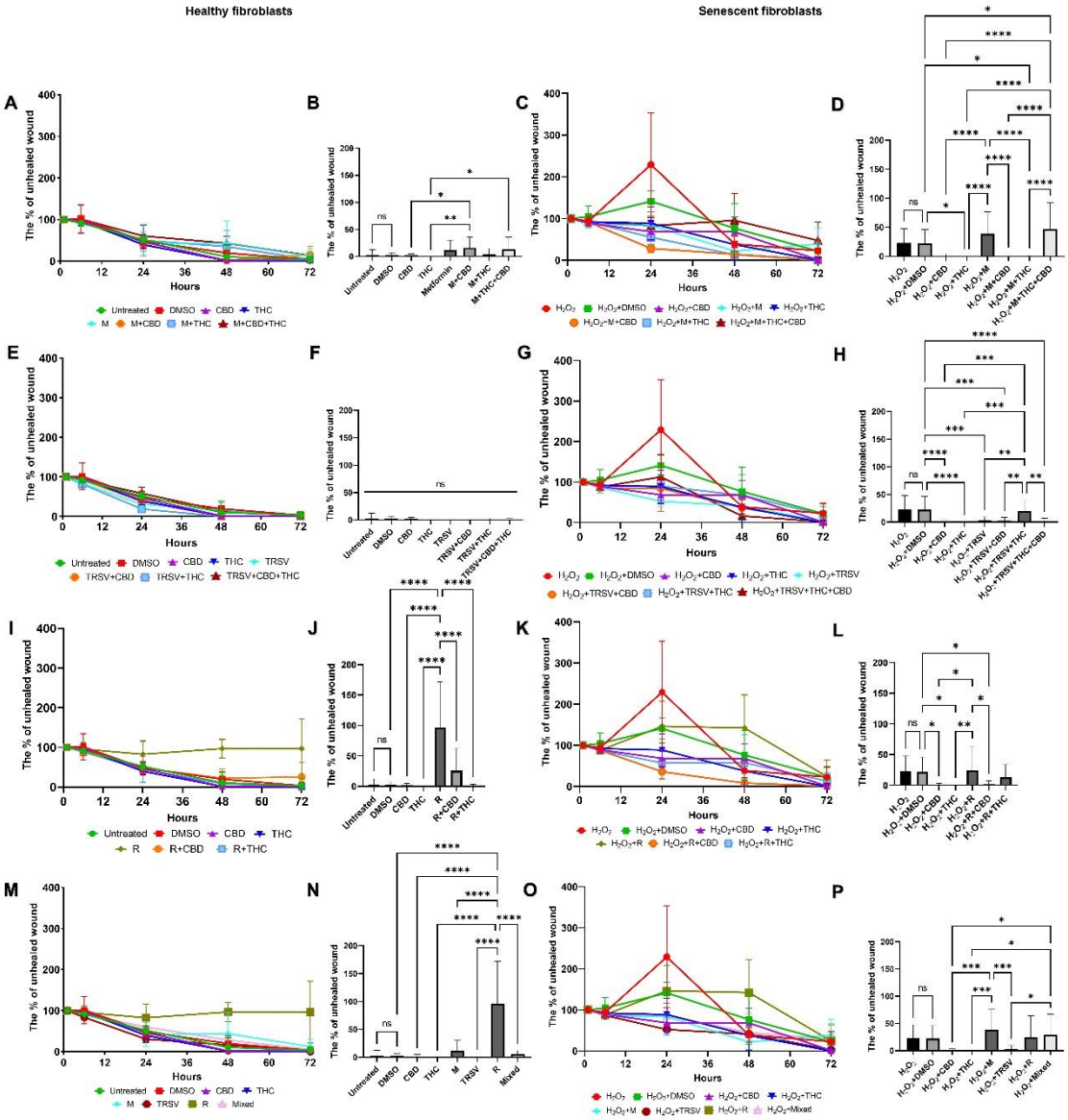

Figure 4.15. The effect of nutrient signaling regulators combined with phytocannabinoids on wound healing. Graphs represented wound healing assay results in CCD-1064Sk 24 PDL dermal fibroblasts, A, E, I, M, the percentage of an unhealed wound in healthy fibroblasts treated with metformin, TRSV and rapamycin combined with pCBs and mixed treatment, which included metformin + TRSV + rapamycin + THC + CBD, respectively; B, F, J, N, the percentage of the unhealed wound after 72 hours of experiment in healthy cells with metformin, TRSV and rapamycin combined with pCBs and mixed treatment, respectively; C, G, K, O, the percentage of an unhealed wound in senescent fibroblasts culture treated with metformin, TRSV and rapamycin combined with pCBs and mixed treatment, respectively; D, H, L, P, the percentage of the unhealed wound after 72 hours in prematurely aged fibroblasts metformin, TRSV and rapamycin combined with pCBs and mixed treatment, respectively. Data were analyzed with an ANOVA test

(Tukey post-hoc multiple comparison test). Bars represent mean ± SD. Significance is indicated within the figures using the following scale: ns, not significant; *, $p<0.05$; **, $p<0.01$; ***, $p<0.001$, ****$p<0.0001$.

The WHA results showed almost complete closure of damaged area in the healthy CCD-1064Sk fibroblasts after 72 h of treatments with NSRs and pCBs (Figure 4.15, A, E, I, M). At the same time, rapamycin significantly delayed the wound healing ($p<0.0001$, Figure 4.15, I-J and M-N). In parallel, in the senescent fibroblasts we detected complete healing after CBD ($p<0.05$, L), THC ($p<0.05$, D), metformin+CBD ($p>0.05$, D), metformin+THC ($p<0.05$, D), TRSV ($p<0.001$, H), TRSV+CBD ($p<0.001$, H), TRSV+THC+CBD ($p<0.0001$, H), rapamycin+CBD ($p<0.05$, L) treatments (Figure 4.15). Also, we found delayed healing after usage of metformin ($p>0.05$), metformin+THC+CBD ($p<0.05$), TRSV+THC ($p>0.05$), rapamycin ($p>0.05$), metformin+TRSV+rapamycin+THC+CBD treatments ($p>0.05$).

The results on BJ-5ta cell line were comparable to CCD-1046Sk (Suppl. Figure 19). In healthy fibroblasts, complete wound closure occurred after 72 h of pCBs exposure and their combinations with NSRs. However, treatments with NSRs alone delayed wound healing: metformin ($p<0.0001$, B), TRSV ($p<0.0001$, F), rapamycin ($p<0.0001$, J), and metformin+TRSV+rapamycin+THC+CBD ($p<0.0001$, N). In SIPS fibroblasts, NSRs combined with pCBs tended to delay repair of the damaged area. The most evident slow down of wound healing was induced by metformin+CBD ($p<0.01$, D), TRSV ($p<0.0001$, H), TRSV+THC ($p<0.0001$, H), rapamycin alone and combined with pCBs ($p<0.0001$, L), mixed treatment, which included metformin + TRSV + rapamycin + THC + CBD ($p<0.01$, P) treatments (Suppl. Figure 19). Nevertheless, the injured zone was completely sealed

after TRSV+THC+CBD exposure ($p>0.05$, H, Suppl. Figure 19), similar to the CCD-1064Sk cell culture experiment (Figure 4.15, H).

In addition, experimental treatment data from CCD-1135Sk, 38 PDL, which corresponds the pre-senescent condition, also demonstrated delayed wound healing induced by NSRs combined with pCBs (Suppl. Figure 20). Hence, substantially retarded healing was detected followed metformin ($p>0.05$, B), metformin combined with pCBs ($p<0.0001$, B), rapamycin ($p<0.0001$, F), and mixed ($p>0.05$, H) treatments (Suppl. Figure 20). Concomitantly, THC ($p>0.05$, B), TRSV+CBD ($p>0.05$, D), and TRSV+THC ($p>0.05$, D) tended to potentiate the healing process after 72 h of the treatments (Suppl. Figure 20).

The knowledge gained from these experiments provides a foundation for investigating the functional roles of NSRs alone in combination with pCBs in dermal healing in an age-dependent manner. The results obtained from three different skin fibroblasts cell lines depicted rapamycin's adverse effects on the speed of wound healing in senescent cultures. At the same time, TRSV combined with pCBs might be a potential tool for enhancing regeneration and repair in injured tissues.

4.5. DISCUSSION

Apart from skin physiology, countless questions remain regarding fibroblast’s role in dermal aging. Hence, all age-related aspects of changes in fibroblasts that include morphological alterations, elevations of biomolecular markers of senescence, changes of

gene expression, changes in functionality, and metabolic activities are potential targets for anti-aging and rejuvenation tools.

The current study established the effects of NSRs (metformin, TRSV, and rapamycin) alone and combined with pCBs on the healthy and senescent skin fibroblasts. Based on the cellular viability test, we determined the 500 μM optimal dose for metformin, 10 μM for TRSV, and 5 μM for rapamycin for the anti-aging experiments. The efficacy of NSRs alone and combined with pCBs were tested by cellular viability MMT and NR assays, RT-PCR, nuclear DAPI staining, WHA assay. The results demonstrated that NSRs revealed preservative and anti-aging properties in dose, time, and age-dependent manner.

During routine microscopical examinations of prematurely aged fibroblasts, we revealed fibroblasts enlargement with evident loss of their elongated spindle-like features, with fibroblasts turning from bipolar into amorphous-like shape. These findings were consistent with the data from other cultures of senescent fibroblasts (Bowman & Daniel, 1975; Mitsui' & Schneider, 1976).

Interestingly, most nuclear studies were focused on genome organization and nuclear structure in young, proliferating, and often transformed cells. However, for the analysis of functional activity in replicative and stress-induced senescence, it would be more relevant to analyze the nucleus of non-proliferating quiescent or senescent cells (Mehta et al., 2007). Our results determined significant nuclear alterations in replicative senescence and SIPS-induced fibroblasts (Figures 2.7, 2.8, 3.8, 4.6, 4.7). For instance, the nuclear area, a parameter that allows identifying size changes, was 149.5 μm^2 in healthy young cells, while it was 194.2 μm^2 in the SIPS fibroblasts of the CCD-1064Sk cell line (Figure 4.9, G, J). Studies presented by other authors reported similar findings on the different cell cultures

of senescent fibroblast. For example, Bridger & Kill (2004) studied nuclear abnormalities in normal dermal fibroblast cultures 1BR and NB1 and compared them with prematurely senescent ones from Hutchinson–Gilford progeria syndrome (HGPS) fibroblasts. They revealed that cellular aging is characterized by a shift in the nuclear area toward larger nuclei (mean=255 μm^2 early passage, and 293 μm^2 late passage). Moreover, it was noted that naturally aged nuclei exerted the same features as HGPS fibroblasts (Bridger & Kill, 2004). In line with these observations, we also found that senescent fibroblasts have larger nuclei due to the cellular size enlargement.

We tested NSRs combined with pCBs on the healthy and senescent dermal fibroblasts based on our earlier experimental findings regarding the positive anti-aging effects of THC and CBD in prematurely aged cells (Chapter 3). We found that in healthy fibroblasts THC induced reduction of area and perimeter of nuclei ($p<0.01$, Figure 4.6, G and I, respectively), while CBD increased ($p>0.05$) nuclear perimeter, and rapamycin substantially ($p<0.0001$) decreased circularity (Figure 4.6, I and H, respectively). The nuclear area and perimeter in senescent fibroblasts increased after TRSV treatment ($p<0.0001$) (Figure 4.6, J and L). Moreover, THC ($p>0.05$) increased nuclei circularity, whereas rapamycin significantly reduced it (Figure 4.6, K).

Remarkably, after 5 days of combined treatments of NSRs with pCBs on senescent fibroblasts, metformin+THC ($p<0.0001$, J), rapamycin+THC ($p<0.0001$, K), and TRSV+CBD ($p<0.0001$, L) increased nuclear area (Figure 4.9). This might be explained as compensatory mechanisms to potentiate nuclear functionality. At the same time, in young healthy cells compared to vehicle, metformin ($p<0.01$, G), rapamycin+CBD ($p>0.05$, H), and TRSV+CBD ($p>0.05$, I) reduced nuclear area (Figure 4.9).

Interestingly, a recent study reported dose-dependent resveratrol-induced premature senescence in BJ fibroblasts, based on increased β-Gal staining, increased expression of p16, p21, and p53 cell-cycle inhibitors, and accumulated senescence-associated heterochromatic foci (SAHF), known as areas of condensed and transcriptionally silenced DNA (Eren et al., 2015). They found that decline in proliferative activity was associated with resveratrol doses higher than 10 μM and that resveratrol did not induce apoptosis at concentrations of 10, 25, 50 μM but starting with 100 μM, the percentage of apoptotic cells was increased to 8.3±1.5 and reached to 37±1.5 after usage of 200 μM and 300 μM and were directly correlated with elevated SAHF appearance. These findings are essential considering the safety and efficacy of resveratrol. In contrast, our studies used 10 μM TRSV, an acetylated form of resveratrol with potentially higher bioavailability (Duan et al., 2016; Liang et al., 2013).

We present the summarized data of nuclear parameters from both CCD-1064Sk and BJ-5ta cell lines presented in Table 4.3 found an interesting tendency. We noticed that treatment of senescent cells by TRSV alone or in combination with THC/CBD increase nuclear parameters, while rapamycin alone and metformin+TRSV+rapamycin+THC+CBD with pCBs reduce it (Table 4.3). Thus, we can speculate that TRSV possesses geroprotective activity toward senescent nuclei by returning the size nuclear area and perimeter parameters to the level of the young cells.

The structural components of the nucleus: nuclear envelope, nucleoli, nuclear bodies, and the nuclear matrix, are intimately linked to the genome, maintaining signaling and ultimately control of the genome functionality (Bridger et al., 2007). Correspondingly, disorganization or defects in nuclear structures and/or architecture are associated with

alterations of normal genome regulation and are commonly found in cancer and severe premature aging diseases, like progeroid syndromes and laminopathies (Foster & Bridger, 2005). This is also supported by the observation of changes in the expression of cell-cycle regulators involved in potentiating senescence phenotypes such as p16, p21, and p53. They are engaged in two well-known theoretical signaling transduction mechanisms responsible for cellular senescence, the p53-p21-pRb pathway and the p16-pRb pathway (Jiang et al., 2018).

We observed that rapamycin ($p<0.0001$) and TRSV+CBD ($p<0.0001$) in healthy cells, as well as metformin+THC ($p<0.01$), metformin+CBD ($p<0.001$), TRSV+THC ($p<0.001$), and TRSV+CBD ($p<0.0001$) in the senescent fibroblasts upregulated *CDKN2A* expression (Figure 4.10, A, B). In parallel, in healthy cells, metformin+CBD, TRSV, and TRSV+THC tended to downregulate *CDKN2A* (Figure 4.10, A), while in SIPS fibroblasts, it was inhibited by TRSV ($p>0.05$) and rapamycin ($p>0.05$) (Figure 4.10 B). Coincidently, in healthy fibroblasts, the *CDKN1A* mRNA levels were reduced by metformin+CBD ($p<0.01$) application, whereas all other treatments, in particular, rapamycin ($p<0.0001$) and TRSV+CBD ($p<0.001$), increased its expression (Figure 4.10, C). In the senescent cells, rapamycin ($p>0.05$), TRSV ($p>0.05$), TRSV+THC ($p>0.05$), and TRSV+CBD ($p>0.05$) had tendency to inhibit *CDKN1A* expression, whereas metformin alone ($p<0.001$) and combined with pCBs ($p<0.001$) increased it (Figure 4.10, D). Interestingly, in the senescent fibroblasts, mRNA transcripts of *TP53* were slightly upregulated by TRSV+CBD ($p>0.05$, similar to CDKN2A) and rapamycin ($p<0.001$, Figure 4.10, F), while the TRSV+THC application ($p<0.01$) substantially decreased *TP53* expression, and other treatments did not change it (Figure 4.10, F).

NSRs and pCBs significantly affected both senescence pathways: the telomere-based p53-p21-pRb typically represents replicative senescence (RS), and the stress-based p16-pRB pathway represents SIPS (Wang et al., 2016). The inhibitory effects of TRSV and its combinations with pCBs on *TP53*, *CDKN2A (p16)*, and *CDKN1A (p21)* discovered in our studies conform to recent studies on the anti-aging properties of resveratrol (Giovannelli et al., 2011; Jiang et al., 2018). For example, adding 30 µM and 60 µM of resveratrol partly downregulated the expression of two senescence markers (p16 and p53) in a concentration-dependent manner, suggesting that resveratrol can suppress mechanical overloading-induced nucleus pulposus cell senescence (Jiang et al., 2018). Furthermore, 4 weeks application of 5 µM of resveratrol on in vitro senescence model of human MRC5 lung fibroblasts lowered the levels of p53 acetylation by about 35% in RS cells (PDL > 50) (Giovannelli et al., 2011).

Besides, Zhao and coworkers (2017) showed metformin-induced mRNA upregulation of *cyclin D1* (*Ccnd1*), a proliferative promoter, and downregulated cell cycle inhibitors *P53*, *P21*, and *P16*, in wounds of aged mice (Zhao et al., 2017). In parallel, they noted resveratrol was less potent in *Ccnd1* promotion and inhibition of *P53*, *P21*, and *P16* than metformin. Moreover, the authors admitted paradoxical suppressive effects of rapamycin on *P53* and *P21* but stimulatory effects on *P16*, which might result in the increased *Ccnd1* level. Both metformin and resveratrol demonstrated an increase in the viability of proliferative cells alongside the epidermis and around hair follicles, ameliorated aging in cutaneous wound healing, with metformin having a more profound anti-aging effect (Zhao et al., 2017).

Based on the free-radical theory of aging (Chapter 1), oxidative stress caused by ROS accumulation is able to potentiate cellular senescence (Gerasymchuk, 2021). In the present study, we also analyzed the influence of NSRs and pCBs on the SIPS dermal fibroblasts tightly associated with ROS generation and corresponded downstream NF-κB activation (Liu et al., 2017; Robbins et al., 2011; Zhang et al., 2013). In healthy dermal fibroblasts, *NF-κB* was upregulated in all treatment groups except metformin ($p>0.05$) following 5 days of NSRs applications (Figure 4.10, G). We also detected increased mRNA levels of *NF-κB* in most of the treatment groups in SIPS fibroblasts except for the TRSV+THC group ($p>0.05$), where *NF-κB* remained slightly downregulated compared to the vehicle (Figure 4.10, H). However, *NF-κB* transcripts in senescent fibroblasts were lower than corresponded levels in the healthy cells. These data indicated the potential protective anti-aging effect of NSRs alone and in combination with pCBs in the prematurely aged fibroblasts and might be used to alleviate aging-related conditions. This idea is based on the substantial body of circumstantial evidence; for instance, the transcriptional activity of NF-κB found increased in a variety of aged tissues and associated with multiple age-related degenerative diseases, including Alzheimer's, diabetes, and osteoporosis. Recently, Robbins and colleagues reported that NF-κB inhibition leads to delayed onset of age-related symptoms and pathologies in murine models (Robbins et al., 2011). They also pointed out that stimulation of NF-κB is involved in the supervision of numerous known lifespan regulators, including insulin/IGF-1, FOXO, SIRT, mTOR, and DNA damage. Thus, the inhibitory tendency of TRSV combined with pCBs towards NF-κB represents a possible therapeutic target for extending cellular and mammalian health span.

There is a large body of data supporting the involvement of NF-κB in regulating metabolic pathways directly linked to Sirtuin modulation (Liu et al., 2017; Ma et al., 2015; Robbins et al., 2011; Ruland, 2011; Zhao et al., 2017). The leading role of Sirtuins on the protection from cellular senescence has mainly been intimately associated with SIRT1 and SIRT6 (Lee et al., 2019). SIRT1 is predominately found in the nucleus and shuttles between the cytoplasm and nucleus and is highly involved in cellular senescence and aging via enzymatic activity of deacetylase towards lifespan extension via ADP-ribosyl-transferase triggered DNA repair (Baur, 2010; Kim et al., 2007; Michishita et al., 2005; Ramis et al., 2015). SIRT6 is primarily localized in the heterochromatic regions and modulates lifespan extension via ADP-ribosylation activities, while its deacetylase activity is focused on DNA repair, genome stability, and telomere maintenance (Michishita et al., 2005).

Sirtuin family modulates the organismal lifespan by interacting with several lifespan regulating signaling pathways, including the insulin/IGF-1 signaling pathway, TOR, AMP-activated protein kinase, FOXO, and the nicotinamide adenine dinucleotide (NAD^+)-dependent sirtuin deacetylases that are commonly dysregulated in aging and ARDs (Bonkowski & Sinclair, 2016; Lee et al., 2019; Tia et al., 2018). Recent data showed a reduction in SIRT1 and SIRT6 but not SIRT2 levels in senescent cells of mouse embryonic fibroblasts, lung epithelial cells, human endothelial cells, and macrophages exposed to oxidants (Anwar et al., 2016; Chen et al., 2018; Sasaki et al., 2006). Moreover, the promotion of premature senescence-like phenotypes in endothelial cells was induced by the reduction of SIRT1 and SIRT6 through targeting their siRNA or miRNA using pharmacological inhibitors (Menghini et al., 2009; Mostoslavsky et al., 2006; Ota et al., 2007). On the other hand, reducing senescence biomarkers in angiotensin II-treated human

coronary artery endothelial cells, primary porcine aortic endothelial cells, and stress-exposed lung cells was associated with overexpression of SIRT1 and SIRT6 (Chen et al., 2018; Kim et al., 2012; Lee et al., 2019; Yao et al., 2012; Zu et al., 2010).

Our previous studies identified the negative impact of senescence on the mRNA levels of *SIRT1* and *SIRT6* in SIPS dermal fibroblasts; this was partially alleviated by pCBs (Chapters 2 and 3). We detected significant rapamycin-induced ($p<0.0001$) upregulation of *SIRT1* and *SIRT6* in healthy fibroblasts, whereas other treatments did not affect *SIRT1* and *SIRT6* expression. However, the "longevity" biomarker *SIRT1* was downregulated after 5 days of TRSV+THC and TRSV+CBD application ($p<0.05$, Figure 4.10, I). In contrast to the healthy cells, in SIPS fibroblasts, we noted rapamycin-induced increase in the expression of *SIRT1* ($p<0.0001$) and *SIRT6* ($p<0.0001$); TRSV+CBD, and TRSV+THC also increased *SIRT1* and *SIRT6* expression ($p<0.0001$), TRSV alone also increased *SIRT1* ($p<0.01$) and *SIRT6* ($p<0.0001$) in SIPS fibroblasts. At the same time, significant increase of the metformin alone and combined with pCBs was not efficient, albeit it exerted tendency to upregulate *SIRT1* ($p<0.05$, Figure 4.10, L). In contrast, *SIRT6* expression was found elevated in response to metformin+THC ($p<0.05$, L) and metformin+CBD ($p<0.01$, L) treatments, but to metformin alone (Figure 4.10, L) (Figure 4.10). These data partially supported our hypotheses about the protective role of pCBs and their combination with NSRs in senescence.

Remarkably, resveratrol was reported to exert neuroprotective effect by modulation of the function of mitochondria and induction of the activity of SIRT1 and the elimination of mutant proteins associated with neurodegenerative diseases (such as Alzheimer's disease) through activation of AMPK by increasing intracellular Ca^{2+} and promoting

AMPK phosphorylation at Thr172 site, leading to the suppression of mTOR activity and enhancement of autophagic and lysosomal clearance of Aβ-amyloid (Kou & Chen, 2017; Wang et al., 2016; Yessenkyzy et al., 2020). Moreover, NSRs was found to reduce the concentrations of the hormonal effectors such as insulin, IGF1, and growth hormone (GH), which stimulated or inhibited the activity of numerous metabolic sensors (i.e., Sirtuins, AMPK, TOR). Bonkowski and Sinclair (2016) showed that Sirtuin-activating compounds such as SRT1720 and SRT2104 can directly activate SIRT1, whereas rapamycin is a direct inhibitor of TOR, and metformin indirectly activates AMPK. In addition, these metabolic regulators mediate downstream activities such as DNA repair, mitochondrial biogenesis and function, stress resistance, stem cell and telomere maintenance, autophagy, chromatin modifications, reduced inflammation, and translation fidelity (Bonkowski & Sinclair, 2016). Also, the inhibitory effects of resveratrol on the mTOR regulation, accompanied by potentiation of autophagic and lysosomal activities in senescent cells, might explain our findings related to increased lysosomal NR accumulation and enhanced cellular viability in prematurely senescent fibroblasts exposed to TRSV and pCBs (Figure 4.14, E). Altogether, these activities improved cellular homeostasis, reduced morbidity, and a more youthful-like state (Bonkowski & Sinclair, 2016; Li et al., 2014).

These results supported the idea that NSRs and pCBs exerted protective activity in cellular senescence and might be used as anti-aging remedies by improving the metabolic functionality in prematurely aged dermal fibroblasts via targeting SIRT1 and SIRT6.

Apart from the metabolic regulation, the AMPK pathway also modulates fibroblasts' functional activity linked to the generation of collagen and other ECM components (Zhao et al., 2017). The UV-induced elevation of MMP-1 expression in HDFs was related to the

potentiation of mTOR phosphorylation. In contrast, augmented phosphorylation of AMPK and liver kinase B1, which are mTOR inhibitors, led to suppression of MMP1-initiated activity towards ECM degradation (Shin et al., 2014). Metformin was reported to ameliorate age-related downregulation of p-acetyl-CoA carboxylase and p-Ampk in the epidermis and around hair follicles as well as the thinner epidermis and reduction in the number of hair follicles and low collagen deposition (Zhao et al., 2017).

Notably, our results discovered stimulatory effects of NRSs combined with pCBs on *COL1A1* gene expression in healthy fibroblasts (Figure 4.11, A). The most prominent increase in *COL1A1* expression was induced by rapamycin ($p<0.001$), TRSV+CBD ($p<0.01$), and metformin+THC ($p<0.05$). Unfortunately, significant inhibitory influence on *COL1A1* was observed in prematurely aged skin cells (Figure 4.11, B). Concomitantly, significant upregulation of *COL3A1* in the senescent fibroblasts was identified after TRSV+CBD ($p<0.0001$) and rapamycin ($p<0.0001$), while other treatments inhibited *COL3A1* expression (Figure 4.11, D). These changes might be related to ROS-induced excessive protein glycation via generation of the advanced glycation end products (AGEs), which contribute to skin aging as it deteriorates the existing collagen by crosslinking. Besides, the progressive increase of AGE during aging causes oxidative damage to cellular macromolecules and modulates the activation of transcription factor NF-κB resulting in apoptosis enhancement and ceased proliferative activity (Soydas et al., 2018). This assertion aligns with our experimental findings, where *NF-κB* was predominantly upregulated in SIPS fibroblasts despite the treatment (Figure 4.10, H).

Almost identical to *COL3A1* findings were observed for *ELN* mRNA levels, which were also increased by rapamycin ($p<0.0001$), TRSV ($p<0.01$), TRSV combined with THC

($p<0.001$), and CBD ($p<0.05$) (Figure 4.11, H). Meanwhile, we discovered slightly opposite tendencies for *MMP2*, responsible for the degradation of ECM components. Thus, mRNA transcripts of *MMP2* in healthy cells were substantially suppressed by metformin ($p<0.05$) inhibition of *MMP2*, while rapamycin ($p<0.01$) increased it (Figure 4.11, E). In senescent fibroblasts, rapamycin ($p>0.05$) was found to inhibit *MMP2* expression, whereas all other NSRs combined with pCBs tended to increase *MMP2* expression. The most noticeable increase in *MMP2* expression was caused by metformin+THC ($p<0.001$), metformin+CBD ($p<0.0001$), TRSV+THC ($p<0.01$), and TRSV+CBD ($p<0.0001$) (Figure 4.11, F).

Interestingly, in recent studies, metformin is often mentioned as a collagen protector in aging and high glucose-associated conditions. For instance, 24 h treatment with 500 μM of metformin significantly increased collagen I and III generation in aged 3T3 fibroblasts, while the activity of MMPs was decreased (Soydas et al., 2018, 2021). Similar results were reported by Shao et al. (2014) – metformin had a direct effect on osteoblast-like cells MG63 and attenuated the suppression on proliferation induced by high glucose with increased expression of collagen type I, osteocalcin, osteoprotegerin, meanwhile suppressing MMP1 and MMP2 (Shao et al., 2014). In contrast, Benazzoug et al. have reported that glucose specifically increases collagen type III synthesis both at the mRNA and protein levels, without alteration of collagen type I production in young and RS cultured human skin fibroblasts (Benazzoug et al., 1998). In conjunction with our findings, positive effects of TRSV might be mediated via the Sirt1 pathway component – peroxisome proliferator-activated receptor γ coactivator, accompanied by NAD+ elevation and AMPK pathway stimulation (Park et al., 2012). Rapamycin is known to inhibit the mTOR pathway

(Lamming et al., 2013), which is also important to promote epithelial cell proliferation (Cai et al., 2012) and angiogenesis (Guang-Tao et al., 2014), explaining potential modulatory effects of metformin and resveratrol on mTOR activity that may be secondary to activation of cell viability and anti-inflammatory impact of these compounds (Zhao et al., 2017).

Senescence is inseparably accompanied by the inflammatory process, ROS-induced gradual damage of cellular components and deterioration of molecular signaling pathways, and alteration of cell-cycle and metabolic regulation that eventually leads to ceased growth and cellular death. Nevertheless, stimulation or inhibition of specific components of ECS, the influence of endocannabinoid (eCBs), or pCBs have the potential to delay or alleviate this process targeting multiple components of the vicious cycle of aging. Thus, the main targets of eCBs/pCBs are cannabinoid receptors CB1 (associated with the analgesic effects of cannabinoids) and CB2 (modulates cytokine release from immune cells and reduces inflammation) (Wang et al., 2022). In the skin, cannabinoid receptor antagonists exacerbate allergic inflammation, whereas receptor agonists attenuate inflammation. Pharmacological inhibition or knockout of CB1/CB2 receptors in mice augmented the hapten dinitrofluorobenzene (DNFB)-induced dermatitis and was linked to the increased levels of eCBs, anandamide and 2-AG. Also, DNFB treatment decreases CB1 mRNA and increases CB2 mRNA (Karsak et al., 2007). Moreover, reduced expression of cannabinoid receptors was observed in contact dermatitis (Caterina, 2014). At the same time, CB1 activation suppressed the expression of two damage-induced keratins, keratin 6 and keratin 16, which are highly upregulated in hyperproliferative disorder psoriasis (Ramot et al., 2013).

In healthy dermal fibroblasts, we identified metformin-stimulated ($p<0.0001$) increased expression of *CB1*; a slight increase was also found in response to

metformin+THC, TRSV+CBD, and rapamycin ($p>0.05$, Figure 4.11, I). In contrast, metformin+THC ($p<0.01$), TRSV+THC ($p<0.0001$), TRSV+CBD ($p<0.01$), and rapamycin ($p<0.01$) significantly increased *CB1* transcripts levels in prematurely aged cells (Figure 4.11, J). In parallel, *CB2* expression was elevated by metformin+THC ($p<0.05$), rapamycin ($p<0.0001$), TRSV ($p<0.01$), TRSV+THC ($p<0.0001$), and TRSV+CBD ($p<0.0001$) (Figure 4.11, L). Our results, together with observations from other authors, might point to anti-inflammatory and anti-aging effect of NSRs and pCBs.

Albeit numerous studies showed a significant positive influence of metformin, resveratrol, and rapamycin on the viability of senescent cells (Benazzoug et al., 1998; Duan et al., 2016; Kou & Chen, 2017; Lamming et al., 2013; Li et al., 2014; Park et al., 2012; Shao et al., 2014; Zhao et al., 2017), our results have not revealed significant improvements in cellular growth induced by NSRs in combinations with pCBs (Figure 4.12). However, we identified the significant reduction in cellular viability caused by rapamycin ($p<0.01$), rapamycin+THC ($p<0.05$), rapamycin+CBD ($p<0.01$), and metformin+TRSV+rapamycin+THC+CBD treatments ($p<0.01$) (Figure 4.12, L). Furthermore, we discovered that rapamycin alone and combined with THC or CBD, and also the metformin+TRSV+rapamycin+THC+CBD treatment that encompassed metformin, TRSV, rapamycin, THC, and CBD exerted a detrimental effect on cellular viability in healthy and senescent dermal fibroblasts (Figure 4.13). These data may suggest that NSRs combined with pCBs have a competitive effect on mTOR, AMPK signaling pathways that eventually diminish their efficacy, thereby reducing cellular viability. Nevertheless, the significant CBD-induced inhibition of dermal fibroblasts viability (Figure

4.12) might be helpful during surgeries and the healing process in patients with hyperproliferative disorders and potential risks of keloids formation.

Zhao et al. also noted that metformin and, to a lesser extent, resveratrol improved the healing process through stimulation of the AMPK pathway, which has been documented to inhibit wound healing (Mills et al., 2008), probably due to its immunosuppressive capability upon systemic administration (Lamming et al., 2013; Mills et al., 2008; Zhao et al., 2017). Most our results were in line with these findings.

Wound healing assay revealed that typically complete wound closure occurred within 72 h (Figure 4.15). Surprisingly, in healthy fibroblasts, we detected rapamycin-induced ($p<0.0001$) delayed wound healing in both cell lines CCD-1064Sk and BJ-5ta (Table 4.4). Additionally, in BJ-5ta fibroblasts, delayed wound closure was found following metformin ($p<0.0001$, B), TRSV ($p<0.0001$, F), and metformin+TRSV+rapamycin+THC+CBD ($p<0.0001$, N) treatments (Suppl. Figure 19, J). These results might be considered in treating hyperproliferative disorders like psoriasis and cosmetological manipulations.

Remarkably, in the senescent fibroblasts of CCD-1064Sk, BJ-5ta, and CCD-1135Sk cultures, we discovered a common trend to potentiate wound healing via TRSV alone and combined with THC or CBD (Table 4.4). However, most other NSRs treatments, such as metformin and its combinations with pCBs, rapamycin, and metformin+TRSV+rapamycin+THC+CBD treatments, substantially delayed wound closure (Table 4.4). Albeit the abovementioned treatments negatively affected wound healing, they might be beneficial in treating hyperproliferative disorders, keloid scars, and time-consuming reconstructive surgeries.

Table 4.4. The effect of nutrient signaling regulators combined with phytocannabinoids on wound closure following 72 h of treatment

Condition	Healthy		Senescent	
	Incomplete	**Complete**	**Incomplete**	**Complete**
CCD-1064Sk, 24 PDL	R **** R+CBD^{ns}	All groups except incomplete	M^{ns}, M+THC+CBD*, TRSV+THC^{ns}, R^{ns}, Mixed^{ns}	CBD*, THC*, M+CBD^{ns}, M+THC*, TRSV***, TRSV+CBD***, TRSV+THC+CBD****, R+CBD*
BJ-5ta, 90 PDL	M****, TRSV****, R****, Mixed****	CBD ^{ns}, THC ^{ns}, M+CBD ^{ns}, M+THC ^{ns}, M+THC+CBD ^{ns}	CBD ^{ns}, THC ^{ns}, M+CBD**, M+THC ^{ns}, M+THC+CBD ^{ns}, TRSV****, TRSV+THC****, R****, R+THC****, R+CBD****, Mixed**	TRSV+CBD ^{ns}, TRSV+THC+CBD ^{ns}

CCD-1135Sk, 38 PDL			CBD ^{ns}, M^{ns}, M+THC**** M+CBD****, M+THC+CBD****, TRSV ^{ns}, TRSV+THC+CBD^{ns}, R****, Mixed ^{ns}	THC ^{ns}, TRSV+CBD ^{ns}, TRSV+THC ^{ns}

CBD, cannabidiol; M, metformin; Mixed, included metformin + TRSV + rapamycin + THC + CBD; R, rapamycin; THC, Δ-9-tetrahydrocannabinol; TRSV, triacetylresveratrol. Data were analyzed with a two-way ANOVA test (Tukey post-hoc multiple comparison test). Significance is indicated within the figures using the following scale: ns, not significant; *, $p<0.05$; **, $p<0.01$; ***, $p<0.001$; ****, $p<0.0001$.

In summary, differential effects exist among CR-based potential anti-aging compounds, namely metformin, triacetylresveratrol, rapamycin in senescence-associated gene regulation, metabolic and functional maintenance, and cutaneous wound healing. We found critical anti-aging mechanisms by downregulation of NF-κB activity, AMPK, and mTOR pathways in young and aged dermal fibroblasts. We also highlighted TRSV as the optimal and promising anti-aging and regenerative agent that can potential be used for treatment or/and prevention of appearance of aging spots and treating cutaneous wounds.

4.6. REFERENCES

Aggarwal, D., Fernandez, M. L., & Soliman, G. A. (2006). Rapamycin, an mTOR inhibitor, disrupts triglyceride metabolism in guinea pigs. *Metabolism: Clinical and Experimental*, *55*(6), 794–802. https://doi.org/10.1016/j.metabol.2006.01.017

Anwar, T., Khosla, S., & Ramakrishna, G. (2016). Increased expression of SIRT2 is a novel marker of cellular senescence and is dependent on wild type p53 status. *Cell Cycle*, *15*(14), 1883–1897. https://doi.org/10.1080/15384101.2016.1189041

Ashcroft, G. S., Horan, M. A., Herrick, S. E., Tarnuzzer, R. W., Schultz, G. S., & Ferguson, M. W. J. (1997). Age-related differences in the temporal and spatial regulation of matrix metalloproteinases (MMPs) in normal skin and acute cutaneous wounds of healthy humans. *Cell and Tissue Research*, *290*(3), 581–591. https://doi.org/10.1007/s004410050963

Bae, J., Kim, N., Shin, Y., Kim, S.-Y., & Kim, Y.-J. (2020). Activity of catechins and their applications. *Biomedical Dermatology*, *4*(1). https://doi.org/10.1186/s41702-020-0057-8

Bai, G. L., Wang, P., Huang, X., Wang, Z. Y., Cao, D., Liu, C., Liu, Y. Y., Li, R. L., & Chen, A. J. (2021). Rapamycin protects skin fibroblasts from UVA-induced photoaging by inhibition of p53 and phosphorylated HSP27. *Frontiers in Cell and Developmental Biology*, *9*(February), 633331. https://doi.org/10.3389/fcell.2021.633331

Barzilai, N., Crandall, J. P., Kritchevsky, S. B., & Espeland, M. A. (2016). Metformin as a tool to target aging. *Cell Metabolism*, *23*(6), 1060–1065. https://doi.org/10.1016/j.cmet.2016.05.011

Bastianetto, S., Ménard, C., & Quirion, R. (2015). Neuroprotective action of resveratrol. *Biochimica et Biophysica Acta - Molecular Basis of Disease*, *1852*(6), 1195–1201. Elsevier B.V. https://doi.org/10.1016/j.bbadis.2014.09.011

Baur, J. A. (2010). Biochemical effects of SIRT1 activators. *Biochimica et Biophysica Acta - Proteins and Proteomics*, *1804*(8), 1626–1634. https://doi.org/10.1016/j.bbapap.2009.10.025

Benazzoug, Y., Borchiellini, C., Labat-Robert, J., Robert, L., & Kern, P. (1998). Effect of high-glucose concentrations on the expression of collagens and fibronectin by fibroblasts in culture. *Experimental Gerontology*, *33*(5), 445–455. https://doi.org/10.1016/s0531-5565(98)00015-1

Benedetti, F., Sorrenti, V., Buriani, A., Fortinguerra, S., Scapagnini, G., & Zella, D. (2020). Resveratrol, rapamycin and metformin as modulators of antiviral pathways. *Viruses*, *12*(12), 1458. MDPI AG. https://doi.org/10.3390/v12121458

Benjamin, D., Colombi, M., Moroni, C., & Hall, M. N. (2011). Rapamycin passes the torch: A new generation of mTOR inhibitors. *Nature Reviews Drug Discovery*, *10*(11), 868–880. https://doi.org/10.1038/nrd3531

Bhansali, S., Bhansali, A., & Dhawan, V. (2019). Metformin promotes mitophagy in mononuclear cells: A potential in vitro model for unraveling metformin's mechanism of action. *Annals of the New York Academy of Sciences*, *1463*(1), 23–36. https://doi.org/10.1111/nyas.14141

Blagosklonny, M. V. (2019). Rapamycin for the aging skin. *Aging*, *11*(24), 12822–12826. Taylor and Francis Inc. https://doi.org/10.4161/cc.5.18.3288

Blagosklonny, M. V. (2021). Anti-aging: Senolytics or gerostatics (unconventional view). *Oncotarget*, *12*(18), 1821–1835. https://doi.org/10.18632/oncotarget.28049

Blanco-Melo, D., Nilsson-Payant, B. E., Liu, W. C., Uhl, S., Hoagland, D., Møller, R., Jordan, T. X., Oishi, K., Panis, M., Sachs, D., Wang, T. T., Schwartz, R. E., Lim, J. K., Albrecht, R. A., & tenOever, B. R. (2020). Imbalanced host response to SARS-CoV-2 drives development of COVID-19. *Cell*, *181*(5), 1036–1045.e9. https://doi.org/10.1016/j.cell.2020.04.026

Bonkowski, M. S., & Sinclair, D. A. (2016). Slowing ageing by design: The rise of NAD+ and sirtuin-activating compounds. *Nature Reviews Molecular Cell Biology*, *17*(11), 679–690. Nature Publishing Group. https://doi.org/10.1038/nrm.2016.93

Boo, Y. C. (2019). Human skin lightening efficacy of resveratrol and its analogs: From in vitro studies to cosmetic applications. *Antioxidants*, *8*(9), 332. https://doi.org/10.3390/antiox8090332

Bowman, P. D., & Daniel, C. W. (1975). Aging of human fibroblasts in vitro: surface features and behavior of aging WI 38 cells. *Mechanisms of Ageing and Development*, *4*, 147–158. https://doi.org/10.1016/0047-6374(75)90016-0

Bridger, J. M., Foeger, N., Kill, I. R., & Herrmann, H. (2007). The nuclear lamina: Both a structural framework and a platform for genome organization. *FEBS Journal*, *274*(6), 1354–1361. https://doi.org/10.1111/j.1742-4658.2007.05694.x

Bridger, J. M., & Kill, I. R. (2004). Aging of Hutchinson-Gilford progeria syndrome fibroblasts is characterised by hyperproliferation and increased apoptosis. *Experimental Gerontology*, *39*(5), 717–724. https://doi.org/10.1016/j.exger.2004.02.002

Bridges, H. R., Sirviö, V. A., Agip, A. N. A., & Hirst, J. (2016). Molecular features of biguanides required for targeting of mitochondrial respiratory complex I and activation of AMP-kinase. *BMC Biology*, *14*(1). https://doi.org/10.1186/s12915-016-0287-9

Cai, N., Dai, S. D., Liu, N. N., Liu, L. M., Zhao, N., & Chen, L. (2012). PI3K/AKT/mTOR signaling pathway inhibitors in proliferation of retinal pigment epithelial cells.

International Journal of Ophthalmology, *5*(6), 675–680. https://doi.org/10.3980/j.issn.2222-3959.2012.06.05

Castel, P., Ellis, H., Bago, R., Toska, E., Razavi, P., Carmona, F. J., Kannan, S., Verma, C. S., Dickler, M., Chandarlapaty, S., Brogi, E., Alessi, D. R., Baselga, J., & Scaltriti, M. (2016). PDK1-SGK1 Signaling Sustains AKT-Independent mTORC1 Activation and Confers Resistance to PI3Kα Inhibition. *Cancer Cell*, *30*(2), 229–242. https://doi.org/10.1016/j.ccell.2016.06.004

Caterina, M. J. (2014). TRP channel cannabinoid receptors in skin sensation, homeostasis, and inflammation. *ACS Chemical Neuroscience, 5*(11), 1107–1116. American Chemical Society. https://doi.org/10.1021/cn5000919

Chang, Y. C., Liu, H. W., Chen, Y. T., Chen, Y. A., Chen, Y. J., & Chang, S. J. (2018). Resveratrol protects muscle cells against palmitate-induced cellular senescence and insulin resistance through ameliorating autophagic flux. *Journal of Food and Drug Analysis, 26*(3), 1066–1074. https://doi.org/10.1016/j.jfda.2018.01.006

Chen, G., Kroemer, G., & Kepp, O. (2020). Mitophagy: An emerging role in aging and age-associated diseases. *Frontiers in Cell and Developmental Biology, 8*, 200. Frontiers Media S.A. https://doi.org/10.3389/fcell.2020.00200

Chen, J., Xie, J. J., Jin, M. Y., Gu, Y. T., Wu, C. C., Guo, W. J., Yan, Y. Z., Zhang, Z. J., Wang, J. le, Zhang, X. L., Lin, Y., Sun, J. L., Zhu, G. H., Wang, X. Y., & Wu, Y.-S. (2018). Sirt6 overexpression suppresses senescence and apoptosis of nucleus pulposus cells by inducing autophagy in a model of intervertebral disc degeneration. *Cell Death and Disease*, *9*(2), 56. https://doi.org/10.1038/s41419-017-0085-5

Chiang, H. M., Lin, T. J., Chiu, C. Y., Chang, C. W., Hsu, K. C., Fan, P. C., & Wen, K. C. (2011). Coffea arabica extract and its constituents prevent photoaging by suppressing MMPs expression and MAP kinase pathway. *Food and Chemical Toxicology*, *49*(1), 309–318. https://doi.org/10.1016/j.fct.2010.10.034

Chung, C. L., Lawrence, I., Hoffman, M., Elgindi, D., Nadhan, K., Potnis, M., Jin, A., Sershon, C., Binnebose, R., Lorenzini, A., & Sell, C. (2019). Topical rapamycin reduces markers of senescence and aging in human skin: An exploratory, prospective, randomized trial. *GeroScience*, *41*(6), 861–869. https://doi.org/10.1007/s11357-019-00113-y

Correia-Melo, C., Marques, F. D., Anderson, R., Hewitt, G., Hewitt, R., Cole, J., Carroll, B. M., Miwa, S., Birch, J., Merz, A., Rushton, M. D., Charles, M., Jurk, D., Tait, S. W., Czapiewski, R., Greaves, L., Nelson, G., Bohlooly-Y, M., Rodriguez-Cuenca, S., … Passos, J. F. (2016). Mitochondria are required for pro-ageing features of the senescent phenotype. *The EMBO Journal*, *35*(7), 724–742. https://doi.org/10.15252/embj.201592862

Cummings, N. E., & Lamming, D. W. (2017). Regulation of metabolic health and aging by nutrient-sensitive signaling pathways. *Molecular and Cellular Endocrinology*, *455*, 13–22. https://doi.org/10.1016/j.mce.2016.11.014

Cunningham, J. T., Rodgers, J. T., Arlow, D. H., Vazquez, F., & Mootha, V. K. (2007). mTOR controls mitochondrial oxidative function through a YY1-PGC-1alpha transcriptional complex. *Nature*, *450*(7170), 736–741. https://doi.org/10.1038/nature06322

Curry, A. M., White, D. S., Donu, D., & Cen, Y. (2021). Human Sirtuin regulators: The "Success" stories. *Frontiers in Physiology*, *12*, 752117. Frontiers Media S.A. https://doi.org/10.3389/fphys.2021.752117

da Luz, P. L., Tanaka, L., Brum, P. C., Dourado, P. M. M., Favarato, D., Krieger, J. E., & Laurindo, F. R. M. (2012). Red wine and equivalent oral pharmacological doses of resveratrol delay vascular aging but do not extend life span in rats. *Atherosclerosis*, *224*(1), 136–142. https://doi.org/10.1016/j.atherosclerosis.2012.06.007

Dinarello, C. A., Simon, A., & van der Meer, J. W. M. (2012). Treating inflammation by blocking interleukin-1 in a broad spectrum of diseases. *Nature Reviews Drug Discovery*, *11*(8), 633–652. https://doi.org/10.1038/nrd3800

Du, L., Chen, E., Wu, T., Ruan, Y., & Wu, S. (2019). Resveratrol attenuates hydrogen peroxide-induced aging through upregulation of autophagy in human umbilical vein endothelial cells. *Drug Design, Development and Therapy*, *13*, 747–755. https://doi.org/10.2147/DDDT.S179894

Duan, J., Yue, W., Jianyu, E., Malhotra, J., Lu, S. E., Gu, J., Xu, F., & Tan, X. L. (2016). *In vitro* comparative studies of resveratrol and triacetylresveratrol on cell proliferation, apoptosis, and STAT3 and NFκB signaling in pancreatic cancer cells. *Scientific Reports*, *6*, 31672. https://doi.org/10.1038/srep31672

Dudás, J., Fullár, A., Romani, A., Pritz, C., Kovalszky, I., Hans Schartinger, V., Mathias Sprinzl, G., & Riechelmann, H. (2013). Curcumin targets fibroblast-tumor cell interactions in oral squamous cell carcinoma. *Experimental Cell Research*, *319*(6), 800–809. https://doi.org/10.1016/j.yexcr.2012.12.001

EL-Arabey, A. A., & Abdalla, M. (2020). Metformin and COVID-19: A novel deal of an old drug. *Journal of Medical Virology*, *92*(11), 2293–2294. John Wiley and Sons Inc. https://doi.org/10.1002/jmv.25958

Eren, M. K., Kilincli, A., & Eren, Ö. (2015). Resveratrol induced premature senescence is associated with DNA damage mediated SIRT1 and SIRT2 down-regulation. *PLoS ONE*, *10*(4), e0124837. https://doi.org/10.1371/journal.pone.0124837

Esam, Z. (2020). A proposed mechanism for the possible therapeutic potential of Metformin in COVID-19. *Diabetes Research and Clinical Practice*, *167*, 108282. Elsevier Ireland Ltd. https://doi.org/10.1016/j.diabres.2020.108282

Fletcher, L., Evans, T. M., Watts, L. T., Jimenez, D. F., & Digicaylioglu, M. (2013). Rapamycin treatment improves neuron viability in an *in vitro* model of stroke. *PLoS ONE*, *8*(7), e68281. https://doi.org/10.1371/journal.pone.0068281

Foster, H. A., & Bridger, J. M. (2005). The genome and the nucleus: A marriage made by evolution. Genome organisation and nuclear architecture. *Chromosoma*, *114*(4), 212–229. https://doi.org/10.1007/s00412-005-0016-6

Fraenkel, M., Ketzinel-Gilad, M., Ariav, Y., Pappo, O., Karaca, M., Castel, J., Berthault, M. F., Magnan, C., Cerasi, E., Kaiser, N., & Leibowitz, G. (2008). mTOR inhibition by rapamycin prevents β-cell adaptation to hyperglycemia and exacerbates the metabolic state in type 2 diabetes. *Diabetes*, *57*(4), 945–957. https://doi.org/10.2337/db07-0922

Fuhrmann-Stroissnigg, H., Niedernhofer, L. J., & Robbins, P. D. (2018). Hsp90 inhibitors as senolytic drugs to extend healthy aging. *Cell Cycle*, *17*(9), 1048–1055-. Taylor and Francis Inc. https://doi.org/10.1080/15384101.2018.1475828

Gao, Y., Wei, Y., Wang, Y., Gao, F., & Chen, Z. (2017). *Lycium barbarum*: A traditional Chinese herb and a promising anti-aging agent. *Aging and Disease*, *8*(6), 778–791. International Society on Aging and Disease. https://doi.org/10.14336/AD.2017.0725

Gerasymchuk, M. (2021). Genomic instability and aging: Causes and consequences. *Genome Stability*, 533–553. https://doi.org/10.1016/B978-0-323-85679-9.00028-3

Gerasymchuk, M., Cherkasova, V., Kovalchuk, O., & Kovalchuk, I. (2020). The role of microRNAs in organismal and skin aging. *International Journal of Molecular Sciences*, *21*(15), 5281. https://doi.org/10.3390/ijms21155281

Giovannelli, L., Pitozzi, V., Jacomelli, M., Mulinacci, N., Laurenzana, A., Dolara, P., & Mocali, A. (2011). Protective effects of resveratrol against senescence-associated changes in cultured human fibroblasts. *Journals of Gerontology - Series A Biological Sciences and Medical Sciences*, *66 A*(1), 9–18. https://doi.org/10.1093/gerona/glq161

Griveau, A., Wiel, C., Ziegler, D. V., Bergo, M. O., & Bernard, D. (2020). The JAK1/2 inhibitor ruxolitinib delays premature aging phenotypes. *Aging Cell*, *19*(4), e13122. https://doi.org/10.1111/acel.13122

Hasan, K. M. M., Rahman, M. S., Arif, K. M. T., & Sobhani, M. E. (2012). Psychological stress and aging: Role of glucocorticoids (GCs). *Age*, *34*(6), 1421–1433. https://doi.org/10.1007/s11357-011-9319-0

Heckman-Stoddard, B. M., DeCensi, A., Sahasrabuddhe, V. V., & Ford, L. G. (2017). Repurposing metformin for the prevention of cancer and cancer recurrence. *Diabetologia*, *60*(9), 1639–1647. Springer Verlag. https://doi.org/10.1007/s00125-017-4372-6

Houde, V. P., Brûlé, S., Festuccia, W. T., Blanchard, P. G., Bellmann, K., Deshaies, Y., & Marette, A. (2010). Chronic rapamycin treatment causes glucose intolerance and

hyperlipidemia by upregulating hepatic gluconeogenesis and impairing lipid deposition in adipose tissue. *Diabetes*, *59*(6), 1338–1348. https://doi.org/10.2337/db09-1324

Howell, J. J., Hellberg, K., Turner, M., Talbott, G., Kolar, M. J., Ross, D. S., Hoxhaj, G., Saghatelian, A., Shaw, R. J., & Manning, B. D. (2017). Metformin inhibits hepatic mTORC1 signaling via dose-dependent mechanisms involving AMPK and the TSC complex. *Cell Metabolism*, *25*(2), 463–471. https://doi.org/10.1016/j.cmet.2016.12.009

Hu, J., Han, H., Cao, P., Yu, W., Yang, C., Gao, Y., & Yuan, W. (2017). Resveratrol improves neuron protection and functional recovery through enhancement of autophagy after spinal cord injury in mice. *Am J Transl Res*, *9*(10), 4607–4616. www.ajtr.org

Huo, X., Zhang, T., Meng, Q., Li, C., & You, B. (2019). Resveratrol effects on a diabetic rat model with coronary heart disease. *Medical Science Monitor*, *25*, 540–546. https://doi.org/10.12659/MSM.910996

Ilnytskyy, Y., Koturbash, I., & Kovalchuk, O. (2009). Radiation-induced bystander effects *in vivo* are epigenetically regulated in a tissue-specific manner. *Environmental and Molecular Mutagenesis*, *50*(2), 105–113. https://doi.org/10.1002/em.20440

Jiang, Y., Dong, G., & Song, Y. (2018). Nucleus pulposus cell senescence is alleviated by resveratrol through regulating the ROS/NF-κB pathway under high-magnitude compression. *Bioscience Reports*, *38*(4), BSR20180670. https://doi.org/10.1042/BSR20180670

Johnson, S. C., Rabinovitch, P. S., & Kaeberlein, M. (2013). MTOR is a key modulator of ageing and age-related disease. *Nature*, *493*(7432), 338–345. https://doi.org/10.1038/nature11861

Karsak, M., Gaffal, E., Date, R., Wang-Eckhardt, L., Rehnelt, J., Petrosino, S., Starowicz, K., Steuder, R., Schlicker, E., Cravatt, B., Mechoulam, R., Buettner, R., Werner, S., Marzo, V. di, Tüting, T., & Zimmer, A. (2007). Attenuation of allergic contact dermatitis through the endocannabinoid system. *Science*, *316*(5830), 1494–1497. https://doi.org/10.1126/science.1142265

Kawarazaki, W., Mizuno, R., Nishimoto, M., Ayuzawa, N., Hirohama, D., Ueda, K., Kawakami-Mori, F., Oba, S., Marumo, T., & Fujita, T. (2020). Salt causes aging-associated hypertension via vascular Wnt5a under Klotho deficiency. *Journal of Clinical Investigation*, *140*(8), 4152–4166. https://doi.org/10.1172/JCI134431

Ketcherside, A., Noble, L. J., McIntyre, C. K., & Filbey, F. M. (2017). Cannabinoid receptor 1 gene by cannabis use interaction on CB1 receptor density. *Cannabis and Cannabinoid Research*, *2*(1), 202–209. https://doi.org/10.1089/can.2017.0007

Khan, N., Syed, D. N., Ahmad, N., & Mukhtar, H. (2013). Fisetin: A dietary antioxidant for health promotion. *Antioxidants and Redox Signaling*, *19*(2), 151–162. https://doi.org/10.1089/ars.2012.4901

Kim, D., Nguyen, M. D., Dobbin, M. M., Fischer, A., Sananbenesi, F., Rodgers, J. T., Delalle, I., Baur, J. A., Sui, G., Armour, S. M., Puigserver, P., Sinclair, D. A., & Tsai, L. H. (2007). SIRT1 deacetylase protects against neurodegeneration in models for Alzheimer's disease and amyotrophic lateral sclerosis. *EMBO Journal*, *26*(13), 3169–3179. https://doi.org/10.1038/sj.emboj.7601758

Kim, E. C., & Kim, J. R. (2019). Senotherapeutics: Emerging strategy for healthy aging and age-related disease. *BMB Reports*, 52(1), 47–55. The Biochemical Society of the Republic of Korea. https://doi.org/10.5483/BMBRep.2019.52.1.293

Kim, M. Y., Kang, E. S., Ham, S. A., Hwang, J. S., Yoo, T. S., Lee, H., Paek, K. S., Park, C., Lee, H. T., Kim, J. H., Han, C. W., & Seo, H. G. (2012). The PPARδ-mediated inhibition of angiotensin II-induced premature senescence in human endothelial cells is SIRT1-dependent. *Biochemical Pharmacology*, *84*(12), 1627–1634. https://doi.org/10.1016/j.bcp.2012.09.008

Kirkland, J. L., & Tchkonia, T. (2020). Senolytic drugs: From discovery to translation. *Journal of Internal Medicine*, *288*(5), 518–536. Blackwell Publishing Ltd. https://doi.org/10.1111/joim.13141

Kleszczynski, K., & Fischer, T. W. (2012). Melatonin and human skin aging. *Dermato-Endocrinology*, 4(3), 245–252. https://doi.org/10.4161/derm.22344

Koide, K., Osman, S., Garner, A. L., Song, F., Dixon, T., Greenberger, J. S., & Epperly, M. W. (2011). The use of 3,5,4′-tri-O-acetylresveratrol as a potential prodrug for resveratrol protects mice from γ-irradiation-induced death. *ACS Medicinal Chemistry Letters*, *2*(4), 270–274. https://doi.org/10.1021/ml100159p

Koturbash, I., Zemp, F. J., Kutanzi, K., Luzhna, L., Loree, J., Kolb, B., & Kovalchuk, O. (2008). Sex-specific microRNAome deregulation in the shielded bystander spleen of cranially exposed mice. *Cell Cycle*, *7*(11), 1658–1667. https://doi.org/10.4161/cc.7.11.5981

Kou, X., & Chen, N. (2017). Resveratrol as a natural autophagy regulator for prevention and treatment of Alzheimer's disease. *Nutrients*, *9*(9), 927. https://doi.org/10.3390/nu9090927

Lago, J. C., & Puzzi, M. B. (2019). The effect of aging in primary human dermal fibroblasts. *PLoS ONE*, *14*(7), e0219165. https://doi.org/10.1371/journal.pone.0219165

Lagoumtzi, S. M., & Chondrogianni, N. (2021). Senolytics and senomorphics: Natural and synthetic therapeutics in the treatment of aging and chronic diseases. *Free Radical Biology and Medicine*, *171*, 169–190. Elsevier Inc. https://doi.org/10.1016/j.freeradbiomed.2021.05.003

Lamming, D. W., Ye, L., Katajisto, P., Goncalves, M. D., Saitoh, M., Stevens, D. M., Davis, J. G., Salmon, A. B., Richardson, A., Ahima, R. S., Guertin, D. A., Sabatini, D. M., & Baur, J. A. (2012). Rapamycin-induced insulin resistance is mediated by mTORC2 loss and

uncoupled from longevity. *Science*, *335*(6076), 1638–1643. https://doi.org/10.1126/science.1215135

Lamming, D. W., Ye, L., Sabatini, D. M., & Baur, J. A. (2013). Rapalogs and mTOR inhibitors as anti-aging therapeutics. *Journal of Clinical Investigation*, *123*(3), 980–989. https://doi.org/10.1172/JCI64099

Laplante, M., & Sabatini, D. M. (2012). MTOR signaling in growth control and disease. *Cell*, *149*(2), 274–293. Elsevier B.V. https://doi.org/10.1016/j.cell.2012.03.017

Lee, J. J., Ng, S. C., Hsu, J. Y., Liu, H., Chen, C. J., Huang, C. Y., & Kuo, W. W. (2022). Galangin reverses H_2O_2-induced dermal fibroblast senescence via SIRT1-PGC-1α/Nrf2 signaling. *International Journal of Molecular Sciences*, *23*(3), 1387. https://doi.org/10.3390/ijms23031387

Lee, S. H., Lee, J. H., Lee, H. Y., & Min, K. J. (2019). Sirtuin signaling in cellular senescence and aging. *BMB Reports*, *52*(1), 24–34. The Biochemical Society of the Republic of Korea. https://doi.org/10.5483/BMBRep.2019.52.1.290

Li, J., Kim, S. G., & Blenis, J. (2014). Rapamycin: One drug, many effects. *Cell Metabolism*, *19*(3), 373–379. https://doi.org/10.1016/j.cmet.2014.01.001

Liang, L., Liu, X., Wang, Q., Cheng, S., Zhang, S., & Zhang, M. (2013). Pharmacokinetics, tissue distribution and excretion study of resveratrol and its prodrug 3,5,4′-tri-O-acetylresveratrol in rats. *Phytomedicine*, *20*(6), 558–563. https://doi.org/10.1016/j.phymed.2012.12.012

Lin, K. L., Lin, K. J., Wang, P. W., Chuang, J. H., Lin, H. Y., Chen, S. der, Chuang, Y. C., Huang, S. T., Tiao, M. M., Chen, J. B., Huang, P. H., Liou, C. W., & Lin, T. K. (2018). Resveratrol provides neuroprotective effects through modulation of mitochondrial dynamics and ERK1/2 regulated autophagy. *Free Radical Research*, *52*(11–12), 1371–1386. https://doi.org/10.1080/10715762.2018.1489128

Liu, S., Liu, S., Wang, X., Zhou, J., Cao, Y., Wang, F., & Duan, E. (2011). The PI3K-Akt pathway inhibits senescence and promotes self-renewal of human skin-derived precursors *in vitro*. *Aging Cell*, *10*(4), 661–674. https://doi.org/10.1111/j.1474-9726.2011.00704.x

Liu, S., Uppal, H., Demaria, M., Desprez, P. Y., Campisi, J., & Kapahi, P. (2015). Simvastatin suppresses breast cancer cell proliferation induced by senescent cells. *Scientific Reports*, *5*, 17895. https://doi.org/10.1038/srep17895

Liu, S., Zheng, Z., Ji, S., Liu, T., Hou, Y., Li, S., & Li, G. (2018). Resveratrol reduces senescence-associated secretory phenotype by SIRT1/NF-κB pathway in gut of the annual fish *Nothobranchius guentheri*. *Fish and Shellfish Immunology*, *80*, 473–479. https://doi.org/10.1016/j.fsi.2018.06.027

Liu, T., Zhang, L., Joo, D., & Sun, S. C. (2017). NF-κB signaling in inflammation. *Signal Transduction and Targeted Therapy*, *2*, e17023. https://doi.org/10.1038/sigtrans.2017.23

Loebsch S., Kloesch. (2014). Anti-inflammatory and pro-apoptotic effects of Curcumin and Resveratrol on the human lung fibroblast cell line MRC-5. *Alternative & Integrative Medicine, 03*(04), 100174. https://doi.org/10.4172/2327-5162.1000174

Ma, L., Zhao, Y., Wang, R., Chen, T., Li, W., Nan, Y., Liu, X., & Jin, F. (2015). 3,5,4′-Tri-O-acetylresveratrol attenuates lipopolysaccharide-induced acute respiratory distress syndrome via MAPK/SIRT1 pathway. *Mediators of Inflammation, 2015*, 143074. https://doi.org/10.1155/2015/143074

Madeo, F., Bauer, M. A., Carmona-Gutierrez, D., & Kroemer, G. (2019). Spermidine: a physiological autophagy inducer acting as an anti-aging vitamin in humans? *Autophagy, 15*(1), 165–168. Taylor and Francis Inc. https://doi.org/10.1080/15548627.2018.1530929

Madiraju, A. K., Erion, D. M., Rahimi, Y., Zhang, X. M., Braddock, D. T., Albright, R. A., Prigaro, B. J., Wood, J. L., Bhanot, S., MacDonald, M. J., Jurczak, M. J., Camporez, J. P., Lee, H. Y., Cline, G. W., Samuel, V. T., Kibbey, R. G., & Shulman, G. I. (2014). Metformin suppresses gluconeogenesis by inhibiting mitochondrial glycerophosphate dehydrogenase. *Nature, 510*(7506), 542–546. https://doi.org/10.1038/nature13270

Manchester, L. C., Coto-Montes, A., Boga, J. A., Andersen, L. P. H., Zhou, Z., Galano, A., Vriend, J., Tan, D. X., & Reiter, R. J. (2015). Melatonin: An ancient molecule that makes oxygen metabolically tolerable. *Journal of Pineal Research, 59*(4), 403–419. Blackwell Publishing Ltd. https://doi.org/10.1111/jpi.12267

Mandrol, P., Bhat, K., & Prabhakar, A. (2016). An *in vitro* evaluation of cytotoxicity of curcumin against human dental pulp fibroblasts. *Journal of Indian Society of Pedodontics and Preventive Dentistry, 34*(3), 269. https://doi.org/10.4103/0970-4388.186757

Martinelli, G., Magnavacca, A., Fumagalli, M., Dell'Agli, M., Piazza, S., & Sangiovanni, E. (2021). *Cannabis sativa* and skin health: Dissecting the role of phytocannabinoids. *Planta Medica,* 1-15. Georg Thieme Verlag. https://doi.org/10.1055/a-1420-5780

Mayack, B. K., Sippl, W., & Ntie-Kang, F. (2020). Natural products as modulators of sirtuins. *Molecules, 25*(14), 3287. MDPI AG. https://doi.org/10.3390/molecules25143287

Mehta, I. S., Figgitt, M., Clements, C. S., Kill, I. R., & Bridger, J. M. (2007). Alterations to nuclear architecture and genome behavior in senescent cells. *Annals of the New York Academy of Sciences, 1100,* 250–263. https://doi.org/10.1196/annals.1395.027

Menghini, R., Casagrande, V., Cardellini, M., Martelli, E., Terrinoni, A., Amati, F., Vasa-Nicotera, M., Ippoliti, A., Novelli, G., Melino, G., Lauro, R., & Federici, M. (2009). MicroRNA 217 modulates endothelial cell senescence via silent information regulator 1. *Circulation, 120*(15), 1524–1532. https://doi.org/10.1161/CIRCULATIONAHA.109.864629

Miao, J., Liu, J., Niu, J., Zhang, Y., Shen, W., Luo, C., Liu, Y., Li, C., Li, H., Yang, P., Liu, Y., Hou, F. F., & Zhou, L. (2019). Wnt/β-catenin/RAS signaling mediates age-related

renal fibrosis and is associated with mitochondrial dysfunction. *Aging Cell*, *18*(5). https://doi.org/10.1111/acel.13004

Michishita, E., Park, J. Y., Burneskis, J. M., Barrett, J. C., & Horikawa, I. (2005). Evolutionarily conserved and nonconserved cellular localizations and functions of human SIRT proteins. *Molecular Biology of the Cell*, *16*(10), 4623–4635. https://doi.org/10.1091/mbc.E05-01-0033

Miller, R. A., Harrison, D. E., Astle, C. M., Baur, J. A., Boyd, A. R., de Cabo, R., Fernandez, E., Flurkey, K., Javors, M. A., Nelson, J. F., Orihuela, C. J., Pletcher, S., Sharp, Z. D., Sinclair, D., Starnes, J. W., Wilkinson, J. E., Nadon, N. L., & Strong, R. (2011). Rapamycin, but not resveratrol or simvastatin, extends life span of genetically heterogeneous mice. *Journals of Gerontology - Series A Biological Sciences and Medical Sciences*, *66 A*(2), 191–201. https://doi.org/10.1093/gerona/glq178

Mills, R. E., Taylor, K. R., Podshivalova, K., Mckay, D. B., & Jameson, J. M. (2008). Defects in skin γδ T cell function contribute to delayed wound repair in rapamycin-treated mice 1. *Journal of Immunology*, *181*(6), 3974–3983. https://doi.org/10.4049/jimmunol.181.6.3974

Mithieux, S. M., & Weiss, A. S. (2005). Elastin. *Advances in Protein Chemistry*, *70*, 437–461. https://doi.org/10.1016/S0065-3233(04)70013-3

Mitsui', Y., & Schneider, E. L. (1976). Increased nuclear sizes in senescent human diploid fibroblast cultures. *Experimental Cell Research*, *100*, 147–152. https://doi.org/10.1016/0014-4827(76)90336-0

Moiseeva, O., Deschênes-Simard, X., St-Germain, E., Igelmann, S., Huot, G., Cadar, A. E., Bourdeau, V., Pollak, M. N., & Ferbeyre, G. (2013). Metformin inhibits the senescence-associated secretory phenotype by interfering with IKK/NF-κB activation. *Aging Cell*, *12*(3), 489–498. https://doi.org/10.1111/acel.12075

Morales, P., Hurst, D. P., & Reggio, P. H. (2017). Molecular targets of the phytocannabinoids-a complex picture. *Progress in the Chemistry of Organic Natural Products*, *103*, 103–131. https://doi.org/10.1007/978-3-319-45541-9

Morales, P., & Reggio, P. H. (2017). An update on non-CB1, non-CB2 cannabinoid related G-protein-coupled receptors. *Cannabis and Cannabinoid Research*, *2*(1), 265–273. https://doi.org/10.1089/can.2017.0036

Mostoslavsky, R., Chua, K. F., Lombard, D. B., Pang, W. W., Fischer, M. R., Gellon, L., Liu, P., Mostoslavsky, G., Franco, S., Murphy, M. M., Mills, K. D., Patel, P., Hsu, J. T., Hong, A. L., Ford, E., Cheng, H. L., Kennedy, C., Nunez, N., Bronson, R., … Alt, F. W. (2006). Genomic instability and aging-like phenotype in the absence of mammalian SIRT6. *Cell*, *124*(2), 315–329. https://doi.org/10.1016/j.cell.2005.11.044

Moyano-Mendez, J. R., Fabbrocini, G., de Stefano, D., Mazzella, C., Mayol, L., Scognamiglio, I., Carnuccio, R., Ayala, F., la Rotonda, M. I., & de Rosa, G. (2014). Enhanced

antioxidant effect of trans-resveratrol: Potential of binary systems with polyethylene glycol and cyclodextrin. *Drug Development and Industrial Pharmacy*, *40*(10), 1300–1307. https://doi.org/10.3109/03639045.2013.817416

Nelson, G., Wordsworth, J., Wang, C., Jurk, D., Lawless, C., Martin-Ruiz, C., & von Zglinicki, T. (2012). A senescent cell bystander effect: Senescence-induced senescence. *Aging Cell*, *11*(2), 345–349. https://doi.org/10.1111/j.1474-9726.2012.00795.x

Olivieri, F., Mazzanti, I., Abbatecola, A. M., Recchioni, R., Marcheselli, F., Procopio, A. D., & Antonicelli, R. (2012). Telomere/telomerase system: A new target of statins pleiotropic effect? *Current Vascular Pharmacology, 10*(2), 216-224.

Onken, B., & Driscoll, M. (2010). Metformin induces a dietary restriction-like state and the oxidative stress response to extend *C. elegans* healthspan via AMPK, LKB1, and SKN-1. *PLoS ONE, 5*(1), e8758. https://doi.org/10.1371/journal.pone.0008758

Ota, H., Akishita, M., Eto, M., Iijima, K., Kaneki, M., & Ouchi, Y. (2007). Sirt1 modulates premature senescence-like phenotype in human endothelial cells. *Journal of Molecular and Cellular Cardiology*, *43*(5), 571–579. https://doi.org/10.1016/j.yjmcc.2007.08.008

Park, D., Jeong, H., Lee, M. N., Koh, A., Kwon, O., Yang, Y. R., Noh, J., Suh, P. G., Park, H., & Ryu, S. H. (2016). Resveratrol induces autophagy by directly inhibiting mTOR through ATP competition. *Scientific Reports*, *6*, 21772. https://doi.org/10.1038/srep21772

Park, S. J., Ahmad, F., Philp, A., Baar, K., Williams, T., Luo, H., Ke, H., Rehmann, H., Taussig, R., Brown, A. L., Kim, M. K., Beaven, M. A., Burgin, A. B., Manganiello, V., & Chung, J. H. (2012). Resveratrol ameliorates aging-related metabolic phenotypes by inhibiting cAMP phosphodiesterases. *Cell*, *148*(3), 421–433. https://doi.org/10.1016/j.cell.2012.01.017

Park, S., Seok, J. K., Kwak, J. Y., Choi, Y. H., Hong, S. S., Suh, H. J., Park, W., & Boo, Y. C. (2016). Anti-melanogenic effects of resveratryl triglycolate, a novel hybrid compound derived by esterification of resveratrol with glycolic acid. *Archives of Dermatological Research*, *308*(5), 325–334. https://doi.org/10.1007/s00403-016-1644-9

Piskovatska, V., Strilbytska, O., Koliada, A., Vaiserman, A., & Lushchak, O. (2019). Health benefits of anti-aging drugs. *Subcellular Biochemistry.* 91, 339–392. Springer New York. https://doi.org/10.1007/978-981-13-3681-2_13

Poulsen, R. C., Watts, A. C., Murphy, R. J., Snelling, S. J., Carr, A. J., & Hulley, P. A. (2014). Glucocorticoids induce senescence in primary human tenocytes by inhibition of sirtuin 1 and activation of the p53/p21 pathway: *In vivo* and *in vitro* evidence. *Annals of the Rheumatic Diseases*, *73*(7), 1405–1413. https://doi.org/10.1136/annrheumdis-2012-203146

Qin, D., Ren, R., Jia, C., Lu, Y., Yang, Q., Chen, L., Wu, X., Zhu, J., Guo, Y., Yang, P., Zhou, Y., Zhu, N., Bi, B., & Liu, T. (2018). Rapamycin protects skin fibroblasts from ultraviolet

B-induced photoaging by suppressing the production of reactive oxygen species. *Cellular Physiology and Biochemistry*, *46*(5), 1849–1860. https://doi.org/10.1159/000489369

Ramis, M. R., Esteban, S., Miralles, A., Tan, D. X., & Reiter, R. J. (2015). Caloric restriction, resveratrol and melatonin: Role of SIRT1 and implications for aging and related-diseases. *Mechanisms of Ageing and Development*, *146–148*, 28–41. Elsevier Ireland Ltd. https://doi.org/10.1016/j.mad.2015.03.008

Ramot, Y., Sugawara, K., Zákány, N., Tóth, B. I., Bíró, T., & Paus, R. (2013). A novel control of human keratin expression: Cannabinoid receptor 1-mediated signaling down-regulates the expression of keratins K6 and K16 in human keratinocytes *in vitro* and *in situ*. *PeerJ*, *1*, e40. https://doi.org/10.7717/peerj.40

Rea, I. M., Gibson, D. S., McGilligan, V., McNerlan, S. E., Denis Alexander, H., & Ross, O. A. (2018). Age and age-related diseases: Role of inflammation triggers and cytokines. *Frontiers in Immunology*, *9*(Apr 9), 586. Frontiers Media S.A. https://doi.org/10.3389/fimmu.2018.00586

Rena, G., Hardie, D. G., & Pearson, E. R. (2017). The mechanisms of action of metformin. *Diabetologia*, 60(9), 1577–1585. Springer Verlag. https://doi.org/10.1007/s00125-017-4342-z

Repetto, G., del Peso, A., & Zurita, J. L. (2008). Neutral red uptake assay for the estimation of cell viability/cytotoxicity. *Nature Protocols*, *3*(7), 1125–1131. https://doi.org/10.1038/nprot.2008.75

Robbins, P. D., Tilstra, J. S., Clauson, C. L., & Niedernhofer, L. J. (2011). NF-κB in aging and disease. *Aging and Disease*, *2*(6), 449–465.

Ruland, J. (2011). Return to homeostasis: Downregulation of NF-κB responses. *Nature Immunology*, *12*(8), 709–714. https://doi.org/10.1038/ni.2055

Sabatini, D. M. (2017). Twenty-five years of mTOR: Uncovering the link from nutrients to growth. *Proceedings of the National Academy of Sciences of the United States of America*, *114*(45), 11818–11825. National Academy of Sciences. https://doi.org/10.1073/pnas.1716173114

Salehi, B., Mishra, A. P., Nigam, M., Sener, B., Kilic, M., Sharifi-Rad, M., Fokou, P. V. T., Martins, N., & Sharifi-Rad, J. (2018). Resveratrol: A double-edged sword in health benefits. *Biomedicines*, *6*(3), 91. MDPI AG. https://doi.org/10.3390/biomedicines6030091

Salminen, A., Kauppinen, A., & Kaarniranta, K. (2012). Emerging role of NF-κB signaling in the induction of senescence-associated secretory phenotype (SASP). *Cellular Signalling*, *24*(4), 835–845. https://doi.org/10.1016/j.cellsig.2011.12.006

Samaraweera, L., Adomako, A., Rodriguez-Gabin, A., & McDaid, H. M. (2017). A novel indication for Panobinostat as a senolytic drug in NSCLC and HNSCC. *Scientific Reports*, *7*(1), 1900. https://doi.org/10.1038/s41598-017-01964-1

San Hipólito-Luengo, Á., Alcaide, A., Ramos-González, M., Cercas, E., Vallejo, S., Romero, A., Talero, E., Sánchez-Ferrer, C. F., Motilva, V., & Peiró, C. (2017). Dual effects of resveratrol on cell death and proliferation of colon cancer cells. *Nutrition and Cancer*, *69*(7), 1019–1027. https://doi.org/10.1080/01635581.2017.1359309

Sarkar, S. (2013). Regulation of autophagy by mTOR-dependent and mTOR-independent pathways: Autophagy dysfunction in neurodegenerative diseases and therapeutic application of autophagy enhancers. *Biochemical Society Transactions*, *41*(5), 1103–1130. https://doi.org/10.1042/BST20130134

Sarpietro, M. G., Spatafora, C., Tringali, C., Micieli, D., & Castelli, F. (2007). Interaction of resveratrol and its trimethyl and triacetyl derivatives with biomembrane models studied by differential scanning calorimetry. *Journal of Agricultural and Food Chemistry*, *55*(9), 3720–3728. https://doi.org/10.1021/jf070070q

Sasaki, T., Maier, B., Bartke, A., & Scrable, H. (2006). Progressive loss of SIRT1 with cell cycle withdrawal. *Aging Cell*, *5*(5), 413–422. https://doi.org/10.1111/j.1474-9726.2006.00235.x

Scheau, C., Badarau, I. A., Mihai, L. G., Scheau, A. E., Costache, D. O., Constantin, C., Calina, D., Caruntu, C., Costache, R. S., & Caruntu, A. (2020). Cannabinoids in the pathophysiology of skin inflammation. *Molecules*, 25(3), 652. MDPI AG. https://doi.org/10.3390/molecules25030652

Sengupta, R., Barone, A., Marasa, J., Taylor, S., Jackson, E., Warrington, N. M., Rao, S., Kim, A. H., Leonard, J. R., Piwnica-Worms, D., & Rubin, J. B. (2015). Novel chemical library screen identifies naturally occurring plant products that specifically disrupt glioblastoma-endothelial cell interactions. *Oncotarget*, *6*(21), 18282–18292. https://doi.org/10.18632/oncotarget.4957

Shao, X., Cao, X., Song, G., Zhao, Y., & Shi, B. (2014). Metformin rescues the MG63 osteoblasts against the effect of high glucose on proliferation. *Journal of Diabetes Research*, *2014*, 453940. https://doi.org/10.1155/2014/453940

Shetty, A. K., Kodali, M., Upadhya, R., & Madhu, L. N. (2018). Emerging anti-aging strategies – Scientific basis and efficacy. *Aging and Disease*, *9*(6), 1165–1184. International Society on Aging and Disease. https://doi.org/10.14336/AD.2018.1026

Shi, W. Y., Xiao, D., Wang, L., Dong, L. H., Yan, Z. X., Shen, Z. X., Chen, S. J., Chen, Y., & Zhao, W. L. (2012). Therapeutic metformin/AMPK activation blocked lymphoma cell growth via inhibition of mTOR pathway and induction of autophagy. *Cell Death and Disease*, *3*(3), e275. https://doi.org/10.1038/cddis.2012.13

Shin, D. J., Kim, J. E., Lim, T. G., Jeong, E. H., Park, G., Kang, N. J., Park, J. S., Yeom, M. H., Oh, D. K., Bode, A. M., Dong, Z., Lee, H. J., & Lee, K. W. (2014). 20-O-β-d-glucopyranosyl-20(S)-protopanaxadiol suppresses UV-induced MMP-1 expression through AMPK-mediated mTOR inhibition as a downstream of the PKA-LKB1 pathway. *Journal of Cellular Biochemistry*, *115*(10), 1702–1711. https://doi.org/10.1002/jcb.24833

Shishodia, S. (2013). Molecular mechanisms of curcumin action: Gene expression. *BioFactors*, *39*(1), 37–55. https://doi.org/10.1002/biof.1041

Singh, N., Ranjan, V., Zaidi, D., Shyam, H., Singh, A., Lodha, D., Sharma, R., Verma, U., Dixit, J., & Balapure, A. K. (2012). Insulin catalyzes the curcumin-induced wound healing: An *in vitro* model for gingival repair. *Indian Journal of Pharmacology*, *44*(4), 458–462. https://doi.org/10.4103/0253-7613.99304

Sorsa, T., Tjäderhane, L., & Salo, T. (2004). Matrix metalloproteinases (MMPs) in oral diseases. *Oral Diseases*, *10*, 311–318. http://www.blackwellmunksgaard.com

Soydas, T., Sayitoglu, M., Sarac, E. Y., Cınar, S., Solakoglu, S., Tiryaki, T., & Sultuybek, G. K. (2021). Metformin reverses the effects of high glucose on human dermal fibroblasts of aged skin via downregulating RELA/p65 expression. *Journal of Physiology and Biochemistry*, *77*(3), 443–450. https://doi.org/10.1007/s13105-021-00823-y

Soydas, T., Yaprak Sarac, E., Cinar, S., Dogan, S., Solakoglu, S., Tuncdemir, M., & Kanigur Sultuybek, G. (2018). The protective effects of metformin in an in vitro model of aging 3T3 fibroblast under the high glucose conditions. *Journal of Physiology and Biochemistry*, *74*(2), 273–281. https://doi.org/10.1007/s13105-018-0613-5

Squarize, C. H., Castilho, R. M., Bugge, T. H., & Gutkind, J. S. (2010). Accelerated wound healing by mTOR activation in genetically defined mouse models. *PLoS ONE*, *5*(5), e10643. https://doi.org/10.1371/journal.pone.0010643

Sun, N., Youle, R. J., & Finkel, T. (2016). The mitochondrial basis of aging. *Molecular Cell*, *61*(5), 654–666. Cell Press. https://doi.org/10.1016/j.molcel.2016.01.028

Szende, B., Tyihák, E., & Király-Véghely, Z. (2000). Dose-dependent effect of resveratrol on proliferation and apoptosis in endothelial and tumor cell cultures. *Experimental and Molecular Medicine*, *32*(2), 88–92. https://doi.org/10.1038/emm.2000.16

Szkudelski, T., & Szkudelska, K. (2015). Resveratrol and diabetes: From animal to human studies. *Biochimica et Biophysica Acta - Molecular Basis of Disease*, *1852*(6), 1145–1154. Elsevier B.V. https://doi.org/10.1016/j.bbadis.2014.10.013

Thoppil, H., & Riabowol, K. (2020). Senolytics: A translational bridge between cellular senescence and organismal aging. *Frontiers in Cell and Developmental Biology*, *7*, 367. Frontiers Media S.A. https://doi.org/10.3389/fcell.2019.00367

Tia, N., Singh, A. K., Pandey, P., Azad, C. S., Chaudhary, P., & Gambhir, I. S. (2018). Role of Forkhead Box O (FOXO) transcription factor in aging and diseases. *Gene, 648*, 97–105. Elsevier B.V. https://doi.org/10.1016/j.gene.2018.01.051

Unni, N., & Arteaga, C. L. (2019). Is dual mTORC1 and mTORC2 therapeutic blockade clinically feasible in cancer? *JAMA Oncology*, *5*(11), 1564–1565. American Medical Association. https://doi.org/10.1001/jamaoncol.2019.2525

Vang, O. (2015). Resveratrol: challenges in analyzing its biological effects. *Annals of the New York Academy of Sciences*, *1348*(1), 161–170. https://doi.org/10.1111/nyas.12879

Wang, C., Zhou, Z., Song, W., Cai, Z., Ding, Z., Chen, D., Xia, F., & He, Y. (2022). Inhibition of IKKβ/NF-κB signaling facilitates tendinopathy healing by rejuvenating inflamm-aging induced tendon-derived stem/progenitor cell senescence. *Molecular Therapy - Nucleic Acids*, *27*, 562–576. https://doi.org/10.1016/j.omtn.2021.12.026

Wang, F., Cai, F., Shi, R., Wang, X. H., & Wu, X. T. (2016). Aging and age related stresses: A senescence mechanism of intervertebral disc degeneration. *Osteoarthritis and Cartilage*, *24*(3), 398–408. W.B. Saunders Ltd. https://doi.org/10.1016/j.joca.2015.09.019

Wang, S. F., Wu, M. Y., Cai, C. Z., Li, M., & Lu, J. H. (2016). Autophagy modulators from traditional Chinese medicine: Mechanisms and therapeutic potentials for cancer and neurodegenerative diseases. *Journal of Ethnopharmacology*, *194*, 861–876. Elsevier Ireland Ltd. https://doi.org/10.1016/j.jep.2016.10.069

Wang, X., Chen, L., & Peng, W. (2017). Protective effects of resveratrol on osteoporosis via activation of the SIRT1-NF-κB signaling pathway in rats. *Experimental and Therapeutic Medicine*, *14*(5), 5032–5038. https://doi.org/10.3892/etm.2017.5147

Widel, M., Krzywon, A., Gajda, K., Skonieczna, M., & Rzeszowska-Wolny, J. (2014). Induction of bystander effects by UVA, UVB, and UVC radiation in human fibroblasts and the implication of reactive oxygen species. *Free Radical Biology and Medicine*, *68*, 278–287. https://doi.org/10.1016/j.freeradbiomed.2013.12.021

Wilkinson, J. E., Burmeister, L., Brooks, S. v., Chan, C. C., Friedline, S., Harrison, D. E., Hejtmancik, J. F., Nadon, N., Strong, R., Wood, L. K., Woodward, M. A., & Miller, R. A. (2012). Rapamycin slows aging in mice. *Aging Cell*, *11*(4), 675–682. https://doi.org/10.1111/j.1474-9726.2012.00832.x

Wu, N., Gu, C., Gu, H., Hu, H., Han, Y., & Li, Q. (2011). Metformin induces apoptosis of lung cancer cells through activating JNK/p38 MAPK pathway and GADD153. *Neoplasma*, *58*(6), 482–490. https://doi.org/10.4149/neo_2011_06_482

Yang, C.-W., Chang, C.-L., Lee, H.-C., Chi, C.-W., Pan, J.-P., & Yang, W.-C. (2012). Curcumin induces the apoptosis of human monocytic leukemia THP-1 cells via the activation of JNK/ERK Pathways. *BMC Complementary and Alternative Medicine*, *12*(1), 22. https://doi.org/10.1186/1472-6882-12-22

Yao, H., Chung, S., Hwang, J.-W., Rajendrasozhan, S., Sundar, I. K., Dean, D. A., Mcburney, M. W., Guarente, L., Gu, W., Rönty, M., Kinnula, V. L., & Rahman, I. (2012). SIRT1 protects against emphysema via FOXO3-mediated reduction of premature senescence in mice. *The Journal of Clinical Investigation*, *122*(6), 2032-2045. https://doi.org/10.1172/JCI60132DS1

Yessenkyzy, A., Saliev, T., Zhanaliyeva, M., Masoud, A. R., Umbayev, B., Sergazy, S., Krivykh, E., Gulyayev, A., & Nurgozhin, T. (2020). Polyphenols as caloric-restriction mimetics and autophagy inducers in aging research. *Nutrients*, *12*(5), 1344. MDPI AG. https://doi.org/10.3390/nu12051344

Yoshizaki, A., Yanaba, K., Yoshizaki, A., Iwata, Y., Komura, K., Ogawa, F., Takenaka, M., Shimizu, K., Asano, Y., Hasegawa, M., Fujimoto, M., & Sato, S. (2010). Treatment with rapamycin prevents fibrosis in tight-skin and bleomycin-induced mouse models of systemic sclerosis. *Arthritis and Rheumatism*, *62*(8), 2476–2487. https://doi.org/10.1002/art.27498

Yu Guang-Tao, Bu Lin-Lin, Zhao Yu-Yue, Liu Bing, Zhang Wen-Feng, Zhao Yi-Fang, Zhang Lu, & Sun Zhi-Jun. (2014). Inhibition of mTOR reduce Stat3 and PAI related angiogenesis in salivary gland adenoid cystic carcinoma. *American Journal of Cancer Research*, *4*(6), 764–775.

Zagórska-Dziok, M., Bujak, T., Ziemlewska, A., & Nizioł-Łukaszewska, Z. (2021). Positive effect of *Cannabis sativa L.* Herb extracts on skin cells and assessment of cannabinoid-based hydrogels properties. *Molecules*, *26*(4), 802. https://doi.org/10.3390/molecules26040802

Zhang, C. S., Li, M., Ma, T., Zong, Y., Cui, J., Feng, J. W., Wu, Y. Q., Lin, S. Y., & Lin, S. C. (2016). Metformin activates AMPK through the lysosomal pathway. *Cell Metabolism*, *24*(4), 521–522. Cell Press. https://doi.org/10.1016/j.cmet.2016.09.003

Zhang, G., Li, J., Purkayastha, S., Tang, Y., Zhang, H., Yin, Y., Li, B., Liu, G., & Cai, D. (2013). Hypothalamic programming of systemic ageing involving IKK-b, NF-kB and GnRH. *Nature*, *497*(May), 211–218. https://doi.org/10.1038/nature12143

Zhao, P., Sui, B. D., Liu, N., Lv, Y. J., Zheng, C. X., Lu, Y. B., Huang, W. T., Zhou, C. H., Chen, J., Pang, D. L., Fei, D. D., Xuan, K., Hu, C. H., & Jin, Y. (2017). Anti-aging pharmacology in cutaneous wound healing: effects of metformin, resveratrol, and rapamycin by local application. *Aging Cell*, *16*(5), 1083–1093. https://doi.org/10.1111/acel.12635

Zhou, H., Ding, S., Sun, C., Fu, J., Yang, D., Wang, X., Wang, C. C., & Wang, L. (2022). *Lycium barbarum* extracts extend lifespan and alleviate proteotoxicity in *Caenorhabditis elegans*. *Frontiers in Nutrition*, *8*, 815947. https://doi.org/10.3389/fnut.2021.815947

Zhu, M., Meng, P., Ling, X., & Zhou, L. (2020). Advancements in therapeutic drugs targeting of senescence. *Therapeutic Advances in Chronic Disease*, *11*, 1–26. SAGE Publications Ltd. https://doi.org/10.1177/2040622320964125

Zou, Z., Tao, T., Li, H., & Zhu, X. (2020). mTOR signaling pathway and mTOR inhibitors in cancer: Progress and challenges. *Cell and Bioscience*, *10*(1), 31. BioMed Central Ltd. https://doi.org/10.1186/s13578-020-00396-1

Zu, Y., Liu, L., Lee, M. Y. K., Xu, C., Liang, Y., Man, R. Y., Vanhoutte, P. M., & Wang, Y. (2010). SIRT1 promotes proliferation and prevents senescence through targeting LKB1 in primary porcine aortic endothelial cells. *Circulation Research*, *106*(8), 1384–1393. https://doi.org/10.1161/CIRCRESAHA.109.215483

CHAPTER 5. GENERAL DISCUSSION AND FUTURE DIRECTIONS

Aging is an ongoing process of gradual deterioration of structural and functional organismal characteristics and time-dependent potentiation of risk of morbidity and mortality. The majority of aging-associated research focused in a few, main areas: (i) the molecular mechanisms of aging on organismal, tissue, and cellular levels; (ii) longevity studies; (iii) anti-aging therapies, and (iv) rejuvenation strategies. In the last couple of decades, a tremendous body of literature and numerous breakthroughs have accumulated in the area of genetic and molecular aspects of cell-cycle regulation, cellular senescence, apoptosis and the corresponding pharmacological possibilities of their ability to correct, alleviate, delay or completely stop aging. Regardless of the progress in this area, the research community are still not able to explain all pathogenetic aspects of aging or propose an efficient method to alleviate or delay aging-related diseases. In parallel, the research community is continuing to look for rejuvenation strategies.

The overall aim of this study was to explore the anti-aging and rejuvenation effects of phytocannabinoids (pCBs) on skin aging by studying the effects of delta-9-tetrahydrocannabinol (THC) and cannabidiol (CBD) during H_2O_2 stress-induced premature senescence (SIPS) on dermal fibroblasts *in vitro*. In addition, we studied the combined effects of pCBs and nutrient signaling regulators (NSRs) metformin, rapamycin, and triacetylresveratrol (TRSV), acetylated analog of resveratrol, as potential anti-aging and rejuvenation tools.

5.1. Summary of major findings

Chapter 2 of this thesis describes the validation of the dermal fibroblasts SIPS models and its use in skin aging research. Here, I explained three-step and one-step H_2O_2-induced models of SIPS for *in vitro* studies that mimic skin aging characteristics designed and tested on different dermal fibroblasts cell-line (CCD-1064Sk, CCD-1135Sk, and BJ-5ta), based on the available literature data (Caldini et al., 1998; Chen & Ames, 1994; Sasaki et al., 2014; Shlush et al., 2011). With the motivation to contribute to developing new anti-aging and rejuvenation strategies, the one-step and three-step *in vitro* SIPS models included different concentrations of H_2O_2 were tested. Firstly, we showed that 25 µM concentration of H_2O_2 was the most optimal for the relatively stable induction of SIPS in different cell lines of dermal fibroblasts. Secondly, our tests found that skin fibroblasts developed similar aging characteristics as cells with replicative senescence (RS) in both SIPS models. We detected increased levels of β-Gal expression, high level of p21 protein, altered levels of cell-cycle regulators (i.e., CDK2 and c-Jun) and extracellular matrix (ECM) components, reduced cellular viability, and delayed wound healing properties. Based on the low cellular recovery, fast exhaustion of the replicative potential, significant increases in senescence biomarkers in the CCD-1135Sk, CCD-1064Sk, and BJ-5ta cultures, along with reduced functional and metabolic activity, the one-step senescence model was chosen as a feasible and reliable method for testing anti-aging compounds.

In **Chapter 3,** we studied the effects of cannabinoid treatments on the skin fibroblasts senescence-associated phenotype. First of all, based on the morphological alterations, β-Gal expression, and cell viability assays, we detected an optimal 2.0 µM concentration of pCBs for the subsequent anti-aging studies. After that, we studied how THC and CBD affected cellular morphology, nuclear architecture, senescence biomarkers, cell-cycle

control, metabolic regulators, and the estimated functional ability to maintain ECM environment and wound healing on healthy and senescent fibroblasts. Both treatments exerted preservative effects on cellular quantitative and qualitative characteristics by reducing morphological alterations in skin cells. Nuclei of senescent fibroblasts resembled healthy counterparts with a lower extent of deviations in the nuclear parameters than the vehicle. These findings accompanied a cannabinoid-induced reduction in main cellular senescence biomarkers like β-galactosidase, p16, and p21 in naturally-aged fibroblasts and SIPS fibroblasts, with CBD – inducing potentiation of *TP53* expression ($p<0.0001$). Moreover, senescent fibroblasts exposed to pCBs demonstrated mild NF-κB downregulation ($p>0.05$), insignificant elevation of CDK2, Cyclin D1, and c-Jun, which is a negative regulator of p53 and p21 expression affecting the modulation of mitogenic signaling and cell-cycle regulation (Schreiber et al., 1999). Beyond that, pCBs exerted anti-aging and rejuvenation effects on dermal cells by potentiating cellular viability and wound closure based on sirtuin-stimulated metabolic regulation and improved generation of ECM components in prematurely aged fibroblasts. Thus, ample evidence points to pCBs as a potential anti-aging and rejuvenation tool.

These are novel findings because the majority of *in vitro* and *in vivo* cannabinoid-orientated studies focused on the effects in the endocannabinoid system regulation or alleviation of neurodegenerative, cardiovascular, diabetes, and cancer, which are combined in the group of age-related diseases (ARD). Furthermore, there is limited attention concerning the usage of pCBs in dermatology. The predominant part of cannabis-associated research projects devoted to skin pathology (i.e., eczema, psoriasis, dermatitis) and surprisingly neglected anti-aging or rejuvenation questions, despite the fact that the market is overloaded with products containing some cannabis ingredients. That is even more

surprising because significant financial input by the cosmetics industry is directed to support the research projects to develop dermatological anti-aging and rejuvenating beauty products. Thus, our study reported research-based evidence of potential use of pCBs for subsequent clinical orientated studies.

In **Chapter 4,** we studied the influence of metformin, rapamycin, and triacetylresveratrol on SIPS fibroblasts to determine possible skin-related anti-aging and rejuvenation effects. For the first time, the combined effect of NSRs and pCBs THC and CBD treatments was tested on the prematurely aged dermal fibroblasts. For the first time, the combined effect of NSRs and THC or/and CBD treatments were tested on the prematurely aged dermal fibroblasts. Moreover, instead of well-known compound resveratrol, we studied its acetylated analog triacetylresveratrol (TRSV), which has higher bioavailability (Duan et al., 2016; Liang et al., 2013). We discovered that THC alone, metformin, TRSV and rapamycin combined with THC/CBD preserve nuclear morphology. Increase in the expression of energy modulators *SIRT1* and *SIRT6* in senescent cells was associated with rapamycin, TRSV, and metformin combined with THC/CBD treatments. At the same time, increase in the expression of ECM components generators (collagen III type, elastin) was predominantly related to TRSV and rapamycin, while rapamycin was also detected to inhibit *MMP2*. Beyond that, TRSV alone and combined with THC or CBD potentiated wound healing, while rapamycin delayed it.

Furthermore, we discovered that rapamycin alone and combined with THC or CBD, and mixed treatment that included metformin, TRSV, rapamycin, THC, and CBD negatively affected cellular viability in healthy and senescent dermal fibroblasts (Figure 4.13). We can speculate that NSRs combined with pCBs have a competitive effect on

mTOR, AMPK signaling pathways that eventually decrease their efficacy, thereby reducing cellular viability.

5.2. Study limitations

In this study, we aimed to detect anti-aging and rejuvenation effects of THC and CBD on the in vitro model of H_2O_2-induced premature senescence of different skin fibroblasts cell lines of. Specifically, we analyzed the impact of pCBs on the changes in components of ECM (collagens, elastin, hyaluronan, and MMPs), cellular viability, morphological deviations, gene expression of aging-related biomarkers, metabolic and functional regulators, and healing activities. We found partial positive effects of THC and CBD as anti-aging and rejuvenation tools alone and combined with popular longevity compounds metformin, rapamycin, and TRSV. These results will likely allow the development of novel anti-aging and rejuvenating strategies in the modern dermatology and beauty industry; nevertheless, they are not without limitations.

First of all, the current study was not done *in vivo*. For instance, in animal experiments, we could evaluate and analyze mutual response not solely of skin fibroblasts, but also of other dermal cells and test the response of immune system and perform multiple biochemical and physical tests. Moreover, animal studies can enable testing trans-epidermal water loss (TEWL), prevention of wrinkle formation, skin turgor, and elasticity, as well as allow to reproduce natural wound healing conditions.

Secondly, we could have used animals to test dose and time-dependent response to pCBs and NSRs. The live organism may react differently to the various doses which may not be aligned with our *in vitro* findings.

The third limitation is related to fibroblasts; they are not the first line of cells in the skin that are affected by external aging. Albeit fibroblasts are the main generators of dermal ECM components and thereby architects and engineers of dermal structure and its health, they are still protected from direct adverse effects by the epidermal layer of the skin.

The fourth limiting factor is associated with test methods. For instance, we could used mRNA-sequencing to determine multiple upregulated or downregulated genes and efficiently distinguish leading pathogenetic pathways in aging.

An additional limitation of this study is the fact that apart from CB1/CB2 receptors expression, we have not analyzed other components of the endocannabinoid system (ECS). In addition to the analysis of CB1/CB2 we in parallel could have analyzed anandamide (AEA) levels and the expression of its degrading enzyme fatty acid amide hydrolase (FAAH), or expression of diacylglycerol lipase (DAGL), which is responsible for 2-arachidonoylglycerol (2-AG) production, and expression of 2-AG degrading enzyme monoacylglycerol lipase (MAGL) (Cintosun et al., 2020; Jeong et al., 2019). It would be interesting to compare the competitive effect of 2-AG, a primary endogenous ligand and physiological cannabinoid receptor agonist for the CB2 receptor (Ibsen et al., 2017). Changes in the expression of ECS component could perhaps explain the effects of CBD and THC alone and in complex with NSRs; it is possible that endocannabinoids may have antagonistic effects, leading to more moderate efficacy of pCBs in decreasing the expression of p16, p21, or p53, and lack of the effect on COL1A1 expression, or reduced cellular viability in certain treatments.

We did not test FGF2, a basic fibroblast growth factor (bFGF), and FGF-β, a growth factor and signaling protein encoded by the FGF2 gene. It exerts a wide range of mitogenic and cell survival activities and is involved in embryonic development, cell growth,

morphogenesis, tissue repair, involved in cancerogenesis (maintains tumor growth and invasion).

5.3. Future studies

While the results presented in this thesis support an anti-aging and rejuvenation potential of THC and CBD alone and combined with NSRs in SIPS, understanding its precise regulation of molecular mechanisms and their regulation requires further research. Several ideas for future work are outlined in the next sections.

5.3.1. Phytocannabinoids impact on nuclear cytoskeletal components of senescent dermal fibroblast

Recent studies showed that nuclei of senescent fibroblasts tended to develop an elongated morphology (Aifuwa et al., 2015). Different authors displayed decreased expression of cytoskeletal proteins such as lamin A/C, F-actin, myosin II, Rho A in senescent nuclei (Aifuwa et al., 2015; Bridger et al., 2007; Frankel et al., 2018; Scaffidi & Misteli, 2006). Moreover, recently found that depolymerization of microtubules and constitutive activation of RhoA prevented the formation of an elongated phenotype in prematurely aged cells (Aifuwa et al., 2015). Thus, it would be interesting to compare the effects of pCBs and NSRs on the abovementioned proteins. In addition, we can compare the activity of adhesive protein vinculin on lamin A/C, F-actin, myosin II, Rho A and find out if stimulating RhoA and vinculin activity or depolymerizing microtubules would not only prevent senescent-induced cell elongation but inhibit cell-cell detachment. These data might also correlate with cell-cycle and metabolic regulation mechanisms and help discover new nuclear-related potential biomarkers of aging.

5.3.2. Role of phytocannabinoids in autophagy stimulation as part of anti-aging effects

Metformin, rapamycin, and resveratrol are well-known NSRs with strong research-based evidence of ARD prevention and symptoms abatement, an extension of longevity, and at least one anti-aging process in common, namely - autophagy (King et al., 2011; Yessenkyzy et al., 2020). Interestingly, recent report show that autophagy reduction prevents the effect of anti-aging calorie restriction in all studied species (Chen et al., 2019; Cheon et al., 2019; Gu et al., 2020; Sarkar, 2013; Wong et al., 2020; Xu et al., 2016) by simultaneous stimulation of TOR and signaling along the insulin/insulin-like growth factor (IGF) pathway (Kenyon, 2010), via AMPK and SIRT1 activation. Furthermore, SIRT1 was affected in prematurely aged fibroblasts in our studies. AMPK and the IGF pathway were not studied and potentially could have been altered in our SIPS model. Hence, it would be beneficial to pay more attention to the impact of THC and CBD on autophagy regulation in *in vitro* and *in vivo* studies.

5.3.3. From genomics to metabolomics

To find robust connections and thereby explain pathogenetic mechanisms in effects of pCBs alone and combined with metformin, rapamycin, or TRSV, it would be very beneficial to look at key transcription factors and target genes by performing RNA sequencing, transcriptome, metabolome, and proteome profiling. The majority of *in vitro* aging studies use genomics (represents DNA and genetic information within a cell) (Ameling et al., 2015; Blumenberg, 2012), transcriptomics (answer questions about RNA and differences in mRNA expression) (Gerasymchuk et al., 2020), followed by the analyses of relevant protein expression as a road map for interpretation of results. At the same time, metabolomics reveals information about substrates and products of metabolism, which are

influenced by genetic and environmental factors, and directly mirror the fundamental biochemical activity and state of cells and/or tissues (Mayer et al., 2018). In addition, previous studies have shown that combining all “omics” or more precisely “Skinomics” (Blumenberg, 2012) may contribute to a better understanding of the pathophysiology of the diseases (Ghosh et al., 2017; Mayer et al., 2018) and, in our situation, it would allow better understanding of anti-aging and rejuvenation properties of pCBs and NSRs in skin aging.

5.3.4. Anti-aging and rejuvenation effects of THC and CBD alone and in combination with metformin, rapamycin, and TRSV on murine skin

One of the most prioritized aspects should be focusing on *in vivo* experiments on naturally aged rats in future studies. Comparing *in vitro* and *in vivo* results based on metabolome and proteome profiling to already obtained data would be very beneficial for potential clinical trials.

5.4. REFERENCES

Aifuwa, I., Giri, A., Longe, N., Lee, S. H., An, S. S., & Wirtz, D. (2015). Senescent stromal cells induce cancer cell migration via inhibition of RhoA/ROCK/myosin-based cell contractility. *Oncotarget*, *6*(31), 30516–30531. www.impactjournals.com/oncotarget/

Ameling, S., Kacprowski, T., Chilukoti, R. K., Malsch, C., Liebscher, V., Suhre, K., Pietzner, M., Friedrich, N., Homuth, G., Hammer, E., & Völker, U. (2015). Associations of circulating plasma microRNAs with age, body mass index and sex in a population-based study. *BMC Medical Genomics*, *8*(1), 1–9. https://doi.org/10.1186/s12920-015-0136-7

Blumenberg, M. (2012). SKINOMICS: Transcriptional profiling in dermatology and skin biology. *Curr Genomics*, *13*, 363–368. https://doi.org/10.2174/138920212801619241

Bridger, J. M., Foeger, N., Kill, I. R., & Herrmann, H. (2007). The nuclear lamina: Both a structural framework and a platform for genome organization. *FEBS Journal*, *274*(6), 1354–1361. https://doi.org/10.1111/j.1742-4658.2007.05694.x

Caldini, R., Chevanne, M., Mocali, A., Tombaccini, D., & Paoletti, F. (1998). Premature induction of aging in sublethally H_2O_2-treated young MRC5 fibroblasts correlates with increased glutathione peroxidase levels and resistance to DNA breakage. *Mechanisms of Ageing and Development*, *105*(1–2), 137–150. https://doi.org/10.1016/S0047-6374(98)00085-2

Chen, Q., & Ames, B. N. (1994). Senescence-like growth arrest induced by hydrogen peroxide in human diploid fibroblast F65 cells (replicatlve castion/mophol /DNA damage/p53 cell cycle checkpoint). *Cell Biology*, *91*(May), 4130–4134. http://www.pnas.org/content/91/10/4130.full.pdf

Chen, X., Lin, S., Gu, L., Zhu, X., Zhang, Y., Zhang, H., Shao, B., Zhuge, Q., & Jin, K. (2019). Inhibition of miR-497 improves functional outcome after ischemic stroke by enhancing neuronal autophagy in young and aged rats. *Neurochemistry International*, *127*, 64–72. https://doi.org/10.1016/j.neuint.2019.01.005

Cheon, S. Y., Kim, H., Rubinsztein, D. C., & Lee, J. E. (2019). Autophagy, cellular aging and age-related human diseases. *Experimental Neurobiology*, *28*(6), 643–657. https://doi.org/10.5607/en.2019.28.6.643

Cintosun, A., Lara-Corrales, I., & Pope, E. (2020). Mechanisms of cannabinoids and potential applicability to skin diseases. *Clinical Drug Investigation*, *40*, 293–304. https://doi.org/10.1007/s40261-020-00894-7

Duan, J., Yue, W., Jianyu, E., Malhotra, J., Lu, S. E., Gu, J., Xu, F., & Tan, X. L. (2016). *In vitro* comparative studies of resveratrol and triacetylresveratrol on cell proliferation, apoptosis, and STAT3 and NFκB signaling in pancreatic cancer cells. *Scientific Reports*, *6*, 31672. https://doi.org/10.1038/srep31672

Frankel, D., Delecourt, V., Harhouri, K., de Sandre-Giovannoli, A., Lévy, N., Kaspi, E., & Roll, P. (2018). MicroRNAs in hereditary and sporadic premature aging syndromes and other laminopathies. *Aging Cell*, *17*(4), 1–17. https://doi.org/10.1111/acel.12766

Gerasymchuk, M., Cherkasova, V., Kovalchuk, O., & Kovalchuk, I. (2020). The role of microRNAs in organismal and skin aging. *International Journal of Molecular Sciences*, *21*(15), 5281. https://doi.org/10.3390/ijms21155281

Ghosh, S., González-Mariscal, I., Egan, J. M., & Moaddel, R. (2017). Targeted proteomics of cannabinoid receptor CB1 and the CB1b isoform. *Journal of Pharmaceutical and Biomedical Analysis*, *144*, 154–158. https://doi.org/10.1016/j.jpba.2016.11.003

Gu, Y., Han, J., Jiang, C., & Zhang, Y. (2020). Biomarkers, oxidative stress and autophagy in skin aging. *Ageing Research Reviews*, *59*(May), 101036. https://doi.org/10.1016/j.arr.2020.101036

Ibsen, M. S., Connor, M., & Glass, M. (2017). Cannabinoid CB1 and CB2 receptor signaling and bias. *Cannabis and Cannabinoid Research*, *2*(1), 48–60. https://doi.org/10.1089/can.2016.0037

Jeong, S., Kim, M. S., Lee, S. H., & Park, B. D. (2019). Epidermal endocannabinoid system (EES) and its cosmetic application. *Cosmetics*, *6*(2), 1–10. https://doi.org/10.3390/COSMETICS6020033

Kenyon, C. J. (2010). The genetics of ageing. *Nature*, *464*(7288), 504–512). https://doi.org/10.1038/nature08980

King, J. S., Veltman, D. M., & Insall, R. H. (2011). The induction of autophagy by mechanical stress. *Autophagy*, *7*(12), 1490–1499. https://doi.org/10.4161/auto.7.12.17924

Liang, L., Liu, X., Wang, Q., Cheng, S., Zhang, S., & Zhang, M. (2013). Pharmacokinetics, tissue distribution and excretion study of resveratrol and its prodrug 3,5,4′-tri-O-acetylresveratrol in rats. *Phytomedicine*, *20*(6), 558–563. https://doi.org/10.1016/j.phymed.2012.12.012

Mayer, R. L., Schwarzmeier, J. D., Gerner, M. C., Bileck, A., Mader, J. C., Meier-Menches, S. M., Gerner, S. M., Schmetterer, K. G., Pukrop, T., Reichle, A., Slany, A., & Gerner, C. (2018). Proteomics and metabolomics identify molecular mechanisms of aging potentially predisposing for chronic lymphocytic leukemia. *Molecular and Cellular Proteomics*, *17*(2), 290–303. https://doi.org/10.1074/mcp.RA117.000425

Sarkar, S. (2013). Regulation of autophagy by mTOR-dependent and mTOR-independent pathways: Autophagy dysfunction in neurodegenerative diseases and therapeutic application of autophagy enhancers. *Biochemical Society Transactions*, *41*(5), 1103–1130. https://doi.org/10.1042/BST20130134

Sasaki, M., Kajiya, H., Ozeki, S., Okabe, K., & Ikebe, T. (2014). Reactive oxygen species promotes cellular senescence in normal human epidermal keratinocytes through

epigenetic regulation of p16INK4a. *Biochemical and Biophysical Research Communications*, *452*(3), 622–628. https://doi.org/10.1016/j.bbrc.2014.08.123

Scaffidi, P., & Misteli, T. (2006). Lamin A-dependent nuclear defects in human aging. *Science*, *312*(5776), 1059–1063. https://doi.org/10.1126/science.1127168

Schreiber, M., Kolbus, A., Piu, F., Szabowski, A., Mö Hle-Steinlein, U., Tian, J., Karin, M., Angel, P., & Wagner, E. F. (1999). Control of cell cycle progression by c-Jun is p53 dependent. *Genes & Development*, *13*, 607–619. www.genesdev.org

Shlush, L. I., Itzkovitz, S., Cohen, A., Rutenberg, A., Berkovitz, R., Yehezkel, S., Shahar, H., Selig, S., & Skorecki, K. (2011). Quantitative digital in situ senescence-associated β-galactosidase assay. *BMC Cell Biology*, *12*, 16. https://doi.org/10.1186/1471-2121-12-16

Wong, S. Q., Kumar, A. v., Mills, J., & Lapierre, L. R. (2020). Autophagy in aging and longevity. *Human Genetics*, *139*(3), 277–290. https://doi.org/10.1007/s00439-019-02031-7

Xu, L., Fan, Q., Wang, X., Zhao, X., & Wang, L. (2016). Inhibition of autophagy increased AGE/ROS-mediated apoptosis in mesangial cells. *Cell Death and Disease*, *7*(11), e2445. https://doi.org/10.1038/cddis.2016.322

Yessenkyzy, A., Saliev, T., Zhanaliyeva, M., Masoud, A. R., Umbayev, B., Sergazy, S., Krivykh, E., Gulyayev, A., & Nurgozhin, T. (2020). Polyphenols as caloric-restriction mimetics and autophagy inducers in aging research. *Nutrients*, *12*(5), 1344. MDPI AG. https://doi.org/10.3390/nu12051344

APPENDIX

Supplementary figures

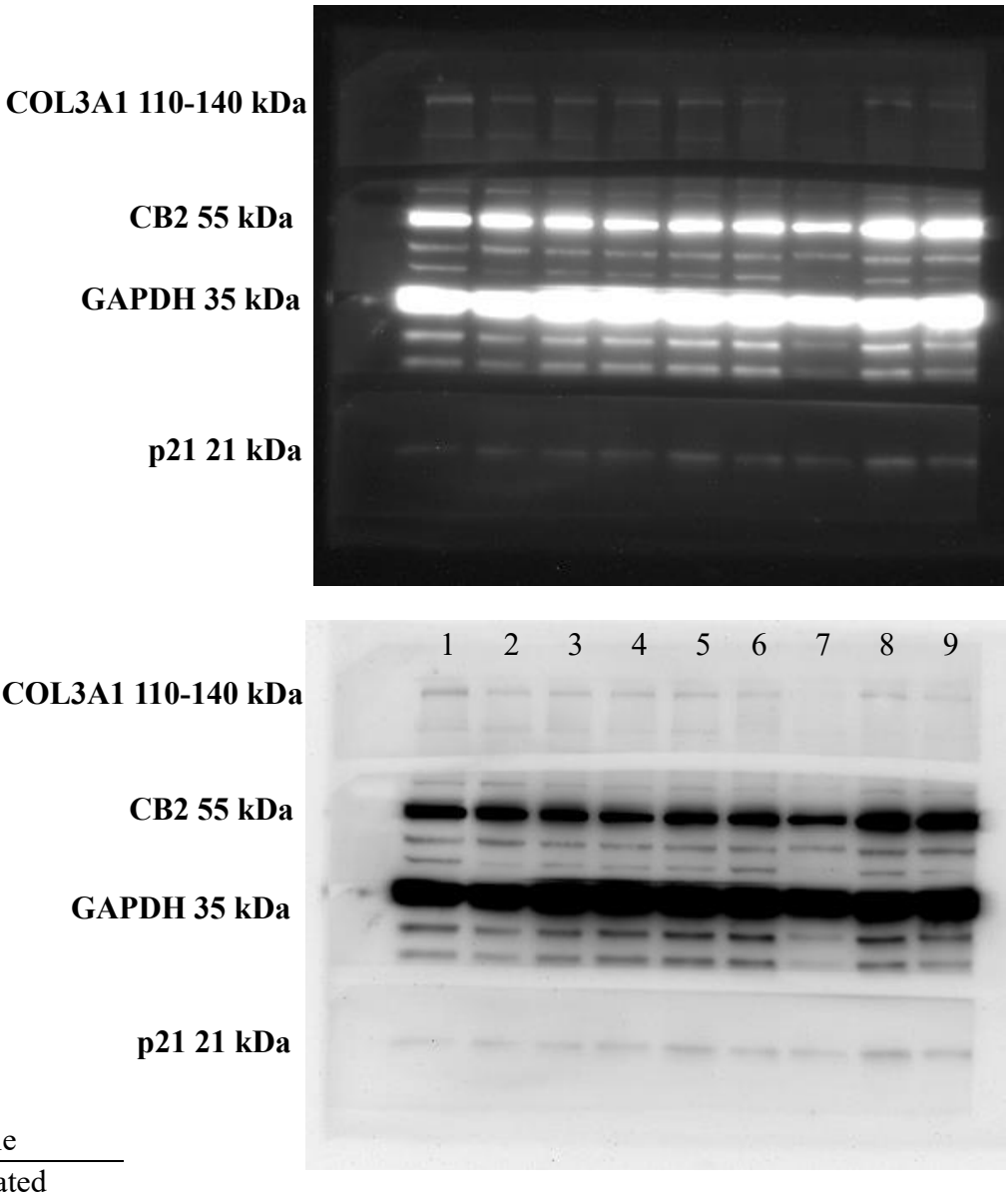

#	Sample
1	Untreated
2	PBS
3	DMSO
4	THC 2.0 μM
5	CBD 2.0 μM
6	H_2O_2 25 μM
7	H_2O_2+DMSO
8	H_2O_2+THC
9	H_2O_2+CBD

Supplementary Figure 1. Western blot images of CCD-1064Sk, 24 PDL. Original Western blots showing the COL3A1, CB2, GAPDH, and p21 bands.

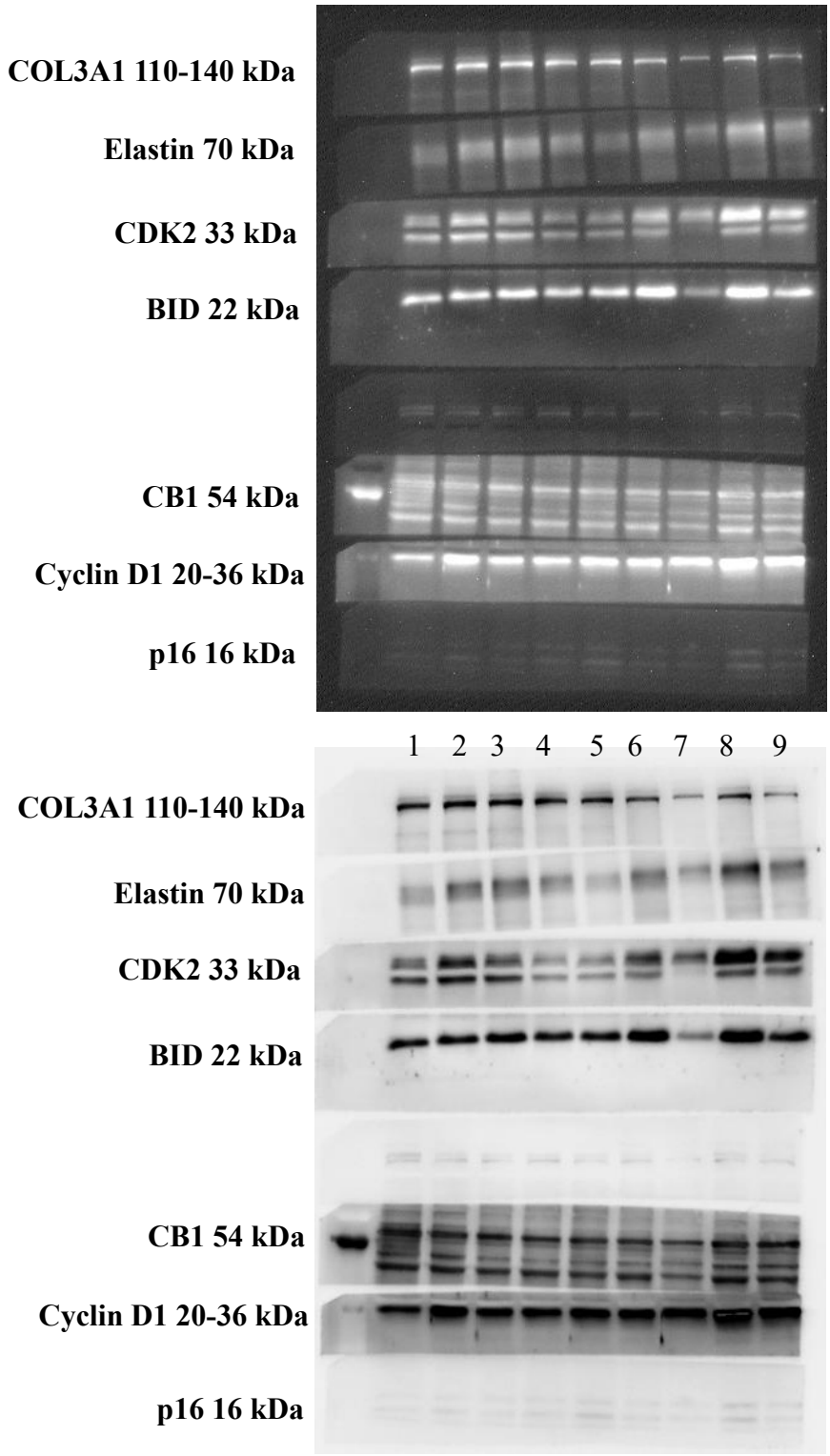

#	Sample
1	Untreated
2	PBS
3	DMSO
4	THC 2.0 μM
5	CBD 2.0 μM
6	H_2O_2 25 μM
7	H_2O_2+DMSO
8	H_2O_2+THC
9	H_2O_2+CBD

Supplementary Figure 2. Western blot images of CCD-1064Sk, 24 PDL. Original Western blots showing the COL3A1, Elastin, CDK2, BID, CB1, Cyclin D1, and p16 bands.

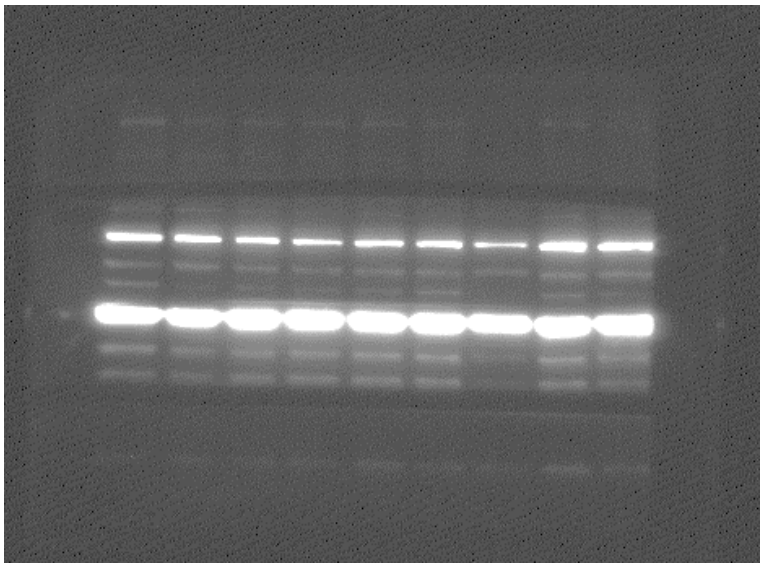

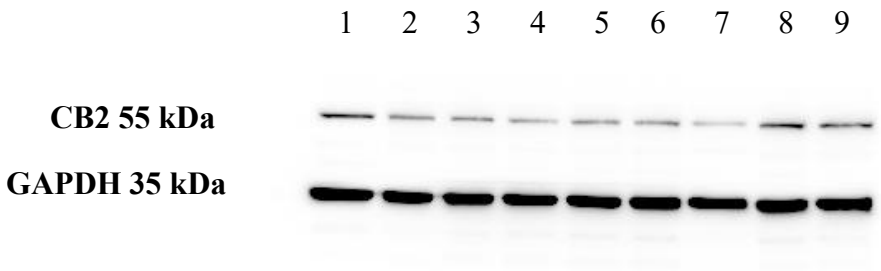

#	Sample
1	Untreated
2	PBS
3	DMSO
4	THC 2.0 µM
5	CBD 2.0 µM
6	H_2O_2 25 µM
7	H_2O_2+DMSO
8	H_2O_2+THC
9	H_2O_2+CBD

Supplementary Figure 3. Western blot images of CCD-1064Sk, 24 PDL. Original Western blots showing the CB2 and GAPDH bands.

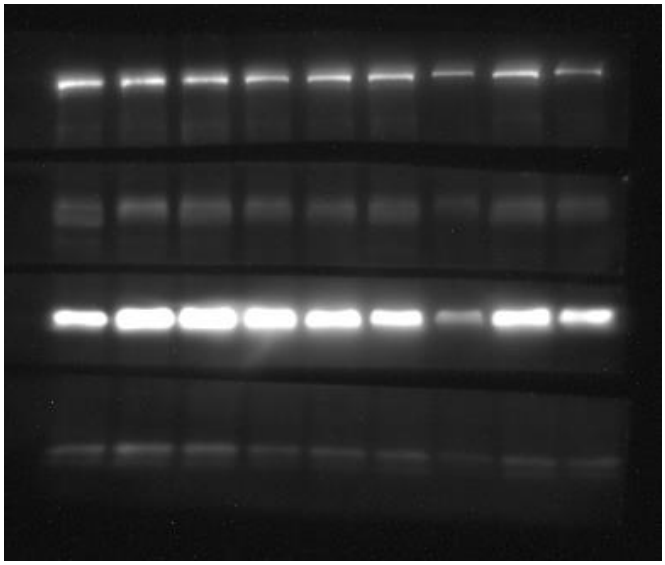

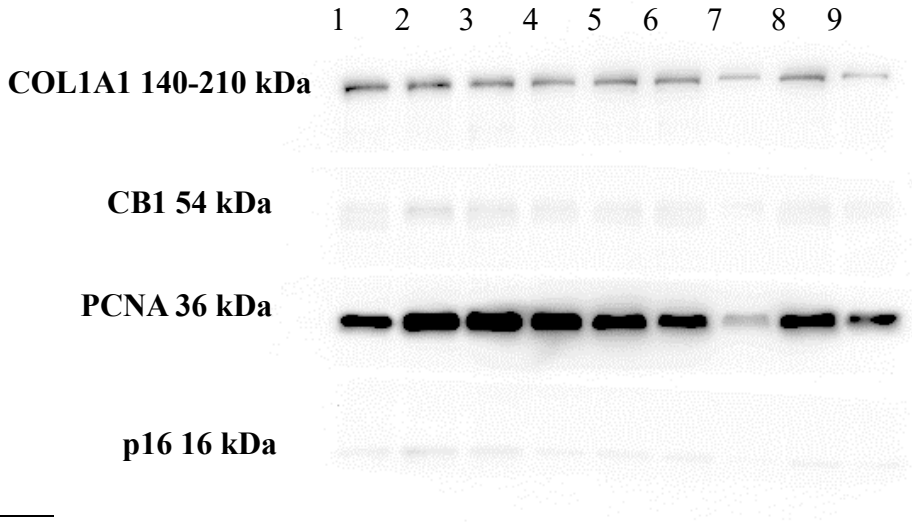

#	Sample
1	Untreated
2	PBS
3	DMSO
4	THC 2.0 μM
5	CBD 2.0 μM
6	H_2O_2 25 μM
7	H_2O_2+DMSO
8	H_2O_2+THC
9	H_2O_2+CBD

Supplementary Figure 4. Western blot images of CCD-1064Sk, 24 PDL. Original Western blots showing the COL1A1, CB1, PCNA and p16 bands.

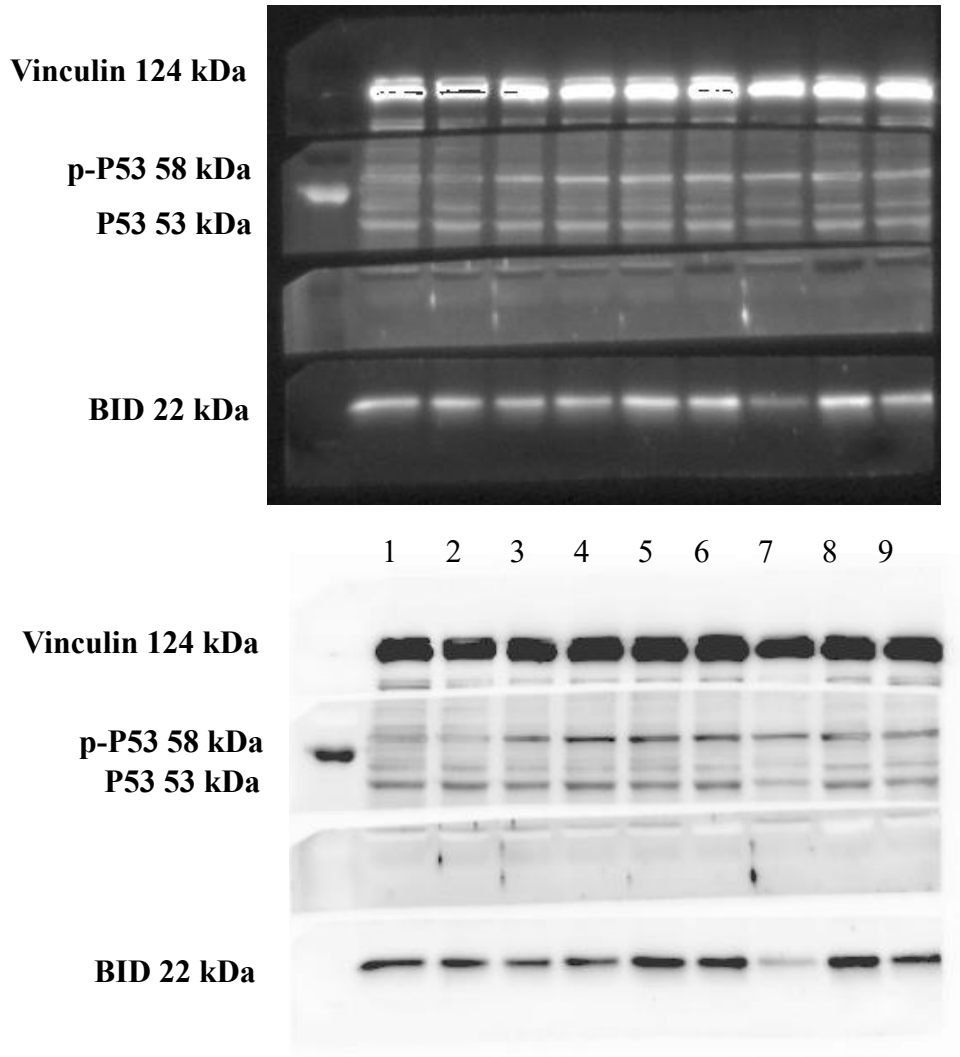

#	Sample
1	Untreated
2	PBS
3	DMSO
4	THC 2.0 µM
5	CBD 2.0 µM
6	H_2O_2 25 µM
7	H_2O_2+DMSO
8	H_2O_2+THC
9	H_2O_2+CBD

Supplementary Figure 5. Western blot images of CCD-1064Sk, 24 PDL. Original Western blots showing the Vinculin, p-P53, P53, and BID bands.

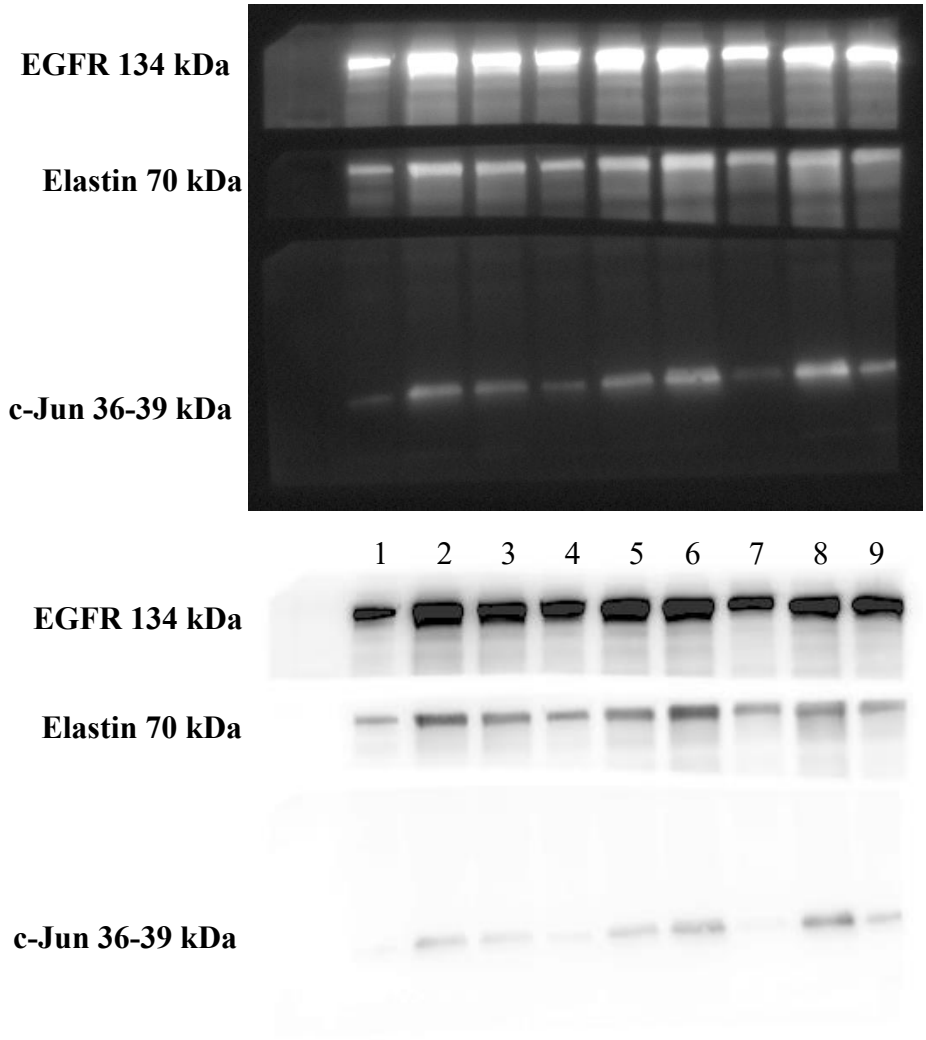

#	Sample
1	Untreated
2	PBS
3	DMSO
4	THC 2.0 μM
5	CBD 2.0 μM
6	H_2O_2 25 μM
7	H_2O_2+DMSO
8	H_2O_2+THC
9	H_2O_2+CBD

Supplementary Figure 6. Western blot images of CCD-1064Sk, 24 PDL. Original Western blots showing the EGFR, Elastin, and c-Jun bands.

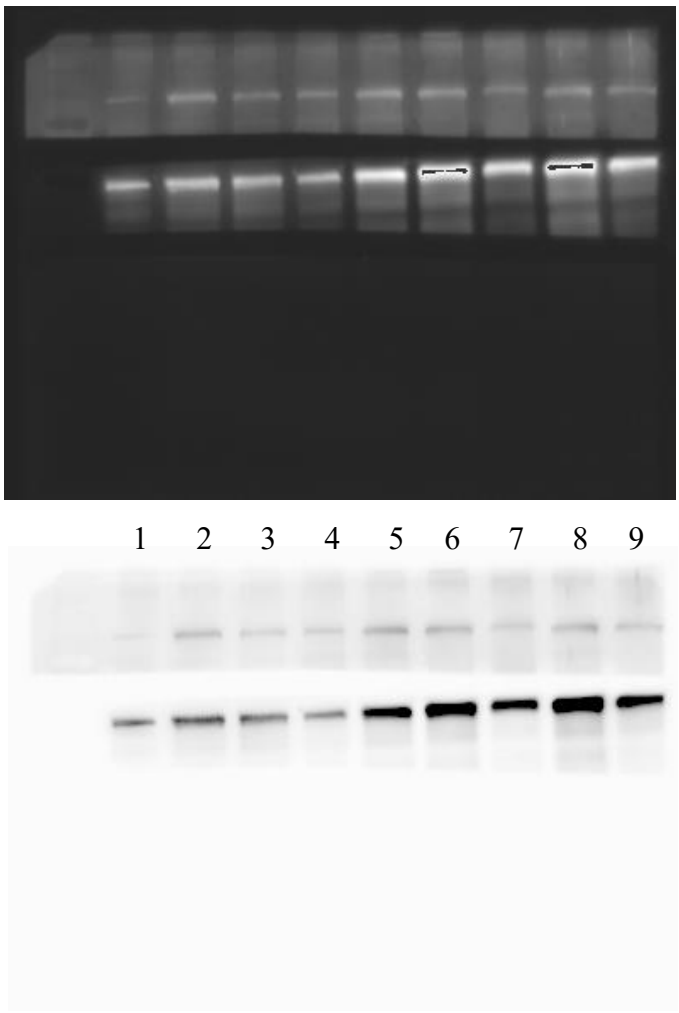

#	Sample
1	Untreated
2	PBS
3	DMSO
4	THC 2.0 μM
5	CBD 2.0 μM
6	H_2O_2 25 μM
7	H_2O_2+DMSO
8	H_2O_2+THC
9	H_2O_2+CBD

Supplementary Figure 7. Western blot images of CCD-1064Sk, 24 PDL. Original Western blots showing the SIRT1, and NF-κB bands.

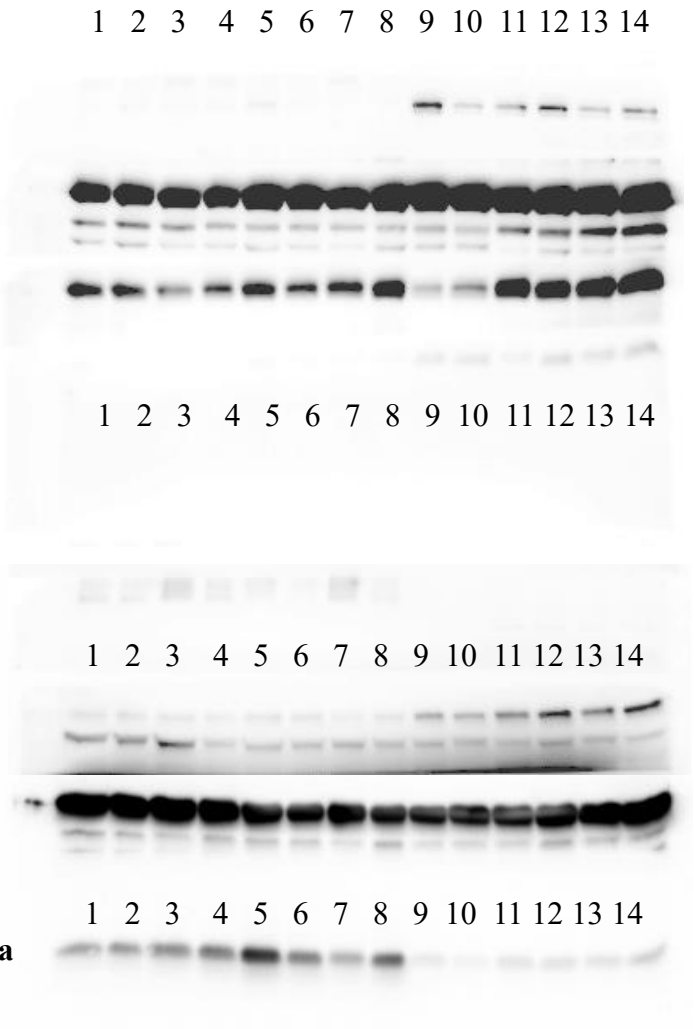

#	Sample
1	1135 40 PDL Untreated
2	1135 40 PDL DMSO
3	1135 40 PDL THC 2.0 µM
4	1135 40 PDL CBD 2.0 µM
5	1064 48 PDL Untreated
6	1064 48 PDL DMSO
7	1064 48 PDL THC 2.0 µM
8	1064 48 PDL CBD 2.0 µM
9	1064 24 PDL Untreated
10	1064 24 PDL H_2O_2 25 µM
11	1064 24 PDLH_2O_2+DMSO
12	1064 24 PDL H_2O_2+THC
13	1064 24 PDL H_2O_2+CBD
14	1064 24 PDL PBS

Supplementary Figure 8. Western blot images of CCD-1135Sk 40 PDL, CCD-1064Sk, 48 PDL, and CCD-1064Sk, 24 PDL. Original Western blots showing the COL1A1, and CB2, Cyclin D1, p27, CB1, GAPDH, and p16 bands.

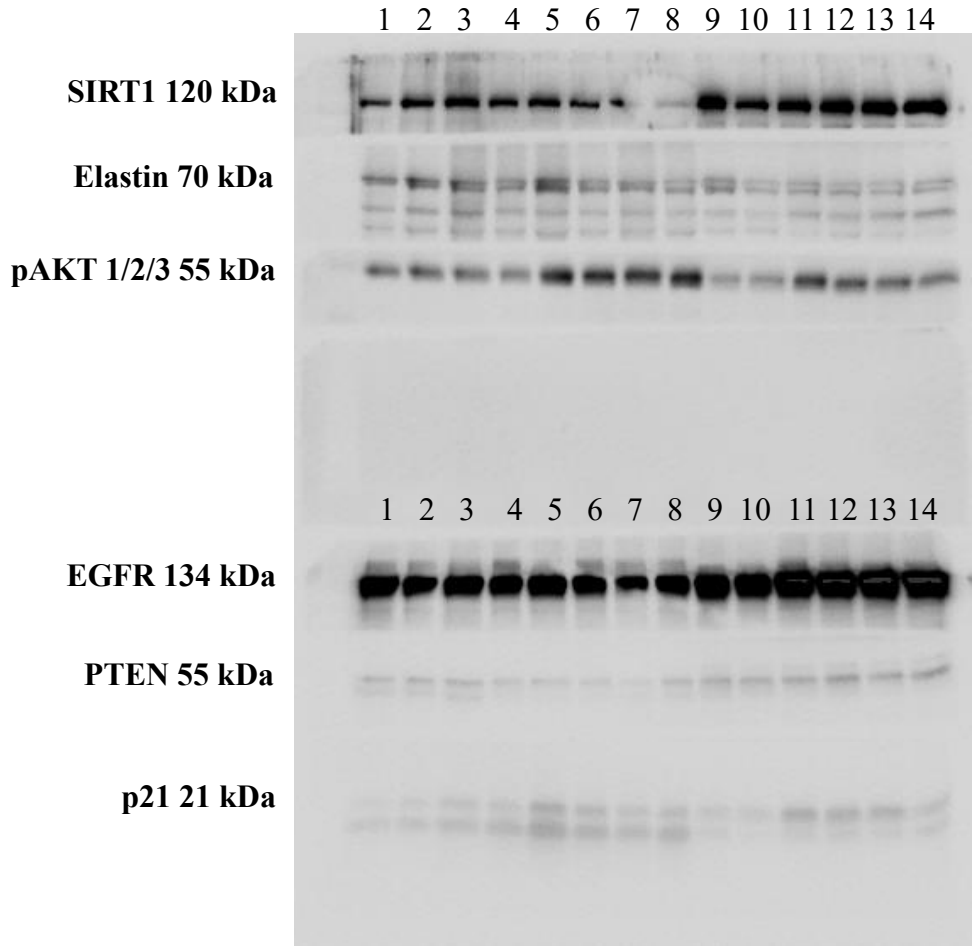

#	Sample
1	1135 40 PDL Untreated
2	1135 40 PDL DMSO
3	1135 40 PDL THC 2.0 μM
4	1135 40 PDL CBD 2.0 μM
5	1064 48 PDL Untreated
6	1064 48 PDL DMSO
7	1064 48 PDL THC 2.0 μM
8	1064 48 PDL CBD 2.0 μM
9	1064 24 PDL Untreated
10	1064 24 PDL H_2O_2 25 μM
11	1064 24 PDLH_2O_2+DMSO
12	1064 24 PDL H_2O_2+THC
13	1064 24 PDL H_2O_2+CBD
14	1064 24 PDL PBS

Supplementary Figure 9. Western blot images of CCD-1135Sk 40 PDL, CCD-1064Sk, 48 PDL, and CCD-1064Sk, 24 PDL. Original Western blots showing the SIRT1, Elastin, pAKT 1/2/3, EGFR, PTEN, and p21 bands.

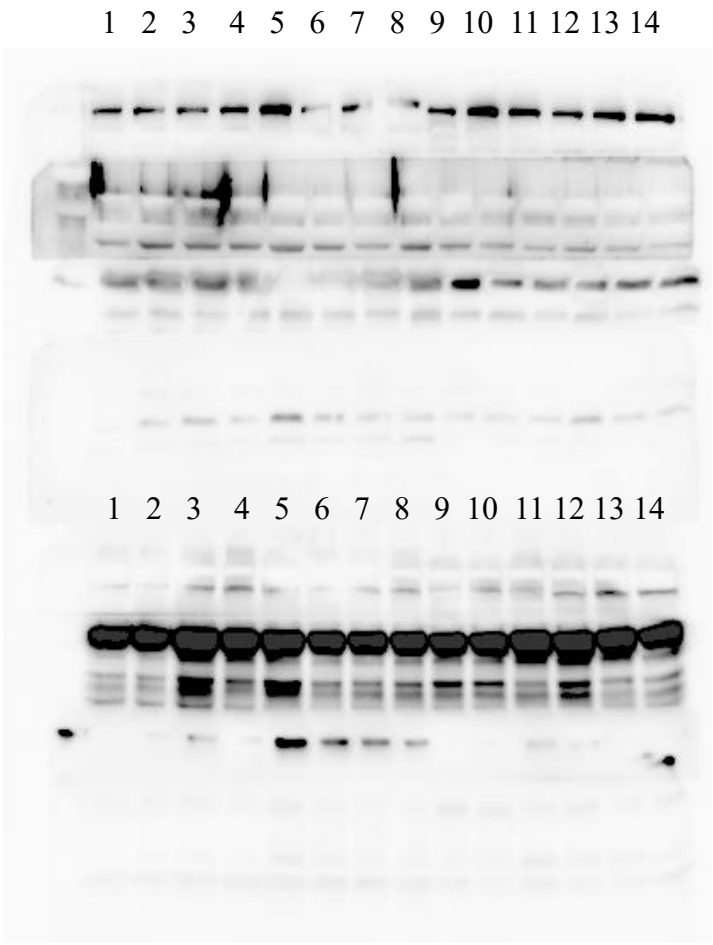

#	Sample
1	1135 40 PDL Untreated
2	1135 40 PDL DMSO
3	1135 40 PDL THC 2.0 µM
4	1135 40 PDL CBD 2.0 µM
5	1064 48 PDL Untreated
6	1064 48 PDL DMSO
7	1064 48 PDL THC 2.0 µM
8	1064 48 PDL CBD 2.0 µM
9	1064 24 PDL Untreated
10	1064 24 PDL H_2O_2 25 µM
11	1064 24 PDLH_2O_2+DMSO
12	1064 24 PDL H_2O_2+THC
13	1064 24 PDL H_2O_2+CBD
14	1064 24 PDL PBS

Supplementary Figure 10. Western blot images of CCD-1135Sk 40 PDL, CCD-1064Sk, 48 PDL, and CCD-1064Sk, 24 PDL. Original Western blots showing the EGFR, p53, c-Jun, BDNF, Vinculin, NF-κB and p27 bands.

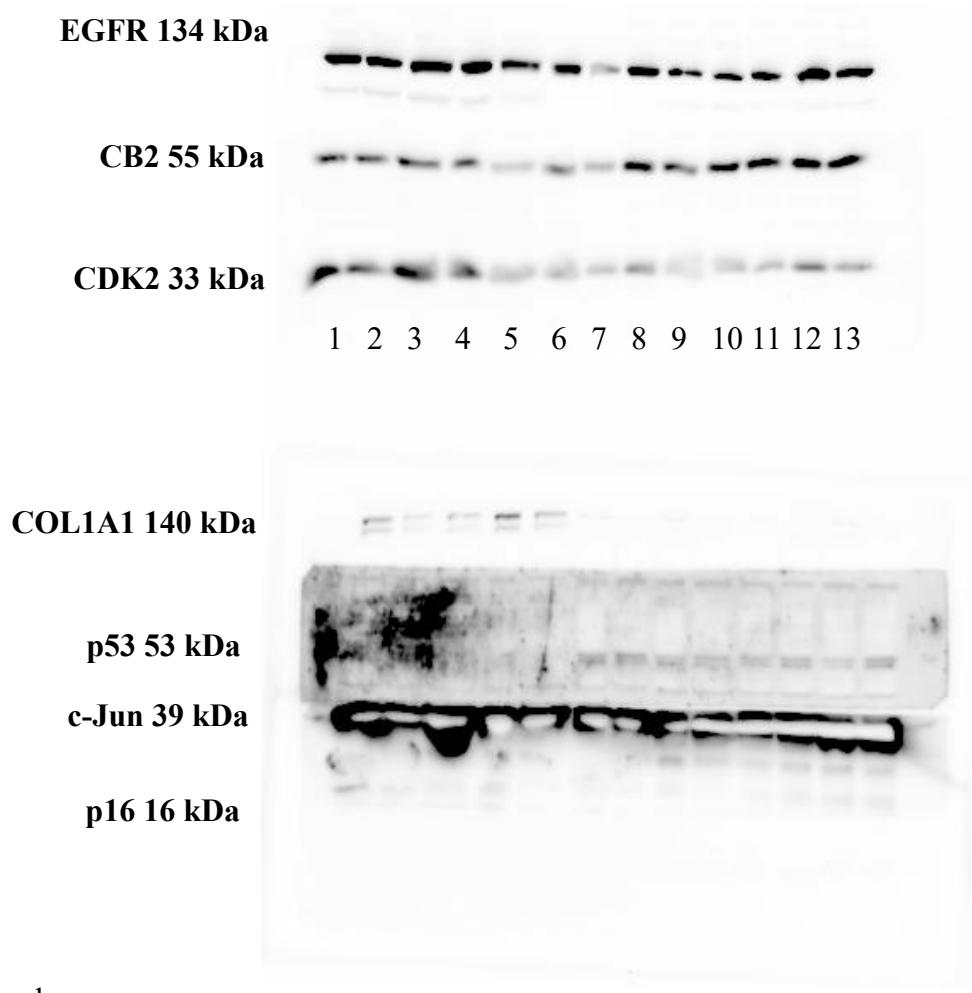

#	Sample
1	1135 40 PDL Untreated
2	1135 40 PDL DMSO
3	1135 40 PDL THC 2.0 μM
4	1135 40 PDL CBD 2.0 μM
5	1064 48 PDL Untreated
6	1064 48 PDL DMSO
7	1064 48 PDL THC 2.0 μM
8	1064 48 PDL CBD 2.0 μM
9	1064 24 PDL Untreated
10	1064 24 PDL H_2O_2 25 μM
11	1064 24 PDLH_2O_2+DMSO
12	1064 24 PDL H_2O_2+THC
13	1064 24 PDL H_2O_2+CBD

Supplementary Figure 11. Western blot images of BJ-5ta, 48 PDL. Original Western blots showing the EGFR, CB2, CDK2, COL1A1, p53, c-Jun, and p16 bands.

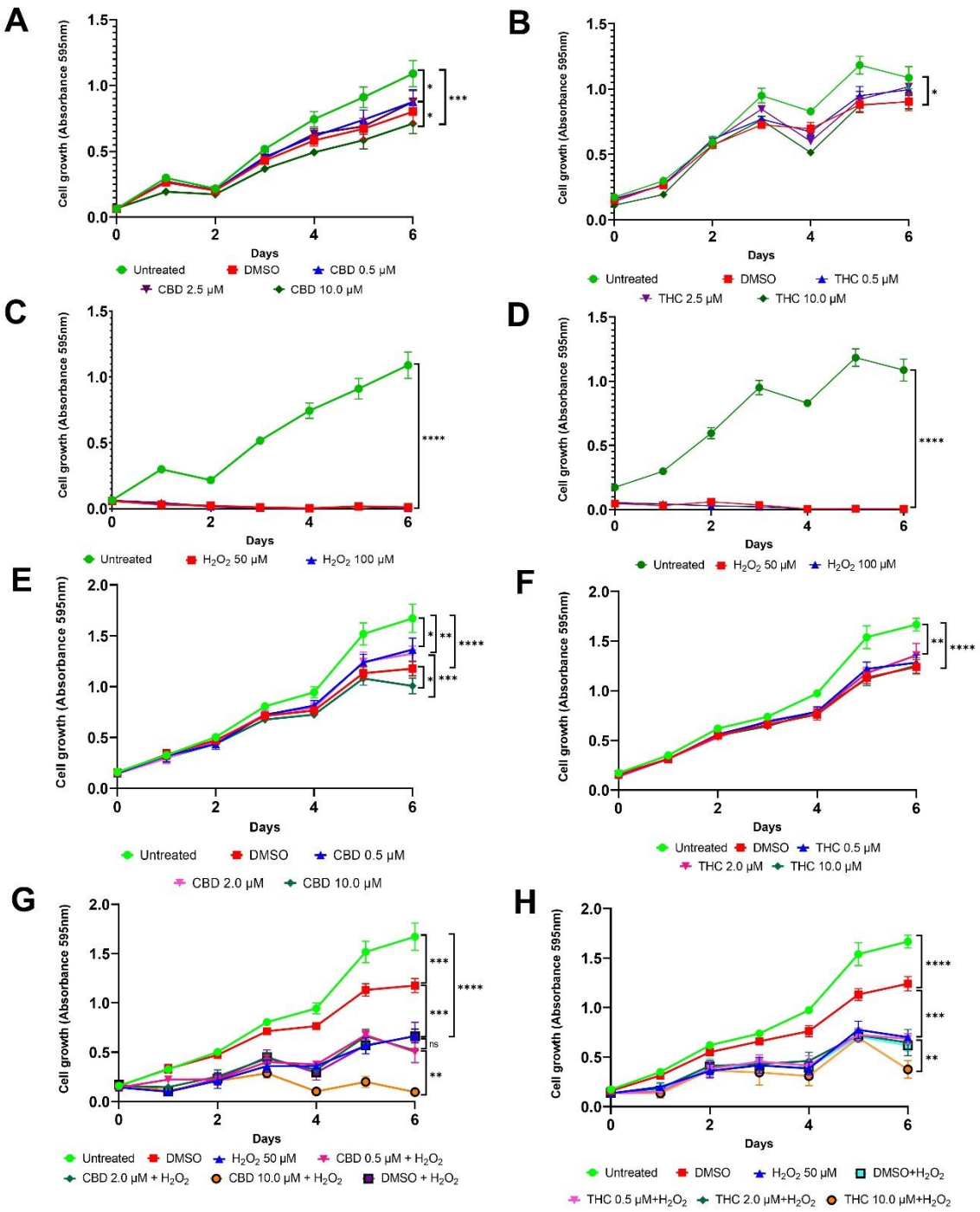

Supplementary Figure 12. Viability of human skin fibroblasts (CCD-1064Sk), 24 PDL treated by different concentrations of THC and CBD. The figure represents gradual changes in cell viability: A, B, HDF treated with 0.5 µM, 2 µM, and 10 µM concentrations of CBD and THC respectively; C, D, 50 µM H_2O_2 and 10 µM H_2O_2-induced senescent fibroblasts; E, F, H_2O_2; G, H, 50 µM H_2O_2-induced senescent fibroblasts treated with 0.5 µM, 2 µM, and 10 µM concentrations of CBD and THC respectively. DMSO, dimethyl sulfoxide (vehicle). Data were analyzed with an ANOVA

test (Tukey post-hoc multiple comparison test). Bars represent mean ± SD. Significance is indicated within the figures using the following scale: ns, not significant; *, p<0.05; **, p<0.01; ***, p<0.001; ****, p<0.0001.

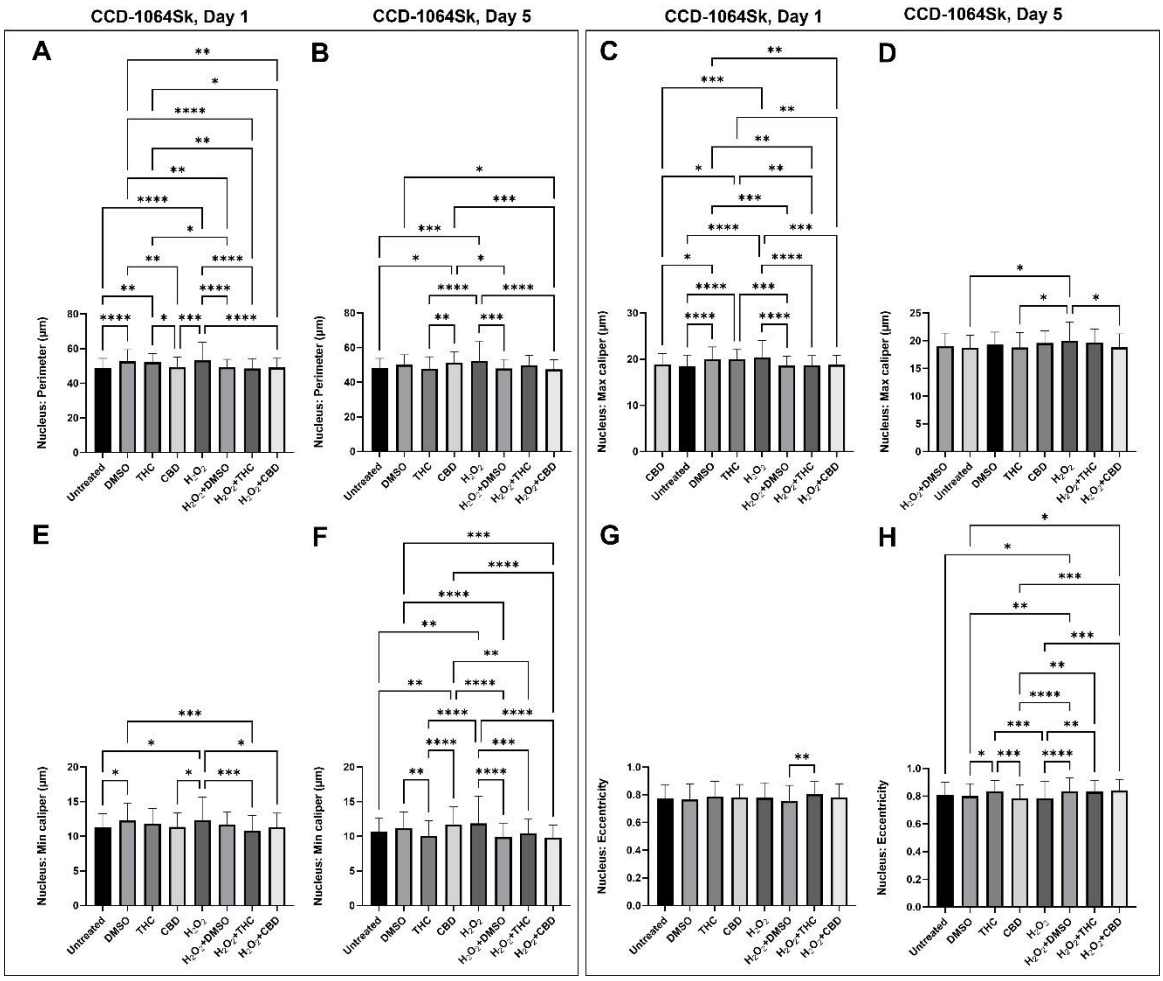

Supplementary Figure 13. DAPI stained nuclei of dermal fibroblasts (CCD-1064Sk), 24 PDL treated with cannabinoids. Graphic representation of nuclear changes on day 1 and day 5 of the experiment respectively: A and B, Nuclear perimeter; C and D, Nuclear max caliper; E and F, Nuclear min caliper; G and H, Nuclear eccentricity. Data were analyzed with an ANOVA test (Tukey post-hoc multiple comparison test). Bars represent mean ± SD. Significance is indicated within the figures using the following scale: ns, not significant; *, p<0.05; **, p<0.01; ***, p<0.001; ****, p<0.0001.

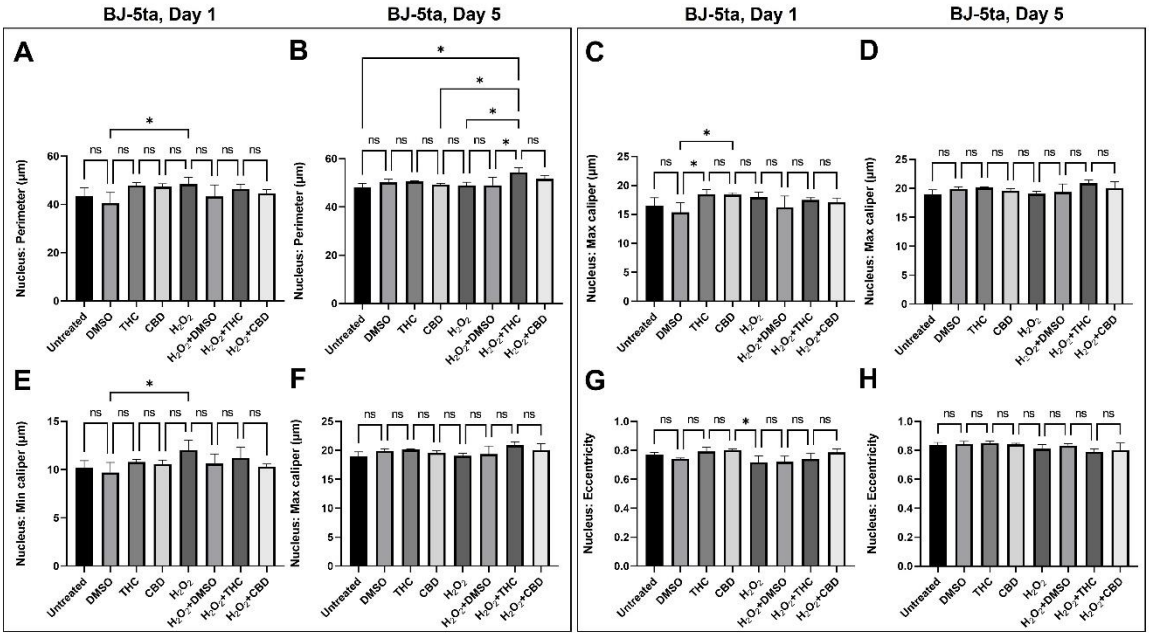

Supplementary Figure 14. DAPI stained nuclei of dermal fibroblasts (BJ-5ta), 90 PDL treated with cannabinoids. Graphic representation of nuclear changes on day 1 and day 5 of the experiment respectively: A and B, Nuclear perimeter; C and D, Nuclear max caliper; E and F, Nuclear min caliper; G and H, Nuclear eccentricity. Data were analyzed with an ANOVA test (Tukey post-hoc multiple comparison test). Bars represent mean ± SD. Significance is indicated within the figures using the following scale: ns, not significant; *, p<0.05; **, p<0.01; ***, p<0.001; ****, p<0.0001.

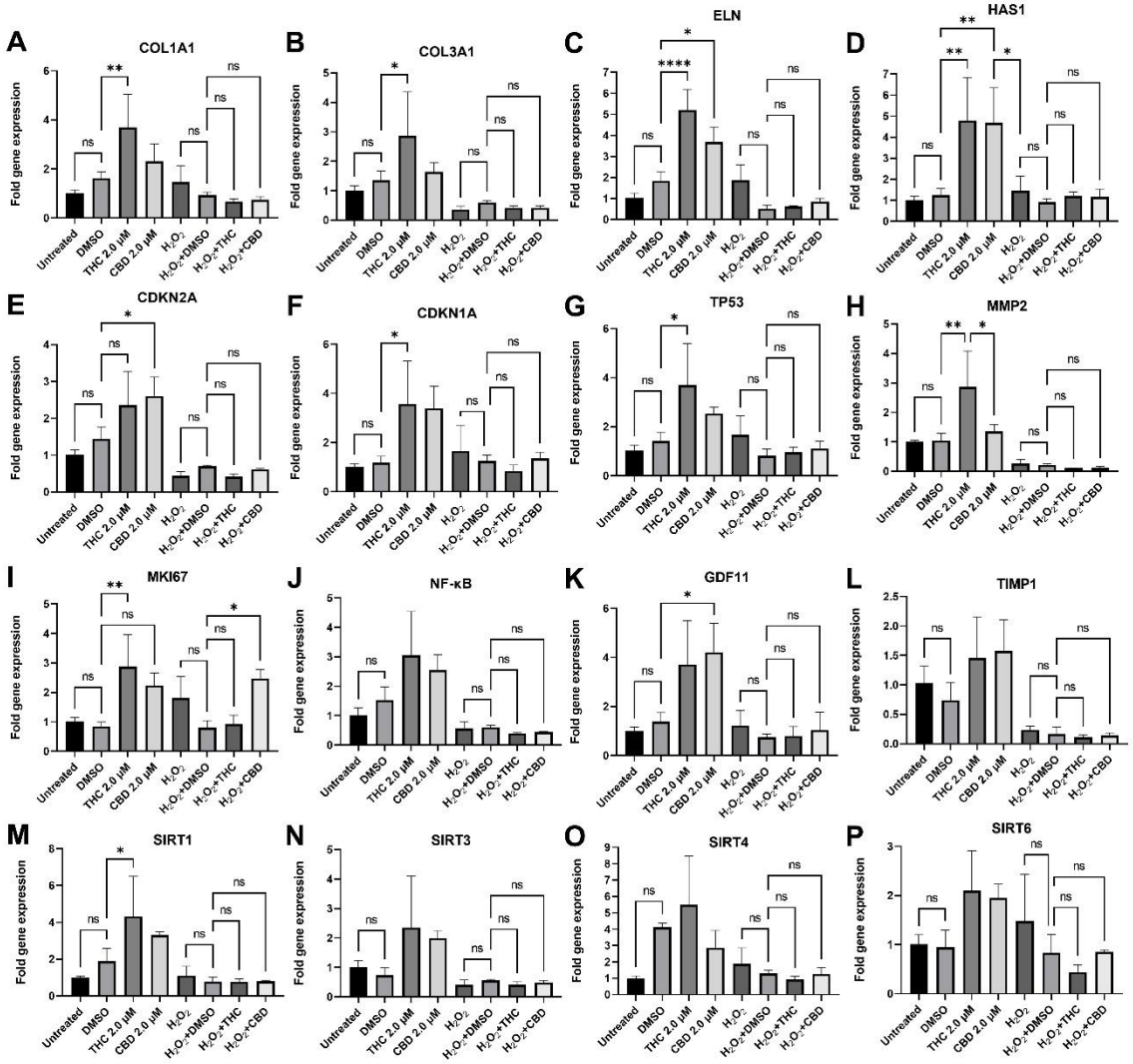

Supplementary Figure 15. Effects of phytocannabinoids on senescence-associated gene expression in CCD-1064Sk dermal fibroblasts. Changes of mRNA expression levels for selected genes measured by as measured by RT-PCR. A. *COL1A1*; B. *COL3A1*; C. *ELN*; D. *HAS1*; E. *CDKN2A*; F. *CDKN1A*; G. *TP53*; H. *MMP2*; I. *MKI67*; J. *NK-κB*; K. *GDF11*; L. *TIMP1*; M. *SIRT1*; N. *SIRT3*; O. *SIRT4*; P. *SIRT6*. Data were analyzed with an ANOVA test (Tukey post-hoc multiple comparison test). Bars represent mean ± SD. Significance is indicated within the figures using the following scale: ns, not significant; *, $p<0.05$; **, $p<0.01$; ***, $p<0.001$; ****, $p<0.0001$.

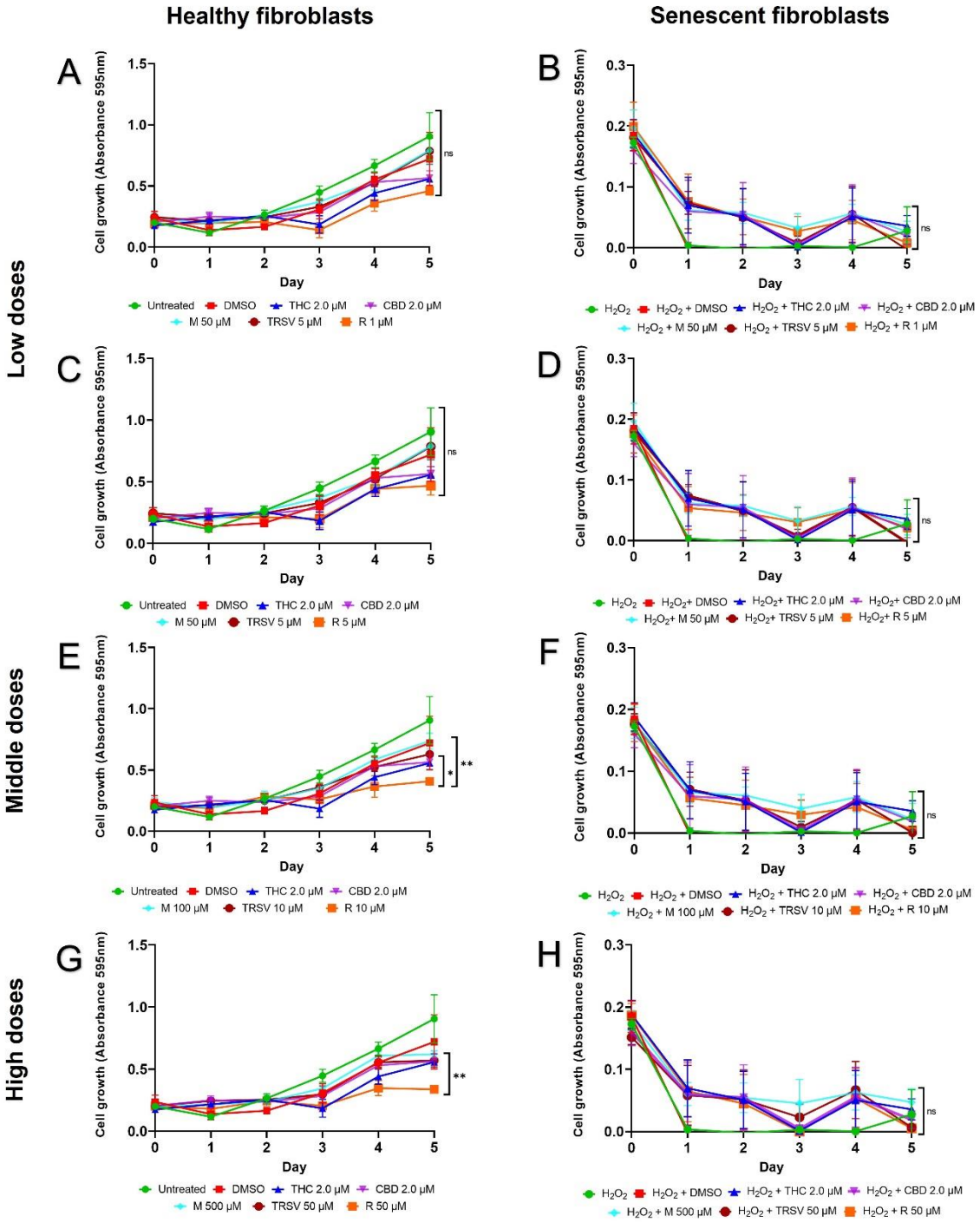

Supplementary Figure 16. Viability of human skin fibroblasts (BJ-5ta), 93 PDL exposed to different concentrations of metformin, triacetylresveratrol, and rapamycin compared to THC and CBD. The figure represents gradual changes in cell viability: A and B, low doses treatments of healthy and senescent cells, respectively: 50 µM metformin (M), 5 µM triacetylresveratrol (TRSV), 1 µM rapamycin (R); C and D, low doses treatments of healthy and senescent cells, respectively: 50 µM metformin (M), 5 µM

triacetylresveratrol (TRSV), 5 µM rapamycin (R); E, F representation of middle doses treatments of healthy and senescent cells, respectively: 100 µM metformin (M), 10 µM triacetylresveratrol (TRSV), 10 µM rapamycin (R); G and H, high doses treatments of healthy and senescent cells, respectively: 500 µM metformin (M), 50 µM triacetylresveratrol (TRSV), 50 µM rapamycin (R). DMSO, dimethyl sulfoxide (vehicle). Data were analyzed with an ANOVA test (Tukey post-hoc multiple comparison test). Bars represent mean ± SD. Significance is indicated within the figures using the following scale: ns, not significant; *, $p<0.05$; **, $p<0.01$.

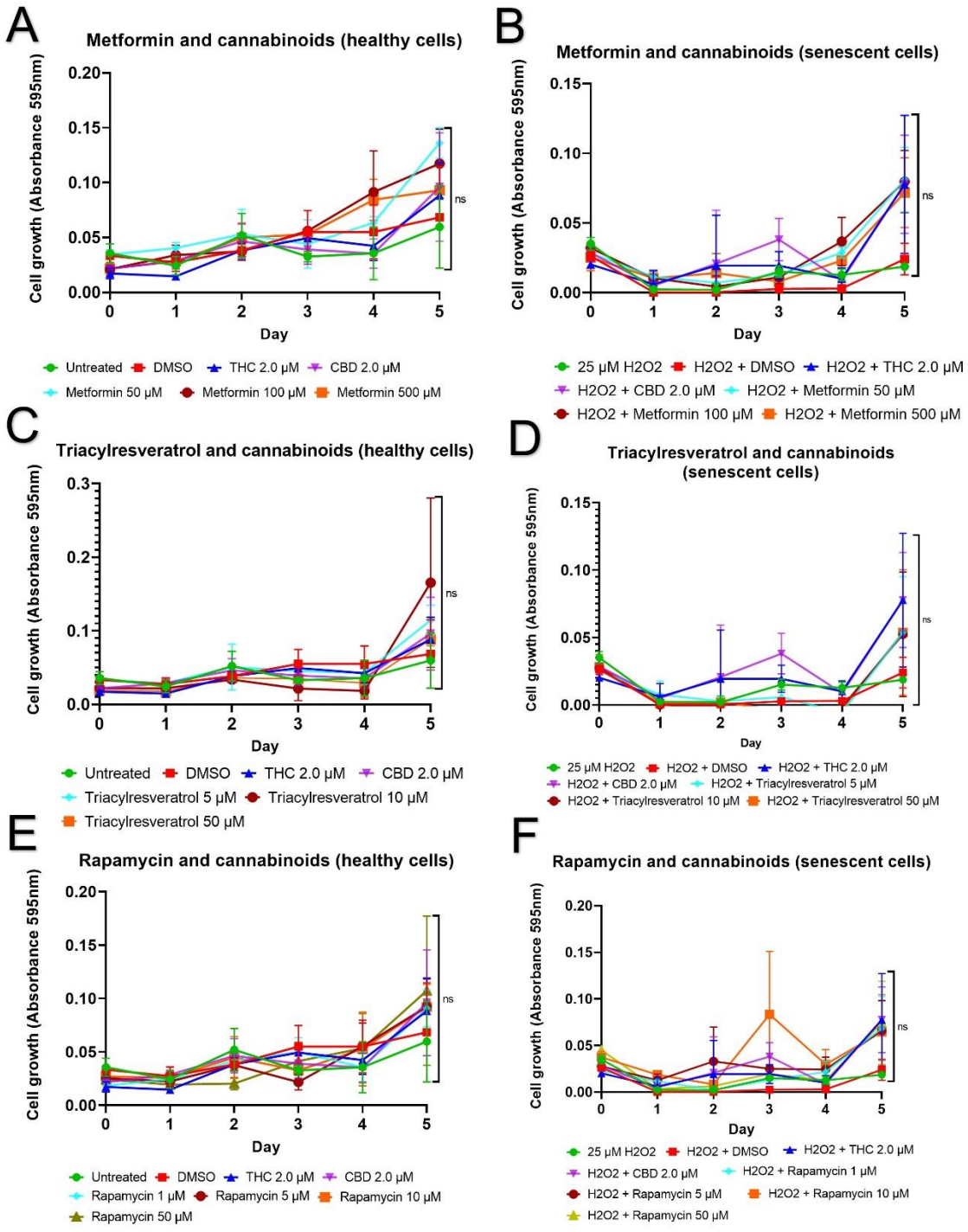

Supplementary Figure 17. 25 µM H_2O_2 model of senescence with two hours cannabinoids and anti-aging drugs treatment in adult human skin fibroblasts cell line (CCD-1135Sk, 36 PDL). The figure represents gradual changes in cell viability: A and B, metformin (M) treatments of healthy and senescent cells, respectively; C and D, triacetylresveratrol (TRSV) treatments of healthy and senescent cells, respectively; E, F

representation of rapamycin (R) treatments of healthy and senescent cells, respectively. DMSO, dimethyl sulfoxide (vehicle). Data were analyzed with an ANOVA test (Tukey post-hoc multiple comparison test). Bars represent mean ± SD. Significance is indicated within the figures using the following scale: ns, not significant.

CCD-1135Sk, p.15

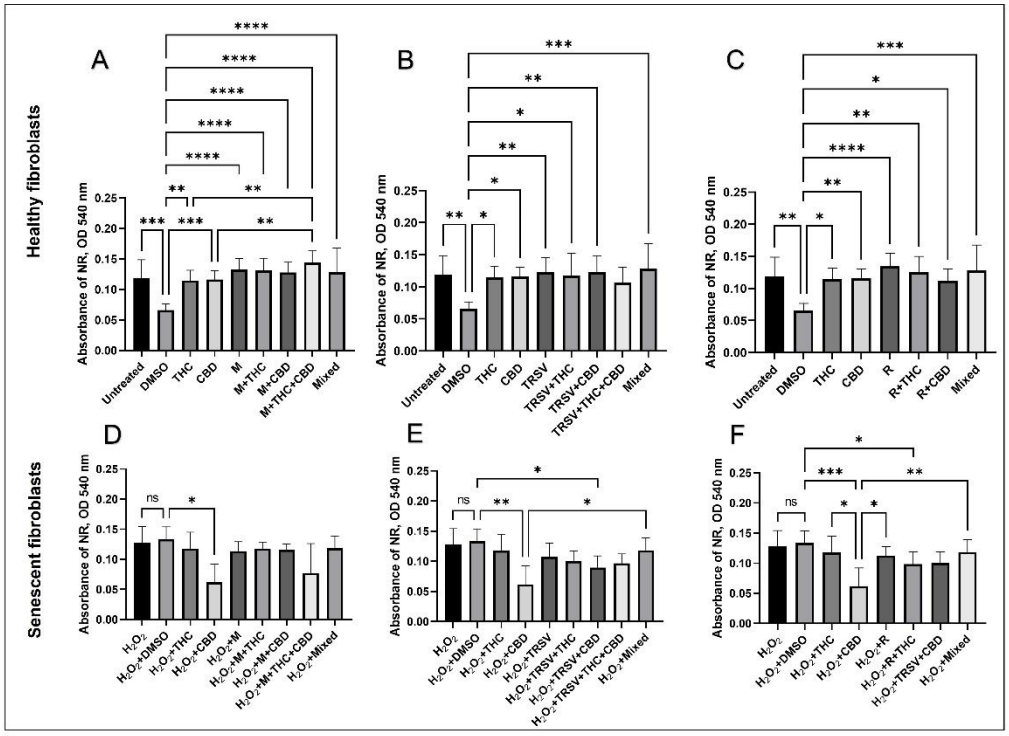

BJ-5ta, p.42

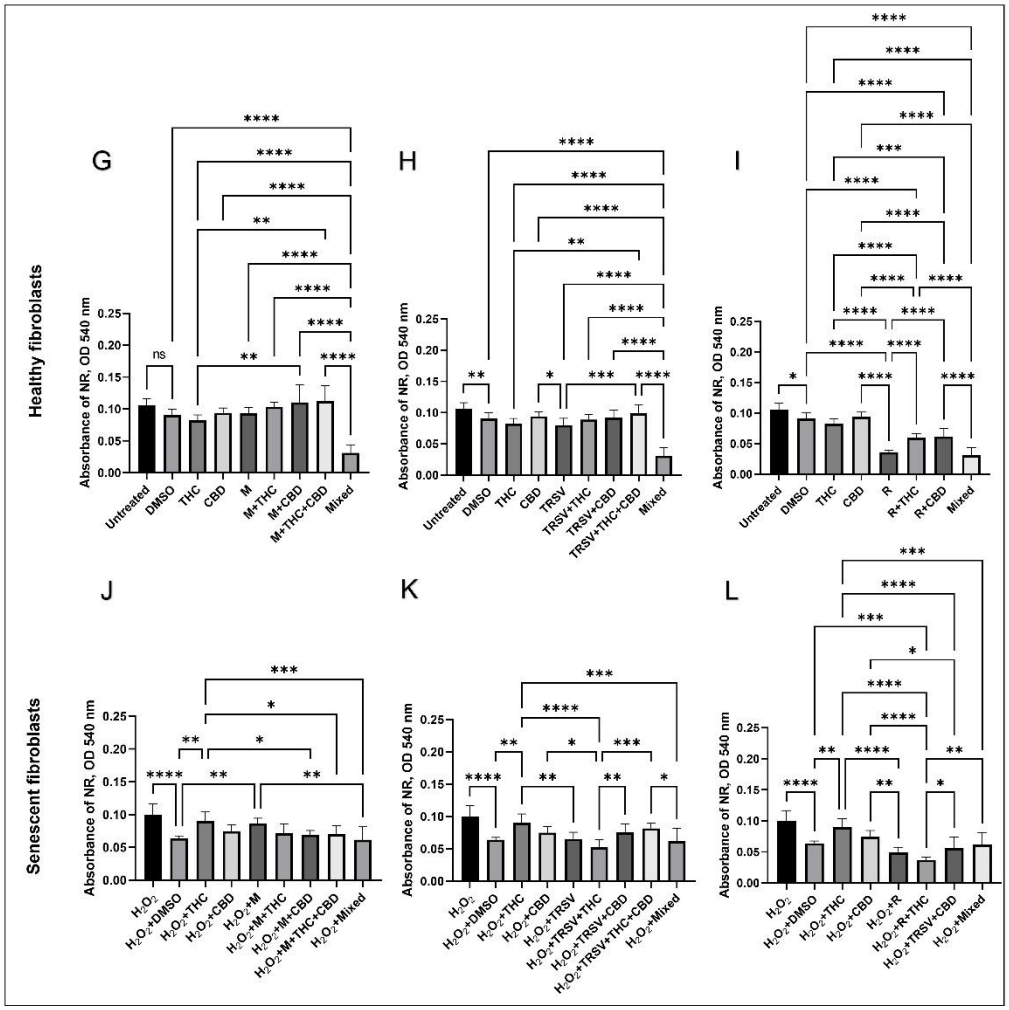

Supplementary Figure 18. Viability of dermal fibroblasts CCD-1135Sk, 38 PDL and BJ-5ta, 90 PDL treated potential anti-aging compounds combined with phytocannabinoids. The graphs represent cell viability of skin fibroblasts estimated by NR assay after experimental treatments of healthy (**A-C, G-I**) and senescent (**D-F, J-L**) cells with nutrient signaling regulators combined with THC and CBD. CBD, cannabidiol; DMSO, dimethyl sulfoxide (vehicle), M, metformin; Mixed, included metformin + TRSV + rapamycin + THC + CBD; R, rapamycin; THC, Δ-9-tetrahydrocannabinol; TRSV, triacetylresveratrol. Data were analyzed with an ANOVA test (Tukey post-hoc multiple comparison test). Bars represent mean ± SD. Significance is indicated within the figures using the following scale: ns, not significant; *, $p<0.05$; **, $p<0.01$; ***, $p<0.001$; ****, $p<0.0001$.

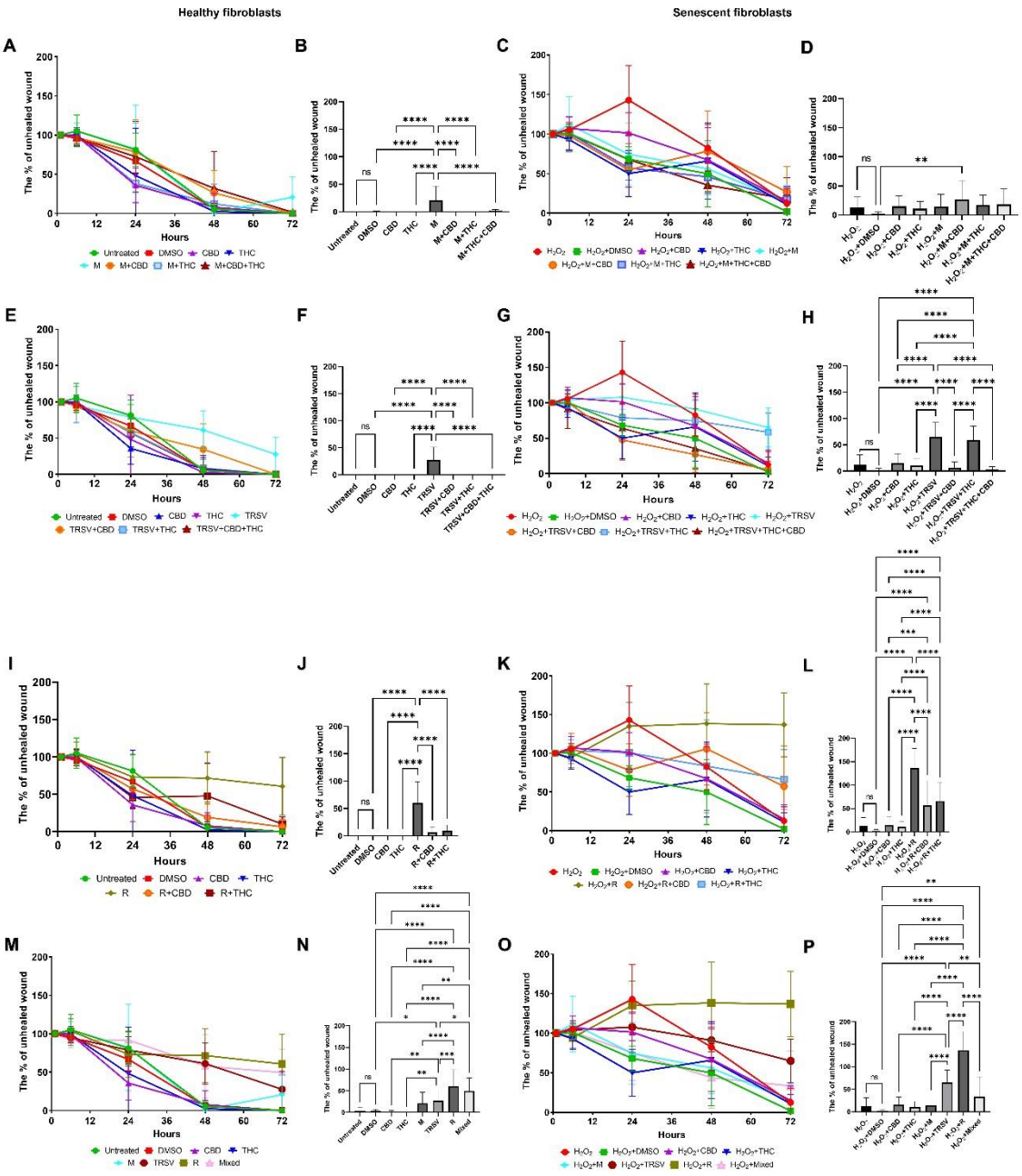

Supplementary figure 19. The effect of nutrient signaling regulators combined with phytocannabinoids on wound healing. Graphs represented wound healing assay results in BJ-5ta 90 PDL dermal fibroblasts. **A, E, I, M**, the percentage of an unhealed wound in healthy fibroblasts treated with metformin, TRSV, rapamycin combined with pCBs and mixed (metformin+TRSV+rapamycin+THC+CBD) treatment, respectively; B, F, J, N, the percentage of the unhealed wound after 72 hours of experiment in healthy cells metformin, TRSV, rapamycin combined with pCBs and mixed (metformin+TRSV+rapamycin+THC+CBD) treatment, respectively; **C, G, K, O**, the percentage of an unhealed wound in senescent fibroblasts culture treated with metformin, TRSV, rapamycin combined with pCBs and mixed

(metformin+TRSV+rapamycin+THC+CBD) treatment, respectively; **D, H, L, P**, The percentage of the unhealed wound after 72 hours in prematurely aged fibroblasts metformin, TRSV, rapamycin combined with pCBs and mixed (metformin+TRSV+rapamycin+THC+CBD) treatment, respectively. Data were analyzed with an ANOVA test (Tukey post-hoc multiple comparison test). Bars represent mean ± SD. Significance is indicated within the figures using the following scale: ns, not significant; *, p<0.05; **, p<0.01; ***, p<0.001, ****p<0.0001.

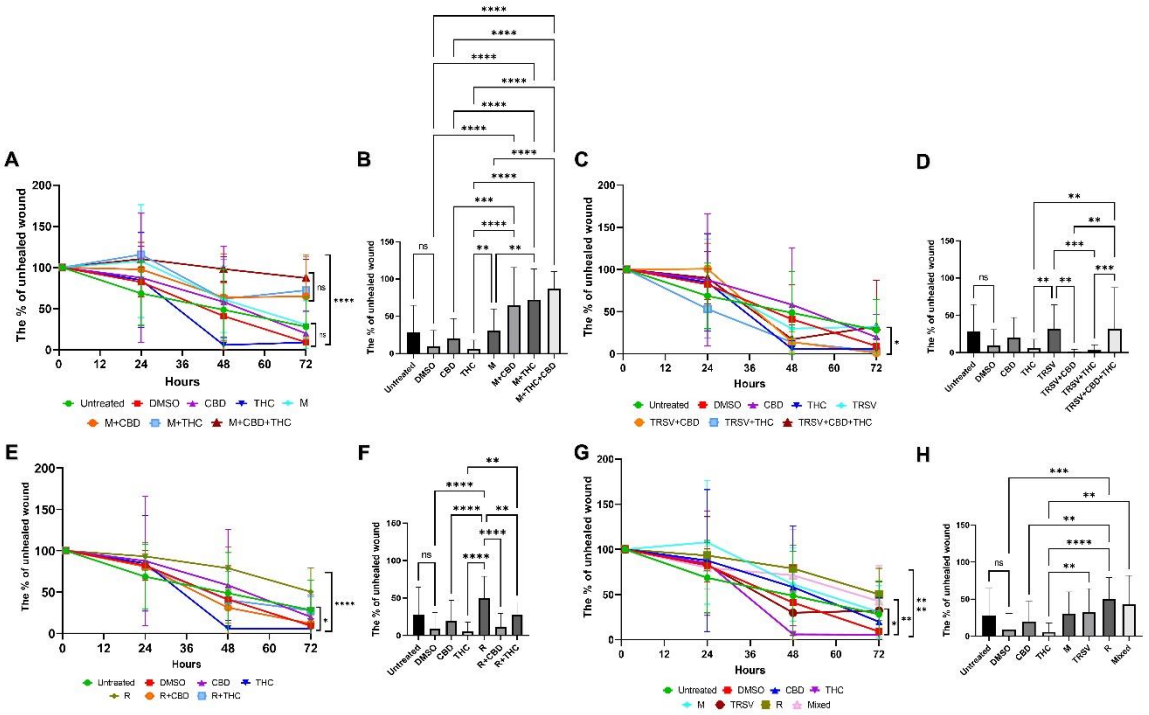

Supplementary figure 20. The effect of nutrient signaling regulators combined with phytocannabinoids on wound healing. Graphs represented wound healing assay results in CCD-1135Sk 38 PDL (pre-senescent condition) dermal fibroblasts. **A, C, E, G**, the percentage of an unhealed wound in healthy fibroblasts treated with metformin, TRSV, rapamycin combined with pCBs and mixed (metformin+TRSV+rapamycin+THC+CBD) treatment, respectively; **B, D, F, H**, the percentage of the unhealed wound after 72 hours of experiment in healthy cells metformin, TRSV, rapamycin combined with pCBs and mixed (metformin+TRSV+rapamycin+THC+CBD) treatment, respectively. Data were analyzed with an ANOVA test (Tukey post-hoc multiple comparison test). Bars represent mean ± SD. Significance is indicated within the figures using the following scale: ns, not significant; *, p<0.05; **, p<0.01; ***, p<0.001, ****p<0.0001.

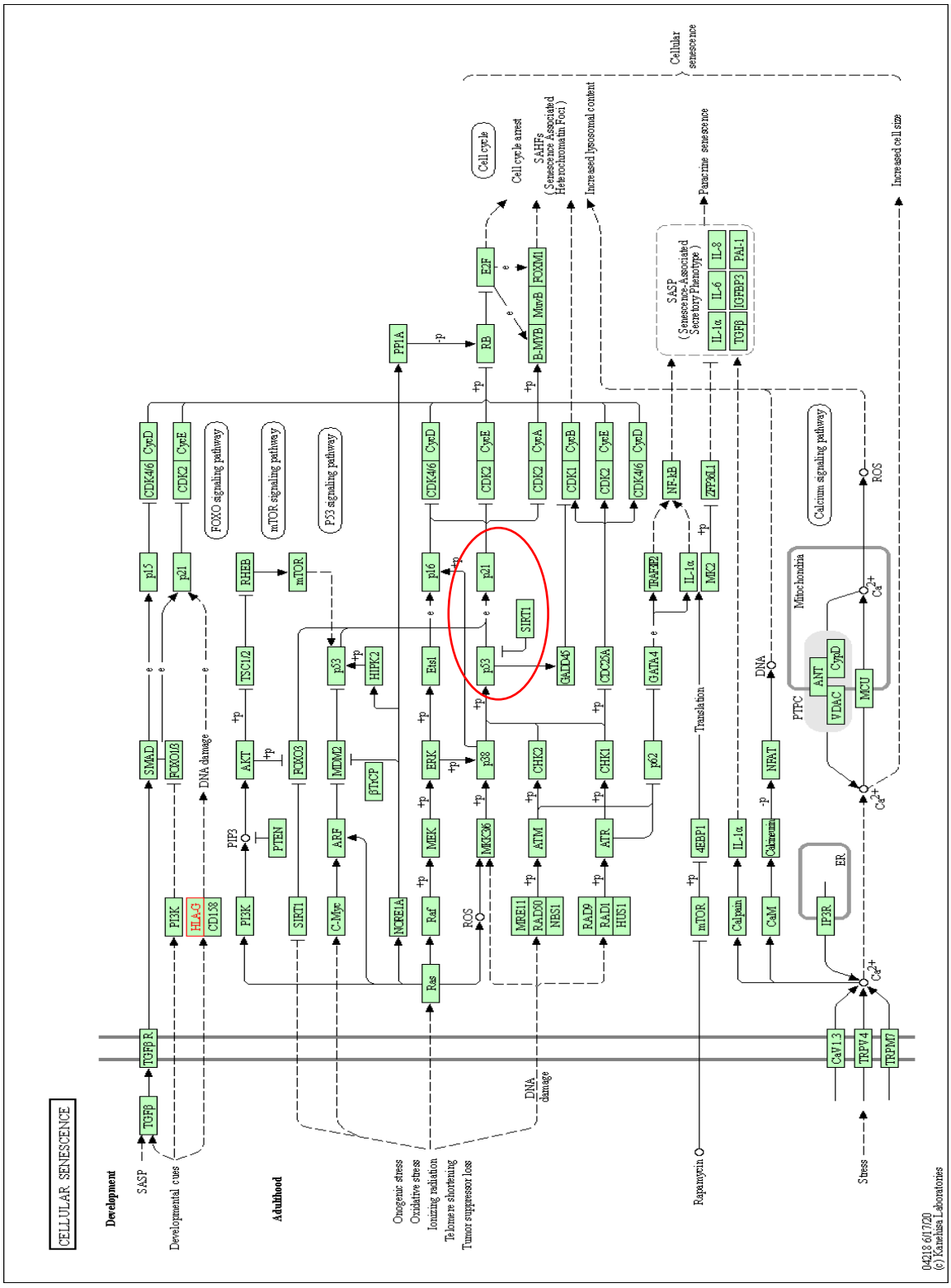

Supplementary Figure 21. Cellular Senescence Pathway. Retrieved from https://www.genome.jp/kegg-bin/show_pathway?hsa04218+3105

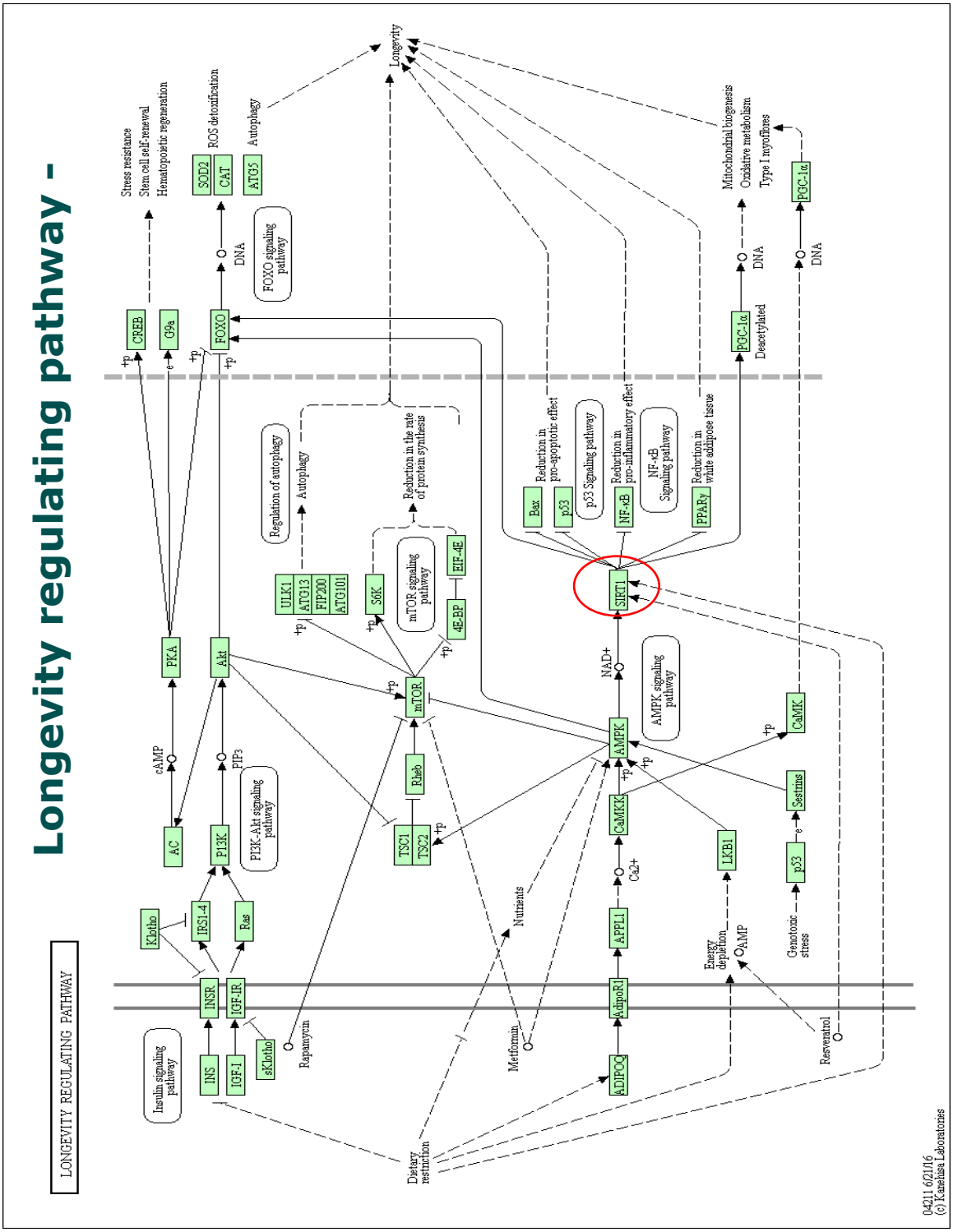

Supplementary Figure 22. Longevity regulating pathway - Homo sapiens (human). Retrieved from https://www.genome.jp/kegg-bin/show_pathway?hsa04211

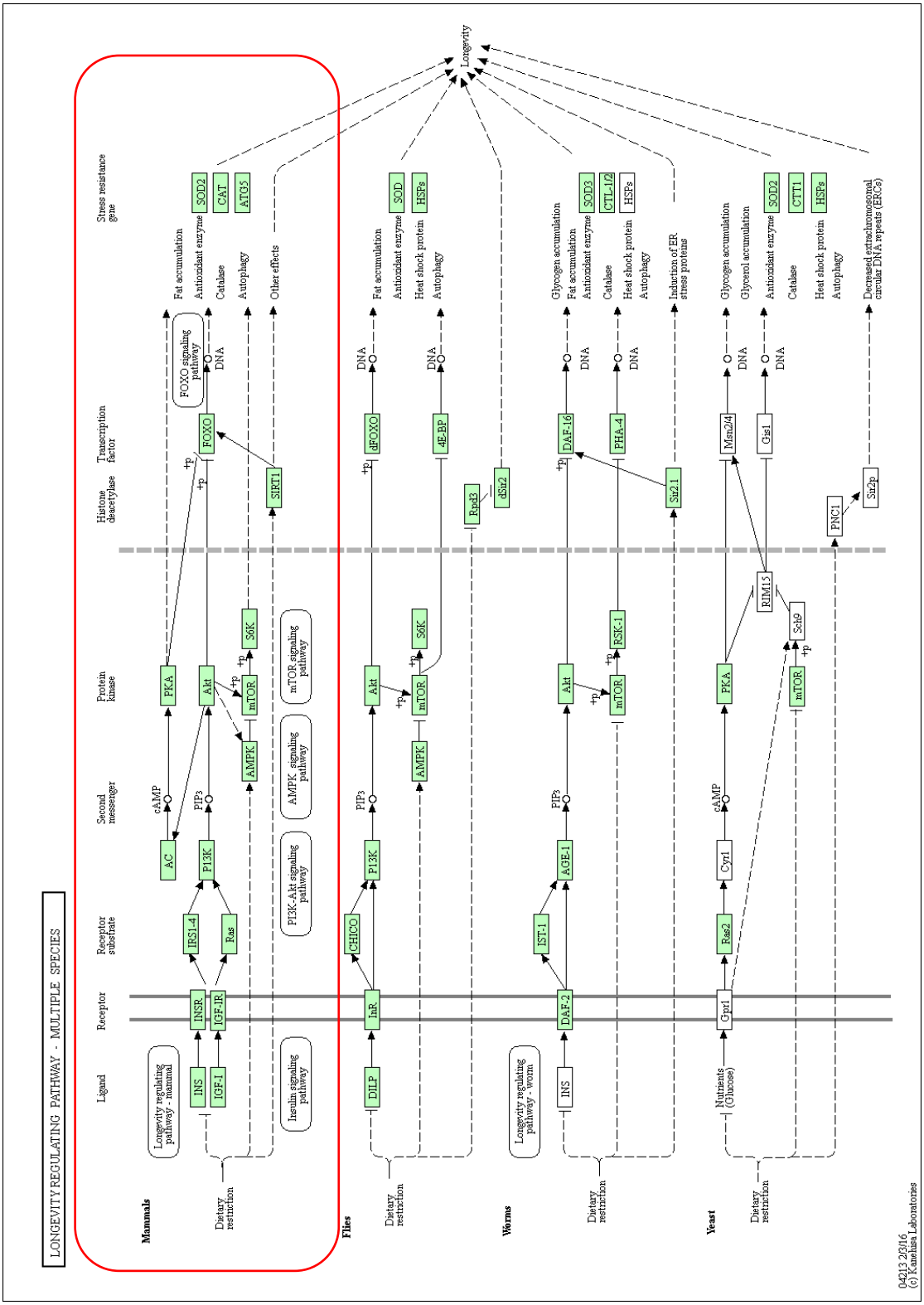

Supplementary Figure 23. Longevity regulating pathway – multiple species. Retrieved from https://www.genome.jp/kegg-bin/show_pathway?hsa04213